LBNL-49061

ERNEST ORLANDO LAWRENCE BERKELEY NATIONAL LABORATORY

The Synthesis and Evaluation of 2,3-Dihydroxyterephthalamides as Actinide Chelators

Christine J. Gramer

Chemical Sciences Division

September 2001

Ph.D. Thesis

REFERENCE COPY
Does Not
Circulate
Library Annex Reference
Lawrence Berkeley National Laboratory
LBNL-49061
Copy 1

DISCLAIMER

This document was prepared as an account of work sponsored by the United States Government. While this document is believed to contain correct information, neither the United States Government nor any agency thereof, nor the Regents of the University of California, nor any of their employees, makes any warranty, express or implied, or assumes any legal responsibility for the accuracy, completeness, or usefulness of any information, apparatus, product, or process disclosed, or represents that its use would not infringe privately owned rights. Reference herein to any specific commercial product, process, or service by its trade name, trademark, manufacturer, or otherwise, does not necessarily constitute or imply its endorsement, recommendation, or favoring by the United States Government or any agency thereof, or the Regents of the University of California. The views and opinions of authors expressed herein do not necessarily state or reflect those of the United States Government or any agency thereof or the Regents of the University of California.

LBNL-49061

The Synthesis and Evaluation of 2,3-Dihydroxyterephthalamides as Actinide Chelators

Christine Julia Gramer
Ph.D. Thesis

Department of Chemistry
University of California, Berkeley

and

Chemical Sciences Division
Seaborg Center/Actinide Chemistry
Ernest Orlando Lawrence Berkeley National Laboratory
University of California
Berkeley, CA 94720

September 2001

This work was supported by the Director, Office of Science, Office of Basic Energy Sciences, Chemical Sciences Division, of the U.S. Department of Energy under Contract No. DE-AC03-76SF00098.

The Synthesis and Evaluation of 2,3-Dihydroxyterephthalamides as Actinide Chelators

Copyright © 2001

by

Christine Julia Gramer

The U.S. Department of Energy has the right to use this document
for any purpose whatsoever including the right to reproduce
all or any part thereof.

The Synthesis and Evaluation of 2,3-Dihydroxyterephthalamides as Actinide Chelators

by

Christine Julia Gramer

B.A. (New College of the University of South Florida) 1996

A dissertation submitted in partial satisfaction of the requirements for the degree of

Doctor of Philosophy

In

Chemistry

in the

GRADUATE DIVISION

of the

UNIVERSITY OF CALIFORNIA, BERKELEY

Committee in charge:

Professor Kenneth N. Raymond, Chair

Professor Heino Nitsche

Professor Jay D. Keasling

Fall 2001

Abstract

The Synthesis and Evaluation of 2,3-Dihydroxyterephthalamides as Actinide Chelators

by

Christine Julia Gramer

Doctor of Philosophy in Chemistry

University of California, Berkeley

Professor Kenneth N. Raymond, Chair

The 2,3-dihydroxyterephthalamides are characterized as chelators for actinide (IV) ions and are investigated as potential nuclear waste remediation agents. Chapter One details the nuclear waste situation in the United States: the formation of nuclear waste, the reason waste cannot remain in its current state, and current approaches to nuclear waste remediation are covered. The properties of the 2,3-dihydroxyterephthalamides as Fe(III) chelators are reviewed, with a discussion of the reasons these ligands are suitable targets as actinide(IV) chelators.

In Chapter Two the coordination chemistry of the 2,3-dihydroxyterephthalamides with the metal ions Zr(IV), Ce(IV), Th(IV), and Pu(IV) is presented. Crystal structures of Zr(IV) and Th(IV) complexes of a simple terephthalamide illustrate that this ligand can accommodate several different coordination geometries about the metal center. Solution thermodynamic studies of the Th(IV) and Pu(IV) complexes of this ligand

indicate that the terephthalamides have very high stability constants with these metals and are suitable as chelators in solutions with basic pH.

In Chapter Three several terephthalamides are presented that function as liquid-liquid extractants of Fe(III). Two different ligand designs were developed to neutralize the charge on the resulting metal complex: one containing an ammonium for an internal cation, and the other utilizing cetylpyridinium as a lipophilic counter cation. The constants for Fe(III) extraction with each were determined. A water-soluble version of one of these ligands incorporates one amine into each side chain and has a higher formation constant with Fe(III) than any previously examined terephthalamide. Parallels between the aqueous formation constants and extraction constants are discussed.

In Chapter Four a shorter synthetic route to the terephthalamides is presented. The route avoids the protection and deprotection of the catecholate oxygens, reducing the time, cost, and hazards associated with the typical synthesis. This method is particularly useful for synthesis of the liquid-liquid extractants discussed in Chapter Three.

In Chapter Five the incorporation of the terephthalamides into a new separation procedure is discussed. The water-soluble polymer polyethyleneimine was functionalized with terephthalamides to produce a water-soluble chelating polymer, and this was used in conjunction with a size-exclusion membrane to remove dilute concentrations of Pu(IV) from aqueous solutions.

Dedication

To my parents Irene and Harold

and my brother Robert

for all of their love and support

Acknowledgements

As my time at Berkeley comes to an end, I am realizing that no matter how hard the scientific writing is, no one tells you that writing this acknowledgement section takes as much time and revision as any one chapter! It's not a matter of trying to remember all of the people with whom I have interacted, but rather every time I sit down to put my thoughts into words I find my mind wandering to the deep feelings of gratitude I have for everyone who has shaped me professionally or personally. Graduate school at Berkeley has been an amazing learning experience so I am going to do my best to acknowledge all of the people who have been a part of it.

First, I want to thank my family for all of their love and support. My parents Irene and Harold have always been an amazing source of support, teaching me about everything from a young age, and encouraging me to do my best while having fun in whatever endeavor I choose. My younger (but not little!) brother Robert is the best brother I could possibly have and no one in the world is special to me in the way he is. My Aunt Wanda, Grandma Julie, Grandpa Pop, Grandma Gisela, and Great-grandma Marie and the rest of my extended family have my gratitude for all of the support they have given to me over the years. I love you all very much.

Next, I must thank my advisor Ken Raymond. This research project covered many areas of chemistry and I have greatly enjoyed the latitude Ken allows in pursing all of these directions. I am also very grateful for the many opportunities that Ken facilitated which I could not have otherwise had– in particular "playing with Plutonium" at

Lawrence Berkeley National Lab, the 3 trips I made to Los Alamos National Lab to do Pu experiments with ligands that I had synthesized, and the many conferences I attended.

All of the researchers who have been a part of the Raymond Group while I have been here have been instrumental in teaching me how to do chemistry research and making sure I take enough beer and coffee breaks. Several of you really stand out as wonderful friends of mine – Dana Caulder (my partner in crime - if anyone has to ask why then they clearly don't know us), Ses Cohen, Carmen Barnes, Christian Bruckner, Lovedog Nicole Wieland, Sharad Hajela (are you opening a bottle of wine to celebrate?), Chris Sunderland (are you opening a second bottle?), Adam "Horsemouth" Johnson, Jide Xu, Cheers Dan Doble, Brendon O'Sullivan (what a great labmate you are!), Stephane Petoud, Anna Davis, Emily Dertz, and Marco Melchior. My favorite Raymond Group member is Darren Johnson. You are a great chemist to have as a colleague during graduate school but I guess I'll admit that its even better to have you as a boyfriend. LMQTPDJ, YLBSB.

I have worked with scientists at various national labs who have all been so generous with their time and taught me so much even if I was not directly working with them. The plutonium work in chapter 2 was done in the labs of Prof. Heino Nitsche at Lawrence Berkeley National Lab with much help from Dr. Petra Panak, Dr. Dawn Shawnessy, and Rich Wilson. Just accomplishing everything else in the maze of equipment was greatly facilitated by the rest of the actinide group there. The work in chapter 5 was all done in collaboration with people at Los Alamos National Lab - Dr. Gordon Jarvinen, Dr. Norm Schroeder, Dr. Barbara Smith, and Dr. Tom Robison.

I have been lucky to have so many wonderful chemistry mentors before Berkeley. The earliest one is probably Ms. Guiliani who in 5th grade taught me about protons, electrons, and made us memorize the periodic table. She taught us so much about chemistry that I don't think I learned more in high school chemistry than I did in her class. I never would have made it here to begin with if it hadn't been for two outstanding chemistry professors at my undergraduate alma mater New College – Dr. Suzanne Sherman and Dr. Paul Scudder. They deserve so much credit for fostering my interest in chemistry, teaching me the fundamentals, and letting me work in their labs to get my first real taste of experimental chemistry. One older student in particular at New College - Duncan Odom – probably already knows how much I appreciated all of his attention, but I'll say it anyway – thanks Duncan for accepting nothing but the best from me. The summer I spent as an intern at Eli Lilly working in the lab of Dr. Ben Anderson and Nancy Harn was such a great experience. I learned so much about working in industry (those 5 foot tall rotovaps are the best!), my first publication arose from that project, and I am surprised we got anything done since we were laughing so much all the time.

I have made some wonderful friends here at Berkeley who probably deserve the most credit for being supportive and keeping me sane in those really tough times: Dana, Glenn, Jay, Amy, Darren, Smullins, Alex, Nicole, Matt, Nate, Nate, Uncle Ian, Emily, Anna, Marco, and Brendon. Josh, you have been my friend both at New College and Berkeley, and I am so glad that you have been one of my best friends for 9 years now. I am also really grateful to my hometown friends – Kira, Rachel, Amy, and Sally – and all of my New College friends (you know who you are) who provided some much needed distraction several times a year and remind me where I came from.

Table of Contents

Dedication i

Acknowledgements ii

Table of Contents iv

List of Figures viii

List of Schemes xiv

List of Tables xiv

CHAPTER ONE: INTRODUCTION 1

OVERVIEW 1

GENERATION OF NUCLEAR WASTE 2

DESCRIPTION OF THE NUCLEAR WASTE PROBLEM 4

CRITICAL FEATURES OF PU LIGANDS 7

ALTERNATE PLUTONIUM EXTRACTION PROCEDURES 8

BIOMIMETIC APPROACH TO PLUTONIUM SEQUESTERING LIGANDS 12

REFERENCES

CHAPTER TWO: CHARACTERIZATION OF 2,3-DIHYDROXYTEREPHTHALAMIDES AS CHELATORS FOR M(IV) IONS 25

INTRODUCTION 25

SYNTHESIS AND X-RAY CRYSTAL STRUCTURES OF M(IV) - ETAM COMPLEXES 26

STABILITY CONSTANT DETERMINATION FOR TH(IV) ETAM COMPLEX 39

PURIFICATION AND PREPARATION OF ^{239}PU(IV) SOLUTION 45

STABILITY CONSTANT DETERMINATION FOR PU(IV) ETAM COMPLEX 49

CONCLUSION 58

EXPERIMENTAL 58

REFERENCES 64

CHAPTER THREE: THE INVESTIGATION OF 2,3-DIHYDROXYTEREPHTHALAMIDES AS LIQUID-LIQUID EXTRACTANTS OF HIGH OXIDATION STATE METALS 67

INTRODUCTION 67

LIGAND DESIGN AND SYNTHESIS 67

AMINO TAMS – THE EFFECT OF PERIPHERAL CHARGE ON THE STABILITY OF AN FE(III) COMPLEX 73

EXPERIMENT DESIGN FOR FE(III) EXTRACTION 84

EFFECTIVENESS OF AMINO TAMS AS EXTRACTANTS 89

EFFECTIVENESS OF ALKYL TAMS AND LIPOPHILLIC CATIONS AS EXTRACTANTS 98

CONCLUSION 106

EXPERIMENTAL 107

REFERENCES 115

CHAPTER FOUR: A STREAMLINED SYNTHESIS OF 2,3-DIHYDROXYTEREPHTHALAMIDES 119

INTRODUCTION 119

GENERAL OUTLINE FOR A SHORTER SYNTHETIC ROUTE 120

SYNTHESIS OF SYMMETRIC TAMS 121

CHARACTERIZATION OF THE ACID CHLORIDE INTERMEDIATE 122

AN ADAPTED PROCEDURE FOR UNEQUIVALENT AMIDE SUBSTITUTION 126

CONCLUSION 130

EXPERIMENTAL 131

REFERENCES 137

CHAPTER FIVE: THE REMOVAL OF DILUTE CONCENTRATIONS OF PU(IV) FROM AQUEOUS SOLUTIONS USING POLYMER FILTRATION AND 2,3-DIHYDROXYTEREPHTHALAMIDE – FUNCTIONALIZED WATER SOLUBLE POLYMERS 140

INTRODUCTION 140

THE USE OF TAMS IN WATER SOLUBLE CHELATING POLYMERS 144

SYNTHESIS OF TAM – WSCP 146

GENERAL PROCEDURE FOR TESTING WATER SOLUBLE CHELATING POLYMERS FOR METAL UPTAKE 149

PU(IV) UPTAKE RESULTS WITH PST 151

PU(IV) UPTAKE RESULTS WITH PDT 154

CONCLUSIONS AND FUTURE WORK 162

EXPERIMENTAL 162

REFERENCES 168

Appendix 1 170

Appendix 2 211

List of Figures

CHAPTER 1

Figure 1-1. Three industrially important ligands used in solvent extraction procedures for the separation of Pu from other metals. 9

Figure 1-2. Structures of several ligands that have been recently investigated in solvent extraction procedures for Pu(IV) extraction. 12

Figure 1-3. The siderophore enterobactin. 14

Figure 1-4. Catecholamide ligands incorporating carboxylate (CAMC) and sulfonate groups (CAMS). 15

Figure 1-5. Hydogen bonding in the protonated and deprotonated TAMs. 16

Figure 1-6. Speciation diagrams and stability constants for catechol, a catecholamide, and a terephthalamide. 17

CHAPTER 2

Figure 2-7. Structure of ethyl 2,3-dihydroxyterephthalamide (H_2ETAM). 26

Figure 2-8. ^{1}H NMR spectra for Th(IV), Zr(IV), and Ce(IV) complexes of ETAM as well as the protonated ligand H_2ETAM. 28

Figure 2-9. ORTEP of the $[Zr(ETAM)_4]^{4-}$ complex (50% probability) illustrating the non-planar approach of the ligand to the metal center. 30

Figure 2-10. ORTEP of the $[Zr(ETAM)_4]^{4-}$ complex (50% probability) showing the square anti-prismatic coordination geometry. 31

Figure 2-11. The idealized 8-coordinate polyhedra are square anti-prism (D_{4d}), bicapped trigonal prism (C_{2v}), and trigonal dodecahedron (D_{2d}). 32

Figure 2-12. ORTEP of $[Th(ETAM)_4]^{4-}$ (50% probability) and numbering scheme. 34

Figure 2-13. ORTEP (50% probability) of first crystal structure of $[Th(ETAM)_3]_2^{4-}$ 37

Figure 2-14. ORTEP (50% probability) of second crystal structure of $[Th(ETAM)_3]_2^{4-}$ 38

Figure 2-15. Spectra collected in the Th – ETAM titration between pH 3 and 1.5. 41

Figure 2-16. UV-Vis spectra collected during the pH titration of Th – ETAM from pH 2.8 to 10.5. 43

Figure 2-17. Speciation Diagram for the Th(IV) – ETAM system. 44

Figure 2-18. Estimated speciation diagram for the complexation of Th(IV) with a hypothetical octadentate TAM ligand. 45

Figure 2-19. UV-Vis-NIR spectrum of the purified $^{239}Pu(VI)$ stock solution. 47

Figure 2-20. Alpha spectra from the unpurified (above) and purified (below) ^{239}Pu samples. 48

Figure 2-21. Spectra from the titration of Pu – ETAM. 50

Figure 2-22. Structures of common ligands for which Pu(IV) stability constants have been reported. 52

Figure 2-23. Speciation diagram for the Pu – ETAM system. Calculated with $1x10^{-4}$ M H_2ETAM and $1x10^{-5}$ M Pu(IV). 54

Figure 2-24. Estimated speciation diagram for the complexation of Pu(IV) with a hypothetical octadentate TAM ligand. 55

Figure 2-25. Graph of pM vs. pH for the Th(IV) and Pu(IV) ETAM systems. 57

CHAPTER 3

Figure 3-26. Alkyl TAMs form charged complexes with Fe(III) and Pu(IV). Incorporating amines into one side chain or using lipophillic counter cations allows the complex to be extracted into organic solvents. 69

Figure 3-27. AminoTAM ligands which were synthesized as potential metal extractants. 70

Figure 3-28. Structure of the ligand DMETAM, and assignment of stepwise protonation states. 74

Figure 3-29. Spectra from batch titration of DMETAM monitored by ^{1}H NMR spectroscopy. 76

Figure 3-30. Tautomers of H_2L for protonation constant and Fe(III) binding constant discussions. 77

Figure 3-31. Visible spectra from the titration of Fe-DMETAM from pH 3 to 1.5. 78

Figure 3-32. Visible spectra from the Fe-DMETAM titration between pH 3 and 6. 79

Figure 3-33. Speciation Diagram for Fe-DMETAM system. 80

Figure 3-34. Structure of a hexadentate ligand with a TREN backbone. 81

Figure 3-35. X-Ray Structure of $[H_4DMETAM]^{2+}$ $2Br^-$. 82

Figure 3-36. Graph of pFe vs. pH for several ligands. 86

Figure 3-37. UV-Vis spectra of the $CHCl_3$ phases from extractant design #1. 88

Figure 3-38. Nomenclature for the protonation states of ligand design #1. 89

Figure 3-39. Plot of Log $[H_2L]$ vs. Log D for two extraction experiments of Fe(III) with the ligand H_3L^1Br. 91

Figure 3-40. Fraction of Fe(III) present as $Fe(HL^1)_3$ as a function of $[HL^1]$ calculated for two different values of K_{ex}. 94

Figure 3-41. Speciation of Fe(III) in a biphasic system containing tiron in the aqueous phase and L in the organic phase. 96

Figure 3-42. Speciation diagrams for the extraction of Fe(III) in the presence of either NTA or EDTA. 98

Figure 3-43. Plot of Log D vs. Log $[H_2L^2]$ for Fe(III) extraction with constant [cetylpyridinium]. 102

Figure 3-44. Fraction of Fe(III) present as $Fe(L^2)_3$ as a function of $[H_2L^2]$ calculated for three different values of K_{ex}. 103

Figure 3-45. Plot of Log D vs. Log $[py^+]$ for Fe(III) extraction with constant $[H_2L^2]$. 104

Figure 3-46. Fraction of Fe(III) present as $Fe(L^2)_3$ as a function of $[py^+]$ calculated for three different values of K_{ex}. 105

CHAPTER 4

Figure 4-47. Two ligand designs were targeted for the shorter synthetic route based on their success as actinide chelators. 121

Figure 4-48. Acid chlorides 9-11 which also contain phenols have been described in the literature. 123

Figure 4-49. Possible structures of acid chlorides arising from the reaction of 2 with $SOCl_2$. 123

Figure 4-50. ^1H NMR spectra of the reaction of 2 with $SOCl_2$. 125

Figure 4-51. X-Ray crystal structure (ORTEP) of 12. Thermal ellipsoids are drawn at the 50% probability level. 126

Figure 4-52. Possible structures of the acid chloride resulting from the reaction of 14 with $SOCl_2$. 128

Figure 4-53. ^1H NMR spectra (D_6-acetone) following the decomposition of 21 to 20, then 14. 129

CHAPTER 5

Figure 5-54. Schematic of the principle of ultrafiltration. 141

Figure 5-55. Polyethyleneimine (PEI) is a water soluble polymer with primary amines that can be functionalized with metal-specific ligands. 142

Figure 5-56. Diagram of the Polymer Filtration process. 143

Figure 5-57. Structure of PEIP, the ligand currently in use at LANL for Pu polymer filtration. 144

Figure 5-58. Possible side chains for TAMs attached to PEI. 146

Figure 5-59. The general procedure for testing Water Soluble Chelating Polymers for metal uptake. 150

Figure 5-60. Graph of D vs. pH for the uptake of Pu(IV) by PST. 152

Figure 5-61. Graph of D vs. pH for Am(III) uptake by PST compared to Pu(IV) uptake 153

Figure 5-62. The graph of D vs. pH for the uptake of Pu(IV) by PDT. 155

Figure 5-63. A comparision of Am(III) and Pu(IV) uptake by PDT is shown in the plot of D vs. pH. 157

Figure 5-64. The graph of D vs. pH shows no difference in D for Pu(IV) uptake as the concentration of PDT varies from 0.1% to 0.001%. 158

Figure 5-65. The graph of D vs. pH for the uptake of Pu(III) in the presence of HAN compared with Am(III) and Pu(IV). 160

Figure 5-66. The graph on top shows the decrease of cpm over time of a basic Pu(IV) solution. The graph on the bottom illustrates the recovery of the cpm when PDT is added after four hours. 161

List of Schemes

Scheme 1-1. Sr-90 and Cs-137 result from the decay of the fission products Br-90 and Te-137 produced when U-235 is bombarded with neutrons to produce Pu. 3

Scheme 2-2. Synthesis of M(IV) – ETAM complexes. 27

Scheme 3-3. Synthetic scheme for the TAMs. 72

Scheme 4-4. The typical TAM synthesis requires protection and deprotection of the catecholate oxygens. 120

Scheme 4-5. The shorter synthesis described here obviates the need for protecting groups and symmetric TAMs can be easily synthesized in one step. 122

Scheme 4-6. The procedure was modified so a TAM with two different amides could be prepared. 127

Scheme 5-7. Synthetic scheme for PDT and PST. 148

List of Tables

Table 1-1. Chart of charge/size ratio for selected tetravalent metals and Fe(III). 20

Table 2-2. Formation constants and hydrolysis constants for the complexation of Th(IV) and Pu(IV) by ETAM. 51

Table 2-3. Stability constants for some common ligands with Pu(IV). 53

Table 3-4. Summary of the Fe(III) stability constants for DMETAM, ETAM and taurTAM. 83

CHAPTER ONE

Introduction

Overview

During the last 60 years the power of the radioactive actinides has been harnessed for both its destructive potential in the form of nuclear weapons and for constructive use as an alternative to fossil fuels. The urgency of weapons development for World War II fueled the need for pure sources of uranium and plutonium, overshadowing the impending need for safe nuclear waste disposal. The majority of the nuclear waste in the United States is the result of actinide purification for nuclear weapons development ("legacy waste"), while a smaller amount is attributable to spent fuel rods from nuclear power plants. [1]

It has become increasingly important that the nuclear waste is treated and stored in a safe manner. Under the auspices of the Department of Energy, waste disposal factors under investigation include identification of the components and characterization of their speciation, separation of the radioactive ions, environmental migration of radionuclides, and finally safe long-term storage options. [1] The ultimate goal of nuclear waste remediation is segregation of the radioactive and non-radioactive components and immobilization of the radioactive materials in a stable form to minimize the cost and hazards associated with storing large volumes of liquid radioactive waste. [1-3]

This thesis deals with one aspect of waste remediation– the selective removal of plutonium from liquid waste. The half-life of Pu-238 is 24,000 years, thus even with the removal of other radioactive metals, the large volumes of waste solutions will persist as a

highly radioactive material for a quarter of a million years. This approach employed here is the investigation of selective chelators for plutonium, based on naturally occurring catecholamide chelators; the development of an economically feasible synthetic route to these ligands; and their application in two different separation processes. This chapter will present the larger background of the nuclear waste problem and other chelators that have been investigated in the capacity for plutonium separation. The facts about the generation and the current status of nuclear waste have been summarized in several thorough publications and are the source for most of the information presented here.[1-6]

Generation of Nuclear Waste

Nuclear waste can generally be classified into two types – defense waste, also called legacy waste, from nuclear weapons development, and commercial waste consisting of spent fuel rods from nuclear power plants. Commercial waste is stored as the entire fuel rod – including the radioactive U-235, U-238, Pu by-products, and metal container – covered in a pool of water. Reprocessing the fuel so the U and Pu can be recovered and reused was the initial plan of the nuclear fuel industry in the 1970's. The benefits of reprocessing have been under debate for the last 30 years, and currently the fuel rods are not reprocessed.

The defense waste is far less simple in composition and is the by-product of plutonium purification. Irradiating many tons of U-238 produces Pu-239 and radioactive fission products, and these small concentrations of Pu (250 ppm) had to be separated and purified to 99.5% purity. Br-90 and Te-137 are the two initial fission products that

quickly decay to the long-lived radioactive fission products Cs-137 and Sr-90 (Scheme 1-1).

$$^{90}_{35}Br \xrightarrow[1.9s]{} {}^{90}_{36}Kr \xrightarrow[32.3s]{} {}^{90}_{37}Rb \xrightarrow[2.6m]{} {}^{90}_{38}Sr \xrightarrow[29.1y]{} {}^{90}_{39}Y \xrightarrow[2.67d]{} {}^{90}_{40}Zr \text{ (stable)}$$

$$^{137}_{52}Te \xrightarrow[2.5s]{} {}^{137}_{53}I \xrightarrow[24.5s]{} {}^{137}_{54}Xe \xrightarrow[3.82m]{} {}^{137}_{55}Cs \xrightarrow[30.3y]{} {}^{137}_{56}Ba \text{ (stable)}$$

Scheme 1-1. Sr-90 and Cs-137 result from the decay of the fission products Br-90 and Te-137 produced when U-235 is bombarded with neutrons to produce Pu.

The plutonium purification procedure involves the selective precipitation of the different oxidation states of Pu, U, Np, and the fission products Cs and Sr. The irradiated U is dissolved in 6M acid and Pu(III), Pu(IV), Cs, and Sr are precipitated with $Bi(PO_4)$ while UO_2^{2+} remains in solution. The Pu(III) is oxidized to Pu(IV) and separated from NpO^{2+} and the fission products by precipitation with LaF_3. This procedure generates large volumes of liquid radioactive waste and sludge and is part of the original source of nuclear waste.

The precipitation procedure was later replaced by a solvent extraction procedure in which a lipophilic ligand coordinates to the metal and transfers it to an organic phase.[7] This is called the PUREX process - Plutonium Uranium Reduction Extraction – and was developed 40 years ago. This process uses 30% tributyl phosphate (TBP) in kerosene to extract $M^{4+}(NO_3)_4 \cdot 2TBP$. In this process, TBP replaces coordinated water molecules to increase the hydrophobicity of the complex and nitrate is coextracted to neutralize the charge. Metal extraction selectivity is seen because the ligand prefers a metal with a

higher effective charge. For a given actinide, the preference is M(IV) > MO_2^{2+} > > M(III) > MO_2^{+}; among metals of the same oxidation state, the preference is for the smaller metal. Separation is achieved by chemical adjustment of the oxidation states, and selective extraction of the actinide. The PUREX process is no longer used because it generates large amounts of waste – the purification one kilogram of Pu results in 340 gallons of high level waste 55,000 gallons of low- to intermediate- level waste and 2.5 million gallons of cooling water.

Description of the Nuclear Waste Problem

Legacy wastes are primarily stored in two locations in the United States – Hanford, Wa and Savannah River, S.C. The liquid waste is contained in underground carbon steel tanks, which hold up to 1.3 million gallons; the Hanford site has 177 of these while Savannah River has 51 tanks. Hanford has 244,000 cubic meters of waste containing 4.46×10^8 Curies and Savannah River has 128,000 cubic meters of waste containing 6.61×10^8 Curies (1 Curie = 3.7×10^{10} disintegrations per second).

Generally the waste is non-homogeneous because it was not stored in its original acidic conditions; NaOH was added to prevent corrosion of the tank walls. This causes large amounts of a metal hydroxide sludge precipitate containing most of the actinides and the $Sr^{2+}$to form on the bottom of the tank. The liquid layer ("supernate"), containing the majority of the Cs^{+} and low quantities of actinides, covers the sludge. Evaporation of the liquid has resulted in the formation of a solid crust, with a composition similar to the supernate, which sits on top of the liquid.

The lack of a predetermined waste remediation procedure and lack of documentation of other material added has resulted in an ill-defined description of the speciation of the radioactive and non-radioactive material in the tanks. For example, NaOH was not added to all of the tanks. Several of the tanks have been used as experimental vessels into which a variety of organic material has been added with the aim of selectively precipitating certain radioactive ions. For instance, tetraphenylborate and ferrocyanide have been added to some tanks to precipitate cesium. However, some of the tetraphenylborate has decomposed due to the elevated temperatures generated by radioactive decay, catalysis by Cu^{2+}, and radiolytic cleavage, which has subsequently resulted in production of high levels of benzene and hydrogen gas. The composition of organic material and pH can vary from top to bottom and side to side in these large tanks, thus further complicating the speciation of the radioactive metal ions.

The waste cannot remain in its current state for several reasons. The current waste form is not secure, and poses hazards to the public. Many of the tanks at Hanford (67 of 177) are known or suspected to have cracks which have allowed at least 750,000 gallons of waste to seep into the ground. The migration of the actinides through the soil and into the ground water has reached the Columbia River, a major source of drinking water. Another safety concern is the threat of fire or explosions. Although the tanks are vented the evolution of benzene, hydrogen, and nitrous oxide gas mentioned above is a major fire hazard, because the gas can build up under the crust before being released when the supernate and crust turn over. While there is no ignition source for a fire, the high temperatures in the tanks resulting from radioactive decay could accelerate potentially explosive reactions. It is unknown if the complex mixture of organic,

inorganic, oxidizing, and reducing materials present could react exothermically to produce an explosion.

All disposal options that are currently being investigated involve eventual immobilization of all radioactive material in a solid matrix. The current disposal strategy (which is not necessarily the best or final method) starts with the separation of the sludge layer. This is combined with melted glass and cooled into the shape of a log ("vitrification"), sealed in a stainless steel tube, and stored in a geological repository. The saltcake is redissolved into the supernate with water. Sr^{2+} and the actinides are removed from the Cs^{+} in the supernate by sorption with mono-sodium titanate. This solid is filtered and vitrified. The Cs^{+} would be removed by either precipitation with tetraphenyl borate, ion-exchange, or solvent extraction.

The procedure outlined above is not necessarily finalized by the DOE. For instance, the precipitation of Cs^{+} with tetraphenylborate was recently halted – even though a half billion dollars have been spent on it – when it was realized that the evolution of benzene was occurring at a greater than anticipated rate. This led to an independent review sponsored by the National Research Council to suggest the best manner in which to deal with the Cs^{+} separation issue. [3] Another major concern is the co-disposal of the actinides and Sr^{2+}. The half-lives are approximately 30 years for Cs^{+} and Sr^{2+} and 24,000 years for Pu-238, and radioactive materials are considered completely decayed after 10 half-lives. Cs^{+} and Sr^{2+} thus need secure storage for 300 years, while Pu requires a quarter-million years. The co-vitrification of Sr^{2+} with Pu will result in a larger volume of waste that will be radioactive for a long period of time. Alternatively,

recovery of the Pu would circumvent the problems associated with long-term storage of such a long-lived isotope.

The knowledge about actinide sequestering agents is fairly limited and a recent comprehensive review summarized the field of Pu(IV) chelators. [8] A better understanding of actinide coordination chemistry would facilitate the development of ligands targeted for separating the short-lived and long-lived isotopes to reduce the volume and cost of waste disposal. The applications for such chelators can be broader and are not limited to nuclear weapons legacy waste. For instance the treatment of waste streams from Pu purification processes, Pu reprocessing from spent nuclear fuel cells, or the development of mammalian plutonium decorporation agents for humans who are exposed to Pu would all benefit from a wider range of plutonium chelating agents.

Critical Features of Pu ligands

Understanding the basic aqueous chemistry of plutonium is essential to developing effective chelators. Plutonium can simultaneously exist in 4 different oxidation states – Pu(III), Pu(IV), PuO_2^+, and PuO_2^{2+}, although Pu(IV) is the one thought to be most prevalent in tank waste. [9,10] Pu(IV) hydrolyzes, forms colloids, and precipitates as the hydroxide above pH 2. One of the difficulties of determining formation constants for ligands with Pu(IV) is the ease with which Pu(IV) undergoes these reactions. Since many different tank conditions can be encountered, the ability of a ligand to form a stable Pu complex over large pH range is desirable. The ligand must show selectivity for Pu(IV) over other metals (Am^{3+}, Na^+, Mg^{2+}, Zn^{2+}, Fe^{2+}, Fe^{3+}, Ce^{3+}) that may be present in tank waste. The ligand must be able to chelate Pu(IV) in the

presence of other ligands that may be present (halides, carbonate, nitrates, citrate, acetate). Since Pu prefers coordination number 8, the geometry of the ligand should be flexible to allow the coordination sphere to adopt a square antiprism or bicapped trigonal prism. Finally, the HSAB principal dictates that the "hard" cation Pu(IV) would prefer oxygen donors to other atoms.

Alternate Plutonium Extraction Procedures

PUREX was the initial solvent extraction procedure developed for actinide separation, but the large volumes of waste generated has prompted the development of new ligands for solvent extraction which would hopefully decrease the waste volume. The structures of several industrially important ligands are shown in Figure 1-1. For Pu reprocessing the spent fuel rods are first dissolved in strongly acidic solutions so the ligands developed had to be effective Pu ligands in high concentrations of H^+. Features of the PUREX process are true for several extraction processes – the extractant is neutral, thus nitrate is coextracted to neutralize the charge, and selectivity is based on charge density.

The TRUEX process– Trans Uranic Extraction – was developed as an alternative to the PUREX process. [11] The bifunctional extractant octyl(phenyl)-N,N-diisobutylcarbamoyl methyl phosphine oxide (CMPO) used in conjunction with TBP is the basis for the TRUEX process. TBP is not effective at extracting transition metals (M^{2+} and M^{3+}) or lanthanides (Ln^{3+}) while being highly efficient and selective for Pu(IV); CMPO is more efficient at extracting Pu(IV), but the selectivity is limited because it is also efficient for trivalent actinides. Thus the TRUEX process is good for all-purpose

actinide extraction. Another benefit to TRUEX is that no third phase is formed, as can happen in PUREX.

An industrially important process that is currently being developed in France for actinide processing is DIAMEX – DIAMide EXtraction. This process was developed for diamides[12-14] – in particular the malonamide N,N'-dimethyl-N,N'-dibutyltetradecylmalonamide (DMDBTDMA) as the chelating ligand. The advantage of using a ligand which is composed only of C, H, O, and N is that the ligand is totally combusible and no phosphate or sulfate by-products are formed upon incineration. This ligand is able to extract the tetra- and tri-valent actinides and is being considered as a replacement for the PUREX process in France.

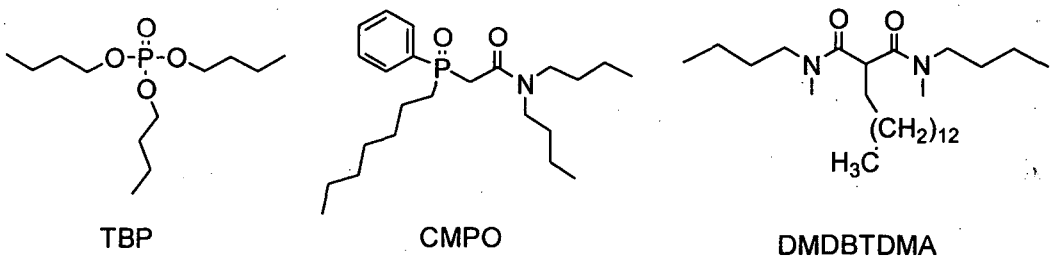

Figure 1-1. Three industrially important ligands used in solvent extraction procedures for the separation of Pu from other metals.

On the laboratory scale, several other classes of ligands are being investigated as extractants (Figure 1-2). [15] A variation on the diamides – the isoxazolones – have recently been investigated for Pu(IV) and Am(III) extraction. [15,16] In particular, 3-phenyl-4-benzoyl-5-isoxazolone (**1**) is particularly promising for acidic waste. Extraction of Pu and U is quantitative from 1 – 6 M HNO_3, however Am(III) is only extracted in solutions of 1 – 2 M HNO_3. The extracted complex is similar to that of the TRUEX

process in that the addition of tri-octyl phosphine oxide, to replace coordinated water molecules, facilitated the extraction.

Although crown ethers are more commonly used as extractants for Cs^+ and Sr^{2+}, they are also effective at extracting Pu(IV) from nitric acid. [17-23] The derivatives that have been most investigated have either 5 or 6 oxygens in the crown and benzyl or cyclohexyl substituents. For example, dicyclohexyl-18-crown-6 extracts Pu(IV) over $UO_2^{2+}$with a stoichiometry of $Pu(DC18C6)_2 \cdot 4NO_3^-$ and an overall formation constant of $10^{5.34}$.

Recently, several research groups have employed calixarenes as a hydrophobic backbone to which ligating groups and hydrophobic substituents are easily attached. Since CMPO is such an efficient actinide chelator, calixarene derivatives with CMPO appended have been extensively investigated. [24] In a series of 13 calix-CMPO derivatives (**2**) , almost all showed higher efficiency for Th(IV) and Pu(IV) extraction than CMPO itself with over 99% extraction of these metals from 1M nitric acid.

Several other attachments to the calixarene backbone have been presented by the Gopalan Group. The ligands investigated include CMPO[25] (**3**) (attached in a different manner than above), acetates (**6**), and hydroxamic acids[26,27] (**4, 5**). In the case of the CMPO derivative, the extraction was only studied at pH 0.33. However, this ligand afforded 90% extraction of Th(IV), which is more efficient than **2** at this pH. The acetate and hydroxamate derivatives were studied at slightly higher pH since these protic ligands are not expected to work as well at the lower pH. In this case Fe(III) was also examined and although all were efficient at pH 2 and 3, the ligands did not show particular selectivity for the tetravalent metal. For example, the hydroxamic acid **3** at pH 2

extracted 95% of the Th(IV) and 99% of the Fe(III). In all cases, the acetate ligand was not as efficient as the hydroxamate ligand, exhibiting only 6% extraction of Th(IV) at pH 2.

Hydroxypyridinone (HOPO) ligands, aromatic versions of hydroxamic acids, have also been investigated. Two examples of octadentate HOPOs, with the carboxylate and the hydroxy in the 2 and 3 positions, respectively, have been prepared with a calixarene scaffold (**7**,**8**).[28] A bidentate isomer with the carboxylate and hydroxy groups in the 2 and 1 positions, respectively, was prepared with an octylamide (**9**) for organic solubility.[29] At pHs 0, 1, and 2, ligands **7** and **8** were much more efficient at Pu(IV) extraction than the corresponding hydroxamic acids, and at low pH were much more selective for Th(IV) over Fe(III). At pH 0, **7** and **8** exhibited 88 and 98% extraction, respectively of Th(IV) and only 29 and 26% extraction of Fe(III). In the case of the bidentate **9**, the extraction of Pu(IV) at pH 0 was 95%, and the extraction was efficient over a range of nitric acid concentrations of 0.1 M to 11 M.

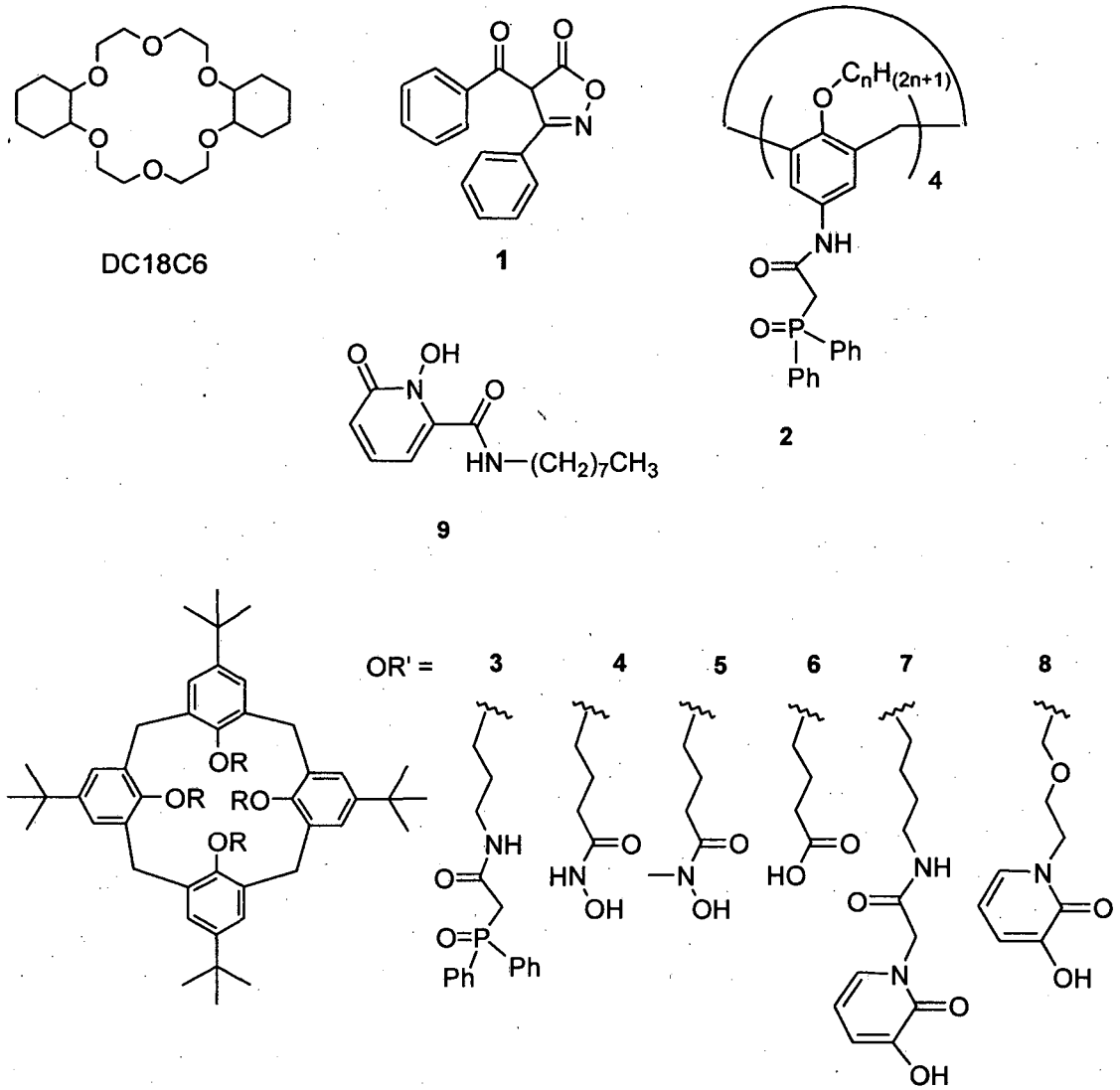

Figure 1-2. Structures of several ligands that have been recently investigated in solvent extraction procedures for Pu(IV) extraction.

Biomimetic Approach to Plutonium Sequestering Ligands

A biomimetic approach to the development of a Pu(IV)-specific chelator has been adopted based on the similarities between Fe(III) and Pu(IV) and the wealth of knowledge about naturally occurring Fe(III)-specific chelators. [30-34] The similarities between Fe(III) and Pu(IV) arise because they are both "hard" cations with high charge to

radius ratio. This is manifested in the low solubility both have at neutral pH (10^{-18} and 10^{-22}, for Fe(III) and Pu(IV), respectively) and the observation that in mammals contaminated with Pu(IV), the Pu(IV) will bind to the Fe(III) sites of the iron-transport protein transferrin.

The siderophores are a class of bacterially-secreted ligands whose function is to retrieve Fe(III) from the environment and deliver it back to the cell. [35] The low solubility of Fe(III) at neutral pH requires that a chelator has a high enough formation constant in order to solubilize Fe(III) upon chelation with the siderophore. The archetype of siderophores is enterobactin which consists of three catechol groups attached by amides to a tri-lactone backbone (Figure 1-3). The overall formation constant for the $Fe(ent)^{3-}$ complex is 10^{49} – the highest known for any ligand with Fe(III). [36] The high stability is largely attributed to the catecholamide which binds the metal through the 6 oxygen atoms of the catechol but is also due to the preorganization imparted by the chiral tri-lactone backbone, which forces all of the catecholamide groups to lie on the same side of the backbone. The electron-withdrawing amides also serve to lower the pKas of the protons such that the ligand is partially deprotonated at neutral pH.

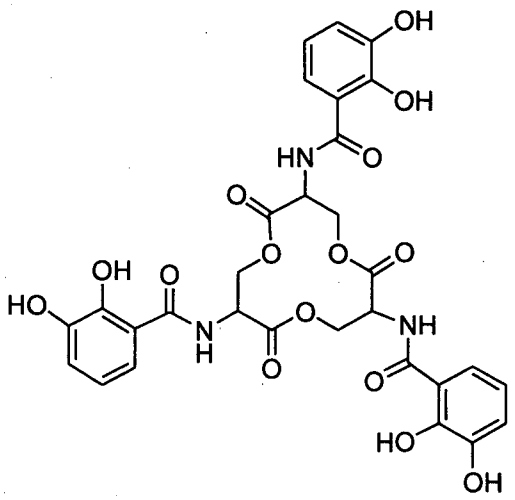

Figure 1-3. The siderophore enterobactin has the highest known formation constant for any ligand with Fe(III), mainly due to the 3 catecholamides which bind Fe(III).

The hypothesis that Pu(IV) is similar to Fe(III) and therefore should be strongly bound by the same ligands is supported by other examples of catecholates from the Raymond Group. The earliest studies of the catecholate anion showed that it formed stable $[ML_4]^{4-}$ complexes with the Pu(IV) analogs Th(IV), U(IV), Ce(IV), and Hf(IV). [37,38] This work showed that the $[Ce(cat)_4]^{4-}$ complex exists not as a Ce(III)semiquinone-triscatechol complex, but as the Ce(IV)tetracatechol. The electrochemical determination of the Ce(III)/Ce(IV) couple when coordinated by catechol indicated that the Ce(IV) complex is 36 orders of magnitude more stable than the Ce(III) tetracatechol complex. Later studies conducted with octadentate catecholamides that include a sulfonate in the 4-position (CAMS), or a carboxylate in the 6-position (CAMC) (Figure 1-4) indicated that these functionalized catecholates are also strong ligands for Pu(IV) and Ce(IV). [39] These results facilitated the development of several multidentate catecholate and

hydroxypyridinone ligands that proved to be effective at removing Pu(IV) and Am(III) from mice. [34,40]

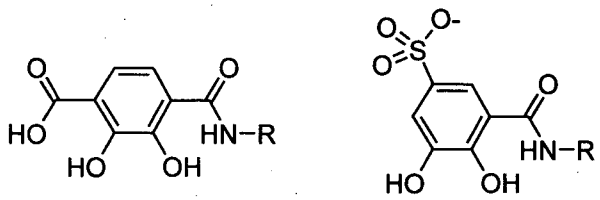

Figure 1-4. Catecholamide ligands incorporating carboxylate (CAMC) and sulfonate groups (CAMS) have been investigated as actinide chelators.

The use of electron withdrawing groups is not limited to a single amide. Catechol derivatives incorporating two amides – the 2,3-dihydroxyterephthalamides – are also excellent Fe(III) chelators (Figure 1-6). [41] The benefit of having two amides is most notable in the lowering of the catecholate pKas without a similar decrease in Fe(III) affinity. The pKas for catechol are 9 and 13, for the CAM they are 8 and 12, while the TAMs have pKas of 6 and 11. [42,43] The overall formation constants for $[Fe(cat)_3]^{3-}$, $[Fe(CAM)_3]^{3-}$, and $[Fe(TAM)_3]^{3-}$ complexes are $10^{43.8}$, $10^{43.7}$, and $10^{42.7}$, respectively. The lower pKas of the TAMs result in a ligand that is available to bind the metal at lower pH values – the TAM complex is fully formed by pH 5, while the CAM complex doesn't fully form until pH 7 and the tris-catechol complex is fully formed at pH 9. The complexation of Fe(III) at lower pH values by the TAMs is also reflected in the pM values. pM is the negative log of the free Fe(III) concentration calculated at a given pH. At every pH the TAMs have a higher pM value than the other two ligands, meaning that there is a lower concentration of free Fe(III) in solution. Several other benefits are gained from the electron withdrawing amides – the ligand is more resistant to oxidation and two

amide sites allow for the functionalization of the ligand to suit whatever purpose is required. Another important feature of these ligands is the internal hydrogen bonding. When the ligand is bound to a metal, a hydrogen bond is formed between the amide hydrogen and the deprotonated, coordinated catecholate oxygen (Figure 1-5). [44] This is seen in all CAMs and TAMs and serves to stabilize the complex by ~1.2 Kcal/mol/hydrogen bond. [45]

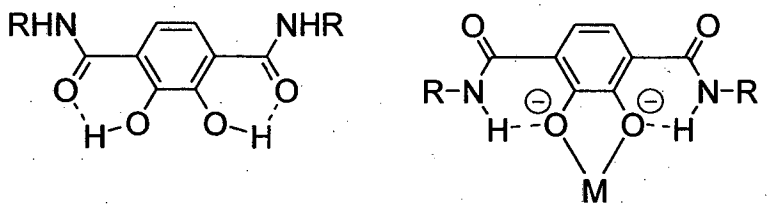

Figure 1-5. Hydogen bonding in the protonated and deprotonated TAMs.

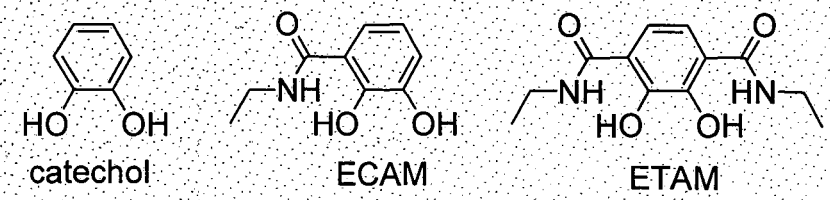

	catechol	ECAM	ETAM
pK_a1	13.0	12.1	11.1
pK_a2	9.2	7.34	6.1
$\log \beta_3$	43.8	43.7	42.7
pM	15.7	19.7	22.8

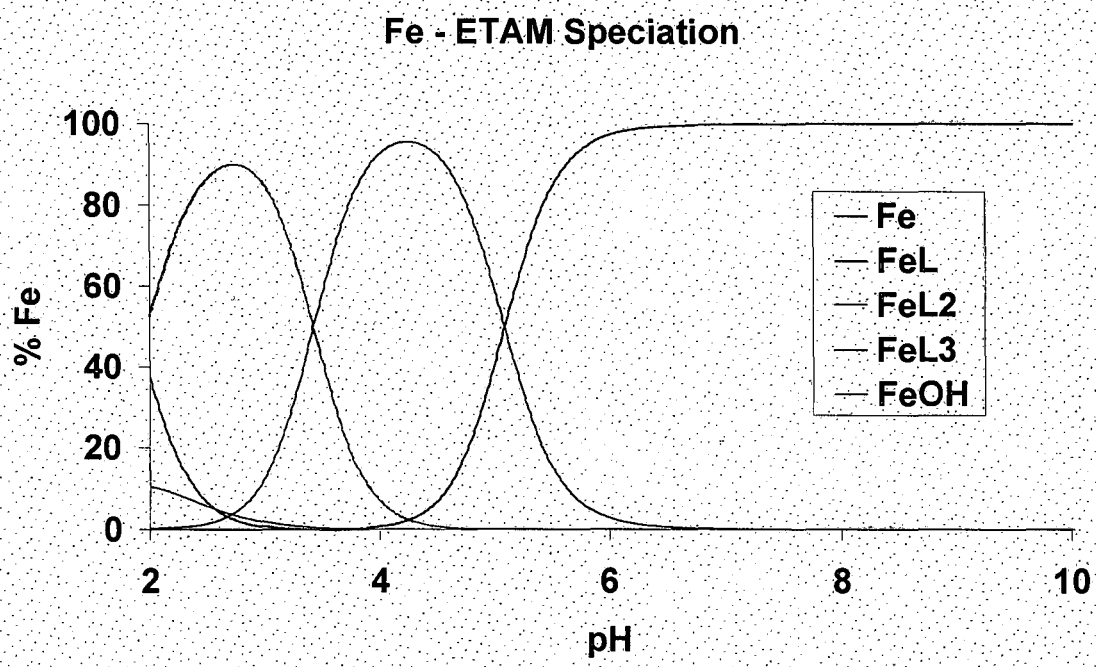

Figure 1-6. Speciation diagrams and stability constants for catechol, a catecholamide, and a terephthalamide illustrate the pH region in which these are effective Fe(III) chelators.

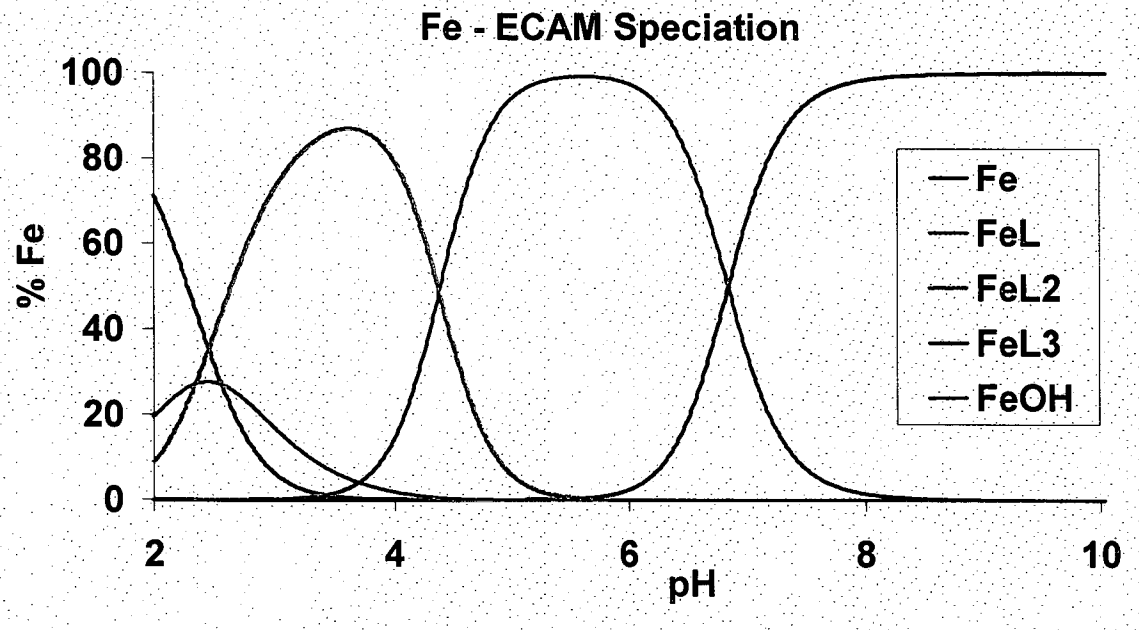
Fe - ECAM Speciation
100
80
60
40
20
0
% Fe
2
4
6
8
10
pH
Fe
FeL
FeL2
FeL3
FeOH

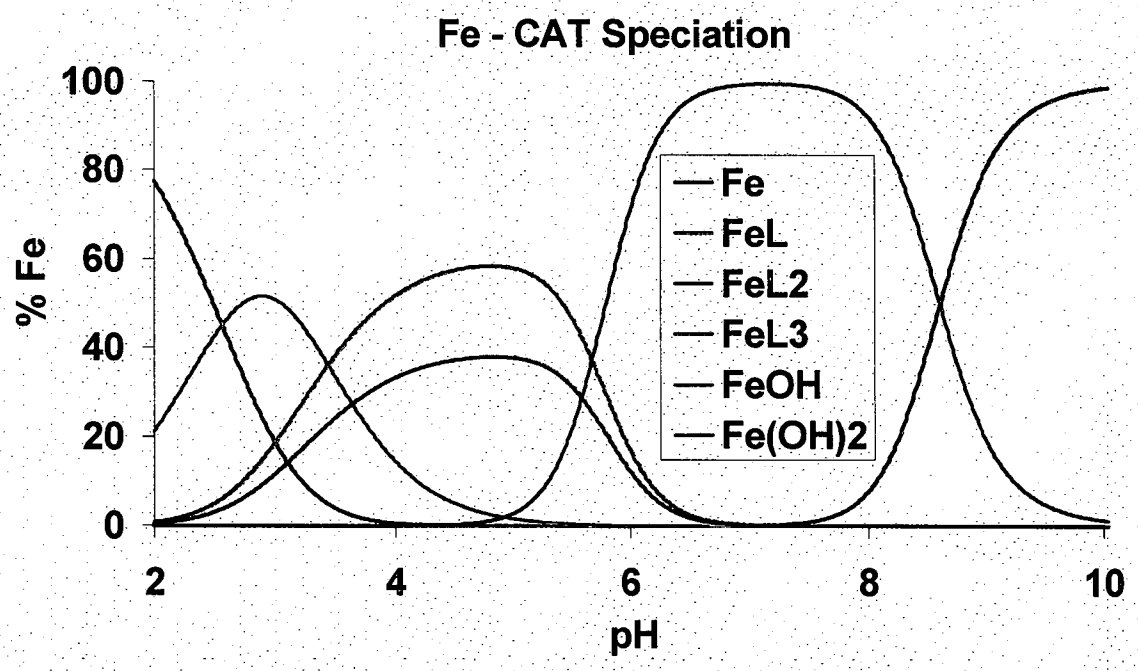
Fe - CAT Speciation
100
80
60
40
20
0
% Fe
2
4
6
8
10
pH
Fe
FeL
FeL2
FeL3
FeOH
Fe(OH)2

The goal of this Ph.D. project is to investigate new chelators for plutonium and develop separation agents that can be incorporated into well-established procedures like liquid-liquid extraction. The most important issues to address are how to chelate plutonium in strongly basic solutions (where hydroxides are easily formed) and how to remove the dilute concentrations of Pu that remain in the waste stream. The previously discussed ligands were developed for acidic waste solutions and are not well suited for the basic conditions of tank waste. The high formation constants that are expected for the actinide – TAM complexes make these ligands well suited for studies in basic solutions and with dilute concentrations of plutonium.

The work presented in this dissertation seeks to characterize the TAMs as actinide chelators and to apply the TAMs as liquid-liquid extractants. Chapter 2 presents the coordination chemistry of the TAMs with Pu(IV) and other tetravalent metal analogs (Table 1-1). Crystal structures of TAM ligands with the actinide analogs Th(IV) and Zr(IV) are presented along with the solution thermodynamic studies of TAM complexes with Th(IV) and Pu(IV). Chapter 3 presents the development of TAMs as liquid-liquid extractants. Two different ligand designs were found that effected the extraction of Fe(III) and Pu(IV) into an organic solvent. The extraction constants for these two methods were determined and the effectiveness of each evaluated. Chapter 4 presents a shorter synthetic route to the TAMs that avoids the protection of the catecholate oxygens required in the typical TAM synthesis. This route decreases the time and cost of synthesizing TAMs so they are more economically feasible extractants. Chapter 5 presents work done in collaboration with researchers at Los Alamos National Lab incorporating TAMs into a polymer-based separation process. The procedure relies on

the water-soluble polymer polyethyleneimine appended with TAM ligands, and a size exclusion membrane. When used in combination, Pu is chelated by the TAM and separated from the waste stream by the size exclusion membrane.

Metal	Radius (Å)	Charge/size ratio
Pu(IV)	0.96	4.2
Ce(IV)	0.92	4.3
Th(IV)	1.05	3.8
Zr(IV)	0.84	4.8
Hf(IV)	0.83	4.8
Fe(III)	0.65	4.6

ref: [46]

Table 1-1. Chart of charge/size ratio for selected tetravalent metals and Fe(III).

References

(1) U. S. Congress, Office of Technology Assesment, *Long-Lived Legacy: Managing High-Level and Transuranic Waste at the DOE Nuclear Weapons Complex*, OTA-BP-O-83 (U.S. Government Printing Office: Washington, D.C., May 1991).

(2) Murray, R. L. *Understanding Radioactive Waste*; 4 ed.; Battelle Press:, 1994.

(3) *Alternatives for High-Level Waste Salt Processing at the Savannah River Site*; National Academy Press: Washington, D.C., 2000.

(4) Hileman, B. In *Chemical and Engineering News*, 1996; pp 14-20.

(5) Levi, B. G. In *Physics Today*, 1992; pp 17-21.

(6) Choppin, G. R.; Wong, P. J. *J Radioanal Nucl Chem Art* **1995**, *203*, 575-590.

(7) Mathur, J. N.; Murali, M. S.; Nash, K. L. *Solvent Extr Ion Exch* **2001**, *19*, 357-390.

(8) Oboyle, N. C.; Nicholson, G. P.; Piper, T. J.; Taylor, D. M.; Williams, D. R.; Williams, G. *Appl Radiat Isotopes* **1997**, *48*, 183-200.

(9) Silva, R. J.; Nitsche, H. *Radiochim Acta* **1995**, *70-1*, 377-396.

(10) Cleveland, J. M. *The Chemistry of Plutonium*; Gordon and Breach Scientific Publishers:, 1970.

(11) Horwitz, E. P.; Kalina, D. G.; Diamond, H.; Vandegrift, G. F. *Solvent Extr. Ion Exch.* **1985**, *3*, 75-109.

(12) Ardois, C.; Mokili, M. B.; Musikas, C.; Abbe, J. C. *J Radioanal Nucl Chem* **1999**, *240*, 751-761.

(13) Courson, O.; Lebrun, M.; Malmbeck, R.; Pagliosa, G.; Romer, K.; Satmark, B.; Glatz, J. P. *Radiochim Acta* **2000**, *88*, 857-863.

(14) Spjuth, L.; Liljenzin, J. O.; Hudson, M. J.; Drew, M. G. B.; Iveson, P. B.; Madic, C. *Solvent Extr Ion Exch* **2000**, *18*, 1-23.

(15) Manchanda, V. K.; Mohapatra, P. K. *Radiochim Acta* **1993**, *60*, 185-188.

(16) Manchanda, V. K.; Mohapatra, P. K.; Veeraraghavan, R. *Anal Chim Acta* **1996**, *320*, 151-154.

(17) Du, H. S.; Wood, D. J.; Elshani, S.; Wai, C. M. *Talanta* **1993**, *40*, 173-177.

(18) Mohapatra, P. K.; Manchanda, V. K. *J Inclusion Phenom Mol Recogn* **1996**, *25*, 257-265.

(19) Shukla, J. P.; Singh, R. K.; Kumar, A. *Radiochim Acta* **1991**, *54*, 73-77.

(20) Yonezawa, C.; Choppin, G. R. *J Radioanal Nucl Chem Art* **1989**, *134*, 233-239.

(21) Bartsch, R. A., Ed. *Metal Ion Separation with Proton-Ionizable Lariat Ethers*; American Chemical Society: Washington, D.C., 1999; Vol. 716.

(22) Sachleben, R. A.; Moyer, B. A.; Case, F. I.; Garmon, S. A. *Separ Sci Technol* **1993**, *28*, 1-23.

(23) Shukla, J. P.; Kumar, A.; Singh, R. K. *Radiochim Acta* **1993**, *60*, 103-107.

(24) Arnaud-Neu, F.; Bohmer, V.; Dozol, J. F.; Gruttner, C.; Jakobi, R. A.; Kraft, D.; Mauprivez, O.; Rouquette, H.; Schwingweill, M. J.; Simon, N.; Vogt, W. *J Chem Soc Perkin Trans 2* **1996**, 1175-1182.

(25) Lambert, T. N.; Jarvinen, G. D.; Gopalan, A. S. *Tetrahedron Lett* **1999**, *40*, 1613-1616.

(26) Gopalan, A. S.; Huber, V. J.; Zincircioglu, O.; Smith, P. H. *J Chem S Ch* **1992**, 1266-1268.

(27) Dasaradhi, L.; Stark, P. C.; Huber, V. J.; Smith, P. H.; Jarvinen, G. D.; Gopalan, A. S. *J Chem Soc Perkin Trans 2* **1997**, 1187-1192.

(28) Lambert, T. N.; Dasaradhi, L.; Huber, V. J.; Gopalan, A. S. *J Org Chem* **1999**, *64*, 6097-6101.

(29) Romanovski, V. V.; White, D. J.; Xu, J. D.; Hoffman, D. C.; Raymond, K. N. *Solvent Extr. Ion Exch.* **1999**, *17*, 55-71.

(30) Raymond, K. N. *Coord. Chem. Reviews* **1990**, *105*, 136-153.

(31) Raymond, K. N.; Garrett, T. M. *Pure & Appl. Chem.* **1988**, *60*, 1807-1816.

(32) Raymond, K. N.; Kappel, M. J.; Pecoraro, V. L.; Harris, W. R.; Carrano, C. J.; Weitl, F. L. In *Actinides in Perspective*; Edelstein, N. M., Ed.; Pergamon Press: Oxford and New York, 1982; pp 491-507.

(33) Raymond, K. N.; Pecoraro, V. L.; Weitl, F. L. In *Development of Iron Chelators for Clinical Use*; Martell, A. E., Anderson, W. F., Badman, D. G., Eds.; Elsevier/North-Holland: New York, 1981; pp 165-187.

(34) Raymond, K. N.; Smith, W. L. In *Structure and Bonding*; Goodenough, J. B., Hemmerich, P., Ibers, J. A., Jorgensen, C. K., Neilands, J. B., Reinen, D., Williams, R. J. P., Eds.; Springer-Verlag: Berlin, Heidelberg, 1981; Vol. 43, pp 159-186.

(35) Drechsel, H.; Winkelmann, G. In *Transition Metals in Microbial Metabolism*; Winkelmann, G., Carrano, C. J., Eds.; Harwood Academic Publishers, 1997.

(36) Loomis, L. D.; Raymond, K. N. *Inorg. Chem.* **1991**, *30*, 906-911.

(37) Sofen, S. R.; Abu-Dari, K.; Freyberg, D. P.; Raymond, K. N. *J. Am. Chem. Soc.* **1978**, *100*, 7882-7887.

(38) Sofen, S. R.; Cooper, S. R.; Raymond, K. N. *Inorg. Chem.* **1979**, *18*, 1611-1616.

(39) Kappel, M. J.; Nitsche, H.; Raymond, K. N. *Inorg. Chem.* **1985**, *24*, 605-611.

(40) Lloyd, R. D.; Bruenger, F. W.; Mays, C. W.; Atherton, D. R.; Jones, C. W.; Taylor, G. N.; Stevens, W.; Durbin, P. W.; Jeung, N.; Jones, E. S.; Kappel, M. J.; Raymond, K. N.; Weitl, F. L. *Rad. Chem.* **1984**, *99*, 106-128.

(41) Garrett, T. M.; Miller, P. W.; Raymond, K. N. *Inorg. Chem.* **1989**, *28*, 128-133.

(42) Martell, A. *Critical Stability Constants*; Plenum Press:, 1977; Vol. 3.

(43) Avdeef, A.; Sofen, S. R.; Bregante, T. L.; Raymond, K. N. *J. Am. Chem. Soc.* **1978**, *100*, 5362-5370.

(44) Garrett, T. M.; Cass, M. E.; Raymond, K. N. *J. Coord. Chem.* **1992**, *25*, 241-253.

(45) Hou, Z. In *Chemistry*; University of California: Berkeley, 1995.

(46) Shannon *Acta Cryst.* **1976**, *A32*, 751.

CHAPTER TWO

Characterization of 2,3-Dihydroxyterephthalamides as Chelators for M(IV) ions

Introduction

The 2,3-dihydroxyterephthalamides (TAM) are attractive targets for chelators of tetravalent metals because these ligands are excellent chelators for Fe(III).[1] In the progression from catechol, to catecholamide (CAM), to TAM, the addition of electron-withdrawing amides lowers the protonation constants of the phenolic oxygens, but does not decrease the strength of Fe(III) binding. Early studies with the catechol dianion and the 8-coordinate, tetravalent metals U(IV), Ce(IV), Th(IV), and Hf(IV) indicated that catechol was a strong chelator of high oxidation state metals.[2,3] Thus, the TAMs are a logical candidate for actinide(IV) chelation.

Understanding the basic coordination chemistry of the TAMs as actinide chelators is crucial for determining under what circumstances these ligands would be best suited for nuclear waste remediation. The formation of the TAM – M(IV) complexes are highly dependent on proton concentration since the ligand is diprotic. Thus, knowing the formation constants for the M(IV) – TAM complexes allow one to calculate the pH range in which the complex is fully formed and best suited as a chelator.

This chapter presents the study of a simple alkyl TAM ligand, ethyl 2,3-dihydroxyterephthalamide (ETAM) (Figure 2-1), with Zr(IV), Ce(IV), Th(IV), and Pu(IV). This includes the crystallographic determination of the Zr(IV) and Th(IV) ETAM structures, and the stability constants for the Th(IV) and Pu(IV) ETAM

complexes. While these metals are all tetravalent, the size of the metals increases in the order Zr(IV) < Ce(IV) ~ Pu(IV) < Th(IV). Ce(IV) is a convenient Pu(IV) analog since the ionic radii are similar,[4] while Zr(IV) and Th(IV) are useful since neither one is electrochemically active. Ultimately, the analogous experiments with Pu(IV) must be conducted and will reveal the extent to which comparisons can be drawn with M(IV) analogs.

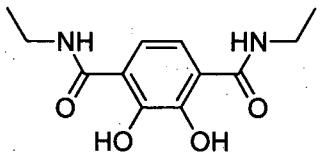

Figure 2-1. Structure of ethyl 2,3-dihydroxyterephthalamide (H_2ETAM).

Synthesis and X-ray Crystal Structures of M(IV) - ETAM complexes

Three complexes with composition $K_4[M(ETAM)_4]$ (M = Zr(IV), Ce(IV), Th(IV)) were prepared by a ligand exchange reaction in which the appropriate $M(acac)_4$ and 4 equivalents of H_2ETAM were heated in refluxing MeOH for 16 hours (Scheme 2-1) then treated with 4 equivalents of methanolic KOH to fully deprotonate the complex. After evaporation, the complex was separated from impurities on a sephadex LH-20 column.

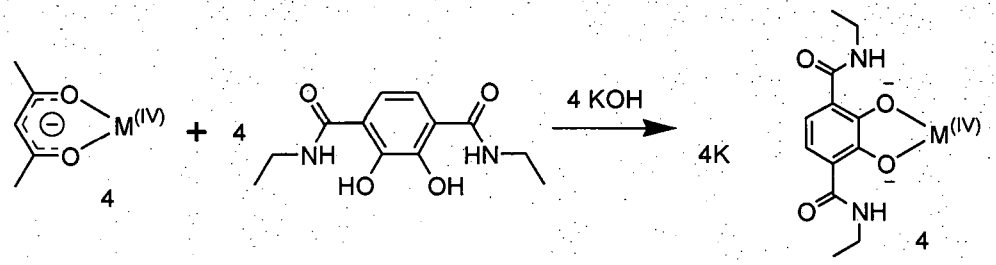

Scheme 2-1. Synthesis of M(IV) – ETAM complexes.

This method produced clean samples of the three metal complexes and their ^{1}H NMR spectra in D_6-DMSO are almost identical (Figure 2-2). The aromatic protons have a chemical shift of ca. 6.6 ppm, while the protons of the ethyl group have chemical shifts of ca. 0.8 and 3.1 ppm. The peak at ca. 2.5 ppm is DMSO, while the large peak at ca. 3.3 ppm is extraneous water, which is present because these compounds are hygroscopic in the solid state. The spectrum of the protonated H_2ETAM is shown at the bottom for comparison. The upfield shift of the coordinated ligand resonances relative to the protonate ligand indicates that the deprotonated, coordinated ligand is more shielded than the protonated ligand. The similarity and simplicity of the spectra suggests that each of these metals is in the same coordination environment and on the NMR time scale all of the ligands are equivalent. The Ce complex has a small impurity of deprotonated, non-coordinated ligand, which illustrates the difference in chemical shift of coordinated and non-coordinated ligand.

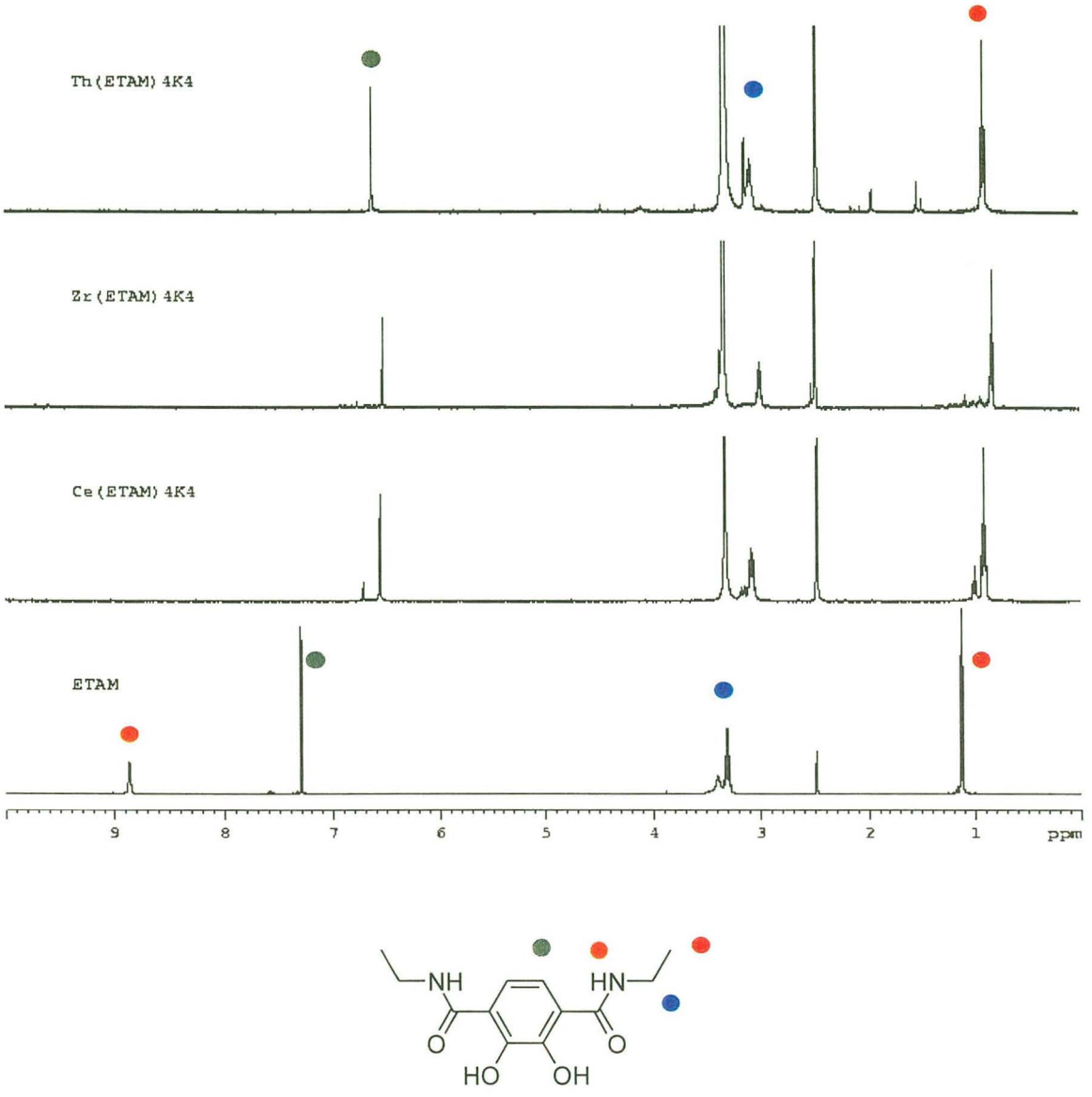

Figure 2-2. ^{1}H NMR spectra for Th(IV), Zr(IV), and Ce(IV) complexes of ETAM as well as the protonated ligand H_2ETAM.

Crystals of the $K_4[Zr(ETAM)_4]$ complex were grown from diffusion of ether into methanolic solutions of the complex. The complex crystallizes in C2/c space group; the Zr lies on a two-fold axis and there are 8 molecules in the unit cell. The ORTEP diagram

(Figure 2-3 and Figure 2-4) shows that the Zr(IV) is coordinated by 8 oxygens in a square antiprismatic geometry. As seen in all metal – TAM complexes, the amide is oriented such that the amide proton can hydrogen bond to the catecholate oxygen.[5] The ligands do not have a propeller arrangement around the metal : the angle formed between the catecholate plane and the Zr(IV) is ~115° and the Zr lays 0.76 or 0.87 Å out of the plane of the catechol. In the view shown in Figure 2-3, the planes of the 2 ETAMs on top intersect each other at 147° and the two catechol planes on the left intersect each other at 25°. The Zr – O bond lengths range from 2.14 Å to 2.27 Å.

One K^+ counterion sits in the cleft above the catecholate oxygens, coordinated by the 4 catecholate oxygens, an ether molecule, an amide oxygen from a neighboring complex, and some disordered solvent (not shown). The other K^+ ion links two adjacent complexes, as it is coordinated only by amide oxygens. In this way, the K^+ ions link all of the $[Zr(ETAM)_4]^{4-}$ and large holes are present in the packed structure that accommodate disordered solvent.

The catechol rings do not lie directly over each other; the ligands are off-set such that the amide of one lies over the catechol ring of the other, and vice versa. This is best seen the view shown in Figure 2-4. This view also clearly shows the square-antiprismatic coordination geometry. The assistance of Dr. Darren Johnson in solving this crystal structure is gratefully acknowledged.

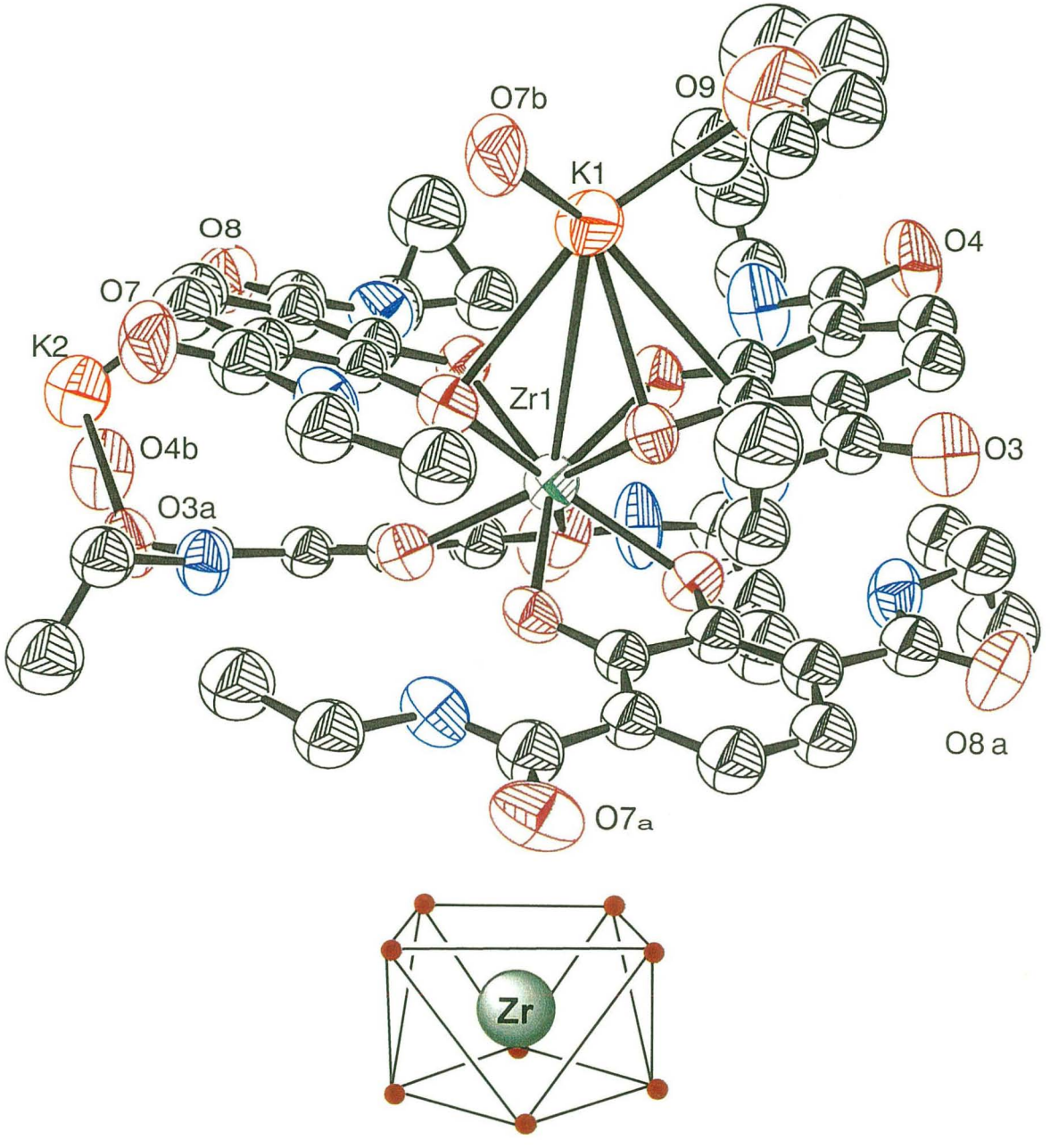

Figure 2-3. ORTEP of the $[Zr(ETAM)_4]^{4-}$ complex (50% probability) illustrating the non-planar approach of the ligand to the metal center, the K^+ which sits in the cleft above the catecholate oxygens, and the K^+ which is coordinated only by amide oxygens. Only the amide oxygens are labeled. Below is a polyhedron in which the maroon dots represent the square anti-prism formed by the coordinating oxygens.

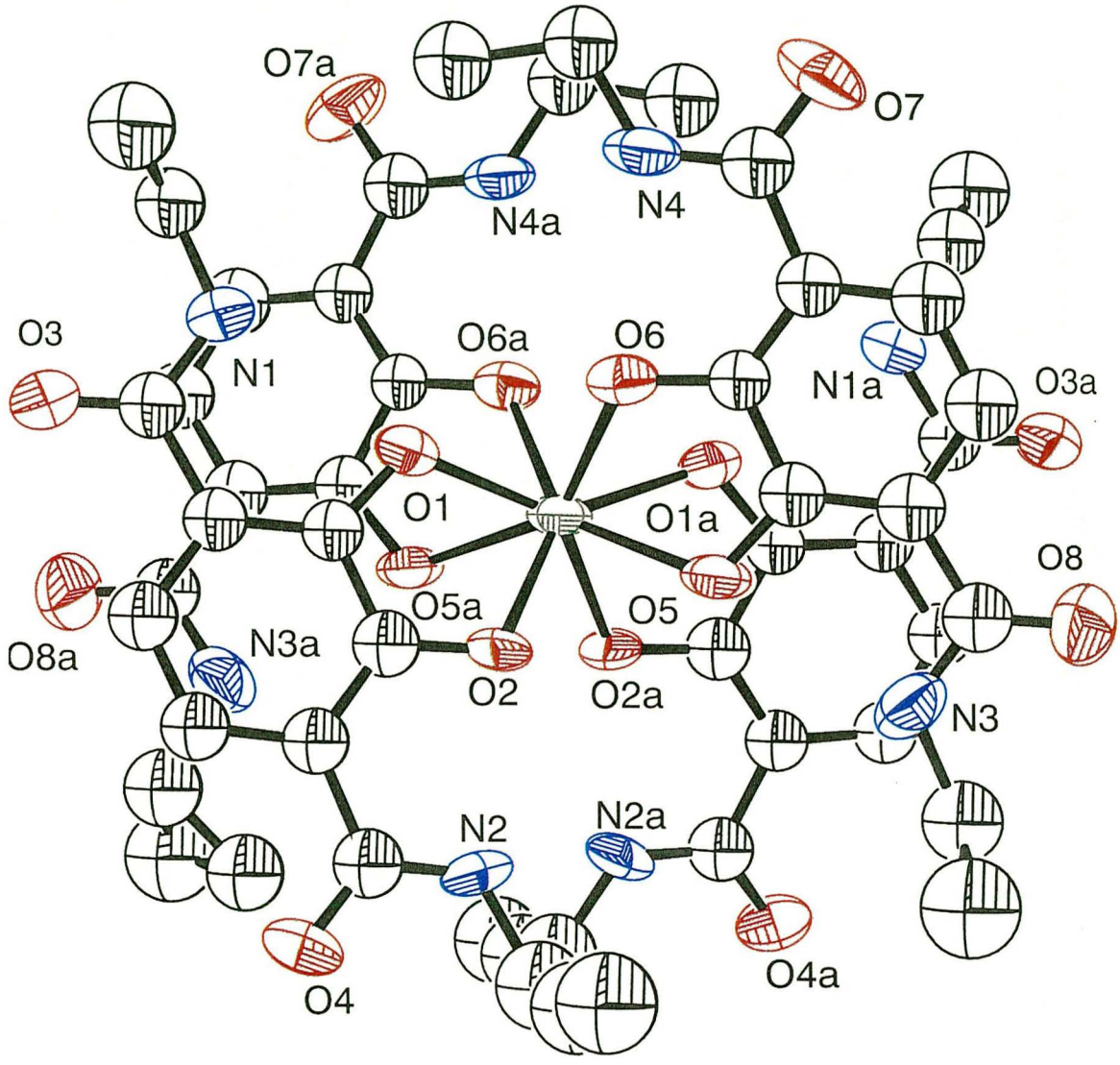

Figure 2-4. ORTEP of the $[Zr(ETAM)_4]^{4-}$ complex (50% probability) showing the square anti-prismatic coordination geometry, orientation of the amides for hydrogen-bonding, and numbering scheme.

Recently, the quantitative shape measure was introduced to compare the coordination polyhedra observed in several 8-coordinate Ce(IV) – hydroxypyridinone

(HOPO) crystal structures with idealized 8-coordinate polyhedra.[6] The 3 idealized 8-coordinate polyhedra are square anti-prism (D_{4d}), bicapped trigonal prism (C_{2v}), and trigonal dodecahedron (D_{2d}) (Figure 2-5). For the shape measure (S), the dihedral angles of adjacent planes from crystal structure coordinates are calculated and compared to the dihedral angles of the D_{4d}, D_{2d}, and C_{2v} geometries.

$$S = \min\left[\frac{1}{m}\sqrt{\sum_{i=1}^{m}(\delta_i - \theta_i)^2}\right]$$

Where m = number of edges; δ = angle between normals of adjacent faces; δ_i = observed dihedral angle along ith edge of δ; θ = same angle of corresponding ideal polytopal shape θ. The smallest S is the one closest to the describing the coordination geometry. In the case of this $[Zr(ETAM)_4]^{4-}$ structure the following shape measures were calculated: $S(D_{4d}) = 3.4^\circ$, $S(C_{2v}) = 4.5^\circ$, and $S(D_{2d}) = 4.6^\circ$. This indicates that the geometry most closely resembles a square anti-prism, as is clear from the ORTEP diagrams.

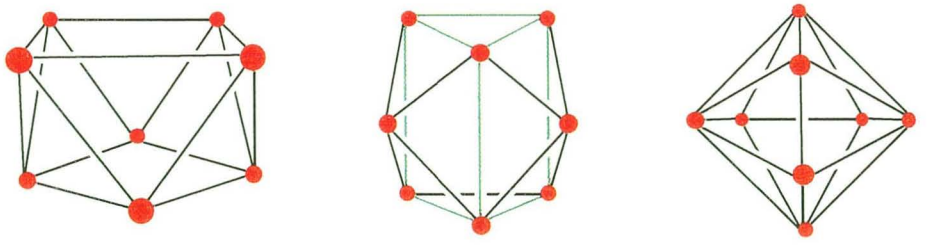

Figure 2-5. The idealized 8-coordinate polyhedra are square anti-prism (D_{4d}), bicapped trigonal prism (C_{2v}), and trigonal dodecahedron (D_{2d}). The red points represent the position of the coordinating atoms. The trigonal prism is shown in green.

Crystals of the K^+ salt of the analogous Th(IV) complex were never formed, so the $[Th(ETAM)_4]^{4-}$ was prepared as the tetra - trimethylbenzylammonium salt by using a stoichiometric amount of $[Me_3BnN]OH$ as the base during the synthesis instead of KOH. This complex crystallizes in P $\bar{1}$ as an 8-coordinate complex (Figure 2-6). This structure is significantly different from the Zr structure. The ligands approach the metal straight on. The shape measure was used to analyze the coordination geometry, which is not as obvious in this structure. The shape measures that were calculated are: $S(D_{4d}) = 6.1°$, $S(C_{2v}) = 4.5°$, and $S(D_{2d}) = 4.8°$. In this complex, the coordination geometry around the Th(IV) lies between bicapped trigonal prismatic (C_{2v}) and trigonal dodecahedron (D_{2d}),but closer to C_{2v}. The Th(IV) – oxygen bond lengths are between 2.38 Å and 2.49 Å.

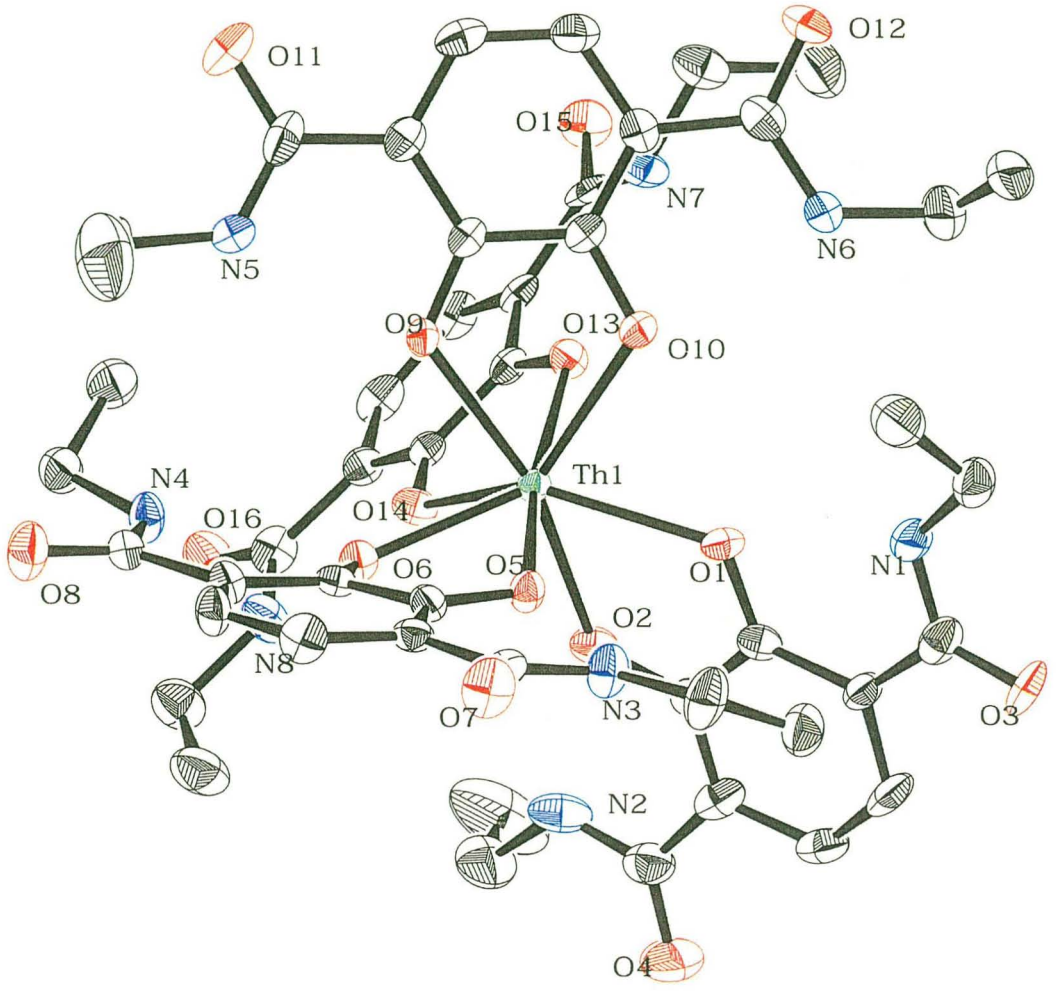

Figure 2-6. ORTEP of $[Th(ETAM)_4]^{4-}$ (50% probability) and numbering scheme.

The $[Th(ETAM)_4]^{4-}$ structure can be compared to the $Th(Me\text{-}3,2\text{-}HOPO)_4$ structure, where Me-3,2-HOPO is the bidentate ligand 6-methyl-3-hydroxypyridin-2-one.[7] In the crystal structure of the HOPO complex, the Th(IV) is 9-coordinate. Four ligands provide 8 oxygens and the 9 coordination spot is filled by an amide oxygen from a neighboring complex. The size of Th(IV) is larger than Zr(IV) (ionic radius of 1.01 Å vs. 0.86 Å) [4] so a coordination number of 8 or 9 is expected. The strong Lewis basicity

of the TAM ligands relative to 3,2-HOPO decreases the effective charge on the metal center and presumably this precludes the $[Th(ETAM)_4]^{4-}$ complex from adding another ligand to its coordination sphere.

These Zr(IV) and Th(IV) ETAM structures have coordination geometries which differ from each other and those in the four crystal structures of $[M(catecholato)_4]^{4-}$ where M = U(IV), Th(IV), Ce(IV), and Hf(IV).[2,3] The latter complexes all have D_{2d} (trigonal dodecahedron) symmetry and all have identical unit cell contents. A small difference was seen in the U(IV)-oxygen bond lengths which was not present in the Th(IV) or Ce(IV) structures and was attributed to a ligand field effect from the $5f^2$ electrons. The Hf(IV) structure also had a small distortion, but this was attributed to the small size of Hf(IV) and the close contacts between adjacent catechol ligands. Th(IV) and Zr(IV) are f^0 and d^0 metals, so there is no electronic preference for a particular coordination geometry. In the TAM structures presented here, the difference is most likely due to the different counter ions: the K^+ coordinating to the catecholate oxygens in the Zr(IV) structure distorts the ligands, which in turn affects the geometry around the metal.

In one case, the Th – ETAM complex was accidentally prepared with a 3:1 ratio of H_2ETAM : Th(IV). The resulting complex crystallized readily from diffusion of either methyl t-butyl ether or diethylether into MeOH. Dark brown tablet-shaped crystals were isolated from both solvent systems, however from the ether diffusion, a single light tan cube crystal also formed with a drastically different appearance than the dark brown crystals. Both crystals were characterized by X-ray crystallography and are the same

complex crystallized as different isomorphs in the same space group P21/C (Figure 2-7 and Figure 2-8)

The complex is a dimer with the formula $[Th(ETAM)_3MeOH]_2 \cdot 4\ NMe_4$. The coordination around the Th(IV) consists of two TAM units bound in the expected catecholate fashion. The third TAM also binds Th(IV) with its catecholate oxygens, however one of the catecholate oxygens bridges to the second Th(IV). The amide that is ortho to this phenol is oriented such that the carbonyl oxygen also binds to the second Th(IV) in a *salicylate* mode. In all other TAM and CAM metal complex structures, the amide is oriented with the oxygen pointing away from the metal such that the amide proton can hydrogen bond to the deprotonated, coordinating catecholate oxygen. In this case, the bridging TAM exhibits both orientations of the amide. In total, each Th(IV) is coordinated by 5 phenolic oxygens, 2 bridging phenolic oxygens, one amide oxygen, and one MeOH, for a total coordination number of 9.

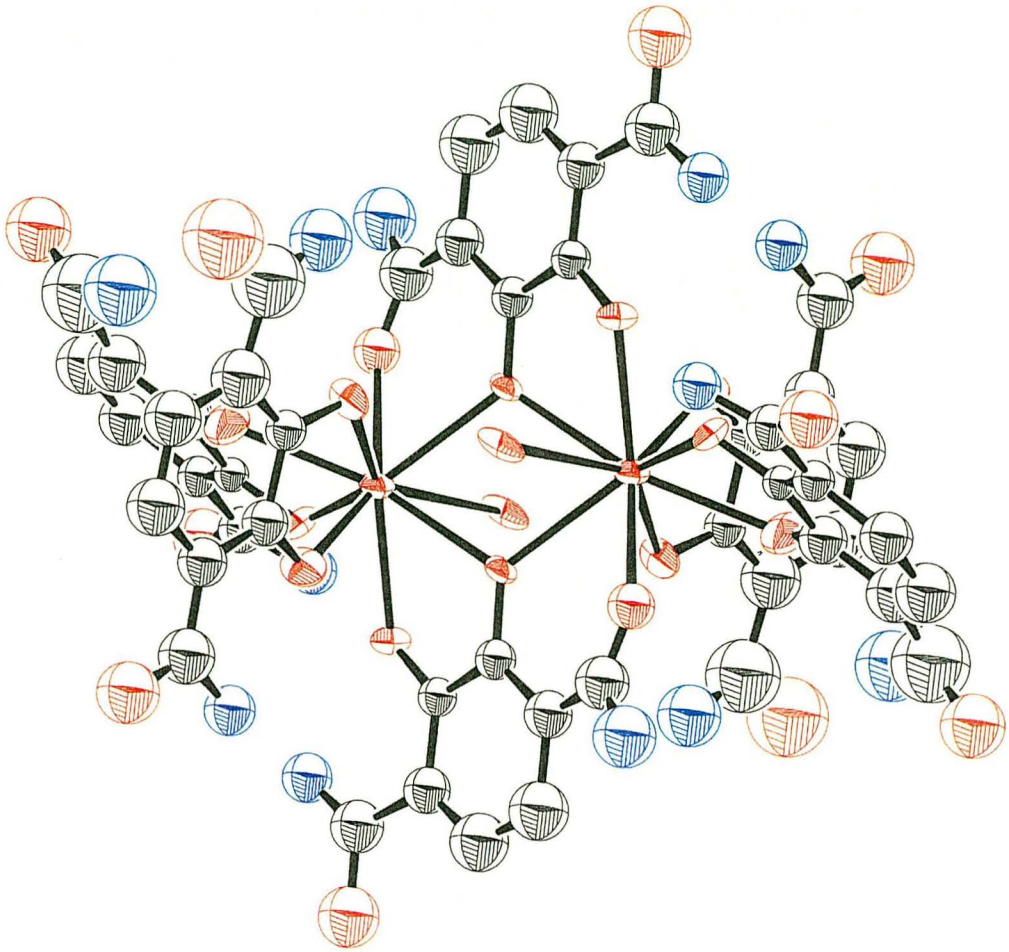

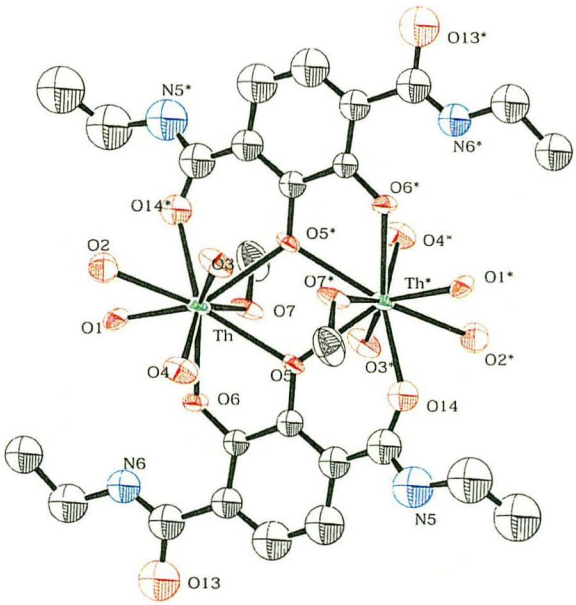

Figure 2-7. ORTEP (50% probability) of first crystal structure of $[Th(ETAM)_3]_2^{4-}$ is shown above. The ethyl groups and methanol carbon have been omitted for clarity. To the left is a detail of the bridging ETAM ligand and the atom numbering scheme.

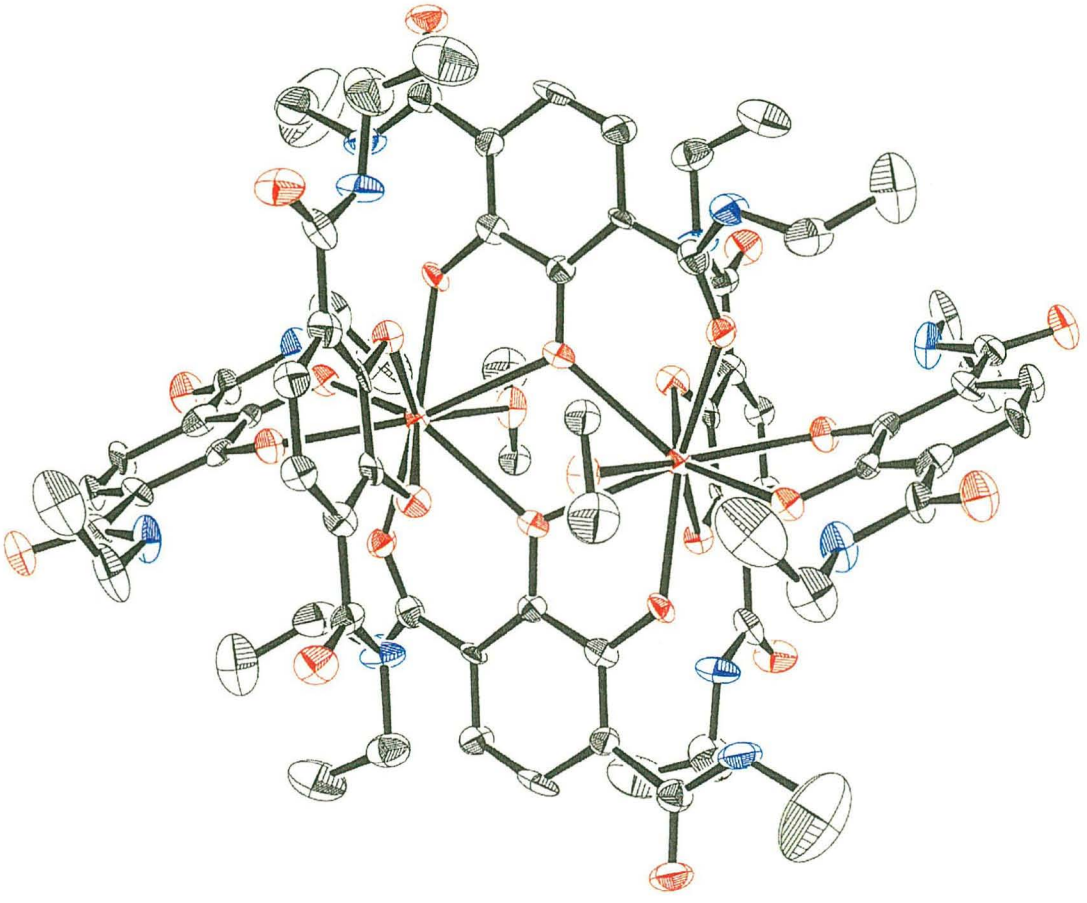

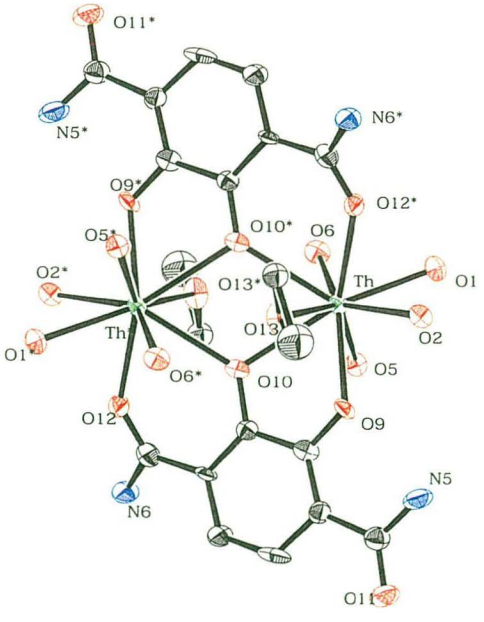

Figure 2-8. ORTEP (50% probability) of second crystal structure of $[Th(ETAM)_3]_2^{4-}$ is shown above. To the left is a detail of the bridging ETAM ligand and the atom numbering scheme.

The bond lengths are very similar between the two structures. In the first structure the bond distances from the Th to the catecholate oxygens range from 2.33 to 2.51 Å. The Th – Th distance is 4.14 Å. In the second structure the bond distances from the Th to the catecholate oxygens range from 2.39 to 2.57 Å. The Th – Th distance is 4.23 Å. In the second structure the carbon of the coordinated methanol is disordered over two sites. Presumably the difference in packing between the two structures is due to the co-crystallized solvent, which is slightly different. The second structure has a lower R-value (3.2%) than the first (6.7%).

There was really no way to know that these were the same complex before solving the structure. The unit cell dimensions are different for the first dimer (a = 13.2437(3) Å, b = 26.7048(2) Å, c = 16.6384(3) Å, β = 106.830(1)°, V = 5632.5(2) Å^3, Z = 2) and the second dimer (a = 18.2603(9) Å, b = 18.5002(9) Å, c = 19.675(1) Å, β = 117.298(1)°, V = 5906.3(5) Å^3, Z =2) but the volumes are similar. The volume of the unit cell is also not diagnostic because in the $[Zr(ETAM)_4]^{4-}$ and $[Th(ETAM)_4]^{4-}$ structures the volumes were 10837.0(9) Å^3 for Z = 4 and 4903.4(2) Å^3 for Z = 2 and neither are dimers.

Stability Constant Determination for Th(IV) ETAM complex

Understanding the thermodynamic metal binding properties of the TAMs is essential for evaluating their utility in nuclear waste remediation applications. Since the TAM ligands are diprotic, the formation of the Th – ETAM complex is dependent on the proton concentration. Thus, the formation constants for the Th-ETAM complex were

determined by titration of a solution containing Th and ETAM with either HCl or KOH. The formation of $[ThETAM]^{2+}$, $Th(ETAM)_2$, $[Th(ETAM)_3]^{2-}$, and $[Th(ETAM)_4]^{4-}$ complexes can be monitored by a change in the UV-Vis spectrum of the solution as a function of pH. The spectra show distinct changes between 250 to 280 nm and 340 to 375 nm, attributed to the π to π^* transition of the ligand.[1] The pK_as for H_2ETAM have been previously reported as 6.0 (1) and 11.1(1).[1]

The stepwise formation constants are defined as:

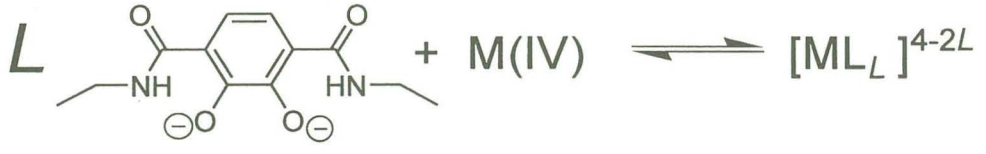

$mM^{4+} + lL^{2-} \rightleftarrows M(L_l)^{4-2l}$ $\quad K_{mlh} = [M(L_l)^{4-2l}] / [M][L^{2-}]^l$

$Th^{4+} + L^{2-} \rightleftarrows Th(L)^{2+}$ $\quad K_{110} = [Th(L)^{2+}] / [Th][L^{2-}]$

$Th^{4+} + 2\,L^{2-} \rightleftarrows ThL_2$ $\quad K_{120} = [ThL_2] / [Th][L^{2-}]^2$

$Th^{4+} + 3\,L^{2-} \rightleftarrows Th(L_3)^{2-}$ $\quad K_{130} = [Th(L_3)^{2-}] / [Th][L^{2-}]^3$

$Th^{4+} + 4\,L^{2-} \rightleftarrows Th(L_4)^{4-}$ $\quad K_{140} = [Th(L_4)^{4-}] / [Th][L^{2-}]^4$

Two different titrations were conducted: one at low pH (3.1 to 1.5) to determine K_{110}, and one throughout the higher pH range (2.7 to 10.5) to determine K_{120}, K_{130}, and K_{140}. The lower pH titration was necessary because the complex is not fully dissociated at pH 2.7 and this is essential to determine K_{110}. For the low pH titration, a solution was prepared with 50 mL 0.1M KCl, 2.5×10^{-4} M H_2ETAM, and 5×10^{-5} M Th(IV). The

solution had an initial pH of 3 and a total of 25 mL of 0.1M HCl was titrated into the cell to lower the pH to 1.5. The spectra, monitoring the disappearance of the ThL^{2+} complex, are shown in Figure 2-9. These spectra represent 60% dissociation of the ThL complex to free Th(IV) and the data were refined using the program pHAB[8] to a value of 17.46(1) for Log K_{110}.

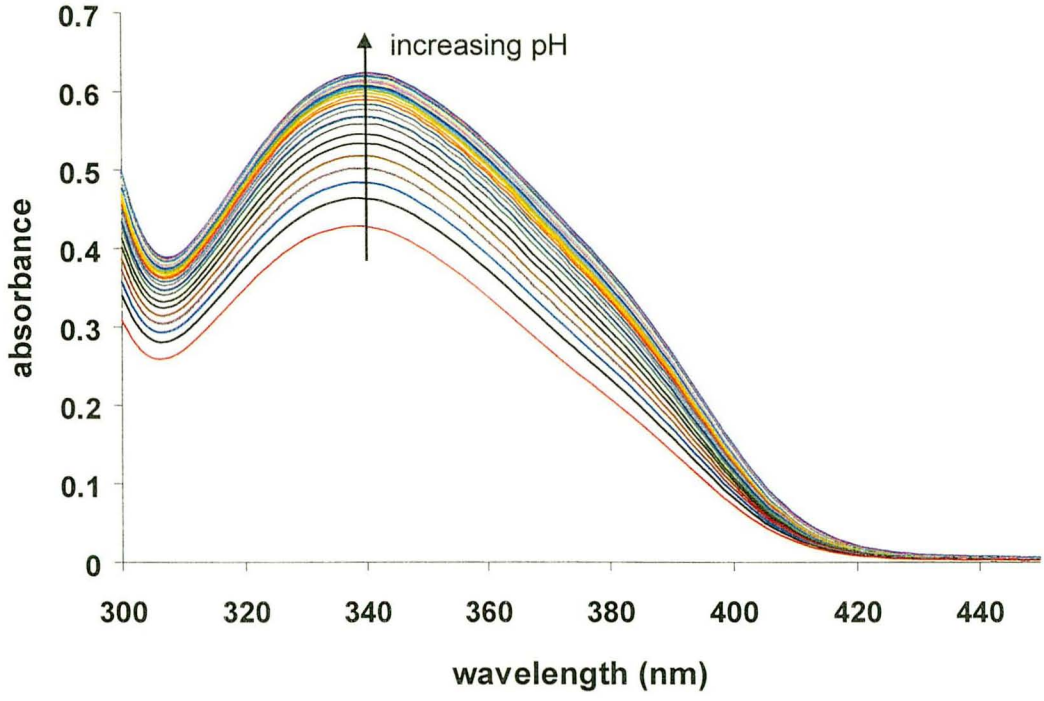

Figure 2-9. Spectra collected in the Th – ETAM titration between pH 3 and 1.5.

$[Th^{4+}] = 5x10^{-5}$ M, $[H_2ETAM] = 2.5x10^{-4}$ M, T = 25°C, ionic strength = 0.1M KCl.

To determine the next 3 formation constants, a titration was set up with $5x10^{-6}$ M Th(IV) and $2.5x10^{-5}$ M H_2ETAM and extra HCl. The solution was titrated from pH 2.8 to 10.5 then back to 2.8, since the system is reversible. In this way, 5 titrations were conducted and in each one spectra were collected for at least 67 pH points. The concentration of Th(IV) and H_2ETAM were carefully chosen to avoid precipitation of the neutral $Th(ETAM)_2$ during the titration and are the minimum that can be used and still obtain sufficient absorbance values. Due to these low concentrations, not enough buffering is afforded by ETAM so three buffers, MES, HEPES, and NH_4Cl, were added at ~ 0.4 mM. In so doing, only the pH and spectra were included in the data analysis. The changes in the spectra are shown in Figure 2-10, and the pH increases as λ_{max} shifts from 340 nM to 380nM.

The program pHAB[8] was used to analyze the data and they fit very well to a simple model of sequential addition of ligand to the metal center. Inclusion of mixed hydroxo species or dimers did not agree at all with the observed data. The hydrolysis constants for Th(IV) tabulated in Table 2-1.[9] In this refinement, log K_{110} determined in the previous experiment, was held fixed at 17.46 while the other three were refined. The log of these constants are 13.23 (47), 8.28 (32), and 6.57 (37), respectively, which amounts to a log β_{140} of 45.02. These numbers are summarized later with the values for the Pu – ETAM system in Table 2-1.

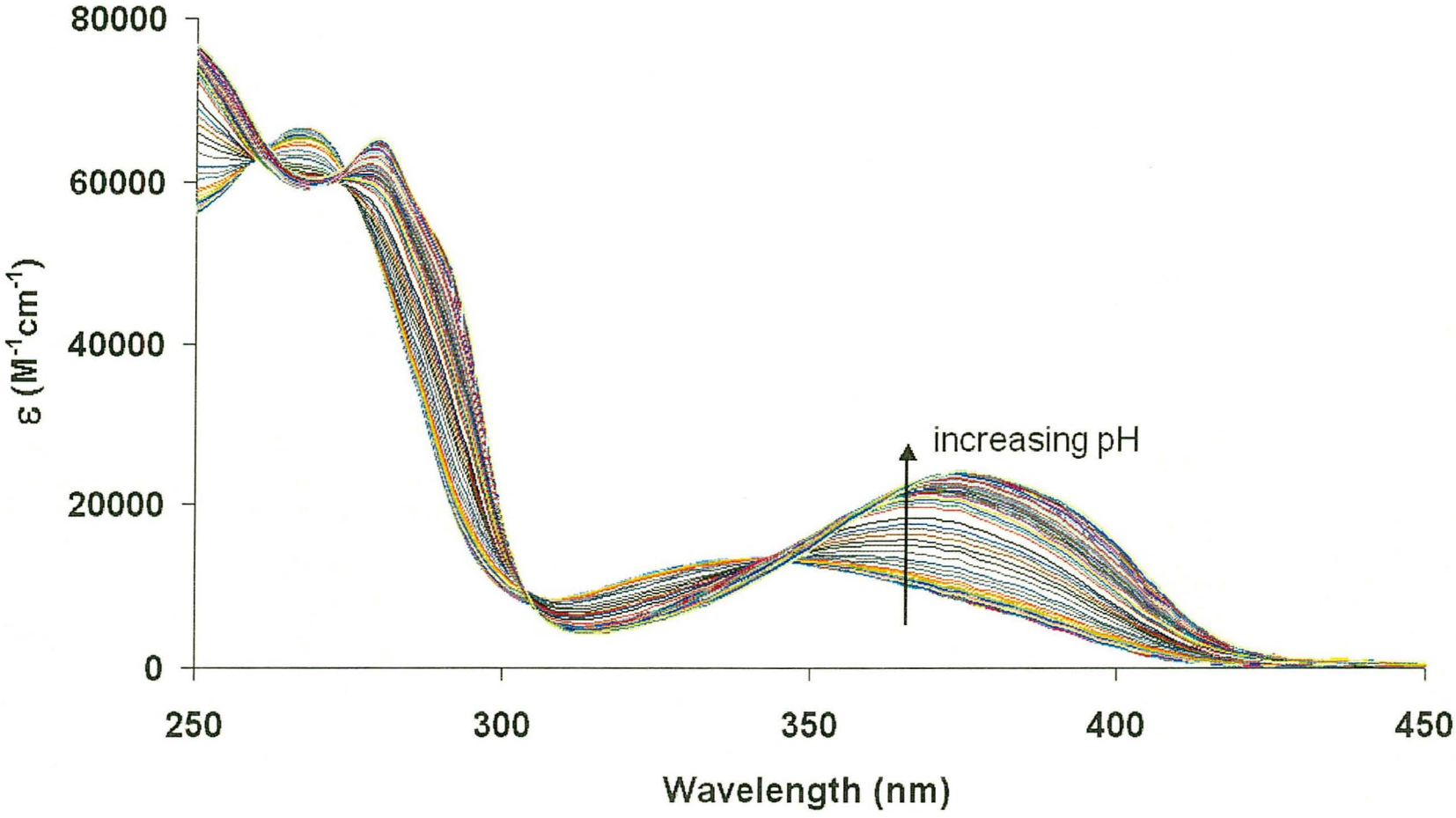

Figure 2-10. UV-Vis spectra collected during the pH titration of Th – ETAM from pH 2.8 to 10.5. $[Th^{4+}] = 5x10^{-6}$ M, $[H_2ETAM] = 2.5x10^{-5}$ M, T = 25° C, ionic strength = 0.1m KCl.

The speciation diagram illustrates how the composition of the solution changes with pH. This indicates that the complex is not fully formed until pH 10 but starts forming at pH 1.

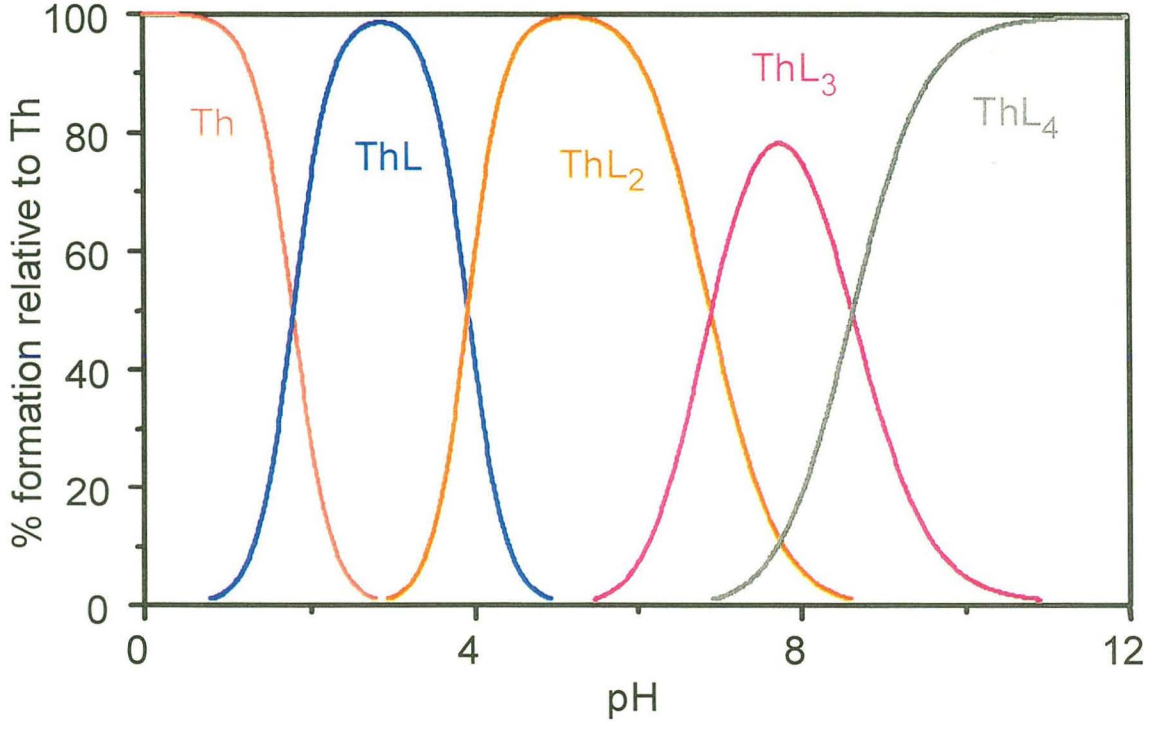

Figure 2-11. Speciation Diagram for the Th(IV) – ETAM system. Calculated with $1x10^{-4}$ M H_2ETAM and $1x10^{-5}$ M Th(IV).

The next step in developing the TAMs as M(IV) chelators is to synthesize octadentate ligands in which 4 TAMs are attached to a backbone, to satisfy the 8-coordinate requirement of the actinides. The speciation diagram for such a ligand can be estimated by using the same overall formation constant – $10^{45.5}$ – although due to the

chelate effect the actual formation constant should be higher. The speciation diagram is shown in Figure 2-12 with the structure of a generic octadentate ligand.

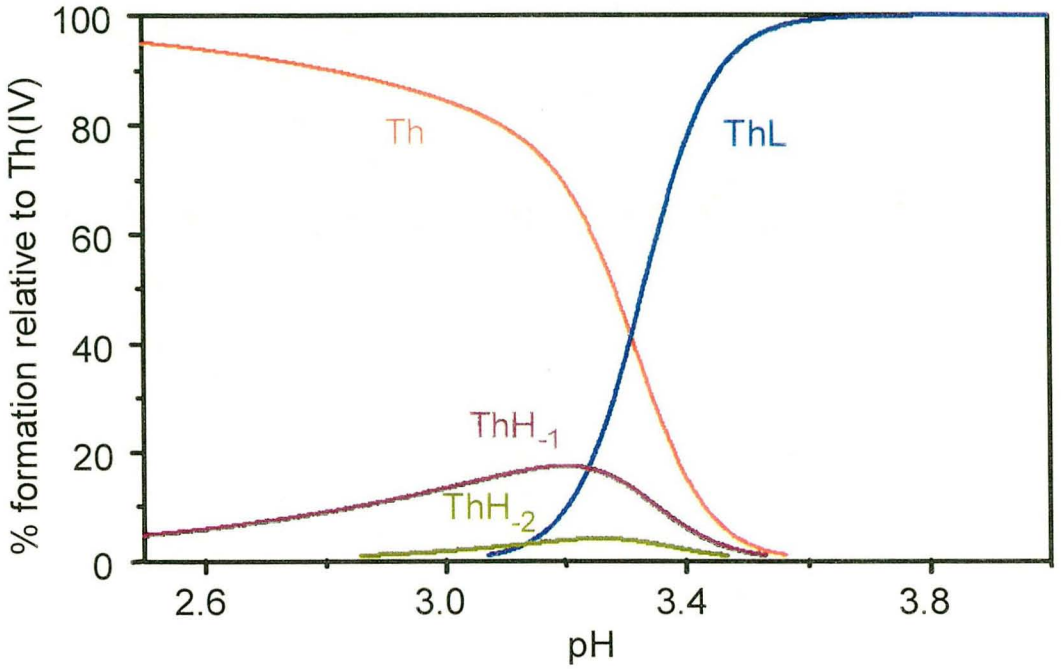

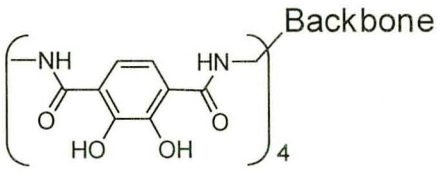

conditions for speciation:
[Th] = 10^{-5} M, [L] = 10^{-4} M
β_{110} = 45.54
pK_as = 11.5, 11.2, 10.8, 10.5, 6.5, 6.2, 5.8, 5.5

Figure 2-12. Estimated speciation diagram for the complexation of Th(IV) with a hypothetical octadentate TAM ligand.

Purification and Preparation of ^{239}Pu(IV) Solution

Before determining the Pu(IV) – ETAM stability constants, a solution of ^{239}Pu first had to be prepared. Dr. Petra Panak has perfected the following procedure and assisted with the purification. The general prcedure[10] involves ion-exchange chromatography to remove any metallic impurities, particularly ^{241}Am. The solution is

then concentrated, oxidized to Pu(VI), and stored in $HClO_4$. When the Pu is needed, the stock solution is reduced electrochemically to Pu(III), then oxidized electrochemically to Pu(IV) to ensure that all of the Pu is present in the desired oxidation state. [11] This solution is generally good for about 1.5 weeks before the Pu disproportionates into Pu(VI), Pu(V), and Pu(III).[12] The Latimer diagram shows that the reduction potentials for the oxidation states are all very close, [13] and once Pu(IV) disproportionates, the overall equilibrium for the species in solution is described by:

$$PuO_2^{+} + Pu(IV) \leftrightarrows Pu(III) + PuO_2^{2+} \quad \text{Log } K = 1.16$$

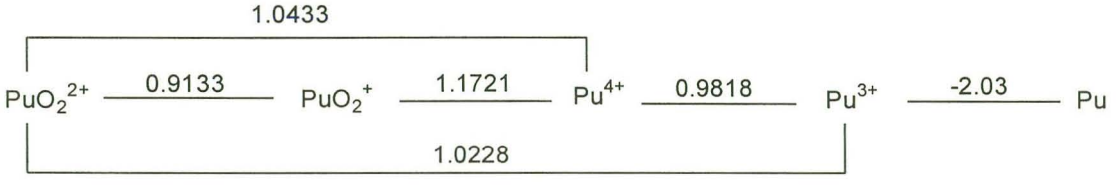

Perchoric acid is used as the medium in which to store the Pu because perchlorate is a weakly coordinating anion, the spectra of the four oxidation states of Pu in perchloric acid are well known ,[14] and the electrochemical potentials are also well known.[11]

The UV-Vis-NIR spectrum of the stock solution was compared with published spectra [14] of Pu^{6+} and Pu^{4+} in $HClO_4$ to ensure that the solution contained exclusively Pu^{6+}. Scintillation counting was used to determine the concentrations of ^{239}Pu in the original solution and the purified solution, and 90% of the Pu was recovered with this purification procedure.

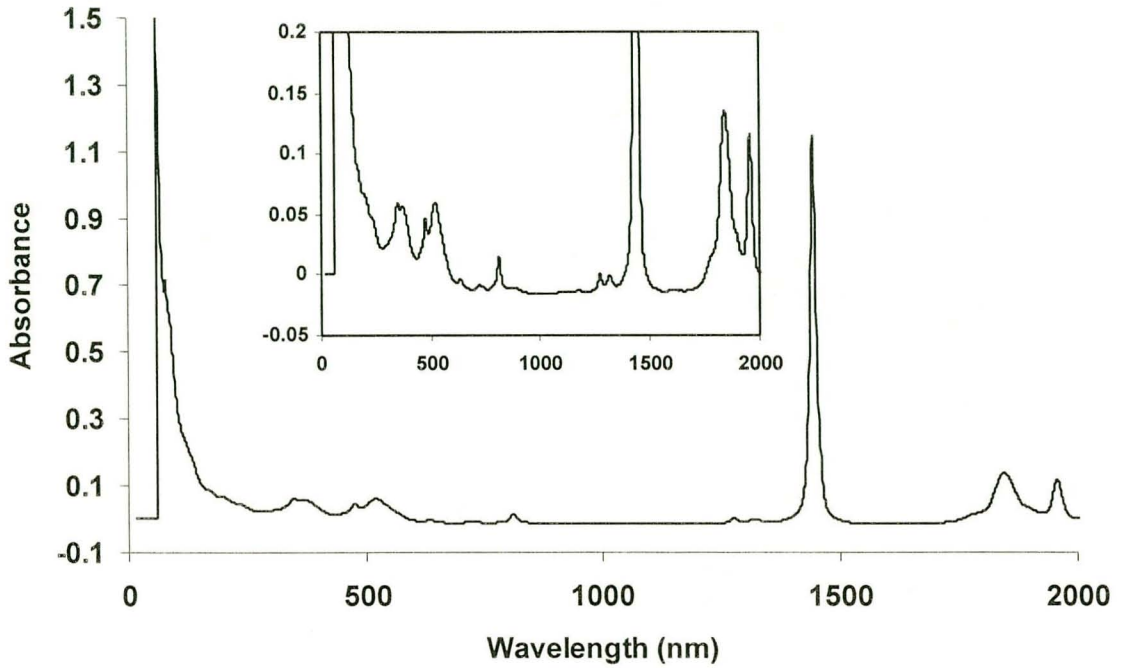

Figure 2-13. UV-Vis-NIR spectrum of the purified ^{239}Pu(VI) stock solution. The inset is a magnification of the spectrum.

Alpha spectroscopy was used to determine the purity of the ^{239}Pu before and after the column. Jerry Bucher assisted with the collection of the spectra. Alpha spectroscopy measures the energy of alpha particles that are ejected when an actinide decays and the energy of the alpha particle is characteristic of the isotope. The alpha spectra of the impure and pure Pu solutions are shown in Figure 2-14. The peaks at 5.10, 5.14, and 5.15 MeV are characteristic of ^{239}Pu. [15] The peaks at 5.44 and 5.48 MeV are characteristic of ^{241}Am. ^{242}Pu has peaks at 4.85 and 4.9 MeV, so the spectra indicate that this isotope is not present. The concentration of ^{241}Am in both samples was calculated by integrating the area under the peaks and accounting for the half-lives of the two isotopes

(24,111 years for ^{239}Pu and 432 years for ^{241}Am). ^{241}Am was present as a 1.4% impurity in the original solution and in the final sample is only present as a 0.003% impurity.

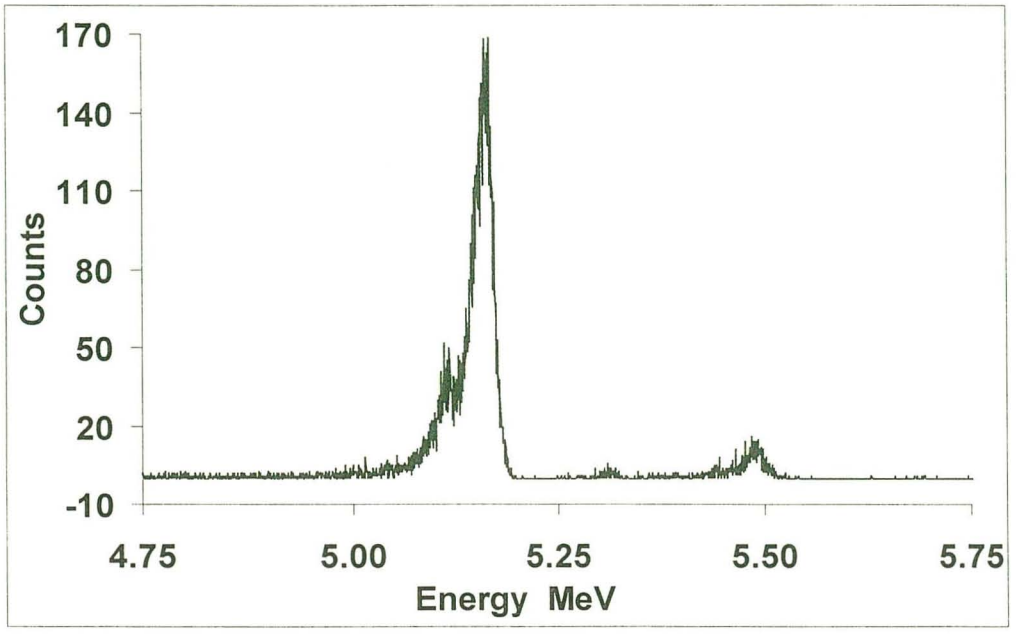

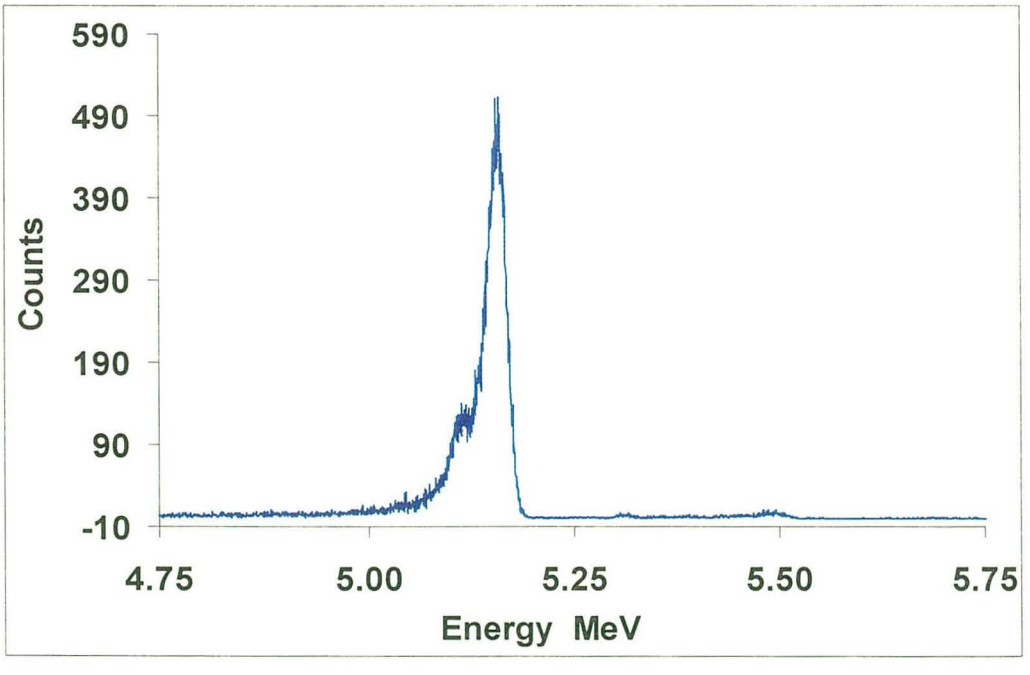

Figure 2-14. Alpha spectra from the unpurified (above) and purified (below) ^{239}Pu samples.

Stability Constant Determination for Pu(IV) ETAM complex

With a pure solution of Pu(IV), the stability constants with H_2ETAM could then be determined. The Pu(IV) – ETAM stability constants were determined in the same way as the Th(IV) constants. The Th(IV) titrations were useful in planning the Pu(IV) titrations for several reasons. Since Th(IV) is being suggested here as a model for Pu(IV), a comparision of the constants will allow us to have a way to evaluate if Th(IV) is a good model. The concentrations and pH range used for the Th(IV) titrations should also be valid for Pu(IV). An initial estimate of the Pu(IV) constants was made by scaling the Th(IV) constants to the ratio of the Th(IV) / Pu(IV) hydrolysis constants.

Spectrophotometric pH titrations were conducted 3 times from pH 2.4 to 10.5, and UV-Vis spectra were recorded from 250 to 550 nM at 150 different pH values, as shown in Figure 2-15. Again, the absorbance seen in the Uv-Vis spectrum are attributed to π to π * transitions of the ligand. The solution contained 50 mL of 0.1M NaClO4, $5x10^{-6}$ M Pu(IV) and $4x10^{-5}$ M H_2ETAM and extra $HClO_4$. In the Th(IV) titration, 5 equivalents of ligand was used, however in this titration 8 equivalents of ligand was used because initial modeling of the titration suggested that extra ligand would suppress hydrolysis of the Pu(IV) at low pH. The hydrolysis constants for Pu(IV) are tabulated in Table 2-1. [9]

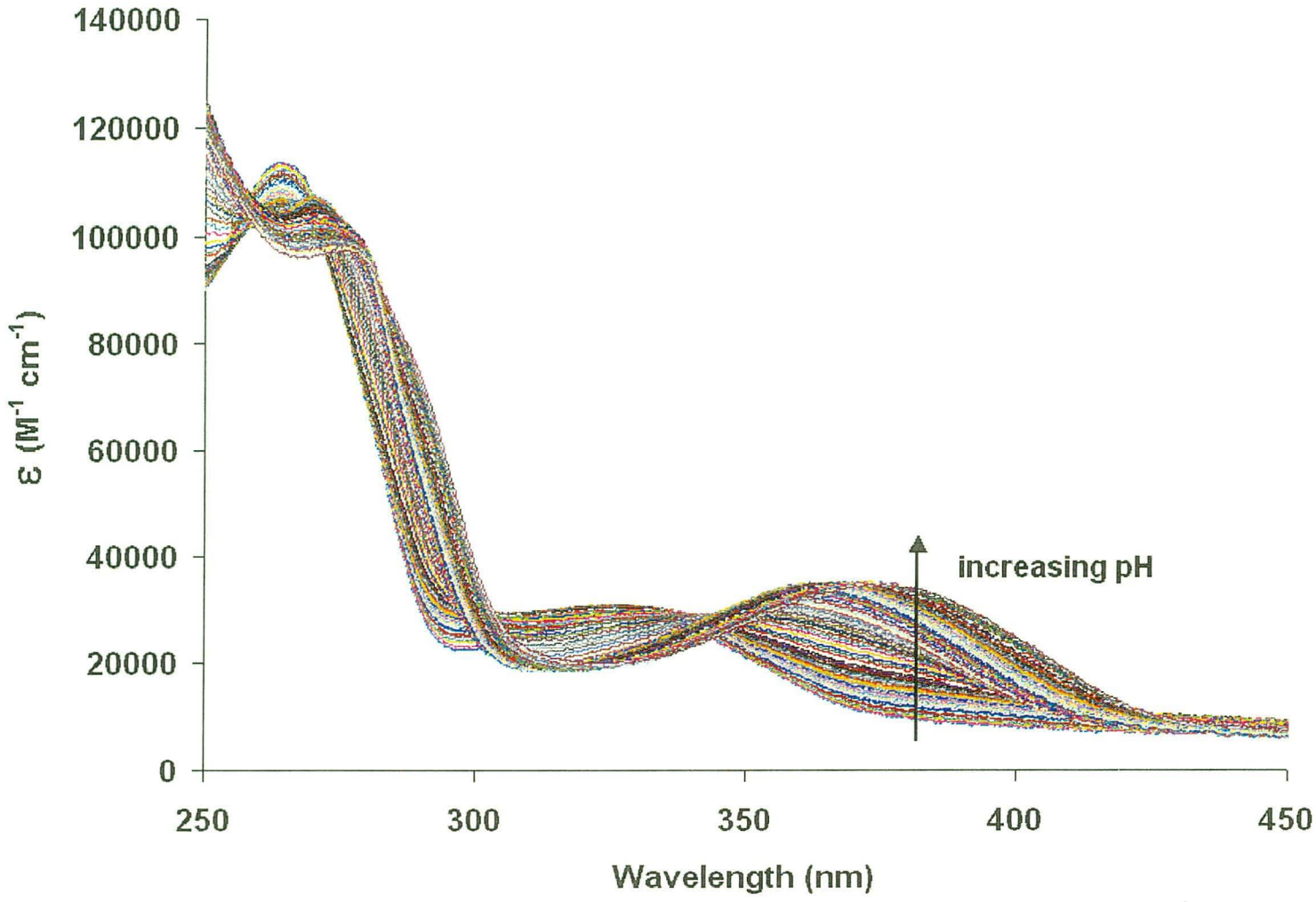

Figure 2-15. Spectra from the titration of Pu – ETAM.

These data were successfully refined with pHAB[8] using a model of stepwise addition of ligands to the metal center. The formation constants are summarized in Table 2-1, along with the Th(IV) constants for comparison. Not surprisingly, the constants for binding Pu(IV) are higher since the metal is a stronger Lewis acid.

Log K_{mlh}	Th(IV)	Pu(IV)
Log K_{110}	17.47 (1)	19.60 (7)
Log K_{120}	13.23 (1)	15.80 (7)
Log K_{130}	8.28 (3)	13.19 (2)
Log K_{140}	6.57 (6)	7.05 (3)
Log β_{140}	**45.54 (5)**	**55.64 (2)**
Log β_{10-1}	-3.8	-0.94
Log β_{10-2}	-7.66	-3.33
Log β_{10-3}	-12.76	-6.59
Log β_{10-4}	na	-10.79

Table 2-1. Formation constants and hydrolysis constants for the complexation of Th(IV) and Pu(IV) by ETAM.

The stability constants of Pu(IV) with several other powerful organic ligands have been reported, and have been tabulated in the Stability Constant Database [16]. The structures are shown in Figure 2-16 and the reported formation constants are summarized in Table 2-2.

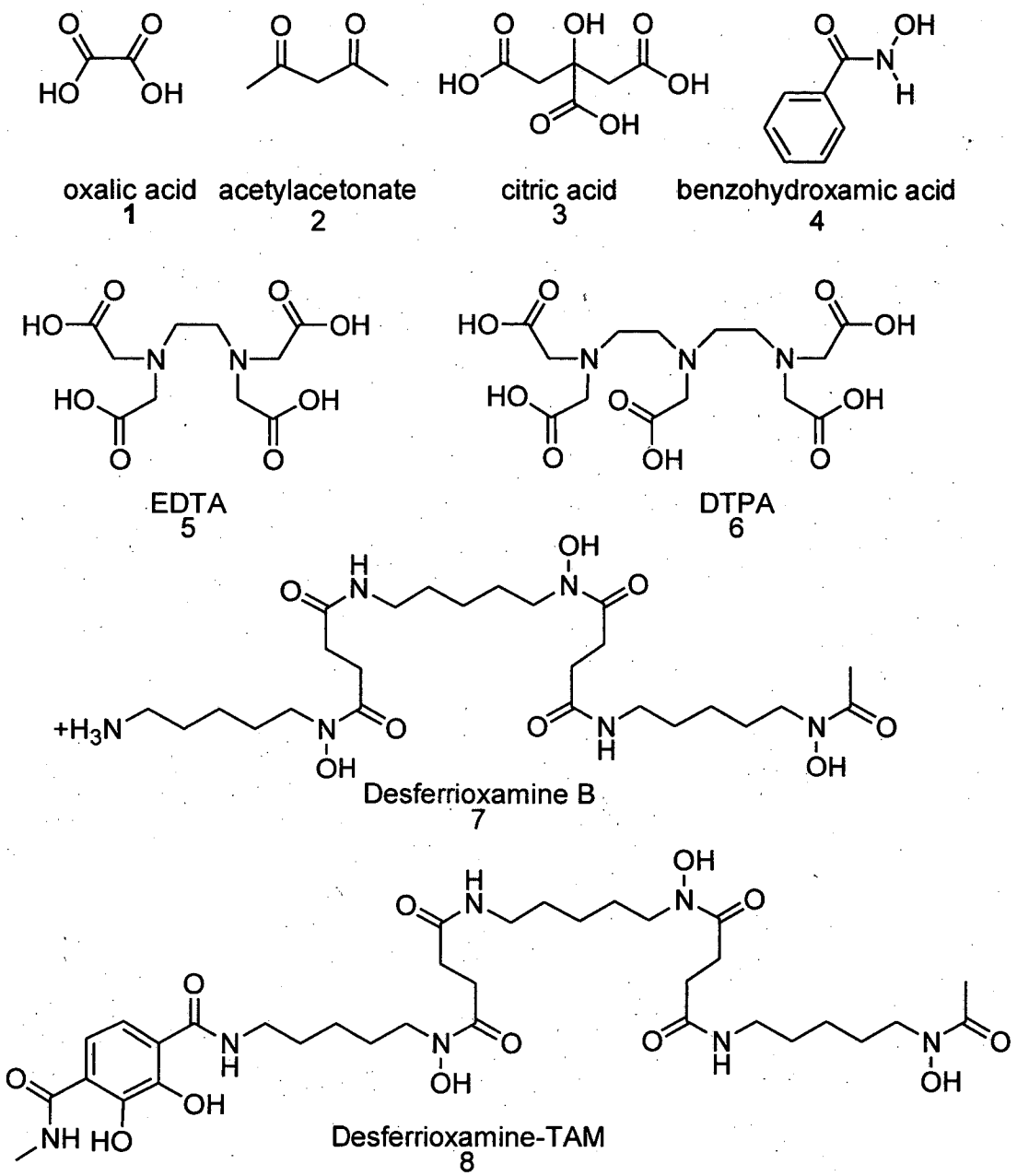

Figure 2-16. Structures of common ligands for which Pu(IV) stability constants have been reported.

ligand	1	2	3	4	5	6	7	8
K_1	8.74	10.5	15.2	12.73	25.6	29.4	30.8	41.7
K_2	8.17	9.2	14.9					
K_3	6.48	8.4						
K_4	4.11	6.0						
temp ^oC	20	25	25	25	20	20	22	25
Ionic Strength	1.0M KNO_3	0.10M $NaClO_4$	0.50M $NaClO_4$	7.0M KNO_3	0.10M $NaClO_4$	0.50M NaCl	none	0.22M KCl
Ref.	17	18	19	20	21	22	23	24

Table 2-2. Stability constants for some common ligands with Pu(IV).

The constants may have been determined at different ionic strengths or temperatures, however they still provide a useful comparison to the TAMs. These ligands, like the catecholates, are commonly considered strong chelating agents for metals such as Fe(III). In particular, the addition of a TAM to DFO(**7**) to produce an octadentate chelator (**8**) raised the formation constant by 11 orders of magnitude over the hexadentate DFO.

The speciation diagram for the Pu – ETAM system, shown in Figure 2-17, illustrates that the TAMs are very strong chelators for Pu : even in 0.1M acid, the complex is only 50% dissociated. The complex is fully formed at pH 9.5. One very important feature of the TAMs is the ability to hinder hydrolysis and precipitation of metal hydroxide species through much of the pH range.

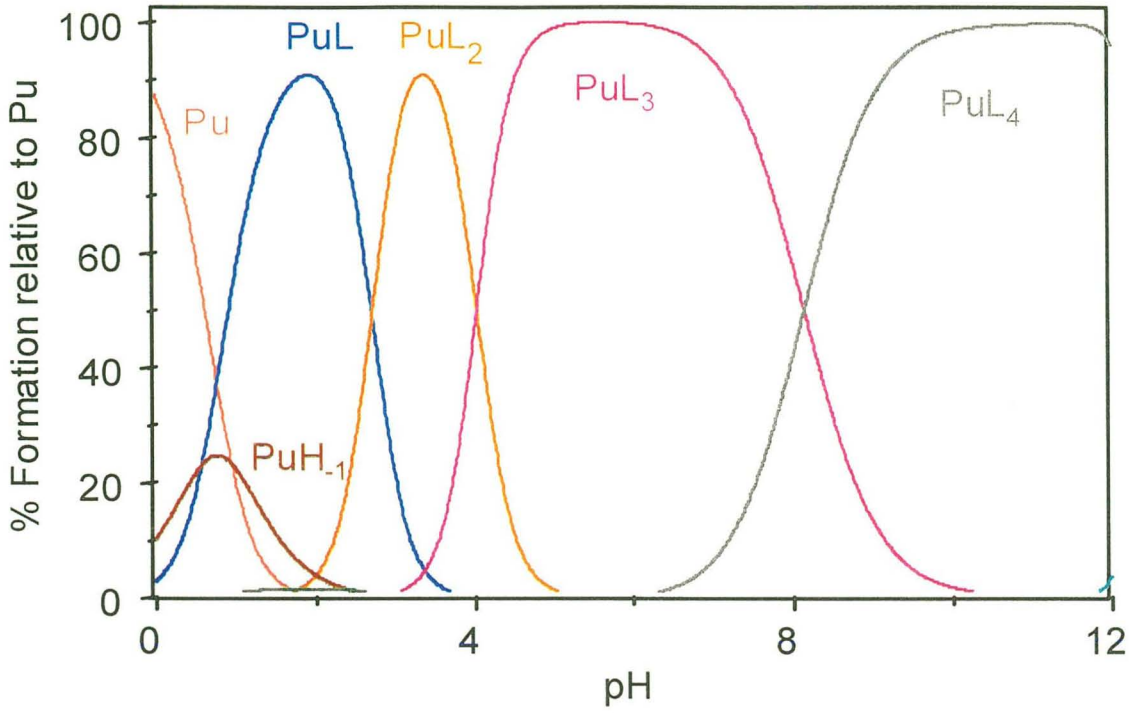

Figure 2-17. Speciation diagram for the Pu – ETAM system. Calculated with $1x10^{-4}$ M H_2ETAM and $1x10^{-5}$ M Pu(IV).

The speciation diagram for a system containing Pu(IV) and a hypothetical octadentate TAM ligand can be estimated from a formation constant of $10^{55.6}$. The diagram, shown in Figure 2-18, indicates that the metal - ligand complex would not form at pH values lower than 2, and substantial hydrolysis of the Pu(IV) would occur below this pH. In actuality, an octadentate ligand should have a higher formation constant than the β_{140} of the corresponding bidentate ligand due to the chelate effect, and the complex wold form at a lower pH.

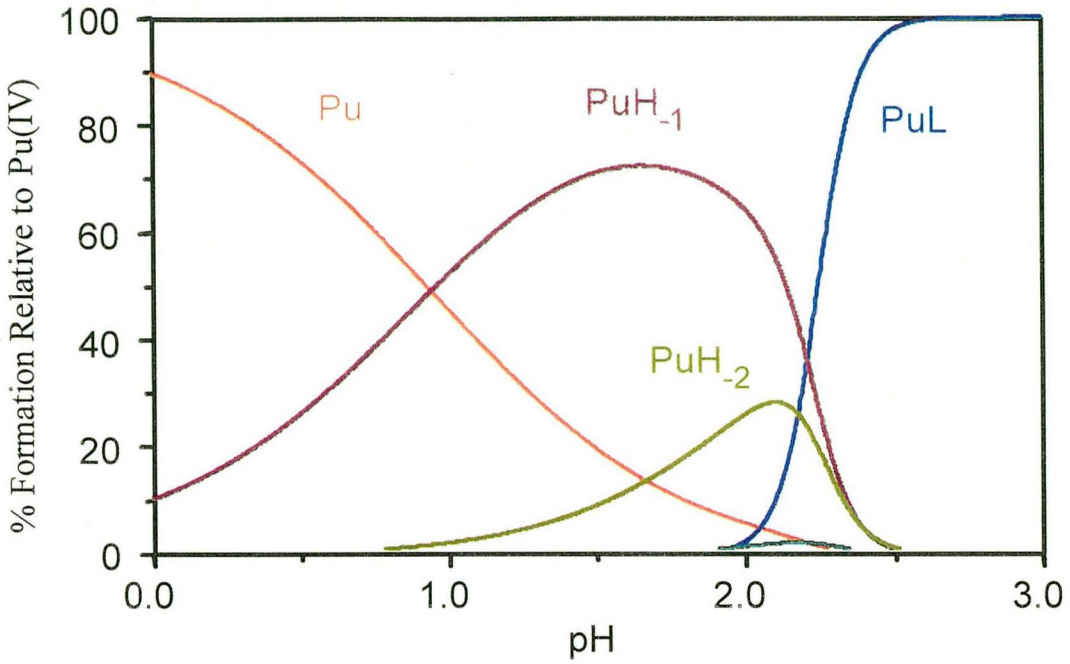

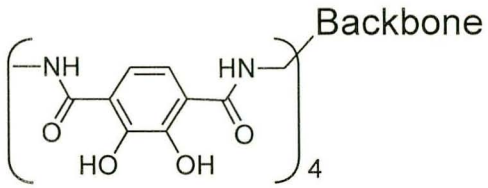

conditions for speciation:
[Pu] = 10^{-5} M, [L] = 10^{-4} M
β_{110} = 55.6
pK_as = 11.5, 11.2, 10.8, 10.5, 6.5, 6.2, 5.8, 5.5

Figure 2-18. Estimated speciation diagram for the complexation of Pu(IV) with a hypothetical octadentate TAM ligand.

Another useful way of comparing the Th(IV) and Pu(IV) constants is to examine their pM values. The pM values are defined as the negative logarithm of the free metal concentration and can be calculated for any pH, concentration of metal, and concentration of ligand. [25] They are useful for comparing ligands of different denticity and number of protonation sites, although in this case the ligand is the same. A higher pM value equates to less free metal in solution, and a stronger chelator at that pH. The standard concentrations for a pM calculation are 1μM metal and 10 μM ligand at a pH of 7.4. In

the case of actinide chelators, it is more useful to look at the entire pH range, and at a variety of ligand and metal concentrations since waste samples can vary widely. The pM value is most useful here for calculating the amount of actinide that would remain in a waste stream after treatment with a TAM. Shown below is a plot of pM vs. pH for the Th(IV) and Pu(IV) ETAM system calculated at three different concentrations of metal and ligand, although there is always a 10 fold excess of ligand: 1μM and 10 μM; 10 μM and 0.1mM; 0.1mM and 1 mM. As the concentrations increase the pM values increase, and in all cases since the ligand is the same, the Pu(IV) has the higher pM value because the formation constants are higher.

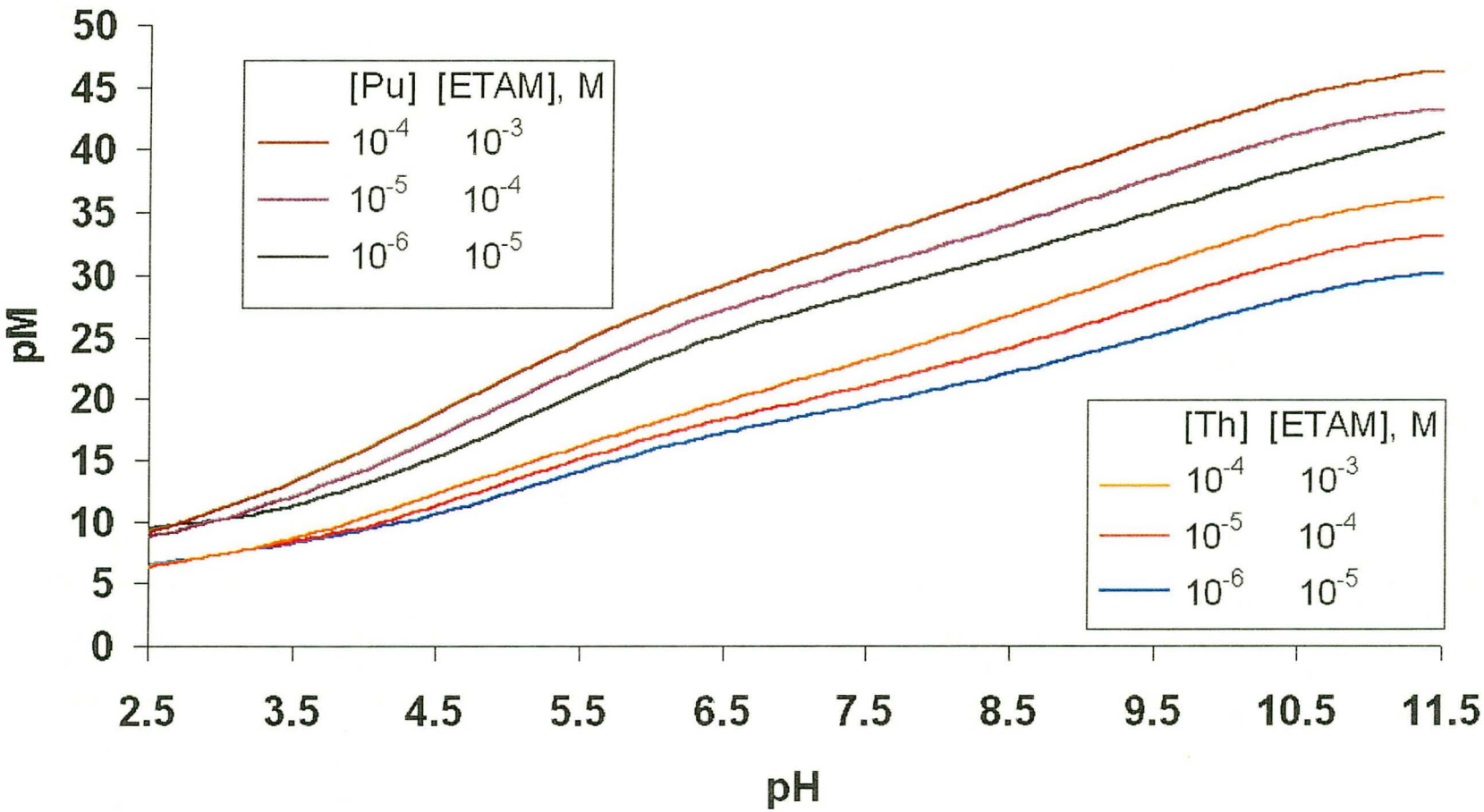

Figure 2-19. Graph of pM vs. pH for the Th(IV) and Pu(IV) ETAM systems.

Conclusion

The simple bidentate 2,3-dihydroxyterephthalamide ligand ETAM has been characterized with respect to its properties as a M(IV) chelator. The complexes of Zr(IV), Ce(IV), and Th(IV) are straightforward to synthesize through a ligand exchange reaction. The crystal structures show that these complexes can adopt different coordination geometries. In the absence of a sufficient amount of ligand to saturate the coordination sphere of Th(IV), the hydrogen bond between the amide proton and catecholate oxygen can be broken to allow the ligand to coordinate with the amide oxygen. The solution thermodynamics shows that the TAMs have very high binding constants with the metals Th(IV) and Pu(IV) and therefore should be well suited for chelating Pu(IV) in a basic waste stream.

Experimental

General. All reagents and solvents were purchased from Aldrich Chemical Company or Fisher Scientific and used as purchased. All solvents were dried over activated alumina and stored over 4Å molecular sieves. All reactions were carried out under Ar and solvents were degassed by evacuating the flask and filling with Ar 3 times. Water was distilled and further purified by a Millipore cartridge system (resisitivity 18 x 10^6 Ω). ^{1}H and ^{13}C NMR spectra were obtained on a Bruker DRX500 (500 MHz) or Bruker AMX400 spectrometer (400 MHz) as noted. All NMR samples were taken in d_6-DMSO. All Microanalyses were performed by the Microanalytical Services Laboratory in the College of Chemistry, University of California, Berkeley. H_2ETAM was synthesized by

published methods. [1] Drs. Darren Johnson, Fred Hollander and Alan are acknowledged for assistance and advice with the X-Ray structures. All of the Pu work was conducted in the laboratory of Professor Heino Nitsche at Lawrence Berkeley National Laboratory with assistance at various times from Dr. Petra Panak, Dr. Dawn Shawnessy, Jerry Bucher, and Richard Wilson.

Metal Complex Synthesis.

$Zr(ETAM)_4K_4$. H_2ETAM (100 mg, 0.4 mmol) was dissolved in 10 mL of degassed MeOH. $Zr(acac)_4$ (48 mg, 0.1 mmol) was dissolved in 5 mL of MeOH and added with filtering to the ligand solution. The reaction was refluxed for 16 hours, then evaporated to a tan solid. This was redissolved in MeOH, degassed, and 0.5 M KOH (0.8 mL, 0.4 mmol) was added. After stirring for 3 hours the solvent was evaporated and the tan solid was dissolved in 0.5 mL MeOH and applied to a sephadex LH-20 column. The desired fraction was collected and evaporated to a tan solid (92 mg, 74% yield). ^1H NMR (d_6-DMSO): δ 0.829 (t, 3H), 3.00 (q, 2H), 6.534 (s, 2H), 10.877 (t, NH). Elemental Analysis calculated (found) for $K_4Zr(ETAM)_4 \cdot 17\ H_2O$: C 37.08 (37.17), H 5.83 (5.98), N 7.21 (7.04). Mass Spec [ES-] m/z : 420.3 $[ZrL_3]^{2-}$ Crystals were grown from diffusion of diethyl ether into 2 mL of ethanol containing 4 mg of the complex.

$Ce(ETAM)_4K_4$. H_2ETAM (100 mg, 0.4 mmol) was dissolved in 10 mL of degassed THF. $Ce(acac)_4$ (51 mg, 0.1 mmol) was dissolved in 5 mL of THF and added with filtering to the ligand solution. The reaction was refluxed for 16 hours, then evaporated to a black solid. This was redissolved in THF, degassed, and 0.5 M KOH (0.8 mL, 0.4

mmol) was added. After stirring for 3 hours the solvent was evaporated and the black solid was dissolved in 0.5 mL MeOH and applied to a sephadex LH-20 column. The desired fraction was collected and evaporated to a black solid (92 mg, 71% yield) ^{1}H NMR (d_6-DMSO): δ 0.912 (t, 3H), 3.08 (q, 2H), 6.564 (s, 2H), 10.688 (t, NH). Elemental Analysis calculated (found) for $K_4Ce(ETAM)_4 \cdot 5H_2O$: C 41.55 (41.49), H 4.79 (4.65), N 7.94 (8.08).

$Th(ETAM)_4K_4$. H_2ETAM (100 mg, 0.4 mmol) was dissolved in 10 mL of degassed MeOH. $Th(acac)_4$ (62 mg, 0.1 mmol) was dissolved in 5 mL of MeOH and added with filtering to the ligand solution. The reaction was refluxed for 16 hours, then evaporated to a tan solid. This was redissolved in MeOH, degassed, and 0.5 M KOH (0.8 mL, 0.4 mmol) was added. After stirring for 3 hours the solvent was evaporated and the tan solid was dissolved in 0.5 mL MeOH and applied to a sephadex LH-20 column. The desired fraction was collected and evaporated to a tan solid (100 mg, 72% yield). ^{1}H NMR (d_6-DMSO): δ 0.91 (t, 3H), 3.086 (q, 2H), 6.63 (s, 2H), 10.874 (t, NH). Elemental Analysis calculated (found) for $K_4Th(ETAM)_4 \cdot 11H_2O$: C 36.31 (36.38), H 4.95 (4.73), N 7.06 (6.90). FAB-MS(-), m/z : 1349.2 $[ThL_4 \cdot 3K]^-$.

$[Th(ETAM)_3]_2 \cdot 4\ Me_4N$. H_2ETAM (76 mg, 0.3 mmol) was dissolved in 10 mL of degassed MeOH. $Th(acac)_4$ (62 mg, 0.1 mmol) was dissolved in 5 mL of MeOH and added with filtering to the ligand solution. The reaction was refluxed for 16 hours, then evaporated to a tan solid. This was redissolved in MeOH, degassed, and 0.5 M KOH (0.6 mL, 0.3 mmol) was added. After stirring for 3 hours the solvent was evaporated and the tan solid was dissolved in 0.5 mL MeOH and applied to a sephadex LH-20 column. The desired fraction was collected and evaporated to a tan solid (94 mg, 86% yield).

Elemental Analysis calculated (found) for $K_4Th_2(ETAM)_6 \cdot 16H_2O$: C 35.88 (35.38), H 4.85 (4.59), N 6.97 (6.76). FAB-MS(-), m/z : 1021 $[Th_2L_6 \cdot 2K]^{2-}$. Crystals were grown from diffusion of either methyl tert-butyl ether or diethyl ether into 1 mL of methanol containing 4 mg of the K^+ salt of the complex and 4 mg of NH_4Cl.

Structure Determination and Refinement.

All X-ray structure data sets were collected on a Siemens SMART Area Detector diffractometer.[26] Crystals were mounted on quartz capillaries in Paratone oil and were cooled in a nitrogen stream on the diffractometer. Peak integrations were performed using Siemens SAINT software package. [27] Space group determinations were done by the software XPREP. The three Th structures were solved and refined using the teXsan software package [28] and the Zr structure was solved and refined using the SHELXTL software package [29]. All hydrogen atoms were fixed at calculated positions and their thermal parameters refined isotropically. For $[Zr(ETAM)_4]^{4-}$ only the Zr, oxygens, and nitrogens of the ligand were refined anisotropically. For the first $[Th(ETAM)_3]_2^{4-}$ dimer, the Th and coordinating oxygens were refined anisotropically. In the other two structures, all non-hydrogen atoms were refined anisotropically. Tables of crystal properties, atom coordinates, and thermal parameters can be found in Appendix 2.

Solution Thermodynamics.

Apparatus. A temperature controlled 100mL titration flask with attached quartz UV-Vis cell has been described in detail elsewhere. [30] An Accumet pH-meter (model AR15 or 15) and a corning glass-bulb electrode were used for electrode potential measurements.

A Hewlett-Packard 8452a spectrophotometer (diode array) was used for the collection of absorbance data and was always turned on for at least 1 h before use to allow the lamp to come to operating temperature. The autoburets, pH meters, and spectrophotometer were controlled by a personal computer using modules of the LABVIEW[31] programming environment, written by Dr. Brendon O'Sullivan. [30]

Standardization of Th(IV) stock solution. [32] A Th(IV) solution was prepared by dissolving $ThCl_4$ in HCl and HNO_3 such that the [Th(IV)] was approximately 5mM and the [H+] was 0.2 M. In a 40 °C temperature controlled cell, 2.5 mL of the Th(IV) solution was diluted into 50 mL of ddH_2O and 4 drops of a 0.1% pyrocatechol violet solution was added. The solution was titrated with 0.1018 M EDTA until the pink color disappeared. This was repeated 5 times for a final concentration of 0.0506 M (0.0002) Th(IV) in the stock solution.

Purification of ^{239}Pu. A modified protocol was used for the purification of the ^{239}Pu [10]: zinc/mercury amalgam was used instead of ferrous sulfamate for the reduction. The anion exchange resin was Dowex. Alpha spectra were collected with a Tennelec TC257 spectrometer. Liquid scintillation counting was performed with a Wallac Guardian 1414LSC and the scintillation cocktail was Eco-Lume (ICN). Bulk electrolysis followed a slight modification of published procedures [11]: a Ag/AgCl reference electrode was used instead of NHE. Electrolysis was conducted in a 100 mL glass beaker fitted with a stir bar, platinum mesh working electrode, Ag/AgCl reference electrode, and platinum counter electrode. An IBM Voltammic analyzer was used to adjust the potential.

Low-pH and Standard Electrode Calibration. The standard electrode calibration was conducted before each titration following published protocol. [30] The electrode used in the

Th(IV) titrations was calibrated by adding 2.000mL of HCl (ca. 0.1M) to 50.0 mL of 0.1M KCl, and the solution was titrated with KOH (ca. 0.1M) to pH 11.6. The electrode used in the Pu(IV) titrations was calibrated by adding 0.800mL of $HClO_4$ (ca. 0.1M) to 20.0 mL of 0.1M $NaCl)_4$, and the solution was titrated with NaOH (ca. 0.1M) to pH 11.6. The data were analyzed using the program GLEE[33] allowing refinement of E° and slope. For low-pH titrations, a correction was made for the junction potential. [30]

Th(IV) ETAM Titrations. Into 50 mL of 0.1 M KCl was added an aliquot of 0.024089 M H_2ETAM solution in MeOH (0.05189 mL, 0.00125 mmmol), an aliquot of a 0.0506 M Th(IV) stock solution (0.0049 mL, 0.00025 mmol), HEPES (4.44 mg, 0.019 mmol), MES (4.7 mg, 0.022 mmol), NH_4Cl (1.6 mg, 0.03 mmmol), and 1.000 mL of 0.0988 M HCl. This was titrated with 0.1003 M KOH from pH 2.8 to 10.5, then back to pH 2.8 with 0.0988 M HCl, with a constant pH increment of 0.05 such that 67 to 82 data points, each consisting of pH and absorbance spectrum, were collected in each direction. This was repeated 3 times, for a total of 5 titrations. An equilibration time of 3 min after addition of the titrant was used. The specifics of data collection of been detailed elsewhere. [30]All absorbance measurements were less than 1.1 absorbance units. The spectrum was recorded from 250 to 550 nm and the data points from 320 to 420 nm were used in the data processing. All data was analyzed using the program pHAB.[8] The pKa values for H_2ETAM are 6.1 and 11.0 and were previously determined. [1]

Pu(IV) ETAM titrations. These were conducted in the same manner as above; however, the electrolyte was 0.1M $NaClO_4$, the acid was ca. 0.1M $HClO_4$, the base was ca. 0.1M NaOH or KOH, and 150 data points were collected over the pH range 2.4 to 10.5.

Low pH titration. An aliquot of a 0.0241 mM H_2ETAM solution in MeOH (0.5189 mL, 0.0125 mmol, 1%MeOH total) and an aliquot of a 0.0506 M Th(IV) stock solution (0.049 mL, 0.0025 mmol) were added to 50 mL of 0.1 M KCl and the pH was lowered from 3.5 to 2.9 with the addition of 0.5 mL of 0.0988 M HCl. The solution was titrated with 0.0998 M HCl with a constant pH increment such that 25 data points were collected. The pH and absorbance data were recorded as described above for the "Th(IV) – ETAM titrations".

References

(1) Garrett, T. M.; Miller, P. W.; Raymond, K. N. *Inorg. Chem.* **1989**, *28*, 128-133.

(2) Sofen, S. R.; Abu-Dari, K.; Freyberg, D. P.; Raymond, K. N. *J. Am. Chem. Soc.* **1978**, *100*, 7882-7887.

(3) Sofen, S. R.; Cooper, S. R.; Raymond, K. N. *Inorg. Chem.* **1979**, *18*, 1611-1616.

(4) Shannon *Acta Cryst.* **1976**, *A32*, 751.

(5) Garrett, T. M.; Cass, M. E.; Raymond, K. N. *J. Coord. Chem.* **1992**, *25*, 241-253.

(6) Xu, J.; Radkov, E.; Ziegler, M.; Raymond, K. N. *IC* **2000**, *39*, 4156-4164.

(7) Xu, J.; Radkov, E.; Raymond, K. N. **in preparation**.

(8) Gans, P.; Sabatini, A.; Vacca, A. *Ann. Chim-Rome* **1999**, *89*, 45-49.

(9) Baes, C. F.; Mesmer, R. E. *The Hydrolysis of Cations*; Wiley: New York, 1976.

(10) Coleman, G. H. *The Radiochemisty of Plutonium*; National Acadmey of Sciences: Springfield, Va., 1965.

(11) Cohen, D. *J. Inorg. Nucl. Chem.* **1961**, *18*, 207-210.

(12) Cleveland, J. M. *The Chemistry of Plutonium*; Gordon and Breach Scientific Publishers:, 1970.

(13) Cotton, F. A.; Wilkinson, G. *Advanced Inorganic Chemistry*; John Wiley and Sons: New York, 1988.

(14) Cohen, D. *J. Inorg. Nucl. Chem.* **1961**, *18*, 211.

(15) Browne, E.; Firestone, R. B. *Table of Radioactive Isotopes*; John Wiley and Sons: New York, 1986.

(16) Stability Constant Database; 1.0 ed.; Academic Software, 1997.

(17) Moskvin, A.; Gelman, A. *Zhur. Neorg. Khim.* **1958**, *3*, 962.

(18) Rydberg, J. *Sv. Kem. Tidskr.* **1955**, *67*, 499.

(19) Nebel, D. *Z. Phys. Chem.* **1966**, *232*, 368.

(20) Barocas, A.; Baroncelli, F.; Biondi, G.; Grossi, G. *J. Inorg. Nucl. Chem.* **1966**, *28*, 2961.

(21) Cauchetier, P.; Guichard, C. *Radiochimica Acta* **1973**, *19*, 137.

(22) Piskunov, E.; Rykov, A. *Radiokhim.* **1972**, *14*, 260.

(23) Jarvis, N. V.; Hancock, R. D. *Inorg Chim Acta* **1991**, *182*, 229-232.

(24) Whisenhunt, D. W.; Neu, M. P.; Hou, Z. G.; Xu, J.; Hoffman, D. C.; Raymond, K. N. *Inorg Chem* **1996**, *35*, 4128-4136.

(25) Weitl, F. L.; Raymond, K. N. *J. Am. Chem. Soc.* **1980**, *102*, 2289-2293.

(26) SMART; Siemens Industrial Automation Inc.: Madison, 1994.

(27) SAINT; 4.024; Siemens Industrial Automation Inc.: Madison, 1994.

(28) teXsan; Molecular Structure Corporation, 1992.

(29) SHELXTL; Siemens Industrial Automation Inc.: Madison, 1994.

(30) Johnson, A. R.; O'Sullivan, B.; Raymond, K. N. *Inorg. Chem.* **2000**, *39*, 2652-2660.

(31) LABVIEW; 5.0.1; National Instruments Corporation: Austin, TX.

(32) Schwarzenbach, G.; Flaschka, H. *Complexometric Titrations*; Methuen and Co. Ltd.: London, 1969.

(33) Gans, P.; O'Sullivan, B. *Talanta* **2000**, *51*, 33.

CHAPTER THREE

The Investigation of 2,3-Dihydroxyterephthalamides as Liquid-liquid Extractants of High Oxidation State Metals

Introduction

Solvent extraction has been tremendously important in the nuclear industry for purification of the actinides. [1,2] The majority of ligands that have been developed as liquid-liquid extractants have targeted acidic waste and there is a lack of ligands that are suited for the basic conditions of tank waste. [3-12] The 2,3-dihydroxyterephthalamides (TAM) are appealing to develop as liquid-liquid extractants because of the high formation constants of the actinide-TAM complexes and their ability to chelate Th(IV) and Pu(IV) at high pH. The high radioactivity of Pu-239 and concern over producing large volumes of mixed waste precluded the study of the TAMs as extractants for Pu(IV). However the ligands presented here were evaluated for Fe(III) extraction. The results from the Fe(III) extraction can be directly applied to Pu(IV) extraction based on the similarities that were presented in Chapter Two between these two metals in their aqueous chemistry with the TAMs.

Ligand Design and Synthesis

The complexation of Fe(III) or Pu(IV) with 3 or 4 TAM^{2-} ligands, respectively, will result in a complex with an overall 3^- or 4^- charge. Such a complex would be recalcitrant to extraction into an organic solvent, so 2 approaches were developed that

would compensate for this charge and produce an extractable metal - TAM complex (Figure 3-1).

In the first approach, the incorporation of an ammonium into one side chain results in a ligand that has an overall -1 charge, and hence a neutral metal complex. The other amide can be an alkyl group chosen to maximize solubility in an organic phase. Throughout this chapter these are referred to collectively as aminoTAMs. This is conceptually similar to lariat ethers – also called ionizable macrocycles – in which a carboxylate attached to a crown ether is used to neutralize the charge on a Cs^+ crown complex. [13,14]

The second approach utilizes a lipophillic counter cation, cetylpyridinium, to achieve phase transfer of the charged alkyl TAM complex. Many examples of ion-pairs have been used for metal extraction where the ligand is usually a neutral crown ether or phosphate and nitrate is coextracted.[4,15,16] A closer example of ion-pair extraction to the approach employed here was presented by Hrdlicka with the extraction of molybdenum(VI) into $CHCl_3$ in the presence of a tetraalkyl phosphonium cation and 2,3-dihydroxynapthalene.[17] His approach was slightly different than the one presented here since he was examining the extraction of oligonuclear anions of Mo(VI) in the presence of tetraalkyl phosphonium cations, and noted "A considerable positive effect on the ion-pair extraction of Mo(VI) is achieved if an o-diphenolic chelating agent…is added to the extraction system".

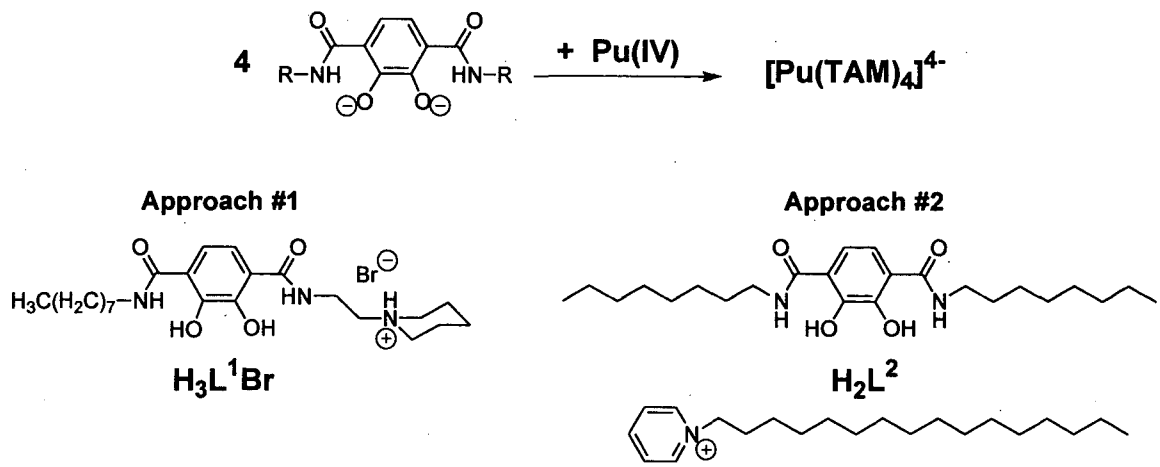

Figure 3-1. Alkyl TAMs form charged complexes with Fe(III) and Pu(IV). Incorporating amines into one side chain or using lipophillic counter cations allows the complex to be extracted into organic solvents.

The specific side chains in the aminoTAM H_3L^1Br - the ethyl piperidinium and the octyl amide – produced a ligand soluble in $CHCl_3$ and whose Fe(III) complex is also soluble in $CHCl_3$ and not water. An iterative process was used to arrive at this ligand design: several ligands had been made which almost worked as extractants, then the promising features were carried on to the next generation of ligands. For approach #2, the alkyl TAM with either octyl, cyclohexyl, or hexyl side chains worked well in this extractant system. The ethylTAM also worked for extraction, however this Fe(III) complex is also soluble in water, so this would not be a very efficient ligand for metal extraction.

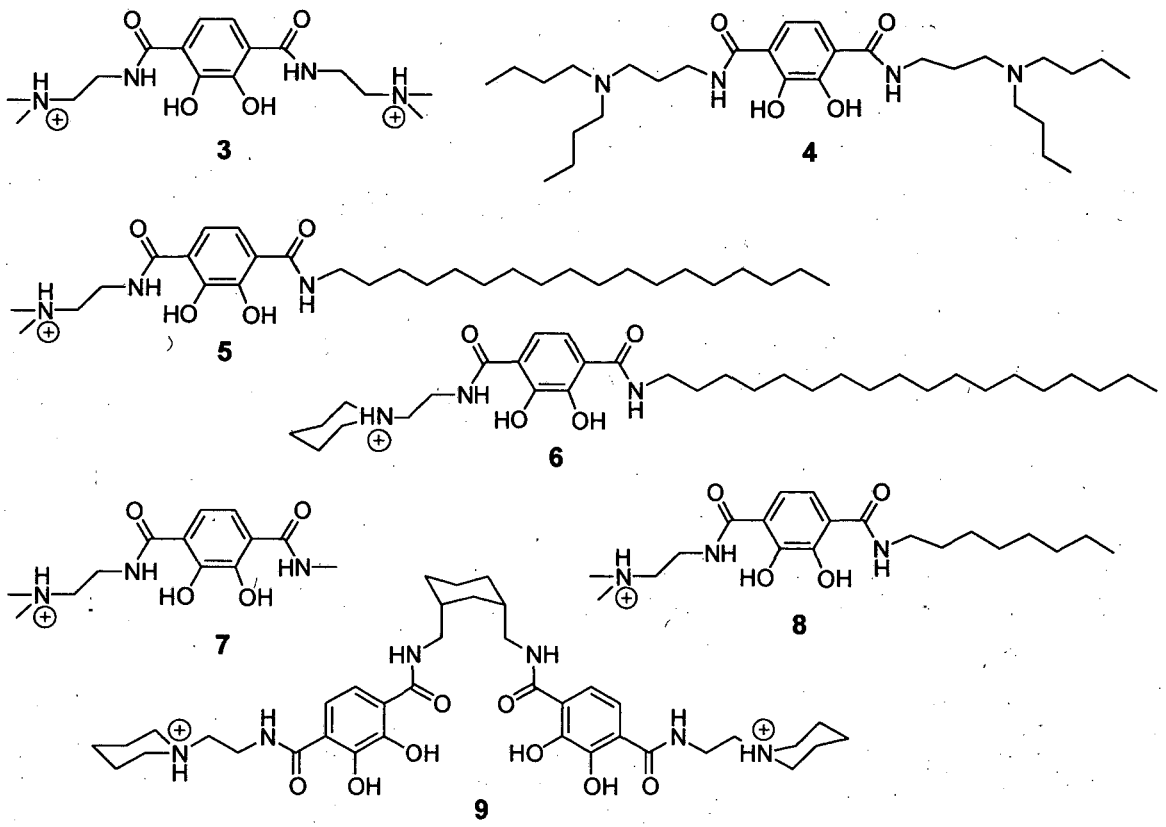

Figure 3-2. AminoTAM ligands which were synthesized as potential metal extractants.

The series of ligands that was synthesized as potential extractants is shown in Figure 3-2. Ligands **3** and **4** were made as the simplest examples of aminoTAMs, since symmetric amide substitution is easy to do. However it was found that these ligands are very soluble in water and it was clear that unsymmetric amide substitution would be necessary to increase hydrophobicity. In addition, the unsymmetric ligands would allow a metal complex to exist as a neutral complex over most of the pH range, whereas ligands **3** and **4** would mostly exist as the 3^+ complex with Fe(III). With this in mind, ligands **5** through **8** were made to examine how lipophillic those amides needed to be. Ligands **5**

and **6** are too lipophillic, and the C_{18} side chain prevents dissolution in many solvents. Ligands **7** and **8** are soluble in water and their Fe(III) complexes partition between water and $CHCl_3$. The balance between these 4 ligands – H_3L^1Br – was found to work well for extraction, and the specific results will be discussed later in this chapter. Finally in an effort to increase the denticity of the extractants, ligand **9** was made, but the large organic substituents and the 2+ charge prevented its dissolution in water or any organic solvent except DMSO and DMF.

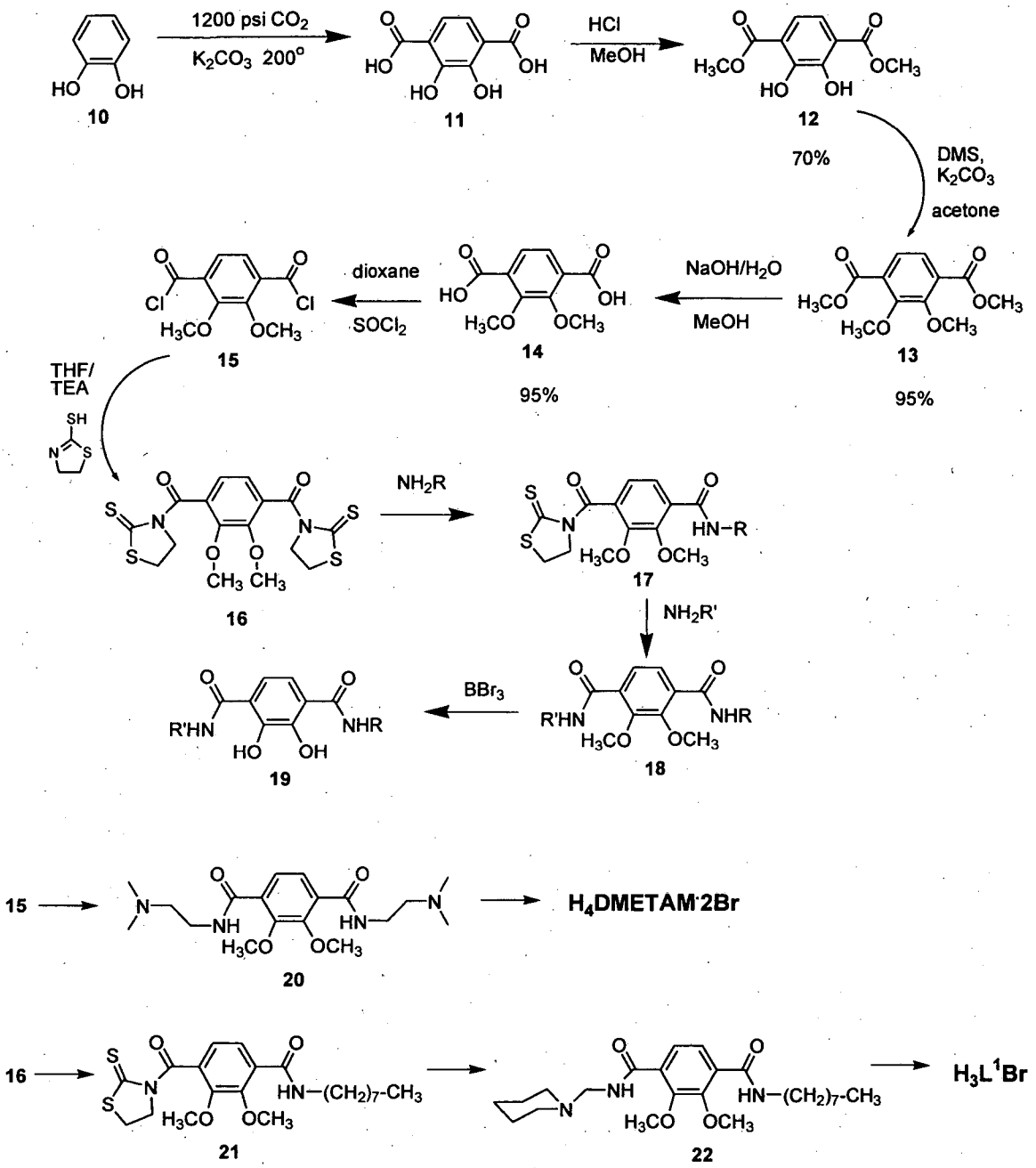

Scheme 3-1. Synthetic scheme for the TAMs.

These ligands were all synthesized by established procedures (Scheme 3-1).[18-21] Catechol is carboxylated to form **11**, the crude material is converted to the methyl ester **12**, the phenolic oxygens are methyl protected to **13**, the esters are saponified to provide

14 which is activated to the acid chloride **15** and coupled with 2-mercaptothiazoline to yield the activated intermediate **16**. This thiaz-activated intermediate is substituted with one equivalent of an amine, and the mono-thiaz-mono-amide TAM intermediate **17** is purified before the second thiaz is substituted with a different amine, yielding the methyl-protected unsymmetric TAM **18**. When two different amides are desired, either the alkyl amine or the diamine has to be used first. It was found that substituting the diamine first eased purification of the resulting **17** since this could be easily separated from any side products or unreacted starting material **16** by extractions, recrystallizations, or column chromatography with silica or alumina gel. This was discovered after H_3L^1Br was synthesized by first installing the octylamide **21**, followed by the ethylpiperidine **22**. The ligands were easily deprotected under standard conditions with BBr_3.

Amino TAMs – The effect of peripheral charge on the stability of an Fe(III) complex

The ligand (N,N'-dimethylaminoethyl)-2,3-dihydroxyterephthalamide (DMETAM, **3**, Figure 3-2 and Figure 3-3) was initially synthesized to study its ability to function as an extractant for actinides. The amines on the side chains allow the metal-ligand complex to exist in a range of charges from 3+ to 3- depending on the pH of the solution. In its neutral state, it was postulated that the complex would be soluble in an organic solvent. However it was found that DMETAM and its Fe(III) complex were highly soluble in water at all pH values and exhibited surprising strength as an Fe(III) chelator. This section will detail some of the aqueous coordination chemistry of DMETAM as an Fe(III) chelator, and the parallels that can be drawn with the hydrophobic amino-TAMs used as extractants.

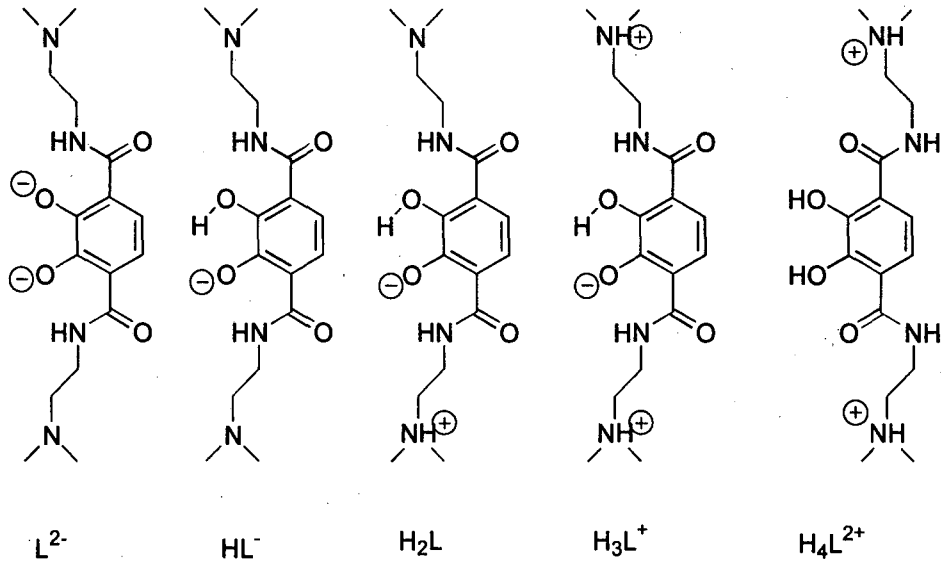

Figure 3-3. Structure of the ligand DMETAM, and assignment of stepwise protonation states.

Before determining Fe(III) formation constants, the protonation constants of the 4 acidic protons were determined. For ethyl-2,3-dihydroxyterephthalamide (ETAM), the pK_as of the two catecholate protons are 6.1 and 11, [19] so it was assumed that the pK_as of DMETAM would be similar to those, with 2 additional pK_as around 9 for the pendant amines. The stepwise protonation constants (K_{MLH}) for this ligand are defined as:

$$L^{2-} + H^+ \rightleftarrows HL^- \qquad K_{011}$$

$$HL^- + H^+ \rightleftarrows H_2L \qquad K_{012}$$

$$H_2L + H^+ \rightleftarrows H_3L^+ \qquad K_{013}$$

$$H_3L^+ + H^+ \rightleftarrows H_4L^{2+} \qquad K_{014}$$

The protonation constants were determined by 4 potentiometric titrations in collaboration with Brendon O'Sullivan. A solution containing DMETAM was titrated with KOH to pH 11, then with HCl to pH 3. The data (400 points in all) were refined with HYPERQUAD. [22,23] The constants of 5.36(2), 8.30(2), 9.39(2), and 10.95(1) are assigned to the following protons, respectively: catechol OH, tertiary amine, tertiary amine, and catechol OH. The protonation constant of one of the catecholate protons for DMETAM (5.36) is significantly lower than for ETAM (6.1). This is attributed to an electrostatic effect of the 2^+ charge on the ligand.

A batch titration monitored by ^{1}H NMR spectroscopy was performed to confirm that the pK_as were assigned to the correct protons (Figure 3-4). The signals in the ^{1}H NMR spectra are assigned to the following protons: the singlet at ca. 7 ppm is the aromatic CH; the triplet between 3.5 and 3.7 ppm is the ethylene CH_2 next to the amide; the triplet between 2.5 and 3.5 ppm is the ethylene CH_2 next to the amine; and the singlet between 2 and 3 ppm are the methyl groups attached to the amine. The signal at ca. 2 ppm is an internal standard of acetonitrile, and the signal at ca. 4.7 ppm is HOD. Seven solutions of DMETAM were prepared at different pD values of 1.5, 5.2, 7.8, 8.2, 8.8, 10.7, and one with a very large concentration of base so the change in chemical shift as a function of pD could be monitored. From low pD through pD 7.8 the only resonance shifting is the aromatic proton, indicating that the low pKa of 5.3 is for one catecholate proton. From pD 7.8 through 10.7 the doublets of the methylene protons and the singlet for the N-methyl groups shift. This indicates that the pKas of 8.3 and 9.4 were correctly assigned to the 2 amines. The aromatic peak has shifted a slight amount in the pD 10.7 spectrum, but the most significant shift comes when the pD of the solution is raised very

high. This indicates that the highest pKa of 10.95 does belong to the second catecholate proton.

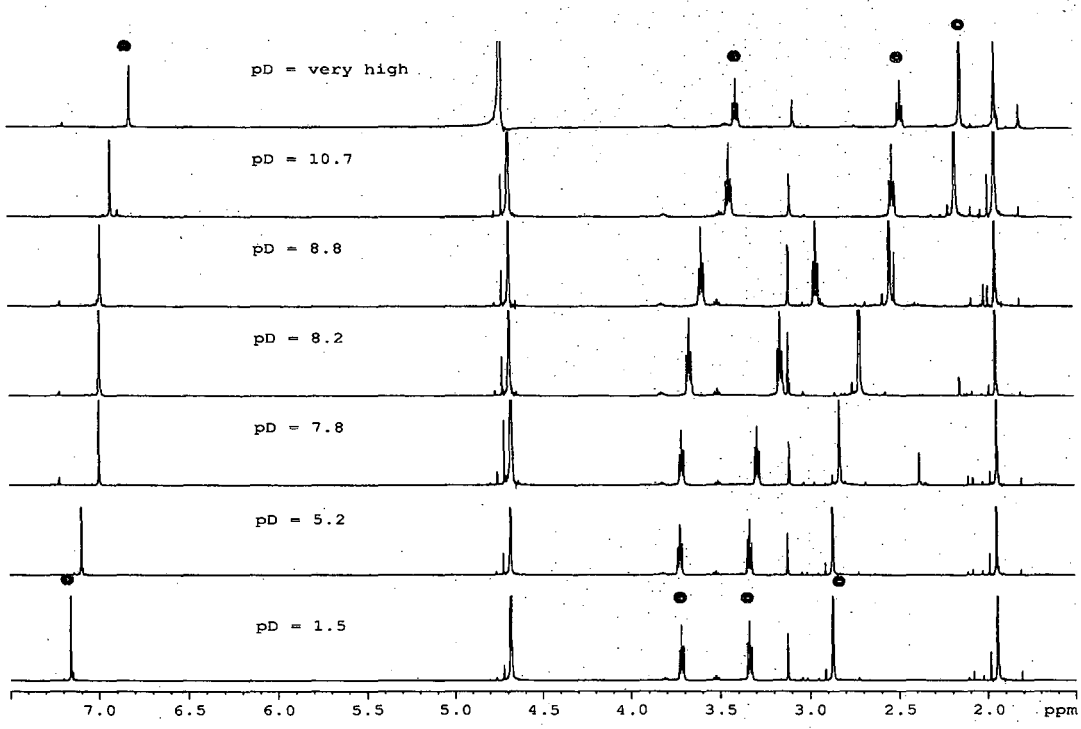

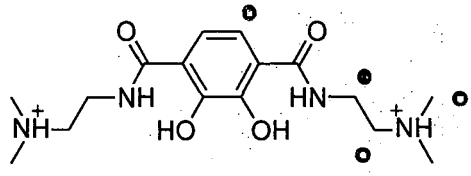

Figure 3-4. Spectra from batch titration of DMETAM monitored by ^{1}H NMR spectroscopy.

Since the TAM ligands are protic, the formation of the complex is dependent on the proton concentration. In conjunction with Brendon O'Sullivan the formation constants for the Fe – DMETAM complex were determined by titration of a solution containing Fe(III) and DMETAM with either HCl or KOH and the changes in the UV-Vis spectrum as a function of pH were monitored. The spectra show distinct changes

between 400 and 800 nm, which is assigned to a ligand to metal charge transfer.[24] Two separate types of titrations were conducted – one from pH 3 to 6 to determine the constants for the formation of the 1:2 and 1:3 complex and one from pH 2.8 to 1.5 to determine the constant for the 1:1 complex.

The assignment of the protons of DMETAM is different for the Fe(III) constants than when determining the protonation constants. The Fe(III) complexation is complete by pH 5, and the two terminal amines do not deprotonate until higher pH values. Thus, when the ligand is deprotonated on the catecholates to coordinate to the metal, the amines are protonated, so the neutral coordinating ligand should be referred to as H_2L. However, this "H_2L" is a tautomer of the "H_2L" named during the pKa determination (Figure 3-5). To avoid confusion during the discussion of the stepwise formation constants, the constants will be referred to as K_1, K_2, K_3, and β_3, instead of the K_{MLH} notation.

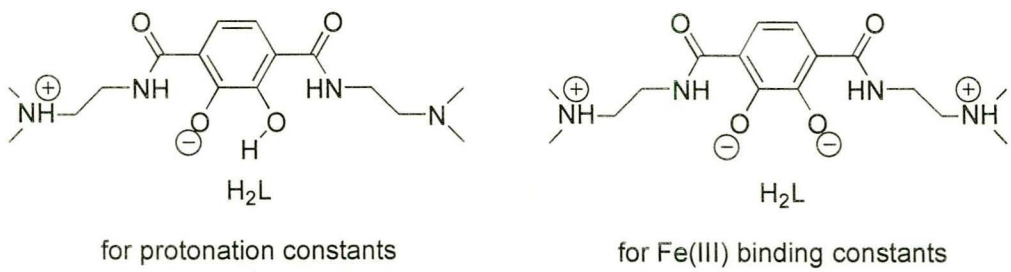

Figure 3-5. Tautomers of H_2L for protonation constant and Fe(III) binding constant discussions.

$$Fe^{3+} + H_2L \rightleftarrows Fe(H_2L)^{3+} \qquad K_1 = [Fe(H_2L)^{3+}] / [Fe][H_2L]$$

$$Fe^{3+} + 2\,H_2L \rightleftarrows Fe(H_2L)_2^{3+} \qquad K_2 = [Fe(H_2L)_2^{3+}] / [Fe][H_2L]^2$$

$$Fe^{3+} + 3\,H_2L \rightleftarrows Fe(H_2L)_3^{3+} \qquad K_3 = [Fe(H_2L)_3^{3+}] / [Fe][H_2L]^3$$

Conditions for each titration were chosen such that the absorbance of the charge transfer bands could be conveniently monitored. The low pH titration performed to determine the K_1 constant contained Fe(III) and ligand concentrations of 2.5×10^{-4} M and the solution was titrated with ~0.1 M HCl to pH 1.5. The spectra, monitoring the disappearance of the $(FeL)^{3+}$ complex, are shown in Figure 3-6. These spectra represent 50% dissociation of the complex to free Fe(III) and the data were refined using the program pHAB [25] to a value of 16.90(2) for Log K_1.

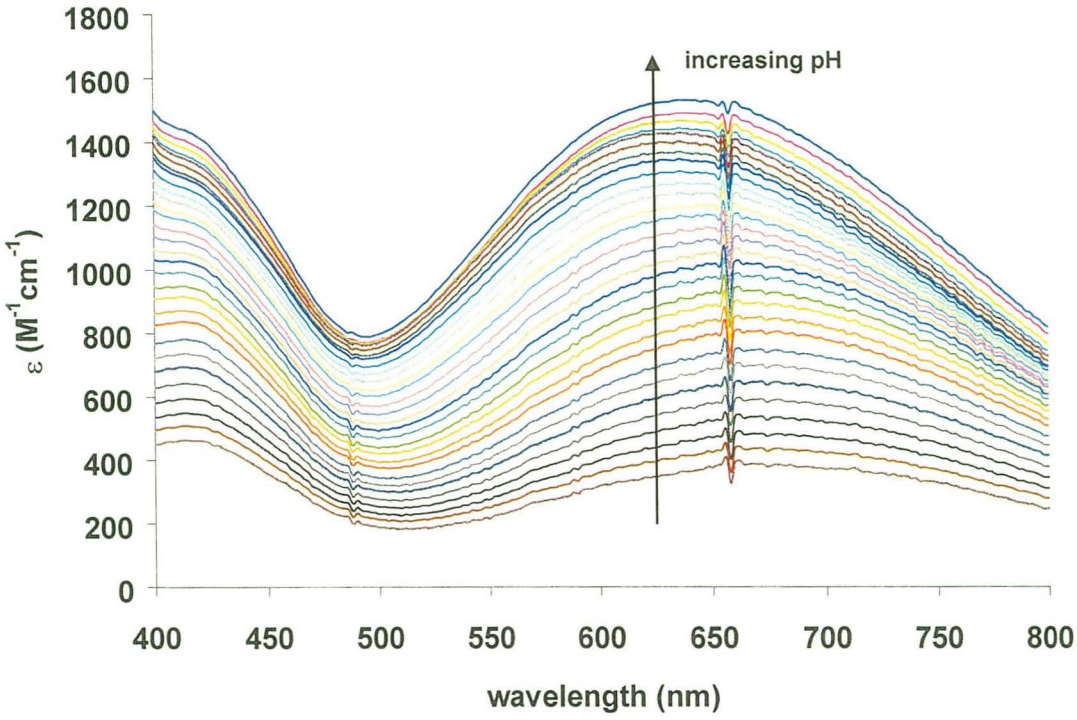

Figure 3-6. Visible spectra from the titration of Fe-DMETAM from pH 3 to 1.5.

For determining K_2 and K_3, a solution was prepared with DMETAM and Fe(III) concentrations of 4×10^{-3} M and 1.3×10^{-4} M for a 1:3 metal:ligand ratio. The solution

was titrated from pH 3 to 6 and back to 3, collecting UV-Vis spectra for at least 25 pH points. The changes in the spectra seen in Figure 3-7 are dominated by a shift of λ_{max} for the ligand to metal charge transfer bands from 590nM to 450nM as the pH increases. These data were refined with pHAB with log K_1 held fixed at 16.90 while K_2 and K_3 were refined. The logs of these constants are 15.78(4) and 12.65(5), respectively, which amounts to a log β_3 of 45.32(4). The speciation is shown in Figure 3-8.

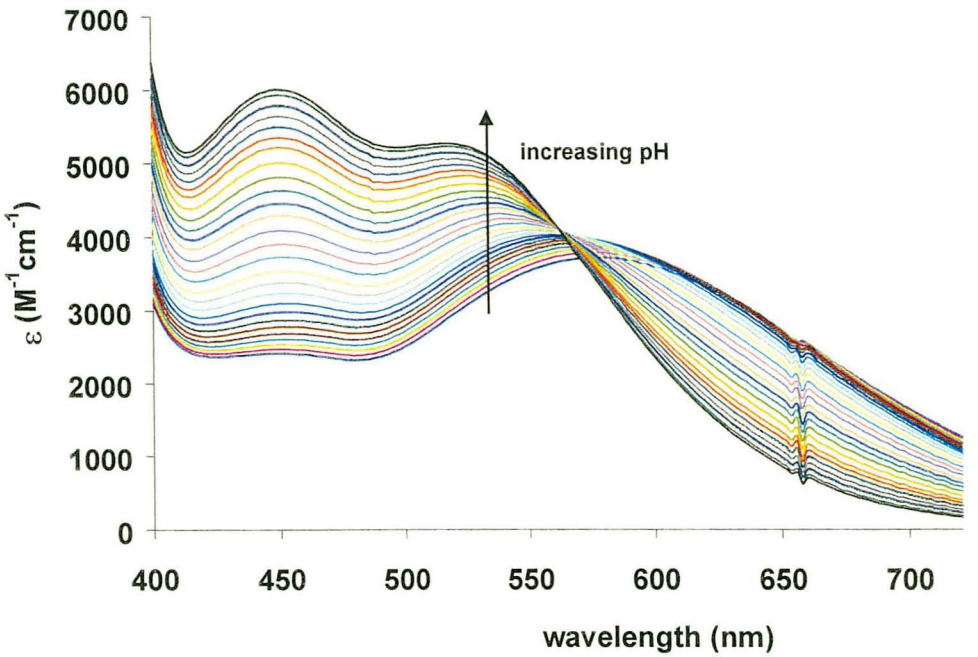

Figure 3-7. Visible spectra from the Fe-DMETAM titration between pH 3 and 6.

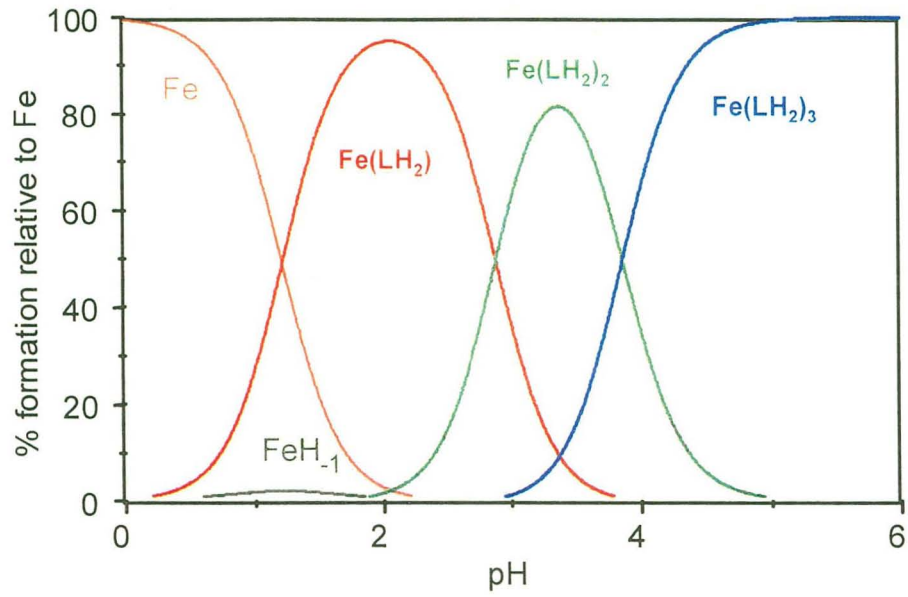

Figure 3-8. Speciation Diagram for Fe-DMETAM system. Calculated with 10^{-5}M Fe(III) and 10^{-4}M DMETAM.

One hypothesis for the stability of the Fe(III) DMETAM complex is that the amines provide a site for extra hydrogen bonding, thereby adding a small amount of stability to the complex. A structural parallel can be drawn between hexadentate ligands synthesized in the Raymond Group in which three bidentate ligands (either TAMs, or 2-hydroxypyridin-3-ones) are attached to a TREN backbone through amide linkages (Figure 3-9). [21] In these ligands, the central amine of the TREN is in the same position relative to the amide as the terminal amines in DMETAM. In the free ligand and Fe(III) complex, the pK_a of the central amine is between 4.3 and 4.6, far less than the expected ammonium pK_a of 9 or 10. This is attributed to a hydrogen bond that is formed between the amine lone pairs and amide protons, in both the free ligand and metal complex. The

X-ray crystal structure of the Fe(III) complex also shows the "inward" orientation of the central nitrogen.

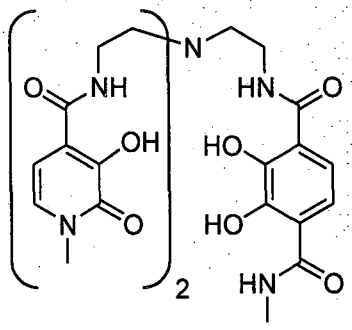

Figure 3-9. Structure of a hexadentate ligand with a TREN backbone.

In the case of DMETAM, the amine protons have pK_as of 8.3 and 9.4, indicative of no hydrogen bonding interaction with the nearby amide protons in the free ligand. The Fe(III) complex is fully formed when the amines are protonated, suggesting that, if hydrogen bonding were contributing to the stability of the complex, it would involve these protons. The crystal structure of the fully protonated ligand, solved by Dr. Dana Caulder, shows no interactions involving the ammonium protons. The expected hydrogen bond between the phenolic hydrogen and amide oxygen is present. [26] In addition, one titration was conducted with the Fe – DMETAM complex up to pH 11 and 6 deprotonations of the metal complex were observed. The pK_as are calculated to be 7.25, 8.19, 8.38, 9.11, 9.36, 10.66, which is a statistical distribution for a mean pK_a of 8.85. This is nearly identical to the mean pKa (8.83) of the free ligand amine pKas of 8.30 and 9.39.

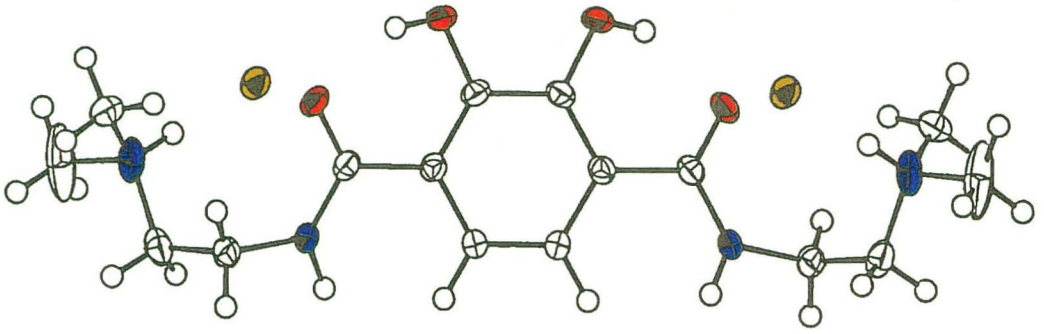

Figure 3-10. X-Ray Structure of $[H_4DMETAM]^{2+}$ $2Br^-$.

The charge of the ligand is probably the dominating factor in the stability of the complex. A TAM ligand containing negatively charged sulfonates (taurTAM) in place of the positively charged amines of DMETAM, was synthesized by Kristy Jurchen and the Fe(III) stability constants were determined by Dr. David VanHorn. The Fe(III) binding constants for these 2 ligands, along with ETAM, are summarized in Table 3-1. Also included in the table are the stoichiometry and charge of the mono-, bis-, and tri-TAM complexes of each ligand. Although the formation constants for the Fe(III) - ETAM system have been previously reported, [19] the values have been recently redetermined by Brendon O'Sullivan with newer titration equipment that was also used for DMETAM titrations.

	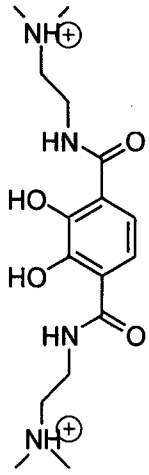 DMETAM	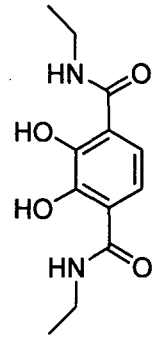 ETAM	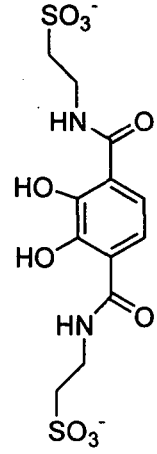 taurTAM
K_1	$[FeL]^{3+}$ 16.90 (2)	$[FeL]^{1+}$ 17.27 (2)	$[FeL]^{-}$ 18.24 (1)
K_2	$[FeL_2]^{3+}$ 15.78 (4)	$[FeL_2]^{-}$ 14.32 (4)	$[FeL_2]^{5-}$ 13.48 (2)
K_3	$[FeL_3]^{3+}$ 12.65 (5)	$[FeL_3]^{3-}$ 11.08 (5)	$[FeL_3]^{9-}$ 8.57 (5)
β_3	45.32 (4)	42.67 (5)	40.29 (7)
pM (at pH 7.4)	25.8	22.8	20.4

Table 3-1. Summary of the Fe(III) stability constants for DMETAM, ETAM and taurTAM.

In this series, K_1 increases as the negative charge on the ligand increases. The charges on the resulting complexes are, respectively, 3^+, 1^+, and 1^-. This suggests that the electrostatic interaction between a 3^+ metal and 4^- ligand contributes greatly to the formation constant. The values for K_2 and K_3 show the reverse of this trend, and decrease as the charge on the ligand, and hence the charge on the metal complex, becomes more negative. It can be inferred that, in the case of taurTAM, the increasing negative charge leads to electrostatic repulsion with the sequential addition of ligands. This is also seen in the difference between the stepwise formation constants. In the case of taurTAM, the addition of each sequential ligand is about 5 orders of magnitude less

favorable than the ligand before. In the case of ETAM, the stepwise decrease is about 3 orders of magnitude for each ligand. The β_3 of DMETAM arises largely from the fact that the addition of the second neutral, zwitterionic ligand to the metal is only $10^{1.12}$ less favorable than the first ligand.

When the TAMs were first characterized as Fe(III) chelators, it was noted that they were extremely efficient at chelating Fe(III) at neutral pH. Another measure of the strength of a particular ligand for Fe(III) binding is the pM value. This is the negative log of the free Fe(III) concentration, and can be calculated at any pH. The pM values that have been calculated for the TAMs are the highest for any bidentate ligand at neutral pH. DMETAM has a lower pK_a than ETAM for one of its phenolic protons without a loss in overall Fe(III) binding strength, so it is not surprising that DMETAM has a higher pM value at neutral pH (and throughout the pH range) than ETAM. The pKas of taurTAM are 11.01 and 6.47, which is reflected in its lower pM value.

Experiment Design for Fe(III) Extraction

Two approaches were described earlier for the extraction of Fe(III) from an aqueous phase (Figure 3-1). To neutralize the charge on the resulting metal complex, one approach utilizes an internal cation (H_3L^1Br) and the other utilizes an alkyl TAM (H_2L^2) and a lipophillic cation. However, in both cases the extraction of Fe(III) from an aqueous phase by a TAM in an organic solvent can be broadly described by the expression:

$$Fe^{3+}_{aq} + 3\ TAM^-_{org} \rightleftarrows Fe(TAM)_{3\ org}$$

In the case of water soluble bidentate TAMs, the mono-, bis-, and tris- Fe(III) complexes are formed as the pH increases and the Fe tris-TAM complex is fully formed

by pH 5. In the case of extraction, it is not expected that any species of lower than 1:3 metal:ligand stoichiometry will form, thus the TAMs should be investigated as extractants over pH 5. In addition, the high formation constants in aqueous solutions will translate into high extraction efficiency when a suitably hydrophobic ligand is used as an extractant.

With this in mind, the experiments were set up as a competition with a water soluble ligand. The competing ligand is essential for several reasons. It ensures that the extraction experiments can be done in a pH range in which the TAMs are well suited (over pH 5) without the Fe(III) precipitating as $Fe(OH)_3$. Second, it ensures that not 100% of the Fe(III) will be extracted, thus resulting in a more accurate determination of the Fe(III) concentration in each phase. The effect of the competing ligand on the observed equilibrium concentrations can then be removed, leaving K_{ex}. The equations used to do this will be described in detail later in this section.

A graph of pFe vs. pH for several ligands, including the TAMs, provides a starting point for choosing a pH and competing ligand which would be competitive with the TAM (Figure 3-11). The ideal extraction experiment would be conducted at a pH where two lines – one for a competing ligand and one for a TAM – cross. This is the pH at which the ligands are equal in Fe chelating strength and the distribution of Fe between two phases would be controlled only by the change in TAM concentration.

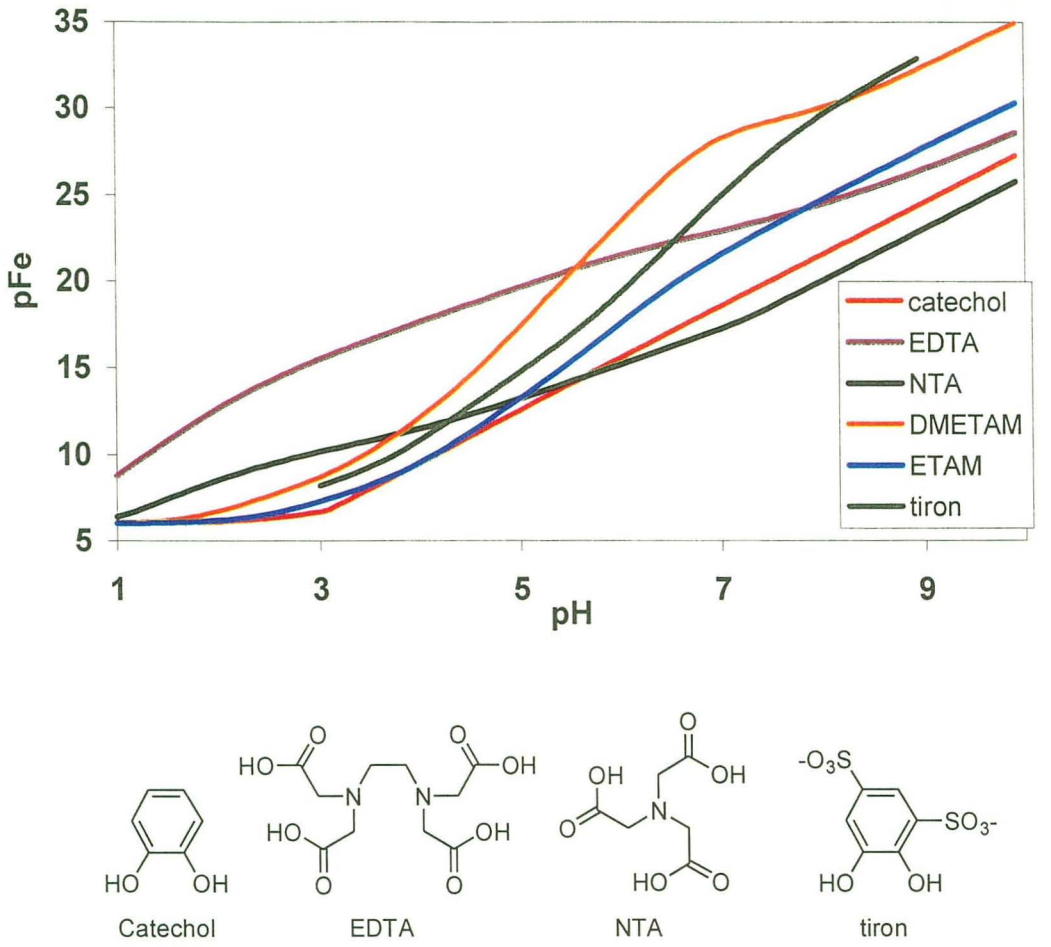

Figure 3-11. Graph of pFe vs. pH for several ligands calculated with 1 μM Fe(III) and 10 μM ligand.

In this graph, both DMETAM and ETAM are included since their Fe(III) stability constants are different ($10^{45.3}$ vs $10^{42.7}$, respectively) and the assumption is made that the extraction constant for a lipophillic TAM will be comparable to a formation constant for a water-soluble ligand. If this assumption is correct, this graph indicates that some good choices are: EDTA between pH 5 and 8, NTA between pH 3.5 and 5.5, or tiron throughout the pH range. Since the extraction constants were not known, the choice of

competing ligand was finalized by a trial-and-error. For extractant design #1 (H_3L^1Br) it was found that at pH 5, NTA releases 100% of the Fe(III) to the TAM (based on equivalents of TAM). Also at pH 5, EDTA is too strong of a chelator and hardly any Fe(III) extracts. Extraction worked well when the competing ligand was changed to tiron, and the pH was raised to 7.4. For extractant design #2 (H_2L^2), tiron cannot be used because tiron and cetylpyridinium precipitate from aqueous solutions. However, this extraction constant is not as high as for ligand design #1 since at pH 5, NTA is sufficient to retain some of the Fe(III) in the aqueous phase.

The solvent extraction experiments were conducted as batch extractions in which the pH, Fe, and competing ligand concentration were held constant in the aqueous phase and the amount of TAM in the organic phase was varied. In the experiments described here, the aqueous phase consists of Fe(III) (at 0.1mM), a ligand such as NTA or tiron (at 5 mM), a pH buffer (0.1M) such as acetic acid / NaOAC or MES (pH 5) or HEPES (pH 7.4), and sometimes cetylpyridinium chloride. The organic phases were prepared with the concentration of the TAM varying from 2 to 50 equivalents, relative to the Fe(III). For extraction design #1, the organic phase was $CHCl_3$. Two milliliters of each phase were shaken vigorously in a capped tube for 2 hours. The tubes were centrifuged to separate the layers, and the Fe(III) concentration was determined. For extractant design #1, the UV-Vis spectrum of the aqueous phase was recorded since the $[Fe(tiron)_3]^{9-}$ is red, its extinction coefficient in water is well known, and the absorbance of the solution can be measured prior to extraction. For extractant design #2, the extinction coefficient for the $(Fe(TAM)_3]\bullet$3cetylpyridinium was determined in ethyl acetate and the UV-Vis of the ethyl acetate phase was recorded to calculate the Fe(III) concentration.

For extractant design #1, the UV-Vis spectra from several of the organic extracts are shown in Figure 3-12. The characteristic "double hump" of the $FeTAM_3$ complex is seen in each spectrum, even when a sub-stoichiometric amount of the H_3L^1Br was used. This indicates that the Fe(III) is always extracted as the $Fe(HL^1)_3$ complex, and not at any lower stoichiometry. In addition, when NTA was initially used as the competing ligand, there was no spectroscopic indication of any $Fe(HL^1)_n$ species in the aqueous phase in the UV-Vis spectra, which would be masked by the $[Fe(tiron)_3]^{9-}$ in later experiments.

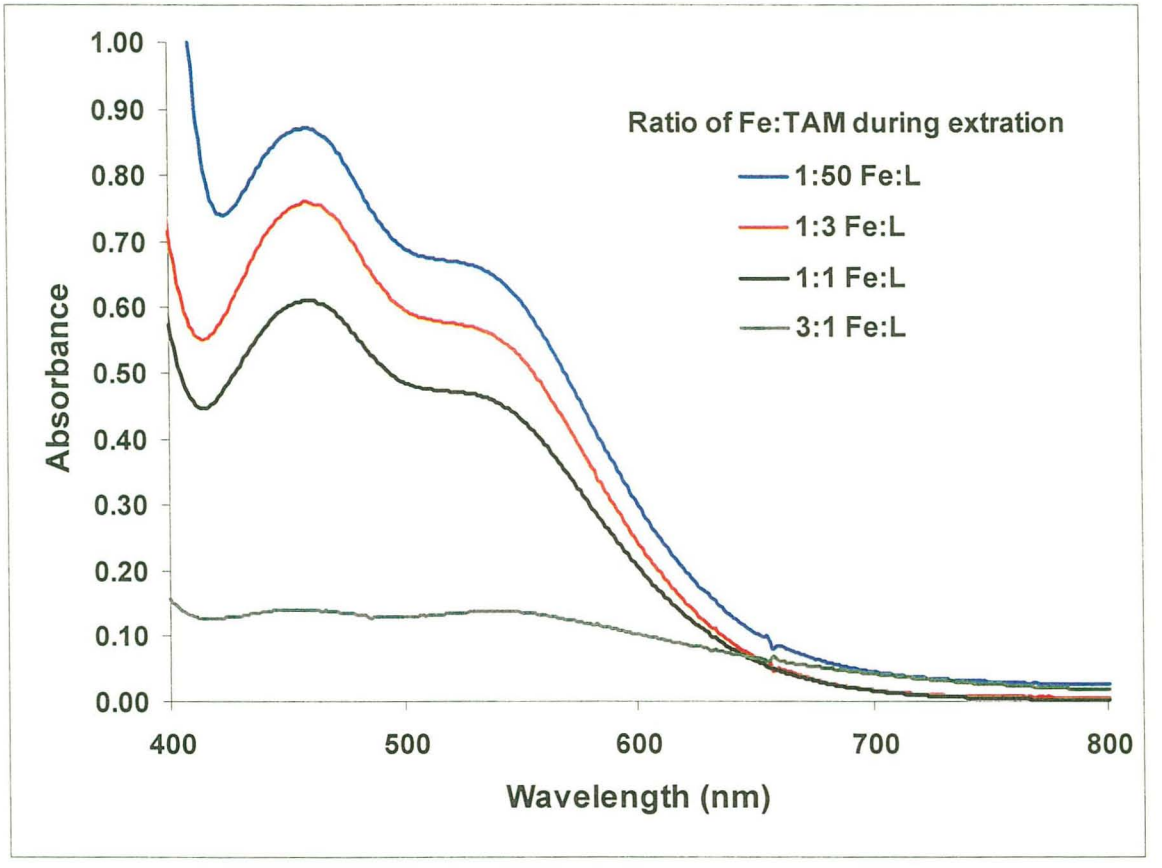

Figure 3-12. UV-Vis spectra of the $CHCl_3$ phases from extractant design #1.

Effectiveness of Amino TAMs as Extractants

In the competition extraction experiment with ligand design #1 (H_3L^1Br), the observed extraction can be described as:

$$[Fe(tiron)_3]^{9-}{}_{(aq)} + N\ H_2L^1{}_{(org)} \rightleftarrows Fe(HL^1)_{n(org)} + N\ Htiron^{3-} \qquad K_{comp} \qquad (1)$$

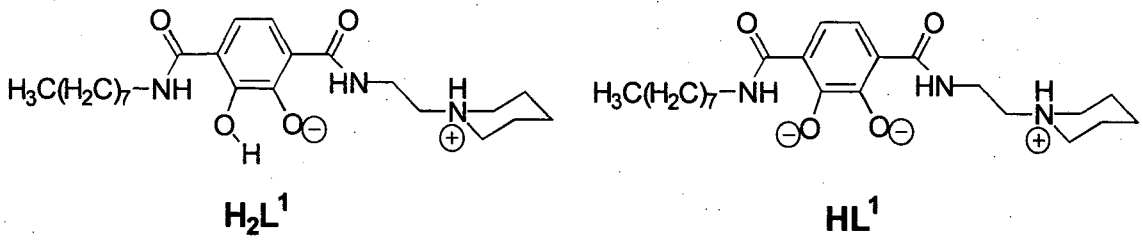

Figure 3-13. Nomenclature for the protonation states of ligand design #1.

The equilibrium contains singly-deprotonated ligand H_2L^1 (Figure 3-13) and $Htiron^{3-}$ because the pH of the experiment was 7.4. Since the pH of each solution is measured and the total concentration of tiron is known, a pM calculation is used to calculate the concentration of free aqueous iron.

$$Fe^{3+} + 3\ Htiron^{3-} \rightleftarrows [Fe(tiron)_3]^{9-} + 3\ H^+ \qquad (2)$$

Substituting this into equation (1) allows the effect of the competing ligand to be removed leaving the extraction expression in equation (3). This will be called $K_{ex(H)}$ since the equilibrium contains one proton per ligand.

$$Fe^{3+} + N\ H_2L^1{}_{org} \rightleftarrows Fe(HL^1)_{n\ org} + N\ H^+ \qquad K_{ex(H)} \qquad (3)$$

The equilibrium constant for this process, K_{ex}, is defined as:

$$K_{ex(H)} = \frac{[Fe(HL)n]_{org}[H]^n}{[Fe^{3+}][H_2L]^n_{org}} \quad (4)$$

The distribution coefficient D is defined as the ratio of the [M] in the organic and aqueous phases:

$$D = [FeHL_3]_{org} / [Fe^{3+}] \quad (5)$$

Substituting (5) into (4), taking the log and rearranging gives:

$$K_{ex(H)} = \frac{D[H^+]^n}{[H_2L]^n_{org}} \quad (6)$$

$$LogD = NLog[H_2L] + (LogK_{ex(H)} - NLog[H^+]) \quad (7)$$

Plotting Log D vs. Log [H_2L^1] (after correcting for the amount of ligand used to complex Fe^{3+}) should give a slope of 3, since this is the stoichiometry of the extracted complex. Subtracting the slope multiplied by pH from the intercept will then yield Log $K_{ex(H)}$.

The data from two of these extraction experiments, which contain between 2 to 5 equivalents of Fe(III), are shown in Figure 3-14 graphed as Log D vs. Log [H_2L]. The slope, intercept, and measured pH for each are 3.0(3), 32.7(1.0), 7.25 and 3.3(2), 33.8(0.8), 7.35. From this, values of 11.4(1.0) and 9.8(8) are calculated for Log $K_{ex(H)}$, respectively.

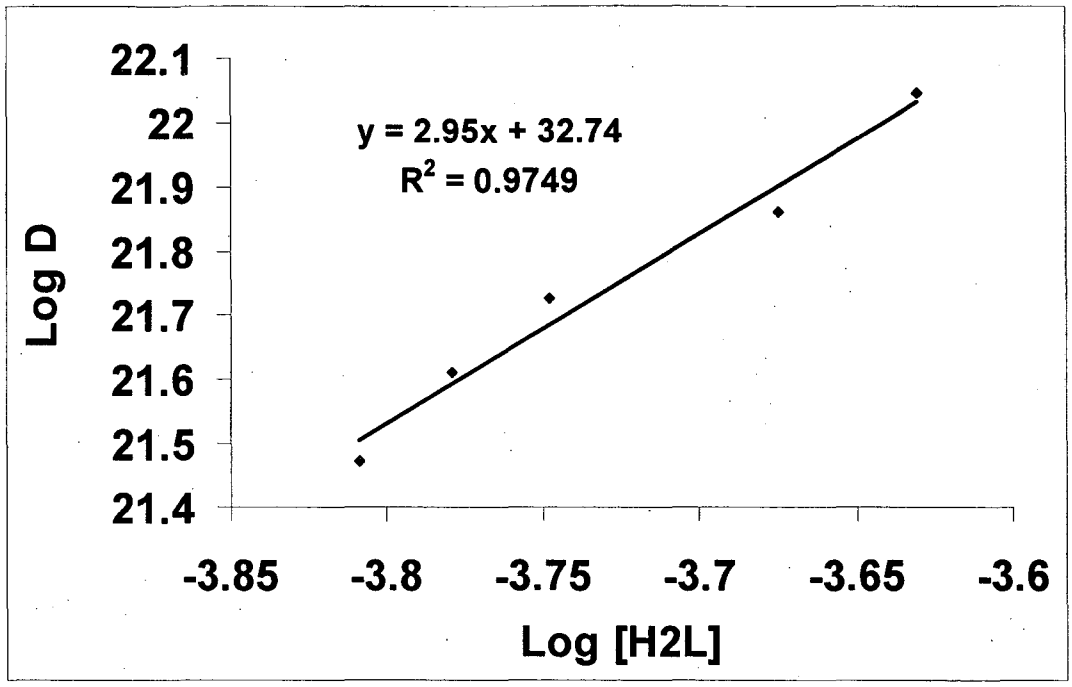

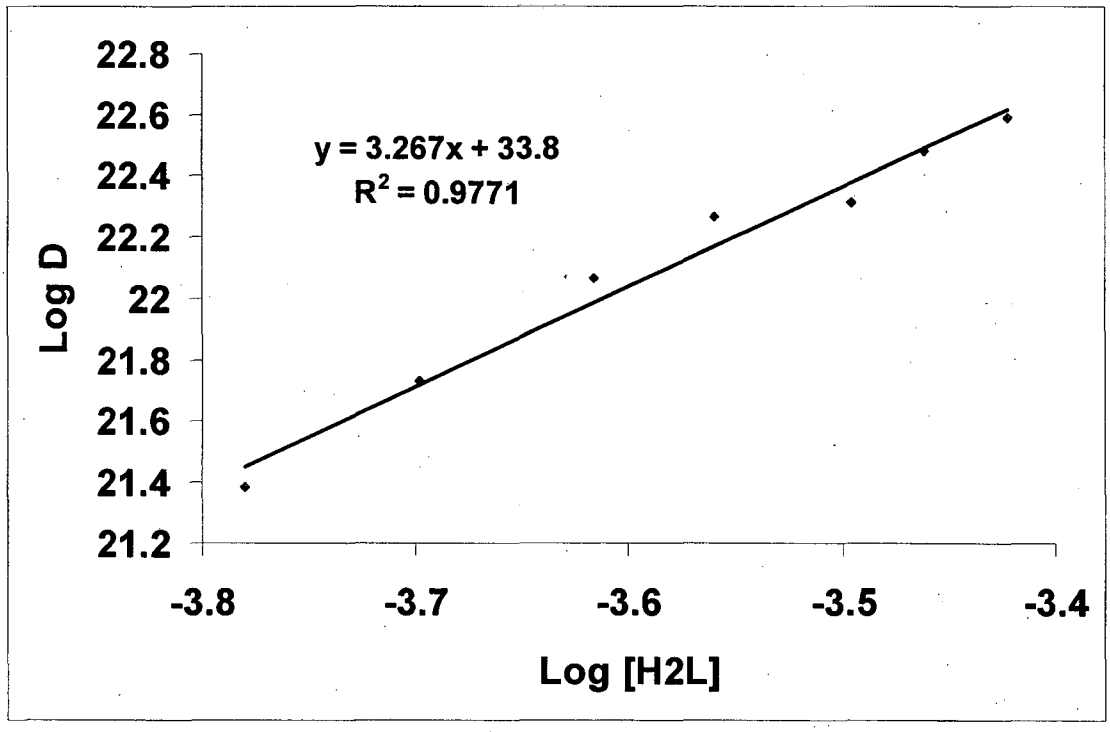

Figure 3-14. Plot of Log [H_2L] vs. Log D for two extraction experiments of Fe(III) with the ligand H_3L^1Br.

In these two experiments, the organic phase contained up to 50 equivalents of ligand, however these data points lie far below the line and are not shown. The deviation of the data point at higher amounts of ligand from a slope of 3 can be explained by a ligand distribution experiment in the absence of Fe(III). Two milliliters of the same ligand solutions used in the extraction experiments were shaken with two milliliters of HEPES buffer for two hours. The UV absorption of the ligand in the $CHCl_3$ phase was recorded to determine the amount that had moved into the aqueous phase. Although there is some range in the data for the amount of ligand partitioning, it is less than 5%. Consequently, in the Fe(III) extraction experiments, the amount of ligand in the organic phase is actually lower than the amount plotted as Log[H_2L]. This is only a significant problem at the higher ligand concentrations where excess ligand is present that can partition into the aqueous phase. Due to this, the points representing greater than 5 equivalents of ligand are not shown and are not used in the calculation of $K_{ex(H)}$.

The average of these extraction constants determined at pH 7.3 is $10^{10.6}$. Since this number is dependent on the protonation of the second catecholate oxygen ($pK_a = 11$), removing this from $K_{ex(H)}$ results in a proton independent extraction constant of $10^{43.6}$.

$$Fe^{3+} + 3\,H_2L^1{}_{org} \rightleftarrows Fe(HL^1)_{3\,org} + 3\,H^+ \qquad K_{ex(H)} \qquad (3)$$

$$3\,H^+ + 3\,HL^{1-} \rightleftarrows 3\,H_2L^1 \qquad 3 \times K_a \qquad (8)$$

$$Fe^{3+} + 3\,HL^{1-}{}_{org} \rightleftarrows Fe(HL^1)_{3\,org} \qquad K_{ex} \qquad (9)$$

$$K_{ex} = K_{ex(H)} * 3(K_a) = 10^{10.6} * 3(10^{11}) = 10^{43.6}$$

This is essentially a formation constant in the organic phase, thus the magnitude is not surprising, and is in line with the formation constants determined for aqueous Fe tris-TAM complexes. The validity of this method of data analysis for determining K_{ex} can be analyzed by comparing the experimentally obtained extraction data with a calculated model of what would be expected for a Log K_{ex} value of 43.6. The program SOLGASWATER [27] is a modeling program that was used to calculate the speciation of Fe(III) under several different conditions.

In the first analysis, the [Fe], [tiron], and pH were fixed at the values used in the experiments, and the [TAM] was varied over the same range that was used in the extraction experiments. The amount of Fe(III) extracted as a function of changing TAM concentration was calculated for two different values of K_{ex}, $10^{43.6}$ and $10^{45.3}$, and the graph in Figure 3-15 shows the fraction of Fe(III) present as $Fe(TAM)_3$. The experimentally observed distribution of the Fe(III) between the TAM and the tiron is graphed as the blue and orange triangles. The value of $10^{45.3}$ was used for the second calculated line since it is the upper bound of K_{ex}. This graph shows that the Log-Log plot

is a reliable way to analyze the extraction data, since the experimentally observed data matches the model calculated in SOLGASWATER.

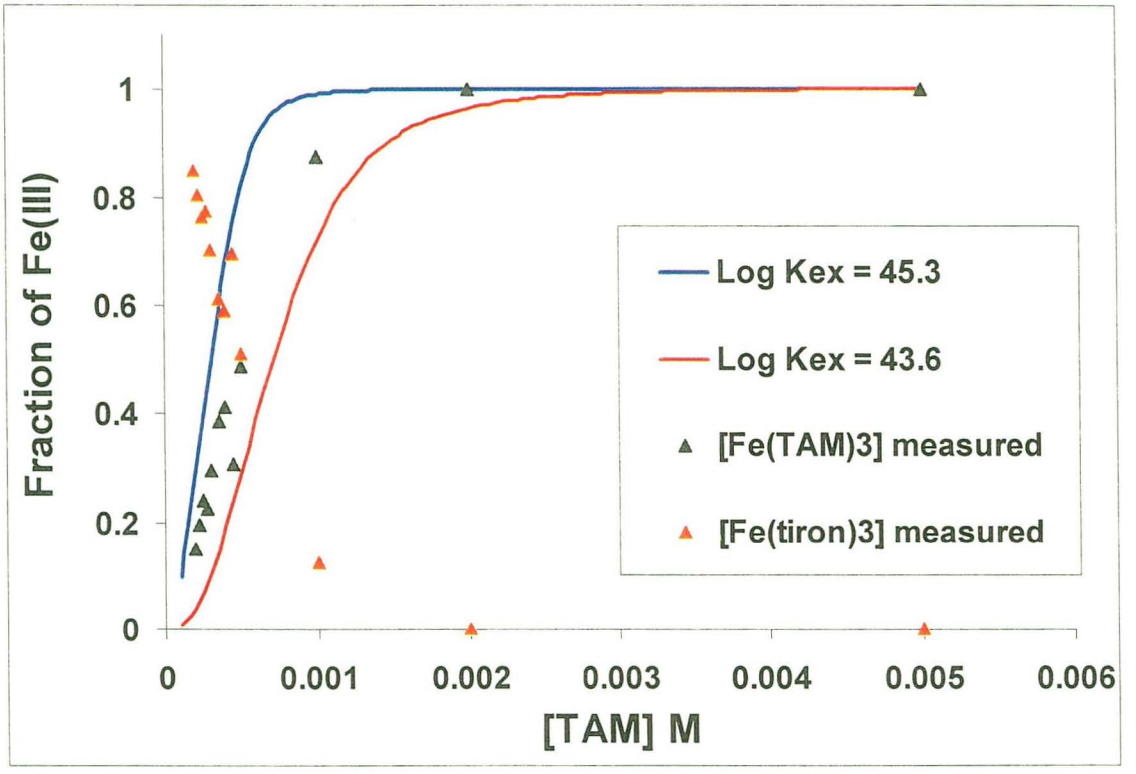

Conditions:

[Fe] = 0.1mM, [Tiron] = 5mM, pH = 7.4, [TAM] = 0.1 to 5mM

Figure 3-15. Fraction of Fe(III) present as $Fe(HL^1)_3$ as a function of $[HL^1]$ calculated for three different values of K_{ex}. The triangles show the experimentally measured concentrations of $Fe(HL^1)_3$ and $Fe(tiron)_3^{9-}$.

The value of Kex of $10^{43.6}$ can also be used to calculate speciation diagrams as a function of pH in the presence of different competing ligands which may be present in waste streams. The extraction experiments were conducted with tiron as a competing ligand, and a speciation for this with fixed amounts of tiron and TAM is shown in Figure 3-16. This illustrates that the TAM is able to extract Fe(III) from tiron, but at higher pH values the high formation constant of the $[Fe(tiron)_3]^{9-}$ ($10^{46.3}$) [28] dominates and the Fe(III) would be extracted back into the aqueous phase. This graph also illustrates that the conditions used for the extraction experiment (i.e. pH 7.4) is the ideal pH for these experiments. At pH 7.4, the $[Fe(tiron)_3]^{9-}$ is present in slightly lower concentration, so varying the amount of TAM allows for a variable extraction of Fe(III). The inflections above pH 8 and 11 can be attributed to the deprotonation of tiron and TAM, respectively. [29]

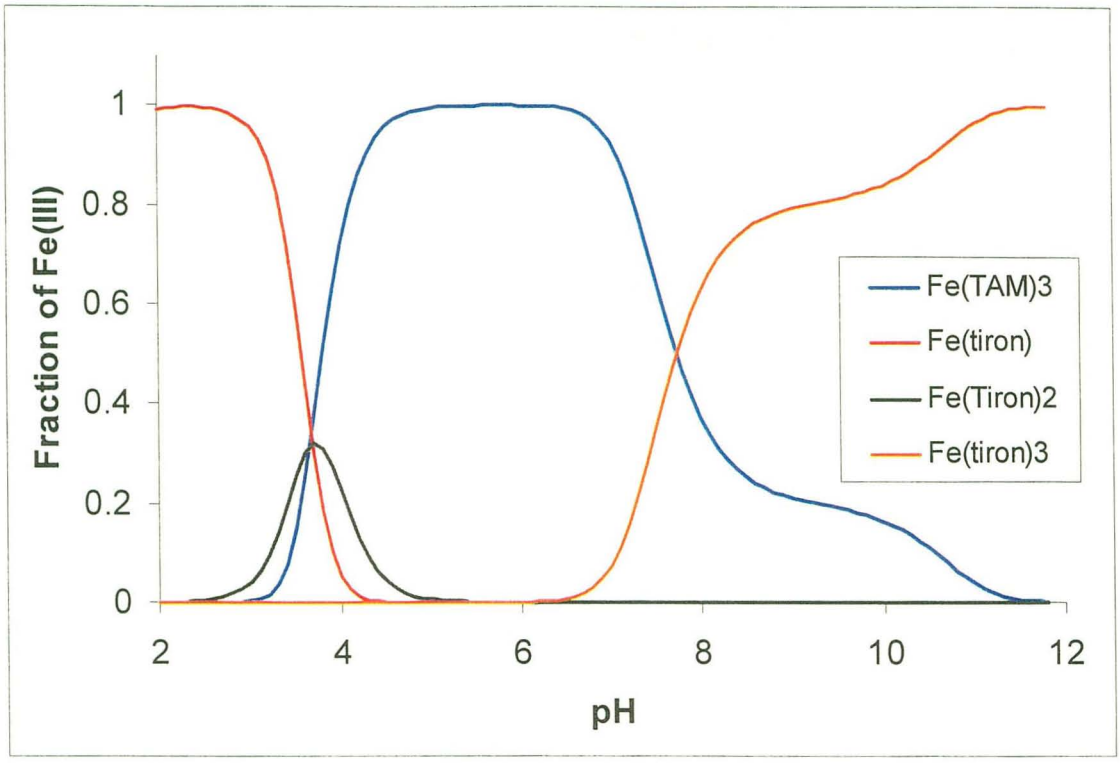

Conditions for speciation:			
[Fe] = 0.1 mM,	pK_a	HTAM	11.00
[Tiron] = 5 mM,		H_2TAM	17.00
[TAM] = 1mM.	Log K_{ex}	$FeTAM_3$	43.6
	pK_a	HTiron	12.6
		H_2Tiron	20.26
	Log K_f	Fetiron	20.7
		$Fetiron_2$	35.9
		$Fetiron_3$	46.9
	reference for constants: [28]		

Figure 3-16. Speciation of Fe(III) in a biphasic system containing tiron in the aqueous phase and L in the organic phase. The [Fe] and [Tiron] are the same as in the extraction experiments.

The speciation diagrams were also calculated with NTA and EDTA as competing ligands. Not only are these ligands relevant since they may be present in waste streams, but they also illustrate that early extraction experiments with these ligands did not work because the pH was not in the right region. In the case of NTA, extraction of Fe(III) is

essentially complete by pH 4.5, hence NTA did not work as a competing ligand at pH 5 and Fe(III) was quantitatively extracted. In the case of EDTA, hardly any of the Fe(III) was extracted at pH 5. This is confirmed by the speciation diagram which shows that at pH 5, the $FeTAM_3$ complex is present in very low concentration and extraction is not complete until pH 6.5.

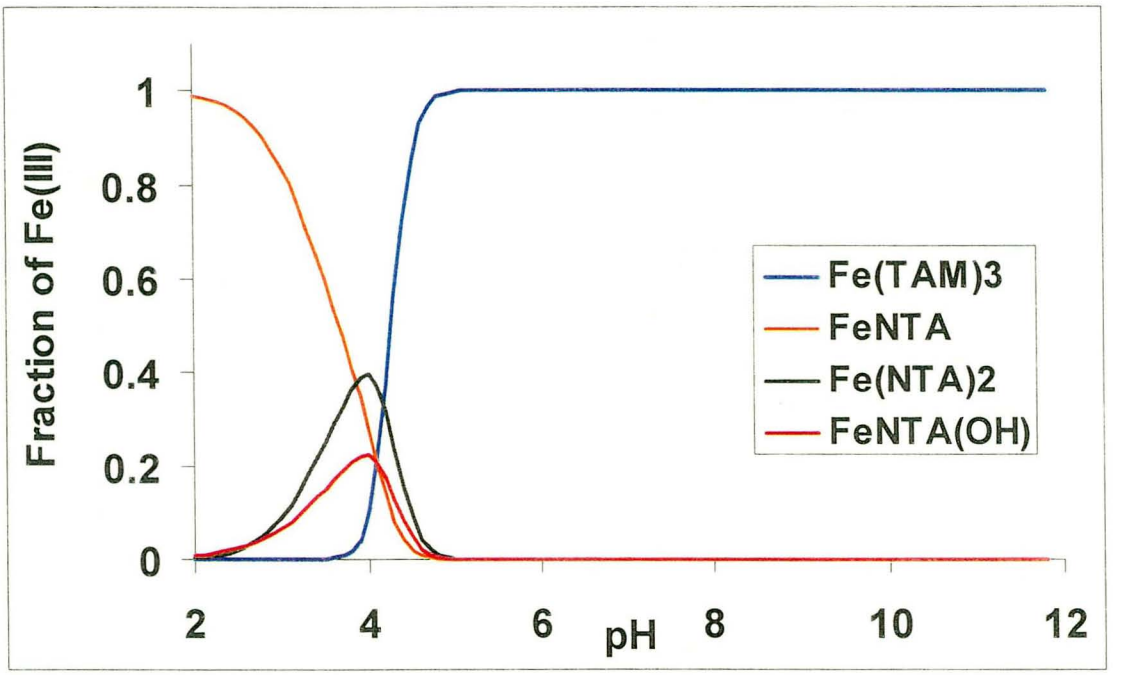

conditions for speciation:	pK_a	HNTA	9.59
[Fe] = 0.1mM		H_2NTA	12.11
[NTA] = 5 mM		H_3NTA	13.61
[TAM] = 1mM	K_f	FeNTA	15.90
Log K_{ex} = 43.6		$Fe(NTA)_2$	23.97
		$H_{-1}FeNTA$	11.80
		$H_{-2}FeNTA$	4.22
		$H_{-3}FeNTA$	-6.50
	reference for constants: [30,31]		

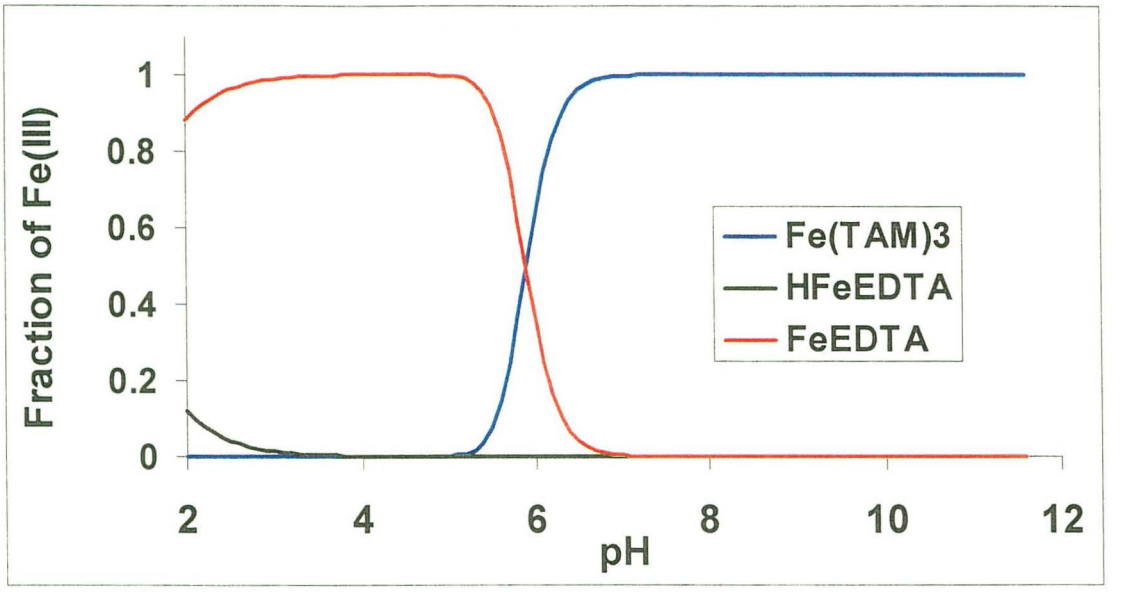

conditions for speciation:			
[Fe] = 0.1mM	pK_a	HEDTA	10.23
[EDTA] = 5 mM		H_2EDTA	16.41
[TAM] = 1mM		H_3EDTA	19.07
Log K_{ex} = 43.6		H_4EDTA	21.08
		H_5EDTA	22.48
		H_6EDTA	22.58
	K_f	HFeEDTA	26.23
		FeEDTA	25.10
		$H_{-1}FeEDTA$	17.61
		$H_{-2}FeEDTA$	8.20
		$H_{-3}FeEDTA$	-4.08
		$H_{-2}Fe_2EDT_2$	38.17
	reference for constants: [32]		

Figure 3-17. Speciation diagrams for the extraction of Fe(III) in the presence of either NTA or EDTA.

Effectiveness of Alkyl TAMs and Lipophillic Cations as Extractants

While the aminoTAMs are efficient at extracting Fe(III), the synthesis is slightly cumbersome. The symmetrically substituted alkylTAMs are much easier to synthesize since both amides can be installed in one step from the acid chloride intermediate **15**.

Recently a shorter synthetic route to the alkylTAMs has been reported which avoids the protecting groups and dramatically decreases the time and cost of synthesizing the alkylTAMs. [33] For this reason, it was advantageous to find a way to use the alkylTAMs as extractants, and it was discovered that a lipophillic cation such as cetylpyridinium (py^+) would act as a phase transfer agent for the charged $Fe(TAM)_3^{3-}$ complex. This is referred to here as extractant design #2 (Figure 3-1).

For ligand design #2, NTA was used as a competing ligand, therefore the aqueous phase is not colored and the absorbance of the organic phase had to be monitored to calculate the concentration of the Fe(III). The determination of the extinction coefficient of the $Fe(L^2)_3 \cdot 3py^+$ complex in ethyl acetate at 440 nm is essential for analyzing extraction data by UV-Vis. A method was developed to determine the extinction coefficient in which the samples were analyzed by UV-Vis spectroscopu and by AA-ICP for an independent measurement of the [Fe]. Thirteen samples were prepared by an extraction method identical to the one used in determining $K_{ex(2H)}$, and the UV-Vis spectra of the organic phase was recorded. Immediately, 1.0 mL was removed, evaporated, digested with 1mL of conc. HNO_3 (low Fe), and diluted to 10 mLs with doubly distilled H_2O for the AA-ICP analysis. The extinction coefficient for the samples at 440 nm is 7273 ± 117, a 1.6% error.

For ligand design #2, two components can limit the extraction – the octylTAM (H_2L^2) or the cetylpyridinium (py^+). The equilibrium expressions are slightly more complicated and the extraction constant can be determined by varying one of these components while the other is held constant.

$$Fe(NTA)_{(aq)} + M\ H_2\ L^2{}_{(org)} + N\ py^+ \leftrightharpoons FeL^2{}_3{\cdot}3py^+{}_{(org)} + HNTA^{2-} + (2M\text{-}1)H^+ \quad K_{comp} \quad (10)$$

Here the ligand is written as fully protonated H_2L^2 because the experiments were conducted at pH 5. Since the pH of each solution is measured and the total concentration of NTA is known, a pM calculation allows the calculation of the concentration of free aqueous iron.

$$Fe^{3+} + HNTA^{2-} \quad FeNTA + H^+ \qquad (11)$$

Substituting this into equation (10) allows the effect of the competing ligand to be removed yielding the extraction process in equation (12).

$$Fe_{(aq)} + M\ H_2L_{(org)} + N\ py+ \leftrightharpoons FeL_3{\cdot}3py^+{}_{(org)} + 2M\ H^+ \quad K_{ex(2H)} \qquad (12)$$

The equilibrium constant for this equilibrium, $K_{ex(2H)}$, is defined as:

$$K_{ex(2H)} = \frac{[FeL_3 3py^+]_{org}[H]^{2M}}{[Fe^{3+}][H_2L]^M_{org}[py+]^n_{aq}} \qquad (13)$$

The distribution coefficient D has the same definition (equation 5), so substituting (5) into (13), taking the log and rearranging gives:

$$K_{ex(2H)} = \frac{D[H^+]^{2M}}{[H_2L]^M_{org}[py+]^n_{aq}} \qquad (14)$$

$$LogD = MLog[H_2L] + NLog[py^+] + LogK_{ex} - 2MLog[H^+] \qquad (15)$$

The extraction then depends on both the TAM and the cetylpyridinium concentrations, so one can be held in excess while the other is varied. In the case of constant py^+ and varying ligand, plotting Log D vs. Log $[H_2L]$ (after correcting for the amount of ligand used to complex Fe^{3+}) should give a slope of 3, since that is the

stoichiometry of the extracted complex. Subtracting the remaining terms from the intercept will then yield Log $K_{ex(2H)}$. Alternatively, in the case of constant ligand and varying py^+, plotting Log D vs. Log $[py^+]$ (after correcting for the amount of cetylpyridinium extracted with Fe^{3+}) should give a slope equal to the amount of py^+ required for extraction. Again, subtracting the remaining terms from the intercept will yield Log $K_{ex(2H)}$.

The experiment with a variable TAM concentration was repeated 3 times with good between the data and the "best" one – the one with slope close to 3 - is shown in Figure 3-18. With the intercept and slope of 21.6 and 2.87 respectively, a pH of 5.5, and a Log[py+] of –2.3, Log K_{ex} is calculated to be –2.1 for the equilibrium described in equation (12). The protonation constants of the TAM (6.1 and 11.0) can be removed to yield a proton independent extraction constant of $10^{48.9}$. This describes the reaction:

$$Fe^{3+}_{(aq)} + L^{2-}_{(org)} + N\ c16py+ \leftrightarrows FeL_3{\cdot}3py^+_{(org)} \qquad (16)$$

This number is clearly too high. In extraction method #1 Log Kex was ca. $10^{45.3}$ and it was observed that Fe(III) was quantitatively removed from NTA at pH 5. Since NTA is used effectively as the competing ligand in this procedure, the extraction constant has to be lower.

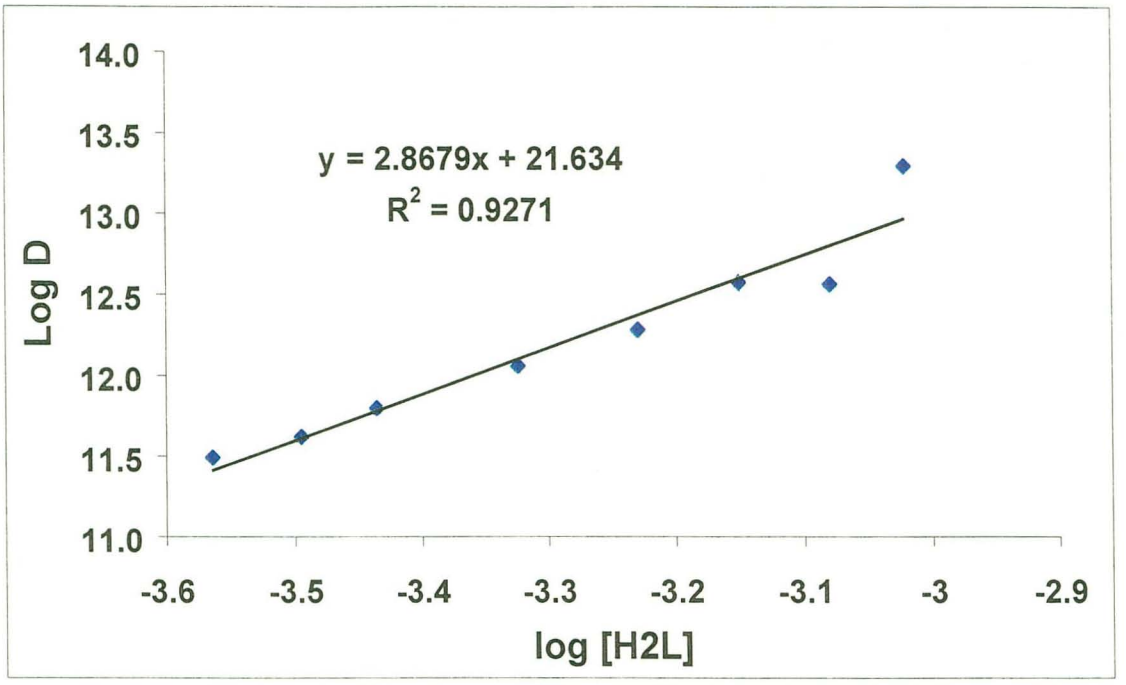

Conditions for experiment: [Fe] = 0.1mM, [NTA] = 5mM, [py^+] = 5mM, [H_2L^2] = 0.5 to 2.5mM, pH = 5.5

Figure 3-18. Plot of Log D vs. Log [H_2L^2] for Fe(III) extraction with constant [cetylpyridinium].

SOLGASWATER was again used to calculate a graph of percent extraction as a function of varying H_2L^2 concentration for several different extraction constants. The calculated points are shown in the second graph where the experimentally observed values are represented by triangles, and the three curves were calculated for Log K_{ex} equal to 43.3, 41.5, and 40. This graph indicates that a Log K_{ex} of 41.5 closely matches the experimentally observed extraction and this number is more reasonable.

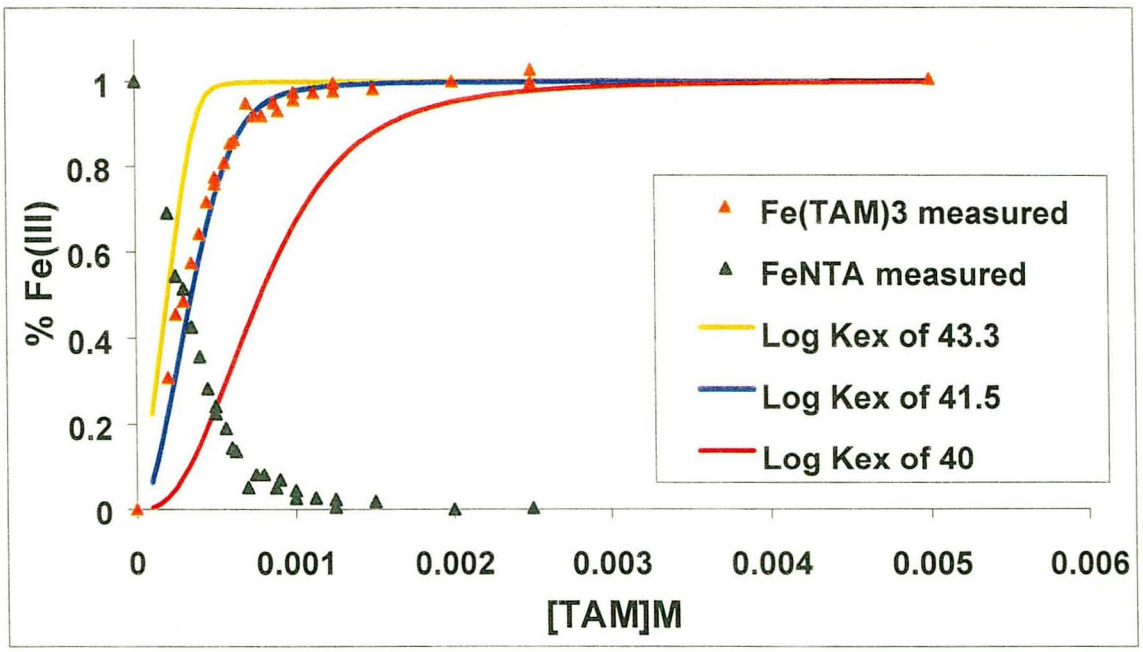

Conditions for calculation: [Fe] = 0.1 mM, [NTA] = 5mM, pH = 5.3, [C8TAM] = 0.1 to 5 mM

Figure 3-19. Fraction of Fe(III) present as $Fe(L^2)_3$ as a function of $[H_2L^2]$ calculated for three different values of K_{ex}. The triangles show the experimentally measured concentrations of $Fe(HL^1)_3$ and Fe(NTA).

Another set of 3 experiments was conducted in which the cetylpyridinium concentration was varied while the $[H_2L^2]$ was held constant at 1.0 mM. The graph of Log D vs. Log $[py^+]$ shown in has an intercept and slope of 20.7 and 2.45 respectively, a pH of 5.5, and a Log[TAM] of –3.1. For this, Log $K_{ex(2H)}$ is calculated as 1.15 for the equilibrium described in equation (12) and removing the protonation constants yields a K_{ex} of $10^{52.2}$ for the equilibrium in equation (16). Again, this value is way too high.

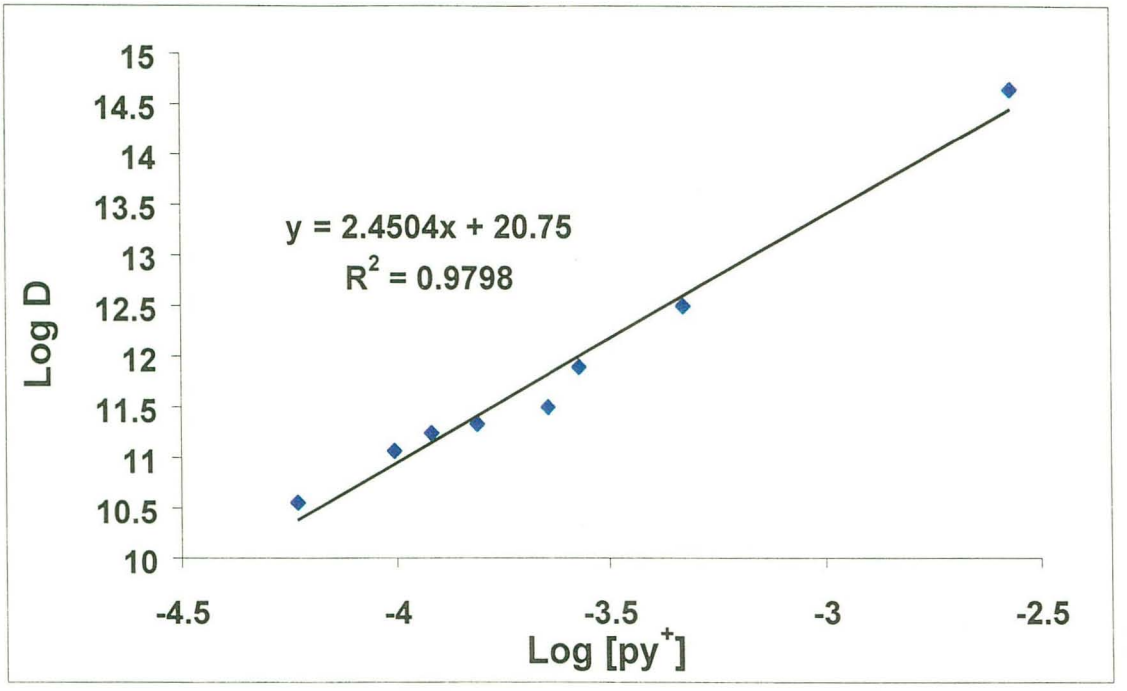

Conditions for experiment: [Fe] = 0.1mM, [NTA] = 5mM, [C8TAM] = 1mM, [C16py+] = 0.1 to 2.5mM, pH 5.5.

Figure 3-20. Plot of Log D vs. Log [py^+] for Fe(III) extraction with constant [H_2L^2].

The data obtained experimentally was again compared to the percent extraction calculated with SOLGASWATER as a function of varying py^+. The calculated points are shown in Figure 3-21 where the experimentally observed values are represented by triangles, and the three curves were calculated for Log K_{ex} equal to 43.3, 41.5, and 40. This graph shows that a Log K_{ex} of 41.5 closely matches the experimentally observed extraction data, just as it did in the case of varying the ligand concentration instead of the cetylpyridinium concentration.

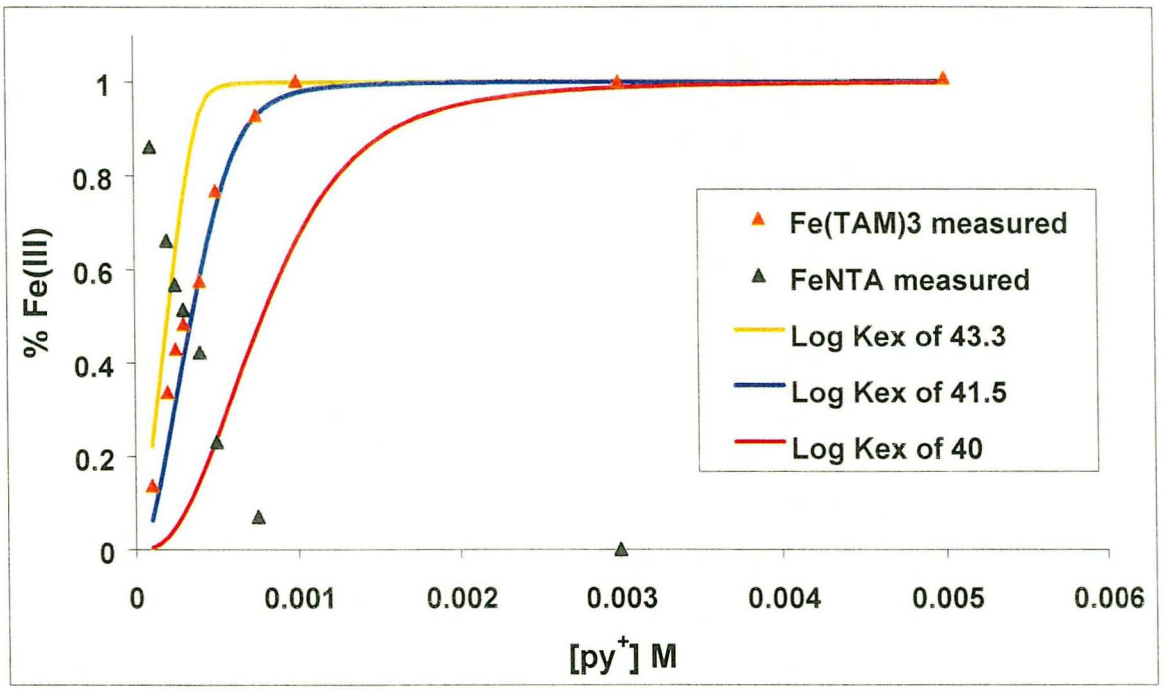

Conditions for calculation: [Fe] = 0.1 mM, [NTA] = 5mM, pH = 5.3,

$[py^+]$ = 0.1 to 5 mM

Figure 3-21. Fraction of Fe(III) present as $Fe(L^2)_3$ as a function of $[py^+]$ calculated for three different values of K_{ex}. The triangles show the experimentally measured concentrations of $Fe(HL^1)_3$ and Fe(NTA).

The approach used here to analyze the extraction data with a Log-Log plot is used extensively in the field of solvent extraction. For ligand design #1, this method provides a reasonable way to calculate K_{ex}, although the error is quite large. For extraction design #2, this approach did not work well for the large number of components involved in the extraction. However, the comparison of the observed Fe(III) extraction with the

calculated extraction based on estimated constants is a convenient way to evaluate the two extraction processes. The numbers estimated for the extraction constants – 10^{45} and 10^{41} – are basically biphasic formation constants and parallel the aqueous formation constants that have been determined for water soluble aminoTAMs and alkylTAMs presented earlier in this chapter. These two approaches each have advantages as extractants. The aminoTAMs have higher extraction constants, but the alkylTAMs are much easier to synthesize.

Conclusion

Two different approaches to the design of TAMs for liquid-liquid extraction of Fe(III) have been presented. The aminoTAMs allow the resulting metal complex to have a neutral charge, while the alkylTAMs can be used in conjunction with a lipophillic cation as a phase transfer agent. The estimated extraction constants parallel the formation constants of the water soluble aminoTAMs and alkylTAMs, respectively. The water soluble aminoTAM DMETAM, was evaluated as an Fe(III) chelator and has the highest formation constants with Fe(III) of any TAM ($10^{45.3}$) and the highest pM value at neutral pH of any bidentate ligand known. These ligands show great promise as extractants since any number of derivatives can be made by changing the amides to suit the specific purpose.

Experimental

General. All reagents and solvents were purchased from Aldrich Chemical Company or Fisher Scientific and used as purchased. All solvents were dried over activated alumina and stored over 4Å molecular sieves. All reactions involving acid chlorides or BBr_3 were carried out under Ar and solvents were degassed by evacuating the flask and filling with Ar 3 times. Water was distilled and further purified by a Millipore cartridge system (resisitivity 18 x 10^6 Ω). ^1H and ^{13}C NMR spectra were obtained on a Bruker DRX500 (500 MHz) or Bruker AMX400 spectrometer (400 MHz) as noted. All NMR samples were taken in $CDCl_3$ unless otherwise noted. All Microanalyses were performed by the Microanalytical Services Laboratory in the College of Chemistry, University of California, Berkeley. Intermediates 10 –14 were synthesized as previousl described. [18-21]

Ligand Synthesis.

2,3-Dimethoxy-1,4-bis(2-mercaptothiazolide) terephthalamide (16). 2,3-dimethoxyterephthalic acid (**14**) (12.38 g, 0.055 mol) was suspended in 40 milliliters of 1,4-dioxane and dissolved with addition of $SOCl_2$ (21 mL, 0.29 mol). The reaction was heated with a 90°C oil bath overnight, the excess $SOCl_2$ and dioxane were removed, and the resulting brown oil was coevaporated three times with $CHCl_3$. Separately, 2-mercaptothiazoline (16.3 g, 0.137 mol) and triethylamine (15 mL) were dissolved in 150 mL of freshly distilled THF. The oil (2,3-dimethoxyterephthaloyl chloride, **15**) was cooled to 0°C and the THF solution was added slowly over one hour. The bright yellow suspension stirred at room temperature for 17 hours then was filtered and washed

generously with water. Recrystallization from isopropanol / 5% dichloromethane afforded yellow crystalline product (12.3 g, 52 %yield). MP 171-173 °C. ^{1}H NMR ($CDCl_3$): δ 3.41 (t, 4H, CH_2), 3.88 (s, 6H, CH_3), 4.64 (t, 4H, CH_2,), 7.06 (s, 2H, CH). ^{13}C NMR ($CDCl_3$): δ 201.0, 166.7, 149.7, 132.4, 123.4, 61.2, 55.5, 29.1. Elemental analysis for $C_{16}H_{16}N_2O_4S_4$ calculated (found): C, 44.84 (44.44); H, 3.76 (3.48); N, 6.54 (6.39).

2,3-Dimethoxy-1,4-bis(N,N-Dimethylaminoethyl)terephthalamide (20). 2,3-dimethoxyterephthalic acid (**14**) (0.525 g, 2.32 mmol) was converted to the acid chloride **15** as described above. This oil was dissolved in 5 mL of $CHCl_3$ and slowly added over 20 minutes to N,N-dimethylethylenediamine (2.7 mL, 24.6 mmol). The reaction was stirred overnight at RT, the solvent and excess diamine were removed with reduced pressure and resulted in a clear solid coated in a brown impurity. The brown impurity was washed off with a small of diethyl ether to afford 0.451 grams of a clear solid (74% yield). MP 80-83°C . ^{1}H NMR ($CDCl_3$): δ 2.27 (s,12H, N-CH_3), 2.50 (t, 4H, CH_2, J=), 3.5 (q, 4H, CH_2, J=), 3.95 (s, 6H, O-CH_3), 7.89 (s, 2H, CH), 8.31 (s, 2H, NH). Elemental analysis for $C_{18}H_{30}N_4O_4$ calculated (found): C, 59.00 (58.94); H, 8.25 (8.42); N, 15.29 (15.29).

2,3-Dihydroxy-1,4-bis(N,N-Dimethylaminoethyl)terephthalamide dihydrobromide salt (DMETAM) (3). Compound 20 (0.255 g, .8 mmol) was dissolved in 40 mL of freshly distilled CH_2Cl_2. The solution was frozen in liquid nitrogen, evacuated, warmed to room temperature and flushed with argon. This was repeated three times. The solution was frozen with liquid nitrogen and boron tribromide (1.1 mL, 11.7 mmol) was added. The yellow, cloudy solution was warmed to room temperature and stirred under

argon for 5 days. The solvent was removed with reduced pressure, the flask was cooled in a dry ice/ isopropanol bath, and 15 milliliters of methanol was slowly added to dissolve the yellow solid. Upon warming the solution was diluted to 100 milliliters with methanol and boiled for 10 hours, refilling the methanol to 100 milliliters when necessary. After stirring for an additional 36 hours a white solid had precipitated (67% yield). MP 280°C(dec.). ^{1}H NMR (D_2O): δ 2.82 (s, 12H, N-CH_3), 3.28 (t, 4H, CH_2, J=), 3.66 (t, 4H, CH_2, J=), 7.08 (s, 2H, CH). ^{13}C NMR (D_2O): δ 169.7, 147.8, 116.9, 56.6, 43.2, 34.7. Elemental analysis for $C_{16}H_{28}N_4O_4Br_2$ calculated (found): C, 38.42 (38.12); H, 5.64 (5.62); N, 11.20 (11.00).

N,N'-Octyl-2,3-Dihydroxyterephthalamide (H_2L^2). Compound **2** (0.46 g, 2.2 mmol) was dissolved in THF and ca. 1.5 mLs of $SOCl_2$ was added. The solution was stirred at RT overnight under Ar then evaporated to a yellow oil. This acid chloride (**13**) was dissolved in CH_2Cl_2 and added slowly to a CH_2Cl_2 solution of octylamine (1.5 mL, 9 mmol) cooled in an ice water bath and allowed to warm to RT under Ar while stirring for 30 min. The solution was extracted with 3 X 1M HCl to remove the excess octylamine. Evaporation of the CH_2Cl_2 yielded a white solid (0.633 g, 90%yield).

2,3-dimethoxyterephthal-1-octylamide-4-(2-(1-piperidyl)ethyl)amide(22). To a 125 mL CH_2Cl_2 solution of **16** (6g, 14mmol) was added a 100 ml solution of octylamine (0.5mL, 3.1mmol) over 1.5h. After stirring overnight, the solution was evaporated to 75mL, extracted with brine (50 mL), 1M KOH (4 x 50mL), brine (50mL) and evaporated to a yellow solid. Soxhlet extraction with hexanes for 24 hours removed the product **21** from the excess **16**, left as a yellow solid in the thimble. Evaporation of the hexanes afforded the 2,3-dimethyoxyterephthal-1-octylamide-4-(2-mercaptothiaxoline) **21**. This

(0.786g, 1.8mmols) was dissolved in 30 ml CH_2Cl_2 and to this was added a 5 ml CH_2Cl_2 solution of 1-(2-aminoethyl)piperidine (0.28mls, 2.0 mmols). The solution was stirred for 18h at room temperature, extracted with 1M KOH/ brine (2x 40 mls) and evaporated to a clear oil (0.60g, 75% yield). 1H NMR, (CDCl3) 8.39 (t, 1H), 7.93-7.87 (two d, 1H each), 7.82 (t, 1H), 3.95 (s, 3H), 3.92 (s, 3H), 3.57-3.53 (q, 2H), 3.47-3.42 (q, 2H), 2.52 (t, 2H), 1.63-1.26 (m, 24H), 0.859 (t, 3H). ^{13}C NMR 164.1, 163.9, 151.6, 151.4, 129.9, 129.8, 126.3, 126.2, 61.5, 61.5, 57.1, 54.3, 39.8, 36.5, 31.7, 29.5, 29.2, 27.0, 26.0, 24.4, 22.6, 14.0.

2,3-dihydroxyterephthal-1-octylamide-4-(2-(1-piperidyl)ethyl)amide (H_3L^1Br).

A 40ml CH_2Cl_2 solution of **22** (0.60g, 1.8 mmol) was flushed with N_2, cooled to –35 °C with an ethylene glycol/dry ice bath and BBr_3 (4mls, 42.4 mmol) was added. The heterogeneous yellow reaction was allowed to warm to room temperature under N_2 and stirred for 6 days. The flask was cooled to –35 °C, carefully quenched by dropwise addition of MeOH and diluted with MeOH to 300 mLs. This was distilled to a final volume of 50 mLs. Addition of 100 mLs of dd H2O caused a brown oil to form, which crystallized after the water was decanted. Trituration with hot EtOAc afforded a white solid (0.57g, 85% yield). ^1H NMR (DMSO) 9.00 (t, 1H), 8.90 (t, 1H), 7.35 (d, 1H), 7.29 (d, 1H), 3.63 (q, 2H), 3.24 (t, 2H), 2.92 (q, 2H), 1.78-1.21 (m, 24H), 0.80 (t, 3H). ^{13}C NMR (CDCl3), 169.6, 169.1, 150.8, 150.2, 116.2, 115.5, 40.5-39.5, 31.6, 29.1, 26.9, 22.9, 22.5, 21.6, 14.3. CHN Calc. (Found) for $H_3L^1Br \cdot H_2O$ 53.28 (53.86), 7.78 (7.75), 8.10 (8.06).

Solution Thermodynamics.

Apparatus. A temperature controlled 100mL titration flask with attached quartz UV-Vis cell has been described in detail elsewhere. [34] An Accumet pH-meter (model AR15 or 15) and a corning glass-bulb electrode were used for electrode potential measurements. A Hewlett-Packard 8452a spectrophotometer (diode array) was used for the collection of absorbance data and was always turned on for at least 1 h before use to allow the lamp to come to operating temperature. The autoburets, pH meters, and spectrophotometer were controlled by a personal computer using modules of the LABVIEW[35] programming environment, written by Brendon O'Sullivan. [34]

Low-pH and Standard Electrode Calibration. The standard electrode calibration was conducted before each titration following published protocol. [34] The data were analyzed using the program GLEE[36] allowing refinement of E° and slope. For low-pH titrations, a correction was made for the junction potential. [34]

DMETAM pKa determination. Into 50 mLs of 0.1M KCl was added DMETAM.2HBr (25mg, 0.05mmoL) and this was titrated with ca. 0.1M KOH to pH 11 then back to pH 3 with 0.1M HCl. This was repeated twice and the data (ca. 400 measurements) were refined with the program HYPERQUAD. [23]

Fe(III) DMETAM Titrations. Into 50 mLs of 0.1 M KCl was added DMETAM·2HBr (9.99 mg, .01997 mmol) and an aliquot of a 0.02514 M Fe(III) stock solution (0.265 mL, .00653 mmol). This was titrated with 0.1007 M KOH from pH 3 to 6, then back to pH 3 with 0.0988 M HCl, with a constant pH increment such that 30 data points were collected in each direction and 4 titrations were conducted in this manner. For the low pH titration, DMETAM.2HBr (6.15 mg, 0.01229 mmol) and an aliquot of a 0.02514 M Fe(III) stock

solution (0.5 mL, 0.01257 mmol) were added to 50 mLs of 0.1 M KCl and titrated with 0.0991 M HCl with a constant pH increment such that 30 data points were collected. An equilibration time of 3 min after addition of the titrant was used. The specifics of data collection of been detailed elsewhere.[34] All absorbance measurements were less than 1.1 absorbance units.

NMR titration. DMETAM (0.1 mmol, 49.9 mg) was dissolved in 10 mLs of D_2O with a small amount of CH_3CN as an internal reference. This was divided into 7 test tubes and the pD was adjusted accordingly with DCl or NaOD. The ^1H NMR spectra were recorded and the pH was measured.

Extraction Experiments.

Preparation of Aqueous Stock Solutions. Fe(III) stock solution of 25.18 mM was prepared by dissolution of $FeCl_3$ in 0.1M HCl and standardized against EDTA.[37] NTA stock solution of 0.091(1) M was prepared by dissolving ~21.4 g Na_2HNTA in 1L ddH_2O and standardized by 3 pH titrations, admitting the NTA concentration as a refinable parameter. Tiron stock solution was prepared analogously to NTA, but dissolved in 0.05 M HCl to prevent oxidation. Cetylpyridinium chloride stock solution of 0.25 M was prepared by dissolving 8.95g of $C_{16}pyCl \cdot H_20$ in 100 mLs ddH_2O.

Preparation of Aqueous Solutions for Extraction.

<u>For Ligand Design #1</u>: Aqueous solutions were prepared by combining the appropriate amount of Fe(III) and tiron stocks to result in a 0.1mM and 5.0 mM solution, respectively, upon dilution with 0.1 M HEPES pH 7.4 buffer. The solution was freshly prepared before use.

For Ligand Design #2: Aqueous solutions were prepared by combining the appropriate amount of Fe(III), NTA, and cetylpyridinium chloride to result in a 0.1mM, 5.0 mM, and 5.0 mM solution, respectively, upon dilution with 0.1 M HOAc/NaOAc pH 5 buffer. The solution was prepared freshly before use.

For solutions of variable cetylpyridinium: An aqueous solution of 1.0mM Fe(III) and 50mM NTA was prepared. An aliquot of this was added to a vial containing varying amounts of cetylpyridinium and 10 mLs of 0.1M HOAc/NaOAc such that the final concentrations were 0.1mM Fe(III), 5.0 mM NTA, and the cetylpyridinium varied from 0.1 to 5 mM. The solution was prepared freshly before use.

Preparation of Organic Solutions. Either H_3L^1Br (50.05 mg, 0.10 mmol) or H_2L^2 (99.14 mg, 0.25 mmol) was dissolved in 10 mls $CHCl_3$ or 25 mLs EtOAc, respectively for 10mM solutions. Solutions between 0.2 and 5mM were prepared by adding the appropriate amount of the 10mM solution with a Gilmont syringe to 10mLs of $CHCl_3$ or EtOAc measured with a volumetric pipet. Solutions were prepared freshly before use.

Extraction Experiment. 2 mLs of the appropriate aqueous phase and organic phase, measured with the same volumetric pipet, were combined in a 15 mL capped conical test tube (Falcon). Between 8 and 15 samples with varying TAM concentration were prepared in this way. The mixture was shaken vigorously for 2 hours on a Glas-Col vortexing table. The test tubes were then centrifuged to separate the layers. Each experiment was repeated 2 or 3 times. The UV-Vis spectra of either the aqueous or the organic phases were recorded for approach #1 and approach #2, respectively. Spectra were recorded on a HP 8453 Diode Array spectrophotometer. For each sample, the

absorbance was recorded 7 times and the numbers were averaged. There was less than 0.3% error in the absorbances.

Determination of Extinction Coefficient of $Fe(L^2)_3 \cdot 3py^+$ in EtOAc. 15 samples were prepared in the same manner described above for the extraction experiments. The absorbances of the organic phases were recorded and 1mL (measured with a volumetric pipet) was removed and placed in individual acid- and EDTA-washed test tubes. The samples were evaporated to dryness in a covered hot water bath. The red residue was digested by adding 1mL of conc. HNO_3 (low Fe) to each test tube and heating in the hot water bath until all of the solids had dissolved (approx. 8 hours). These were then carefully transferred to a 10 mL acid- and EDTA-washed volumetric flask, the test tubes were rinsed three times with 1 mL of ddH_2O, the washings were transferred to the volumetric flask, and the sample was diluted to 10 mLs with ddH_2O. The Fe(III) content was analyzed by AA-ICP. The extinction coefficient for each sample was calculated and the average is 7273 ± 117 $mol^{-1}cm^{-1}$ at 440 nM.

References

(1) Mathur, J. N.; Murali, M. S.; Nash, K. L. *Solvent Extr Ion Exch* **2001**, *19*, 357-390.

(2) Logsdail, D. H.; Mills, A. L., Eds. *Solvent Extraction and Ion Exchange in the Nuclear Fuel Cycle*; Halstead Press: New York, 1985.

(3) Mohapatra, P. K.; Manchanda, V. K. *J Inclusion Phenom Mol Recogn* **1996**, *25*, 257-265.

(4) Otu, E. O.; Westland, A. D. *Solvent Extr. Ion Exch.* **1990**, *8*, 759-781.

(5) Romanovski, V. V.; White, D. J.; Xu, J. D.; Hoffman, D. C.; Raymond, K. N. *Solvent Extr. Ion Exch.* **1999**, *17*, 55-71.

(6) Shukla, J. P.; Singh, R. K.; Kumar, A. *Radiochim Acta* **1991**, *54*, 73-77.

(7) Spjuth, L.; Liljenzin, J. O.; Hudson, M. J.; Drew, M. G. B.; Iveson, P. B.; Madic, C. *Solvent Extr Ion Exch* **2000**, *18*, 1-23.

(8) Yonezawa, C.; Choppin, G. R. *J Radioanal Nucl Chem Art* **1989**, *134*, 233-239.

(9) Arnaud-Neu, F.; Bohmer, V.; Dozol, J. F.; Gruttner, C.; Jakobi, R. A.; Kraft, D.; Mauprivez, O.; Rouquette, H.; Schwingweill, M. J.; Simon, N.; Vogt, W. *J Chem Soc Perkin Trans 2* **1996**, 1175-1182.

(10) Du, H. S.; Wood, D. J.; Elshani, S.; Wai, C. M. *Talanta* **1993**, *40*, 173-177.

(11) Horwitz, E. P.; Kalina, D. G.; Diamond, H.; Vandegrift, G. F. *Solvent Extr. Ion Exch.* **1985**, *3*, 75-109.

(12) Manchanda, V. K.; Mohapatra, P. K.; Veeraraghavan, R. *Anal Chim Acta* **1996**, *320*, 151-154.

(13) Bartsch, R. A.; Bitalac, L. P.; Cowey, C. L.; Elshani, S.; Goo, M. J.; Huber, V. J.; Ivy, S. N.; Jang, Y. C.; Johnson, R. J.; Kim, J. S.; Luboch, E.; McDonough, J. A.; Pugia, M. J.; Son, B.; Zhao, Q. *J Heterocycl Chem* **2000**, *37*, 1337-1350.

(14) Bartsch, R. A.; Cowey, C. L.; Elshani, S.; Goo, M. J.; Huber, V. J.; Ivy, S. N.; Johnson, R. J.; Kim, J. S.; Luboch, E.; McDonough, J. A.; Pugia, M. J.; Son, B.; Zhao, Q. *J Heterocycl Chem* **2001**, *38*, 311-331.

(15) Bond, A. H.; Dietz, M. L.; Chiarizia, R. *Ind Eng Chem Res* **2000**, *39*, 3442-3464.

(16) Khopkar, S. M.; Gandhi, M. N. *J Sci Ind Res India* **1996**, *55*, 139-155.

(17) Hrdlicka, A. *Solvent Extr. Ion Exch.* **1991**, *9*, 259-276.

(18) Weitl, F. L.; Raymond, K. N.; Durbin, P. W. *J. Med. Chem.* **1981**, *24*, 203-206.

(19) Garrett, T. M.; Miller, P. W.; Raymond, K. N. *Inorg. Chem.* **1989**, *28*, 128-133.

(20) Garrett, T. M.; McMurry, T. J.; Hosseini, M. W.; Reyes, Z. E.; Hahn, F. E.; Raymond, K. N. *J. Am. Chem. Soc.* **1991**, *113*, 2965-2977.

(21) Cohen, S. M.; O'Sullivan, B.; Raymond, K. N. *IC* **2000**, *39*, 4339-4346.

(22) Gans, P.; Sabatini, A.; Vacca, A. *Talanta* **1996**, *43*, 1739.

(23) Gans, P.; Sabatini, A.; Vacca, A. In;: Leeds, U.K. Florence, Italy.

(24) Karpishin, T. B. In *Chemistry*; University of California, Berkeley, 1992.

(25) Gans, P.; Sabatini, A.; Vacca, A. *Ann. Chim-Rome* **1999**, *89*, 45-49.

(26) Garrett, T. M.; Cass, M. E.; Raymond, K. N. *J. Coord. Chem.* **1992**, *25*, 241-253.

(27) Eriksson, G. In;: Umea, Sweden.

(28) Shridah, M.; Ohzeki, K. *Analyst* **1986**, *111*, 197.

(29) Manjula, V.; Bhattacharya, P. *J. Inorg. Biochem.* **1991**, *41*, 63.

(30) Anderegg, A. *Pure and Appl. Chem.* **1982**, *54*, 2693.

(31) Motekaitis, R.; Martell, A. *J. Coord. Chem.* **1994**, *31*, 67.

(32) Anderegg, G. **1978**.

(33) Gramer, C. J.; Raymond, K. N. *Organic Letters* **2001**, *in press*.

(34) Johnson, A. R.; O'Sullivan, B.; Raymond, K. N. *IC* **2000**, *39*, 2652-2660.

(35) LABVIEW In; 5.0.1 ed.; National Instruments Corporation: Austin, TX.

(36) Gans, P.; O'Sullivan, B. *Talanta* **2000**, *51*, 33.

(37) Schawarzenbach, G.; Flaschka, H. *Complexometric Titrations*; Methuen and Co. Ltd.: London, 1969.

CHAPTER FOUR

A Streamlined Synthesis of 2,3-Dihydroxyterephthalamides

Introduction

Catecholate ligands incorporating a variety of electron withdrawing substituents have been extensively investigated for their extraordinarily high affinity for high-oxidation state metals.[1-12] The catecholate anion is highly sensitive to oxidation[12] unless the aromatic ring is substituted with electron withdrawing groups, which also precludes its incorporation into useful materials. Catechol derivatives containing one or more carboxylates or amides - 2,3-dihydroxybenzamides (CAM), carboxamido-2,3-dihydroxyterephthalates (CAMC), and 2,3-dihydroxyterephthalamides (TAM) - display higher Fe(III) affinity, are harder to oxidize, and are more acidic than catechol.[13,14] The increased acidity of these ligands relative to catechol broadens their utility because they can fully complex Fe(III) in lower pH solutions. These properties prompted successful investigations of CAMs and CAMC derivatives as in vivo decorporation agents for Pu(IV) and the in vitro stability of complexes with Ce(IV), a Pu(IV) analog.[15-17]

Until recently, the TAMs had only been characterized as Fe(III) chelators. As described in chapter 2, the strength of the TAMs as M(IV) chelators has been shown by the direct spectrophotometric titration of Pu(IV) with a TAM. The overall formation constant for the $[Pu(ETAM)_4]^{4-}$ was calculated as $10^{55.6}$. The application of the TAMs as actinide extractants, discussed in Chapter 3, has been achieved by the appropriate functionalization of the side chains such that lipophilic, neutral complexes can be

extracted into an organic solvent. The implementation of the TAMs as practical, large-scale actinide sequestering agents would require that any ligand be accessed through an efficient synthesis. Described in this chapter is a shorter synthetic route to the TAMs that decreases the time, cost, and hazards associated with the synthesis.

The typical TAM synthesis[13,14,18] involves six steps (Scheme 4-1) in an overall 30% yield: carboxylation of catechol to form **2**, conversion of the carboxylic acids to methyl esters **3**, methyl or benzyl protection of the catecholate oxygens **4**, saponification of the esters to provide **5**, activation to the acid chloride, coupling with the desired amine, and deprotection of the catecholate oxygens to yield the desired TAM. The CAMC synthesis differs in that it requires the saponification of only one ester of **4** followed by amide bond formation and hydroxyl deprotection.

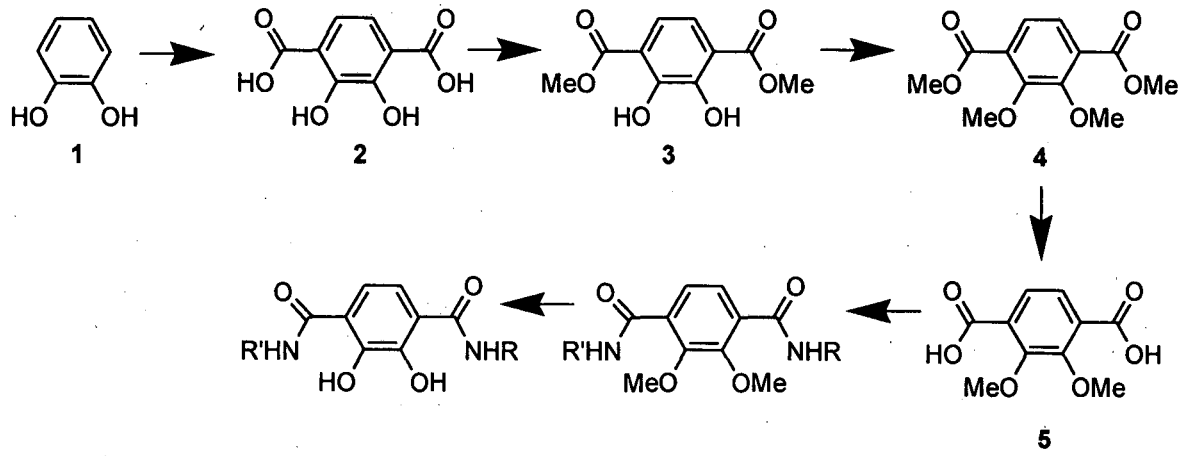

Scheme 4-1. The typical TAM synthesis requires protection and deprotection of the catecholate oxygens.

General outline for a shorter synthetic route

The more efficient synthesis described here for TAMs does not require protection of the phenolic oxygens; the direct activation of 2,3-dihydroxyterephthalic acid **2** with $SOCl_2$ is followed by reaction with an amine.[19] By avoiding the protecting group the number of synthetic steps is reduced from seven to three. This eliminates two steps involving the hazardous reagents dimethyl sulfate and BBr_3, decreases the synthetic time from approximately nine days to two days, increases the overall yield to 75%, and decreases the cost for alkyl TAMs tenfold. This synthetic sequence also broadens the diversity of available TAMs since deprotection of methyl ether protecting groups with BBr_3 is incompatible with certain functional groups that might be desired in the amide side chains. Finally, this procedure has been adapted to allow for the preparation of CAMC ligands and the installation of two *different* amides, generating a much wider

range of compounds. Two ligand designs were developed for the extraction of metals from aqueous solution and these ligands were synthesized as a demonstration of this synthetic route (Figure 4-1).

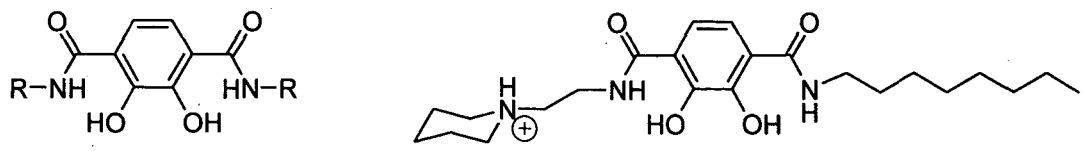

Figure 4-1. Two ligand designs were targeted for the shorter synthetic route based on their success as actinide chelators.

Synthesis of symmetric TAMs

For the current synthesis, compound **2** was activated with an excess of $SOCl_2$ in refluxing dioxane for 6 h (Scheme 4-2) followed by evaporation to yield the crude acid chloride as a yellow oil. Although a variety of organic solvents were used successfully for the activation, the use of dioxane ensures the removal of excess $SOCl_2$ during evaporation. Coupling the crude acid chloride with octylamine, cyclohexylamine, or ethylamine in $CHCl_3$ at 0°C followed by extraction with 1M HCl and recrystallization yields the pure product in 40 - 90% yield. Compound **8** had the low yield due to the work-up, although the reaction appeared to be quantitative from the NMR spectrum of the crude product. Compound **8** was first isolated as the triethylammonium salt of the deprotonated ligand, and its solubility in water during the recrystallization resulted in the loss of some product.

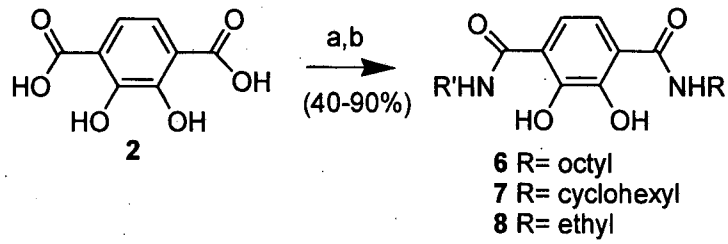

Scheme 4-2. The shorter synthesis described here obviates the need for protecting groups and symmetric TAMs can be easily synthesized in one step.

Characterization of the acid chloride intermediate

Activation of the dicarboxylic acid **2** with $SOCl_2$ was proposed based on previous work on the $SOCl_2$ activation of 2,3-dihydroxybenzoic acid, for which there was originally some confusion about the product composition.[20-22] The product was first reported as 2,3-dihydroxybenzoyl chloride **9** based on the previously reported formation of 2,4-dihydroxybenzoyl chloride **11**,[23] although characterization was limited to a melting point of 84 °C for the sublimed crystals (Figure 4-2). However it was later shown that the phenol groups react to form a sulfite ester, a convenient and effective in situ protecting group. The resulting sublimed crystals of 2,3-dioxosulfinylbenzoyl chloride **10** were characterized by melting point and elemental analysis. This acid chloride has been useful for several syntheses requiring the installation of a catecholamide.[24-28] The formation of the catecholate sulfite ester is also precedented; the synthesis of 1,2-dioxosulfinyl benzene from the reaction of catechol with $SOCl_2$ has been reported.[29,30]

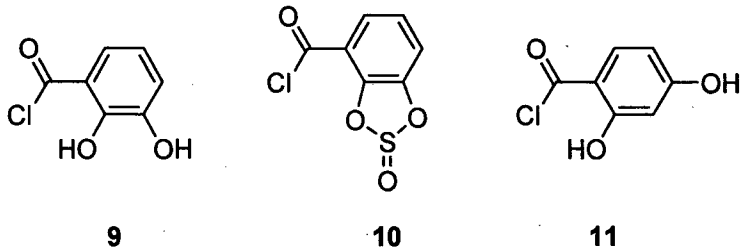

Figure 4-2. Acid chlorides 9-11 which also contain phenols have been described in the literature. 10 was originally reported with the structure of 9 based on analogy to 11 but 9 has never been isolated.

The key intermediate for making the symmetric TAMs is the product of the reaction between **2** and $SOCl_2$. By analogy to **10** and **11**, both 2,3-dihydroxyterephthaloyl chloride **12** and 2,3-dioxosufinylterephthaloyl chloride **13** could be considered as products (Figure 4-3). The composition of the intermediate was elucidated by ^{1}H NMR spectroscopy and X-ray crystallography.

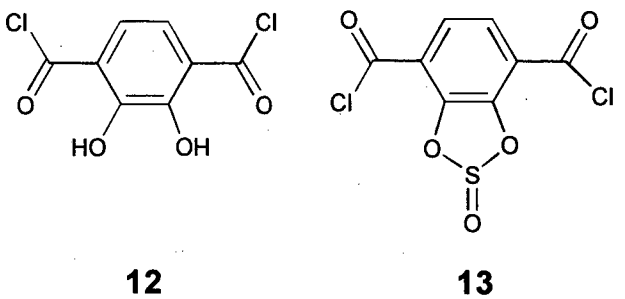

Figure 4-3. Possible structures of acid chlorides arising from the reaction of 2 with $SOCl_2$.

The product isolated from refluxing dioxane as described above – a yellow oil - exhibits a singlet in the ^{1}H NMR spectrum at ca. 8 ppm. This was tentatively assigned as the labile intermediate **13** since two decomposition products were observed in the ^{1}H NMR spectra (D_8-THF) as **13** decomposed. The decomposition of **13** via loss of SO_2 to form the less reactive phenol acid chloride **12** was observed as the singlet at 8 ppm disappeared and another appeared at ca. 7.5 ppm. This compound further decomposed when water was introduced into the NMR tube (in the form of wet D_8-THF): the singlet at ca. 7.5 ppm disappeared and a singlet at ca. 7.2 ppm appeared which corresponds to the starting material **2**.

The opposite situation was seen in the forward reaction of **2** with $SOCl_2$ in d_8-THF as the ^{1}H NMR spectra were monitored over the course of one day (Figure 4-4). At 2 hours, the signal for **2** was disappearing while several other sets of peaks were appearing: a doublet of doublets centered around 7.37 ppm, the singlet at ~7.5 ppm (assigned as compound **12**), a second doublet of doublets centered around 7.85 ppm, and another singlet at ~ 8 ppm (assigned as compound **13**). By 24 hours everything was converted to **13** as evidenced by the singlet at 8 ppm, with the exception of a small peak at 7.5 ppm for the remaining **12**. The two doublets of doublets could be the intermediate with one acid chloride and one carboxylic acid, with and without the sulfite ester, although they were never isolated and characterized. The NMR spectra indicate that the acid chlorides and sulfite ester are forming simultaneously. Therefore, for this synthesis it is best to reflux the solution as described above to allow the sulfite ester protecting group to form which will ensure complete formation of the acid chlorides.

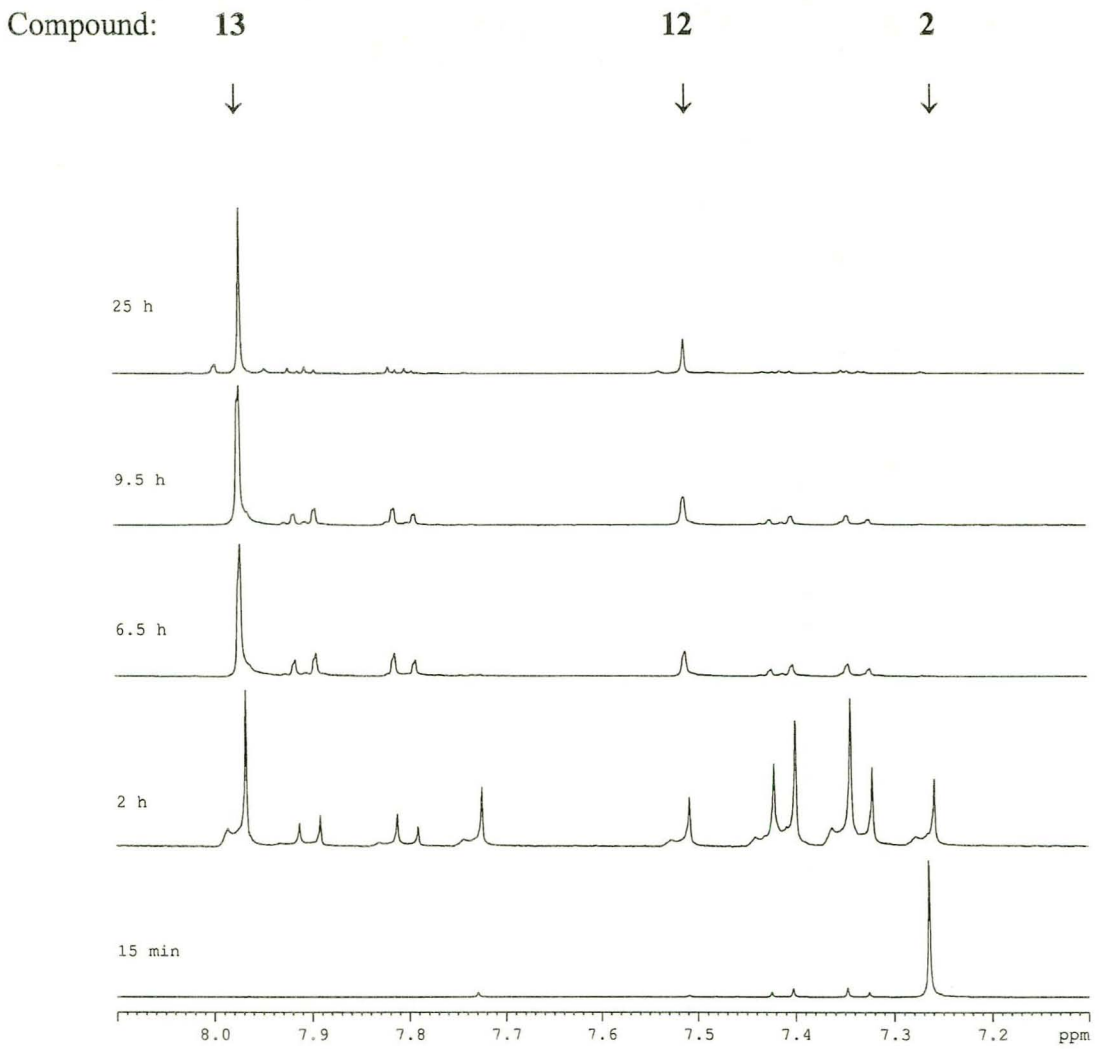

Figure 4-4. ^{1}H NMR spectra of the reaction of 2 with $SOCl_2$.

A yellow solid results from the decomposition of the yellow oil **13** or the incomplete reaction of **2** with $SOCl_2$. Sublimation of this yellow solid yielded crystals suitable for X-ray diffraction. This confirmed that the activated intermediate with a ^{1}H NMR signal at 7.5 is **12** and not an ester polymer formed from the reaction of the phenol oxygens with the acid chloride (Figure 4-5). As is seen with all TAMs in the solid state, the carbonyl is oriented such that the oxygen is hydrogen-bonded to the phenolic

proton.[31] The stability of this chelate hydrogen bond possibly in part hinders the formation of a polymeric ester. An amine can be coupled with a mixture of **12** and **13** without a loss in yield and the transitory protecting group is easily cleaved during the aqueous workup following the amine coupling.

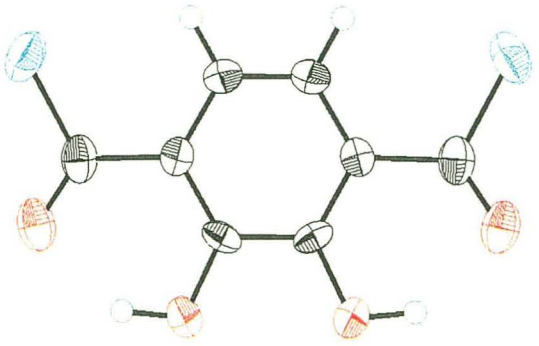

Figure 4-5. X-Ray crystal structure (ORTEP) of 12. Thermal ellipsoids are drawn at the 50% probability level.

An adapted procedure for unequivalent amide substitution

This procedure was modified so a TAM with two different amide linkages can be prepared (Scheme 4-3). This methodology is demonstrated with the synthesis of ligand **19** and is general for most amides. Ligand **19** was chosen because of its ability to extract Fe(III) from aqueous solutions and is very amenable to this synthetic route. This synthesis is best suited for intermediates that can be purified by extractions and recrystallizations since the unprotected catecholate oxygens preclude purification by column chromatography.

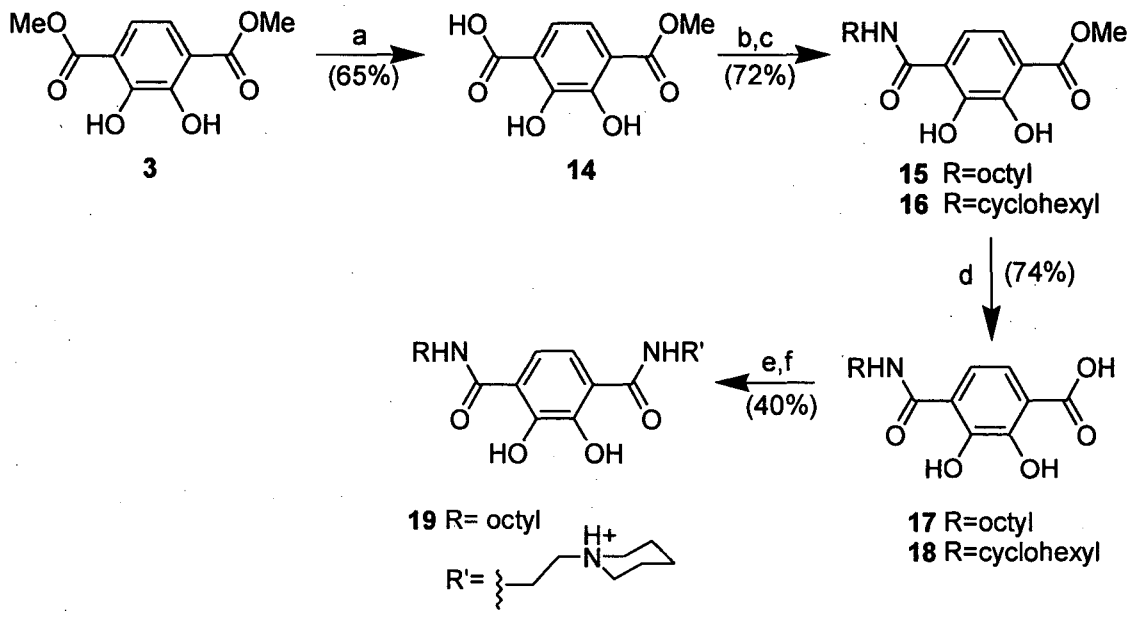

Scheme 4-3. The procedure was modified so a TAM with two different amides could be prepared.

Mono-saponification of the dimethyl ester **3** with aq. $NaHCO_3$ affords **14** in 70% yield. This procedure was carried out in warm water due to the limited solubility of **3** in water. Cooling the reaction mixture after ca. 5 hours precipitated any unreacted starting material, while the deprotonated product remained in solution. Subsequent acidification resulted in precipitation of only the product **14** and any small amounts of **2** that formed remained in solution. MeOH, which increases the solubility of **3**, was avoided as a solvent, since it prevented the separation of **3**, **14**, and **2**. The acid chloride was prepared by treatment of **14** with $SOCl_2$ in refluxing dioxane. The crude acid chloride was then coupled to octylamine in the presence of TEA to yield **15**. The TEA·HCl was removed by extraction with HCl, however this did not remove the excess octylamine. This was circumvented by boiling the resulting solid in water and filtering while hot. This also

removes any unreacted **14**, which is soluble in acidic water only when hot. Compound **15** was then converted to the acid **17** by stirring in thoroughly degassed 1M KOH. Halting the synthesis at this point provides the CAMC ligands. Finally **17** was activated with $SOCl_2$ and treated with one equivalent of 1-(2-ethylamino)piperidine to afford **19** in 40% yield. The octylamide was installed first because in general it was found that installing the more hydrophobic of the two amides first eased the separation of the product from the excess amine. For monitoring the progress of any reaction, thin layer chromatography was used with one of three solvent systems: 5:4:1 benzene: ethyl formate: formic acid, 5:4:1:1 ethyl acetate: acetone: methanol: water, or 4:3:1:1 ethyl acetate: acetic acid: methanol: water.

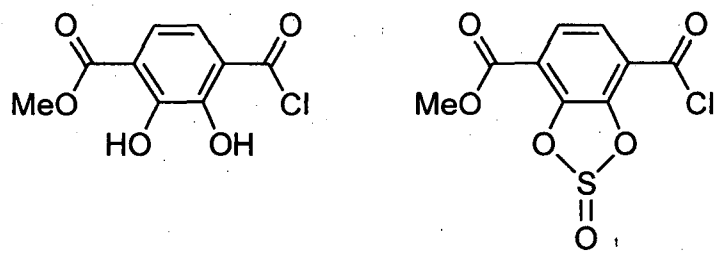

20 **21**

Figure 4-6. Possible structures of the acid chloride resulting from the reaction of 14 with $SOCl_2$.

After activating mono-ester **14** with $SOCl_2$, one product was initially observed in the ^1H NMR spectrum which is tentatively assigned as **21** (Figure 4-6). As with **13**, the decomposition of this to the acid chloride **20** then to the starting material **14** was observed (Figure 4-7). The doublet of doublets for **21** is centered at 7.9ppm (D_6-

acetone). After 2 days, these signals were gone and two doublets of doublets appeared – one centered about 7.44 ppm for **20**, and one centered about 7.32 ppm for the starting material **14**. After an additional 3 days, only the signals for **14** remained. In addition, the singlet for the methyl ester protons of the three different compounds also appeared and disappeared. If the activation reaction was carried out at lower temperatures or for a shorter amount of time, the ^{1}H NMR spectrum of the crude product contained signals for **20** and **21**. Sublimation of the resultant yellow solid afforded a pure yellow powder, confirmed by elemental analysis, ^{1}H, and ^{13}C NMR as the acid chloride **20**.

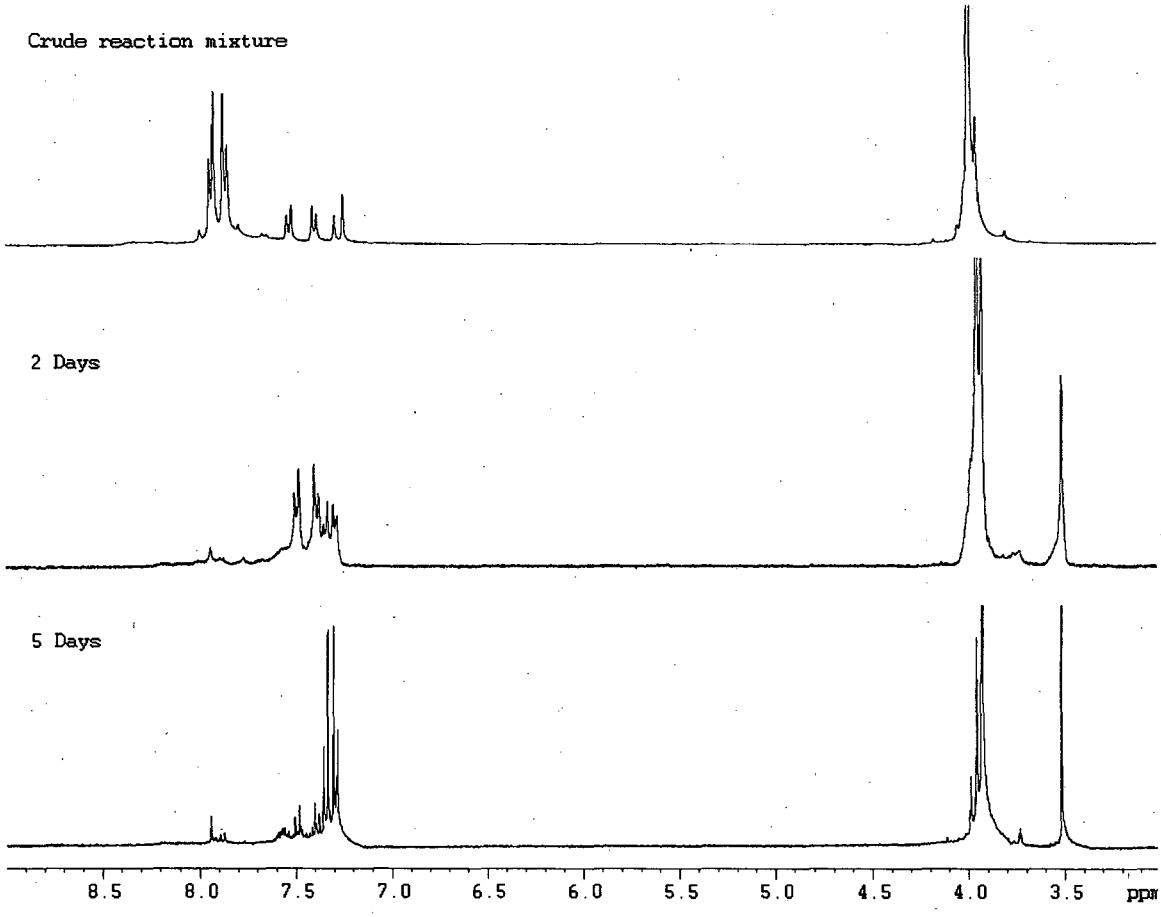

Figure 4-7. ^{1}H NMR spectra (D_6-acetone) following the decomposition of 21 to 20, then 14.

Conclusion

In summary, a synthesis for 2,3-dihydroxyterephthalamides has been developed that obviates the need for protection of the catecholates. The synthesis has been adapted to permit the introduction of two different amide linkages and can be used for the synthesis of the CAMC ligands. These routes avoid the costly BBr_3 deprotection and shorten the synthesis of a symmetric TAM from one week to one day. This methodology would enable broad application in large-scale production of sequestering agents based on this class of ligands.

Experimental

General. All reagents and solvents were purchased from Aldrich Chemical Company or Fisher Scientific and used as purchased. All solvents were dried over activated alumina and stored over 4Å molecular sieves. All reactions were carried out under Ar. Thionyl chloride was purified by distillation from triphenyl phosphite. Water was distilled and further purified by a Millipore cartridge system (resisitivity 18 x 10^6 Ω). All melting points were obtained using a Mel-Temp melting point apparatus (Laboratory Devices). Thin layer chromatography (TLC) was performed using alumina-backed silica plates and visualized with a 254 nm UV lamp. All organic extracts were dried over $MgSO_4$ and solvents were removed with a rotary evaporator. ^1H and ^{13}C NMR spectra were obtained on a Bruker DRX500 (500 MHz) or Bruker AMX400 spectrometer (400 MHz) as noted. All NMR samples were taken in $CDCl_3$, d_6-DMSO, d_8THF, or d_6-acetone as noted. All Microanalyses were performed by the Microanalytical Services Laboratory in the College of Chemistry, University of California, Berkeley. Compounds **2-5** and **8** were synthesized by published methods.[13,14]

2,3-Dihydroxy terephthaloyl chloride (12)

2 (0.207 g, 1.05 mmols), suspended in 15 mLs of 1,4-dioxane, dissolved upon addition of thionyl chloride (0.4 mLs, 5.4 mmols) and the solution turned pale yellow. The solution was stirred for 12 hours at 45 °C under Ar. The liquids were removed and the yellow solid was coevaporated 3 times with dry $CHCl_3$. Crystals suitable for X-ray diffraction

were grown by sublimation (45-65 °C, 0.1 torr). ^{1}H NMR ($CDCl_3$): δ 7.66 (s, 2H, 2 CH), 9.74 (s, 2H, 2 OH).

N,N'-Octyl-2,3-Dihydroxyterephthalamide (6)

2 (0.46 g, 2.2 mmol) was dissolved in THF and ca. 1.5 mLs of $SOCl_2$ was added. The solution was stirred at RT overnight under Ar then evaporated to a yellow oil. This acid chloride (**13**) was dissolved in CH_2Cl_2 and added slowly to a CH_2Cl_2 solution of octylamine (1.5 mL, 9 mmol) cooled in an ice water bath and allowed to warm to RT under Ar while stirring for 30 min. The solution was extracted with 3 X 1M HCl to remove the excess octylamine. Evaporation of the CH_2Cl_2 yielded a white solid (0.633 g, 90%yield).

N,N'-Cyclohexyl-2,3-Dihydroxyterephthalamide (7)

2 (0.2g, 1.0 mmol) was suspended in $CHCl_3$ and ca. 1.5 mLs of $SOCl_2$ was added. The solution was heated at reflux overnight under Ar then evaporated to a yellow oil. This acid chloride (**13**) was dissolved in CH_2Cl_2 and added slowly to a CH_2Cl_2 solution of cyclohexylamine cooled in an ice water bath and allowed to warm to RT under Ar while stirring overnight . The solution was extracted with 3 X 1M HCl to remove the excess cyclohexylamine. Evaporation of the CH_2Cl_2 yielded a white solid (0.25 g, 60 %yield). MP 250 °C, NMR ($CDCl_3$): δ 7.05 (s, 2H, arom. CH), 6.69 (d, 1H, NH), 3.96 (m, 1H, CH), 1.23-2.03 (m, 1H, CH_2). ^{13}C NMR (CDCl3): δ 168.0, 150.5, 117.8, 116.3, 48.8, 48.7, 32.5, 31.1, 25.6, 25.3. Anal. Calcd (found) for $C_{20}H_{28}O_4N_2$: C 66.64 (66.94); H 7.83 (7.97); N 7.77 (7.79).

N,N'-Ethyl-2,3-Dihydroxyterephthalamide (8)

2 (0.1g, 0.5 mmol) was suspended in $CHCl_3$ and ca. 1.5 mLs of $SOCl_2$ was added. The solution was heated at reflux overnight under Ar then evaporated to a yellow oil. This acid chloride (**13**) was dissolved in CH_2Cl_2, cooled in an ice water bath, and gaseous ethylamine was bubbled through the solution. The cloudy yellow reaction mixture was allowed to warm to RT under Ar while stirring overnight . The off-white solid ($2H_3NEt^+ETAM$) was filtered, dissolved in boiling water, and the product precipitated as a white solid with addition of HCl (0.53 g, 40% yield). (Unreacted **2** was recovered from the filtration supernatant by extraction with water and evaporation of the CH_2Cl_2.) Melting point, ^{1}H NMR, ^{13}C NMR, and elemental analysis matched those previously published.[7]

2,3-Dihydroxy methyl benzoate 4-carboxylic acid (14)

3 (0.506 g, 2.2 mmols) was suspended in 150 mLs of distilled, deionized water and $NaHCO_3$ (0.125 g, 1.49 mmols) was added. The suspension was heated at 40 °C and all solids dissolved. After 12 hours the reaction was cooled to room temperature; the unreacted starting material precipitated and was filtered (0.162 g, 100% recovery). The supernatant was acidified with HCl and the resulting white precipitate was filtered and dried in a vacuum oven (0.203 g, 0.96 mmols, 65% yield). mp 223-226 °C. ^{1}H NMR (D_6-DMSO): δ 3.85(s, 3H, CH_3), 7.15 (dd, 1H, CH), 7.22 (dd, 1H, CH), 10.4 (br s, 1H, OH). ^{13}C NMR (D_6-DMSO): δ 53.1, 116.9, 117.4, 118.6, 119.0, 119.3, 149.9, 150.0,

151.4, 169.1, 169.2, 172.0. Anal. Calcd (found) for $C_9H_8O_6$: C 50.95 (50.70); H 3.80 (3.97).

2,3-Dihydroxy methyl benzoate 4-carbonyl chloride (20)

14 (0.537 g, 2.5 mmols) was dissolved in 25 mLs of 1,4-dioxane with the addition of $SOCl_2$ (1.3 mLs, 17.8 mmols) and the reaction turned pale yellow. The solution was heated at 45-50 °C for 12 hours under Ar. The liquids were removed and the yellow solid was coevaporated 3 times with dry $CHCl_3$ and sublimed (45-65 °C, 0.1 torr). mp 88-96 °C. ^{1}H NMR ($CDCl_3$): δ 3.40(s, 3H, CH_3), 7.40 (dd, 1H, CH), 7.53 (dd, 1H, CH), 9.62 (s, 1H, OH), 11.02 (s, 1H, OH). ^{13}C NMR ($CDCl_3$): δ 53.1, 117.2, 119.1, 120, 121.6, 151.2, 151.5, 169.7. Anal. Calcd (found) for $C_9H_7O_5Cl$: C 46.88 (46.5); H 3.06 (2.97).

2,3-Dihydroxy methyl benzoate 4-octylamide (15)

14 (0.250g, 1.2 mmol) was dissolved in 15 mLs of dry THF with the addition of 1 mL of $SOCl_2$ and stirred for 12 hours under Ar. The solvent was evaporated and the yellow oil was dissolved in 15 mLs of dry CH_2Cl_2, cooled with a dry ice/acetone bath and added slowly to octylamine (1mL, 6 mmols) dissolved in 5 mLs of CH_2Cl_2 under Ar and cooled in a dry ice/acetone bath. The reaction was allowed to warm to room temperature for 2 hours while stirring, then extracted with 1M HCl (2 x 30 mLs), dried, and evaporated to a white solid. The solid was boiled in 25 mLs of water and filtered while hot to afford **15** as a white solid (0.273 g, 0.85 mmols, 72% yield). MP 130-134 °C. ^{1}H NMR ($CDCl_3$): δ 0.84 (t, 3H), 1.2 (m, 10H), 1.5 (m, 2H), 3.28 (m, 2H), 3.88 (s, 3H), 7.21 (d, 1H), 7.35 (d, 1H), 8.95 (t, 1H, NH), 10.3 (bs, 1H, OH), 13.0 (bs, 1H, OH)., ^{13}CMR ($CDCl_3$): δ 14.1,

22.6, 27.0, 29.2, 29.3, 29.4, 31.8, 40.0, 52.7, 114.5, 115.5, 118.3, 150.0, 151.7, 168.3, 170.1, FAB-MS(+), m/z : 324. Anal. Calcd (found) for $C_{17}H_{25}O_5N$: C 63.14 (62.81), H 7.79 (7.79), N 4.33 (4.13).

2,3-Dihydroxybenzoic acid 4-octylamide (17)

15 (0.485 g, 1.5 mmol) was suspended in 5 mLs distilled, deionized water and upon addition of 15 mLs of 1M KOH the solid dissolved. N_2 was bubbled through the solution for 10 minutes then it was stirred for 2 hours under Ar. Addition of HCl precipitated **17** as a white solid (0.345 g, 1.1 mmols, 74% yield). MP 197-200 °C. ^{1}H NMR ($CDCl_3$): δ 0.82 (t, 3H), 1.2 (m, 10H), 1.5 (m, 2H), 3.27 (m, 2H), 7.22 (d, 1H), 7.33 (d, 1H), 8.92 (t, 1H, NH), 12.83 (bs, 1H, OH). ^{13}CMR ($CDCl_3$): δ 14.3, 22.5, 26.8, 29.0, 29.1, 31.6, 115, 116.5, 118, 119, 150.3, 151.7, 168.9, 172.1, FAB-MS(+) m/z: 310, Anal. Calcd (found) for $C_{16}H_{23}O_5N$: C 62.12 (62.05), H 7.49 (7.64), N 4.53 (4.84).

N-octyl, N'-ethylpiperidine-2,3-Dihydroxyterephthalamide (19)

17 (0.100 g, 0.32 mmols) was dissolved in 10 mLs of dry dioxane with 1mL of $SOCl_2$ and heated at reflux for 5 hours under Ar. Evaporation afforded a yellow-brown oil which was dissolved in 10 mLs of $CHCl_3$, cooled in an ice water bath, and added slowly to 1-(2-aminoethyl)piperidine (0.06 mLs, 0.42 mmols) dissolved in 10 mLs of $CHCl_3$ under Ar cooled in an ice water bath. The reaction was stirred for 3 hours in an ice water bath, then 3 hours at room temperature and extracted with $NH_4CH_3CO_2$ (pH 9, 0.1M, 2x 20 mLs) and HCl (1M, 20 mLs). Evaporation yielded a tan oil which upon trituration with EtOAc (3 mLs) afforded **19** as a white solid. ^{1}H NMR ($CDCl_3$): δ 0.87 (t, 3H),

1.26-1.67 (mult, 20H), 2.62-2.74 (mult, 5H), 3.43 (quart, 2H), 3.62 (t, 2H), 6.98 (d, 1H), 7.04 (d, 1H), 7.06 (bs, 1H, NH), 8.35 (bs, 1H, NH). Anal. Calcd (found) for $C_{23}H_{38}O_4N_3Cl$: C 60.58 (60.28), H 8.4 (8.54), N 9.21 (8.86).

References

(1) Raymond, K. N.; Müller, G.; Matzanke, B. F. In *Topics in Current Chemistry*; Boschke, F. L., Ed.; Springer-Verlag: Berlin, Heidelberg, 1984; pp 50-102.

(2) Raymond, K. N. *Coord. Chem. Reviews* **1990**, *105*, 136-153.

(3) Telford, J. R.; Raymond, K. N. In *Comprehensive Supramolecular Chemistry*; Atwood, J. L., Davies, J. E. D., MacNicol, D. D., Vogtle, F., Eds.; Elsevier Science Ltd.: Oxford, 1996; Vol. 1, pp 245-266.

(4) Raymond, K. N.; Kappel, M. J.; Pecoraro, V. L.; Harris, W. R.; Carrano, C. J.; Weitl, F. L. In *Actinides in Perspective*; Edelstein, N. M., Ed.; Pergamon Press: Oxford and New York, 1982; pp 491-507.

(5) Raymond, K. N.; Garrett, T. M. *Pure & Appl. Chem.* **1988**, *60*, 1807-1816.

(6) Raymond, K. N.; Freeman, G. E.; Kappel, M. J. *Inorg. Chem. Acta* **1984**, *94*, 193-194.

(7) Karpishin, T. B.; Dewey, T. M.; Raymond, K. N. *J. Am. Chem. Soc.* **1993**, *115*, 1842-1851.

(8) Dewey, T. M.; Du Bois, J.; Raymond, K. N. *Inorg. Chem.* **1993**, *32*, 1729-1738.

(9) Branca, M.; Micera, G.; Dessi, A.; Sanna, D.; Raymond, K. N. *Inorg. Chem.* **1990**, *29*, 1586-1589.

(10) Borgias, B. A.; Cooper, S. R.; Koh, Y. B.; Raymond, K. N. *Inorg. Chem.* **1984**, *23*, 1009-1016.

(11) Cooper, S. R.; Koh, Y. B.; Raymond, K. N. *J. Am. Chem. Soc.* **1982**, *104*, 5092-5102.

(12) Pierpont, C. G.; Lange, C. W. In *Progress in Inorganic Chemistry*; Karlin, K. D., Ed.; John Wiley & Sons, Inc., 1994; Vol. 41, pp 331-442.

(13) Weitl, F. L.; Raymond, K. N.; Durbin, P. W. *J. Med. Chem.* **1981**, *24*, 203-206.

(14) Garrett, T. M.; Miller, P. W.; Raymond, K. N. *Inorg. Chem.* **1989**, *28*, 128-133.

(15) Raymond, K. N.; Smith, W. L. In *Structure and Bonding*; Goodenough, J. B., Hemmerich, P., Ibers, J. A., Jorgensen, C. K., Neilands, J. B., Reinen, D., Williams, R. J. P., Eds.; Springer-Verlag: Berlin, Heidelberg, 1981; Vol. 43, pp 159-186.

(16) Lloyd, R. D.; Bruenger, F. W.; Mays, C. W.; Atherton, D. R.; Jones, C. W.; Taylor, G. N.; Stevens, W.; Durbin, P. W.; Jeung, N.; Jones, E. S.; Kappel, M. J.; Raymond, K. N.; Weitl, F. L. *Rad. Chem.* **1984**, *99*, 106-128.

(17) Kappel, M. J.; Nitsche, H.; Raymond, K. N. *Inorg. Chem.* **1985**, *24*, 605-611.

(18) Rodgers, S. J.; Ng, C. Y.; Raymond, K. N. *J. Am. Chem. Soc.* **1985**, *107*, 4094-4095.

(19) Gramer, C. J.; Raymond, K. N. *Organic Letters* **2001**, *in press*.

(20) Corey, E. J.; Bhattacharyya, S. *Tetrahedron Letters* **1977**, *45*, 3919-3922.

(21) Corey, E. J.; Hurt, S. D. *Tetrahedron Letters* **1977**, *45*, 3923-3924.

(22) Weitl, F. L.; Raymond, K. N. *J. Am. Chem. Soc.* **1979**, *101*, 2728-2731.

(23) Scott, A. W.; Kearse, W. O. *Journal of Organic Chemistry* **1940**, 598-605.

(24) Husson, A.; Besselievre, R.; Husson, H.-P. *Tetrahedron Letters* **1983**, *24*, 1031-1034.

(25) Lowe, C.; Pu, Y.; Vederas, J. C. *Journal of Organic Chemistry* **1992**, *57*, 10-11.

(26) Pu, Y.; Lowe, C.; Sailer, M.; Vederas, J. C. *The Journal of Organic Chemistry* **1994**, *59*, 3642-3655.

(27) Slama, S.; Stong, J. D.; Neilands, J. B.; Spiro, T. G. *Biochemistry* **1978**, *17*, 3781-3785.

(28) Corey, E. J.; Cashman, J. R.; Kanter, S. S.; Wright, S. W. *Journal of the American Chemical Society* **1984**, *106*, 1503-1504.

(29) Anschutz, R.; Posth, W. *Chem. Ber.* **1894**, *27*, 2751-2753.

(30) Green, A. *Journal of the Chemical Society* **1927**, 500-503.

(31) Garrett, T. M.; Cass, M. E.; Raymond, K. N. *J. Coord. Chem.* **1992**, *25*, 241-253.

CHAPTER FIVE

The Removal of Dilute Concentrations of Pu(IV) from Aqueous Solutions using Polymer Filtration and 2,3-Dihydroxyterephthalamide-Functionalized Water Soluble Polymers

Introduction

The removal of actinides from waste streams presents challenging separation problems due to the complex and unique mixture of radioactive and non-radioactive components each stream contains. The usual approaches to separating actinide ions from solutions involve liquid-liquid extraction[1-5] or solid-supported chelators.[6-9] Although many advances have been made in the development of new extractants, ion exchange materials, and ligands for solid supports, any one of these techniques has the disadvantages of slow kinetics and mixed waste or colloid formation, and none are ideal for the removal or concentration of dilute amounts of radionuclides. Thus new approaches to waste stream remediation are required that can function in ways for which older techniques are not suited.

Ultrafiltration (UF) used in combination with water soluble chelating polymers (WSCP) has recently been developed as a very effective way to remove or concentrate Pu(IV) from dilute waste streams,[10-14] although UF was first investigated as a separation technique 30 years ago.[15] Separation is achieved with a molecular weight cutoff membrane that retains higher molecular weight species ("retentate") while allowing the smaller molecules and ions to freely pass through the membrane ("permeate"), illustrated

in Figure 5-1. The metal ion separation is accomplished by chelating the metal with a ligand that is covalently attached to a water-soluble polymer. This process can be conducted in two ways: as a separation or a concentration method. In the separation method (diafiltration), the retentate is replenished with water at the same rate that the water is permeating the membrane. The small molecules are essentially washed from the solution. For concentration (ultrafiltration), the retentate is not replenished with water and thus the volume is reduced.

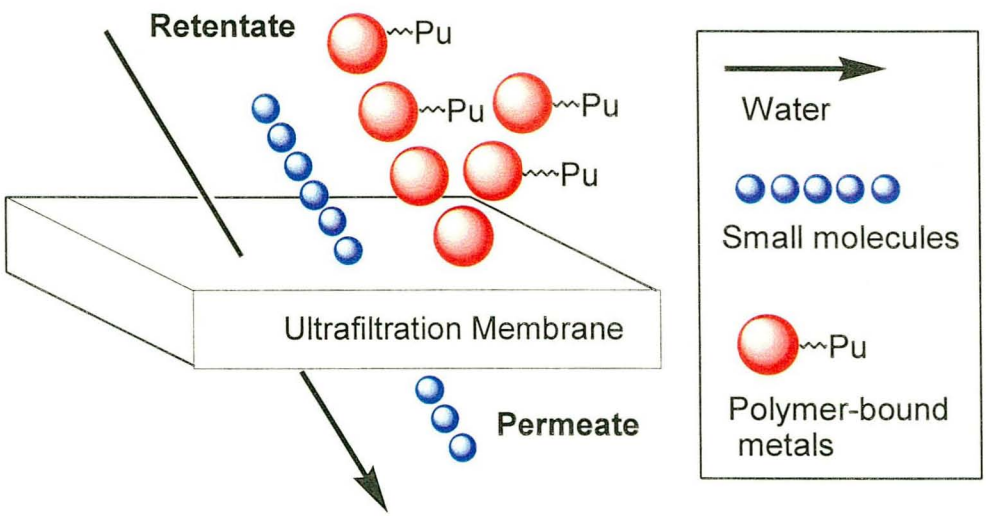

Figure 5-1. Schematic of the principle of ultrafiltration.

Approximately ten years ago Drs. Barbara Smith and Gordon Jarvinen of Los Alamos National Lab started investigating the UF technique as a way to remove and recover metals from a waste stream with a metal chelator covalently linked to a water-soluble polymer. When UF and WSCP are used together, the technique has been called polymer-supported ultrafiltration, liquid-phase polymer-based retention, polyelectrolyte-

enhanced ultrafiltration, and polymer-assisted ultrafiltration, however these researchers at LANL refer to it as polymer filtration (PF). The scaffold they selected for the WSCP is polyethyleneimine (PEI) (Figure 5-2), a water-soluble polymer with a molecular weight of at least 30,000. PEI is a polymerized aziridine with a ratio of 1°:2°:3° nitrogens of 1:2:1 and functionalization of the primary amines with ligands such as phosphonic acids produces the WSCP.[16]

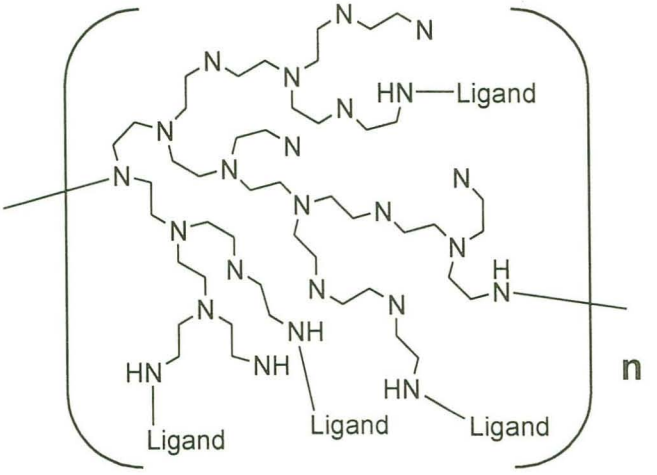

Figure 5-2. Polyethyleneimine (PEI) is a water soluble polymer with primary amines that can be functionalized with metal-specific ligands.

The effectiveness of PF has been demonstrated in several industrial processes, including recovering Zn from an electrochemical plating bath, removing Cu from a waste stream resulting from printing circuit boards, and the removal of Pu-239 from LANL waste streams. The technology has currently been licensed to two companies – one for non-radioactive work and one for radioactive work. The hardware consists of a reservoir (feed tank) that contains the waste stream and WSCP, a peristaltic pump, and a column

housing the size-exclusion membrane (Figure 5-3). The process was first conducted with a bench-top unit that can process between 10 - 50 mL per minute and has been scaled up to a unit that can process 0.5 – 1 L per minute, or approximately 200 L per day.

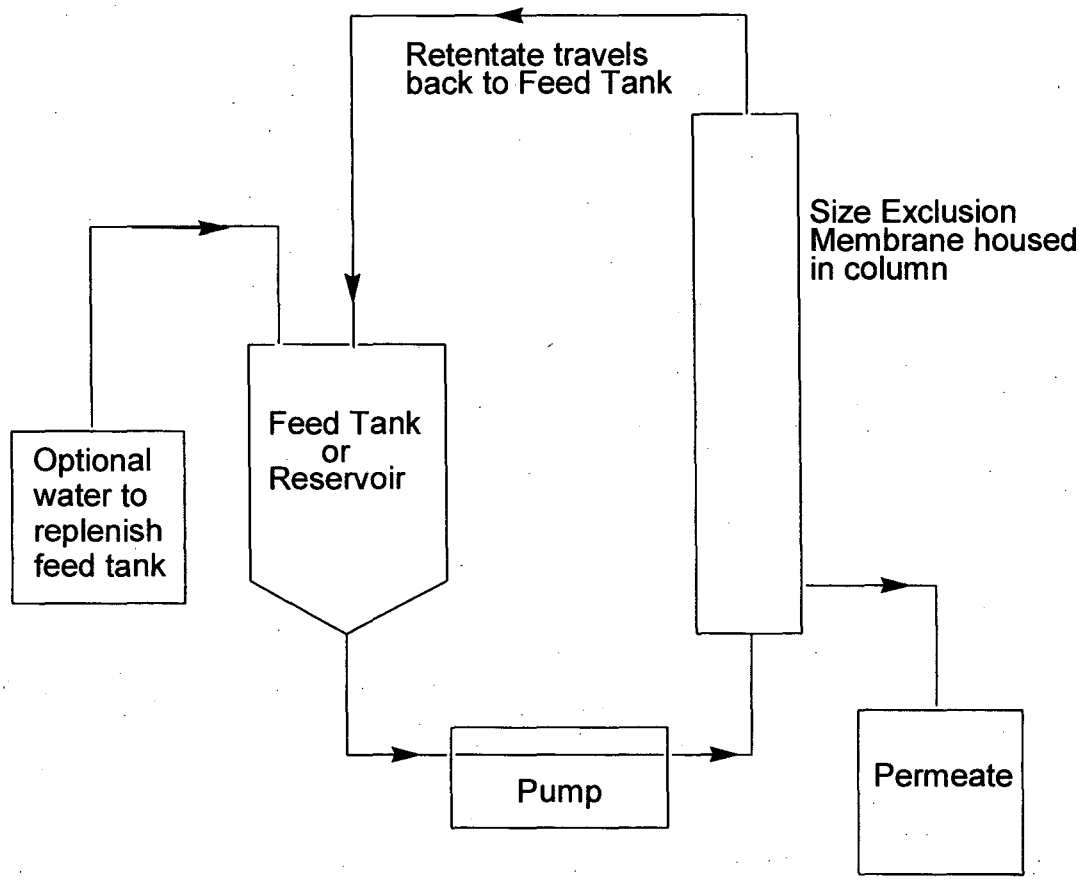

Figure 5-3. Diagram of the Polymer Filtration process.

PF has several advantages over other separation techniques. The WSCP in the retentate can either be reused or disposed. For reuse, the solution conditions are adjusted to release the metal, and a second PF step yields the metal in the permeate and the metal-free WSCP in the retentate. In addition, volatile organic solvents are avoided;

equilibrium is attained rapidly in this homogeneous system; mixed-waste is not produced; and a small number of steps are needed.

The plutonium processing facility at LANL has used PF extensively. In this facility, ultra-pure $^{238}PuO_2$ pellets are being produced as heat sources for solar-powered batteries used in NASA space missions. Pu-238 is very expensive and highly radioactive and thus the researchers were interested in recovering the Pu-238 from the processing waste streams either to recycle it or remove it to reduce the cost of disposal. The "aqueous scrap recovery process" was developed for Pu recycling, however the last recovery step is to precipitate the Pu(III) with oxalate.[17] This does not achieve low enough alpha activity in the waste stream for the caustic waste line limit (the limit for sending to the LANL general waste processing facility) of 4.5 millicuries per liter, thus the PF process was adopted to remove more Pu-238. Currently, the most commonly used WSCP at LANL has phosphoric acid binding groups (Figure 5-4) which, upon oxidation, produce phosphate that can interfere with both glass waste forms and Pu-purification ion exchange columns used in the Pu-238 disposal or recovery.

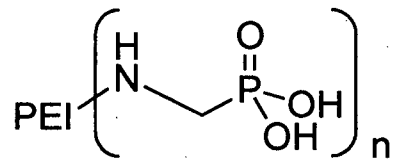

Figure 5-4. Structure of PEIP, the ligand currently in use at LANL for Pu polymer filtration.

The use of TAMs in Water Soluble Chelating Polymers

A collaboration was forged between the Raymond Group and the LANL researchers in 1997 to investigate PEI functionalized with several HOPO and TAM ligands for the recovery of Pu-238 with PF. The TAM derivatives were investigated as the chelating agent for several reasons. First, the TAMs are expected to have selectivity for Pu(IV) over trivalent metals such as Am(III) and Fe(III).[18-25] Second, the TAMs are totally oxidizable. Finally, the second amide group allows us to install functional groups that can improve the solubility of the WSCP in water throughout the entire pH range. HOPO derivatives previously prepared by Drs. Tom Mohs and Jide Xu had problems with solubility in certain pH ranges, depending on the specific ligand.

The rationale for choosing an appropriate side group for the TAMs was to increase the water solubility. As was seen earlier (Chapter 2), DMETAM is only soluble in water, thus N,N'-dimethylethylenediamine was chosen as a side group, affording compound **5-7**. Other side groups, illustrated in Figure 5-5, include taurine (containing a sulfonate, compound **5-10**), ethanolamine (containing a hydroxyl), b-alanine (containing a carboxylate), and finally, no amide substituent, just the benzoic acid. PDT (**5-7**) and PST (**5-10**) were considered the most promising, so they were synthesized first and worked so well that no other derivatives were investigated.

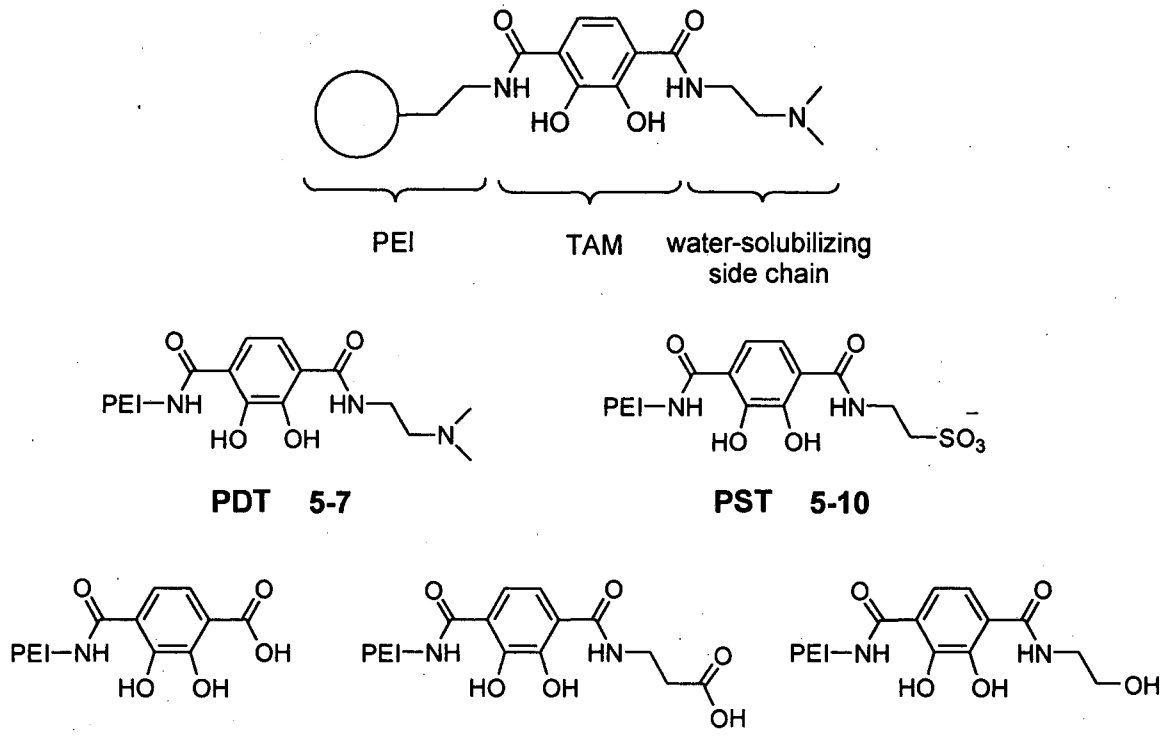

Figure 5-5. Possible side chains for TAMs attached to PEI.

Synthesis of TAM – WSCP

The synthesis is shown in Scheme 5-1and generally follows the procedure outlined in Chapter 2. Both PDT and PST were synthesized via the benzyl-protected thiazolide-activated TAM **5-4** since the PEI may not be robust enough for the BBr_3 deprotection that is required for methyl protecting groups. The first amide was substituted with either N,N-dimethylethylenediamine or taurine by slow addition of the amine to a dilute solution of excess **5-4**. Compound **5-5** was separated from the bis-substituted side-product by flash silica chromatography. Compound **5-8** was difficult to purify, forming emulsions with most biphasic extraction systems and the sulfonate

prevented purification by chromatography. The unreacted **5-4** was removed by precipitation from a THF solution by addition of an excess of water. The presence of the product, and absence of the starting material was confirmed by NMR, TLC, and mass spectometry. The crude product was used to couple to the PEI, since the remaining impurities and side products – taurine, 2-mercaptothiazoline, or TAM bis-substituted with taurine - would not interfere with the PEI coupling. For the coupling of the second thiaz-activated site to the PEI amines, the "molecular weight" of the primary amines of PEI needed to be calculated so the amount of required TAM precursor could be calculated for a 1:1 ratio. This was done by estimating that if the polymer is roughly 25% 1° amines, then every fourth (CH_2CH_2NH) unit should have one catecholate unit attached.

$$\frac{(8C \times 12\ g) + (4N \times 14\ g) + (20H \times 1\ g)}{1\ mol\ 1^{o}\ amine} = \frac{172\ g\ PEI}{1\ mol\ 1^{o}\ amine}$$

Coupling **5-5** with PEI was conducted in a CH_2Cl_2 / MeOH mixture and coupling **5-8** with PEI was conducted in water. The PEI is highly soluble in water and sparingly soluble in polar organic solvents, although addition of methanol or water to an organic solvent dramatically increases the dissolution of the PEI. In both cases, the progress of the reaction was monitored by the disappearance of the yellow color, which occurred over one day. At this stage both **5-6** and **5-9**, even though benzyl-protected, were sufficiently soluble in water to use an UF unit to remove all small molecules including 2-mercaptothiazolide and unreacted TAM.

Finally, the benzyl groups were deprotected with HBr/HOAc. After 1 week, the reaction solution was diluted with water and again, the UF unit was used to remove the

small molecules such as HOAC and toluene (from the cleaved benzyl groups). This however raises the pH to neutral since HBr and HOAc permeate the UF membrane and it was apparent that traces of Fe(III) were present in the solution since the solutions turned a pale pink color. The Fe(III) was removed by adding EDTA, adjusting the pH to approximately 3 with HCl (where EDTA is preferentially chelated by EDTA and not TAMs) and separating the FeEDTA complex with the UF unit. This diafiltration was continued with three different "washing" solutions - EDTA at pH 3, pH 3 water, and pure Millipore water - until the WSCP was free of Fe(III), EDTA, and other small molecules and the pH was neutral. The WSCP was then obtained by lyophilizing the retentate and a tan solid resulted.

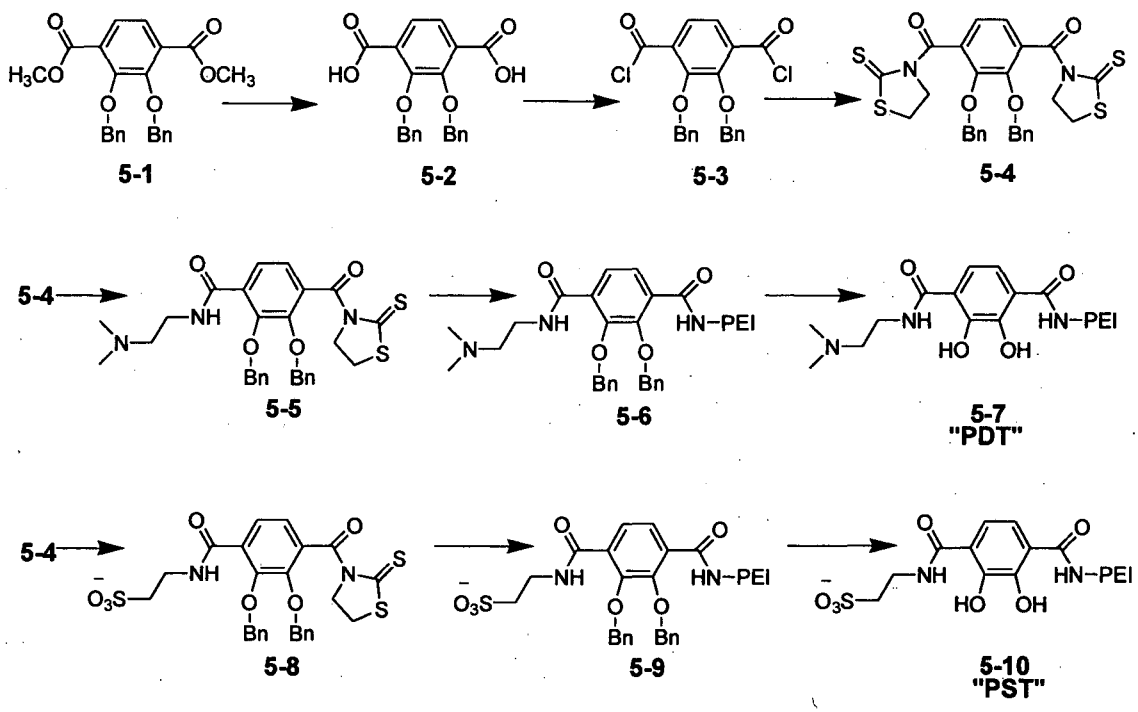

Scheme 5-1. Synthetic scheme for PDT and PST.

General procedure for testing Water Soluble Chelating Polymers for metal uptake

The general procedure for the metal retention experiments, shown in Figure 5-6, was to prepare a 0.01% solution of the polymer by diluting 0.100 mL of a 1% stock solution (prepared by dissolving 100 mg in 10 mL dd H_2O and filtering through a 5 micron filter) in 10 mL of 0.1 M $NaNO_3$. This experimental solution was spiked with an appropriate amount of the radionuclide, stirred for 15 minutes to reach equilibrium, the pH was recorded, and two samples were removed. The first sample of approximately 0.1 grams is the "feed" whose exact weight was recorded by tareing a scintillation vial containing 10 mL of Ultima Gold Scintillation Cocktail and recording the weight after adding the feed sample. The second sample would become the "permeate" and is obtained after polymer filtration with a centricon tube. The centricon tubes consist of two test-tube shaped parts which each hold approximately 2 mL. The two pieces snap together in the middle and the 10,000 MWCO membrane filter is attached to the bottom of the top half. Samples of ca. 1 mL are placed in the top half and after centrifuging for 30 minutes ca. 0.8 mL is collected as the permeate. Again, the exact weight of the permeated was recorded. The samples were then scintillation counted to determine the amount of actinide present. The pH of the experimental solution was adjusted with either NaOH or HCl and the process was repeated. The distribution coefficients (D), as a function of pH, were determined at 8 pH values in each experiment.

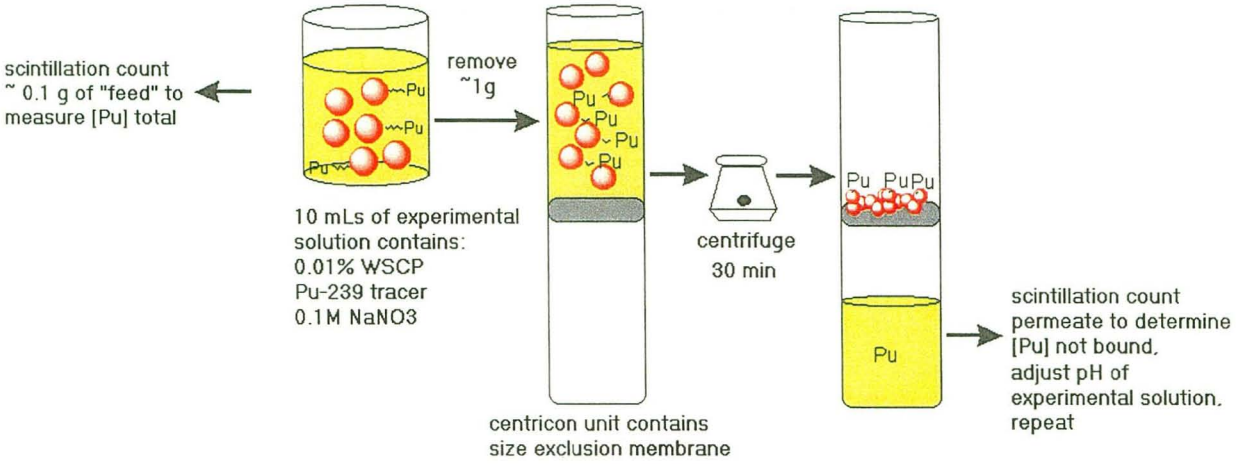

Figure 5-6. The general procedure for testing Water Soluble Chelating Polymers for metal uptake.

To calculate the distribution coefficients, first the background counts per minute (cpm) were subtracted from the sample cpm, and this was divided by the weight of the sample to yield a cpm per gram for both the feed and permeate samples. The amount of Pu bound to the WSCP is equal to:

$$\text{Bound Pu} = \text{feed cpm/g} - \text{permeate cpm/g}$$

The distribution coefficients at each pH were then calculated as:

$$D = (\text{bound cpm/g} / \text{permeate cpm/g}) * \text{phase ratio}$$

The phase ratio is a concentration of WSCP and is calculated as:

$$\text{phase ratio} = g\ H_2O\ /\ g\ WSCP$$

In most cases discussed here, the WSCP solution was 0.01% by weight, so the phase ratio is 10,000 (10g H_2O / 0.001g WSCP).

The % extraction was also calculated and is calculated as:

$$\%E = \text{Bound} / \text{Feed}$$

Pu(IV) uptake results with PST

Before any Pu(IV) uptake experiments were conducted, a qualitative titration was performed on a 0.01% solution of PST in 0.1M $NaNO_3$ to determine the approximate solubility of PST at different pH values. As the solution was titrated from high to low pH, PST precipitated around neutral pH. The solution first appeared cloudy around pH 8 and noticeable small particles formed at pH 6.5. If the pH was lowered too quickly, larger particles would form. The solids would not dissolve at low pH, but would redissolve if the pH was raised.

In the Pu(IV) uptake experiments, two different procedures were tried in an attempt to circumvent the precipitation of PST. It was found that if the experiment was conducted from low to high pH, a copious amount of precipitate would form which would not redissolve at higher pH. Since precipitation will change the phase ratio, the calculated D will also be incorrect. The method which suppressed precipitation was to add excess NaOH to the PST solution before adding the Pu(IV). In this case the pH started at 12.1 and as the pH of the solution was slowly lowered to 2, only small amounts

of precipitate formed. This was repeated 3 times to ensure reproducibility. The data that were collected from low to high pH do not correspond well to this data.

The data collected from high to low pH are shown as blue diamonds in Figure 5-7. As expected for the proton-dependent metal binding of the catecholates, PST functions the best at the higher pH values with D values around 10^7. These points represent extraction of greater than 99%. As the pH drops to approximately 8.5 (where the polymer starts precipitating) D starts to decrease, however even at the lower pH values of 4 and 2.3, high Pu(IV) uptake is still observed (99%, and 82% respectively).

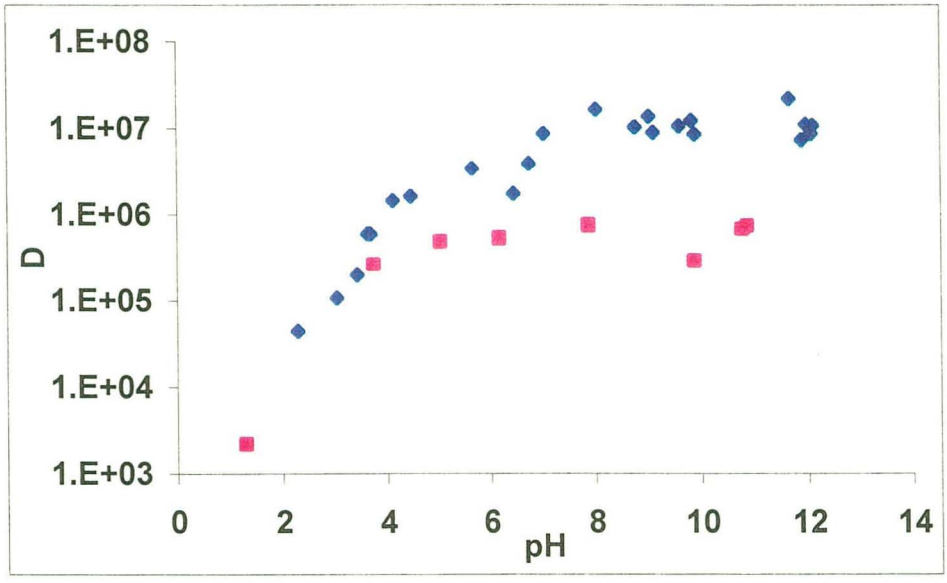

Figure 5-7. Graph of D vs. pH for the uptake of Pu(IV) by PST. The blue data were obtained starting at pH 12 and slowly lowering the pH and the pink data were obtained starting at low pH and raising the pH.

These can be compared to the experiment where the initial pH was 1.4 and the substantial amount of polymer precipitate would not dissolve as the pH was increased.

The Ds (illustrated as pink squares in Figure 5-7) at each pH point here are lower than those for the other experiments because not as much of the polymer was actually in solution and available to chelate the Pu(IV).

An Am(III) uptake experiment was conducted to compare the efficiency of these chelators for the Ac(III) and Ln(III) ions relative to Pu(IV). The graph in Figure 5-8 clearly indicates that the TAM ligands are more efficient chelators for Pu(IV) by the lower Ds for Am(III) throughout the pH range. The point at pH 12 represents 96% uptake and at pH 2.2, only 2.7% of the Pu(IV) is chelated.

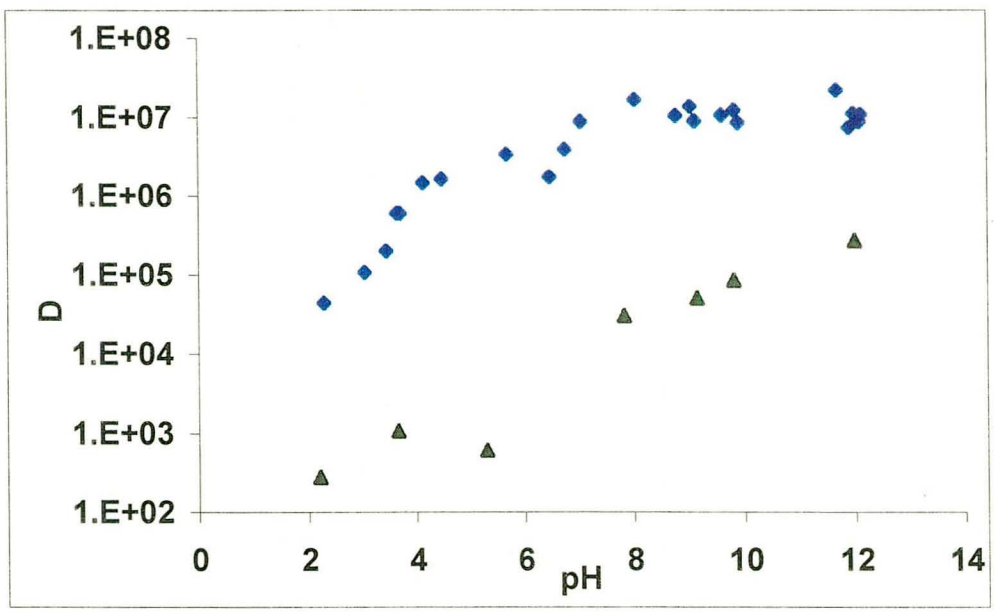

Figure 5-8. Graph of D vs. pH for Am(III) uptake by PST (triangles) compared to Pu(IV) uptake (diamonds).

Pu(IV) uptake results with PDT

Before doing any metal ion uptake experiments, a qualitative pH titration conducted in 0.1M $NaNO_3$ confirmed that PDT is soluble from pH 1.5 to 12.5. The Pu(IV) uptake experiment was conducted twice from pH 1.5 to 11.4. Since the TAMs have pKas of 6 and 11 for the catecholate protons, the distribution coefficients increase as a function of pH (Figure 5-9). At the highest D is 4.8×10^6 at pH 11.4 (99.8% extraction). The largest increase is at pH 4.5, where D is 1.3×10^6 (99.3% extraction). A low pH value where PDT still exhibits strong uptake is pH 2.9, where D is 1×10^5 (91.1% extraction).

These data can be directly compared to PEIP, the phosphoric-acid based ligand currently in use at LANL.[4] At pH 2, PEIP has a D of $10^{4.7}$ (98 % uptake) and this increases to $10^{6.4}$ (99.97 % uptake) by pH 6. Thus, under identical conditions, PDT is not as effective in the lower pH region, but equally effective at higher pH for Pu(IV) uptake. This also indicates that PDT would be a suitable replacement for PEIP in the LANL process.

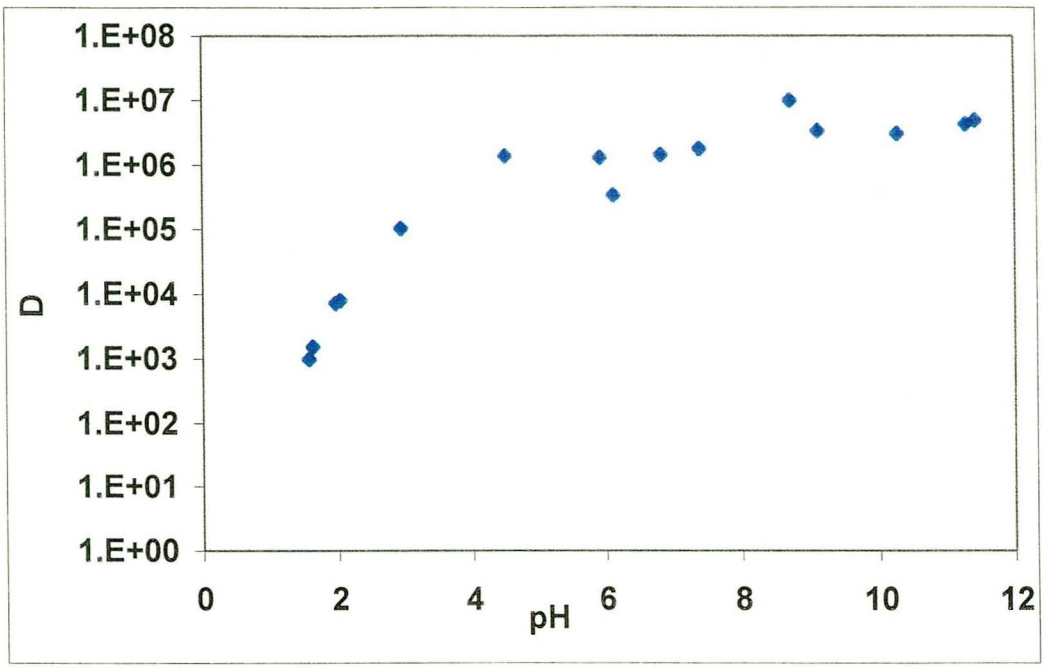

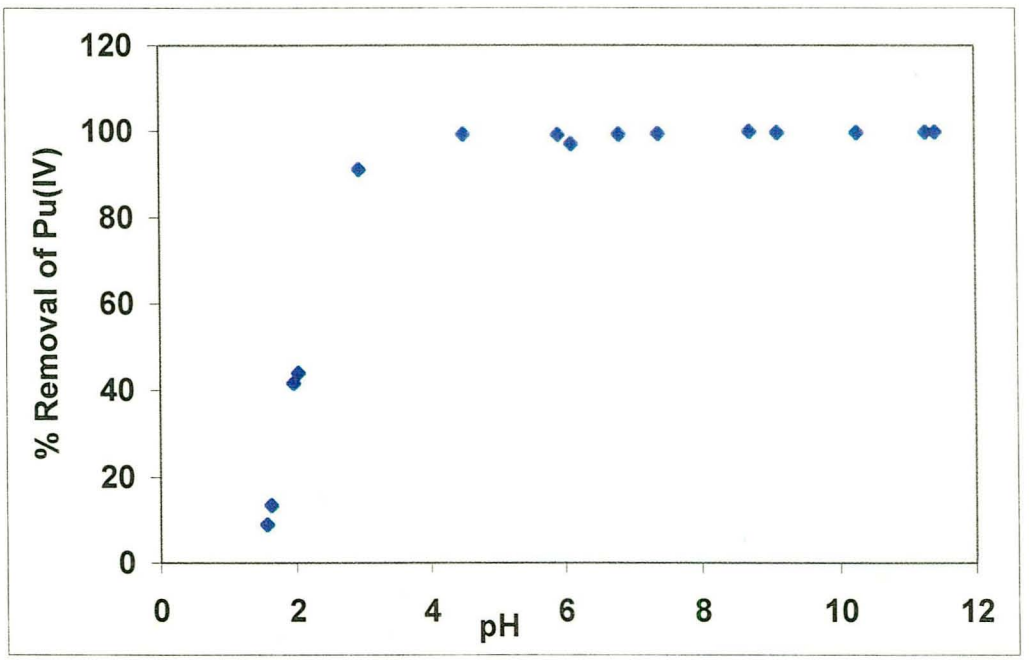

Figure 5-9. The graph of D vs. pH for the uptake of Pu(IV) by PDT is shown above. The same data are plotted as % extraction vs. pH in the graph below.

The selectivity of TAMs for higher oxidation state metals is seen by comparing these results to the Am(III) uptake results (Figure 5-10). Again, the distribution coefficients increase with increasing pH, however this happens between pH 7 and 9. The distribution coefficient at pH 10.9 is 2.1×10^6 (99.5% extraction), comparable with Pu(IV), and the biggest difference between the two metals is seen at pH 4.5 where D is 1.6×10^3 for Am(III) (14% extraction) and 1.3×10^6 for Pu(IV) (99.3% extraction).

This is very different from the Am(III) uptake seen with PEIP since PEIP does not discriminate as much between the trivalent and tetravalent actinides.[4] At pH 2, the D is almost 10^4 (89.7% uptake) and this increases to almost 10^5 by pH 6 (98.7% uptake).

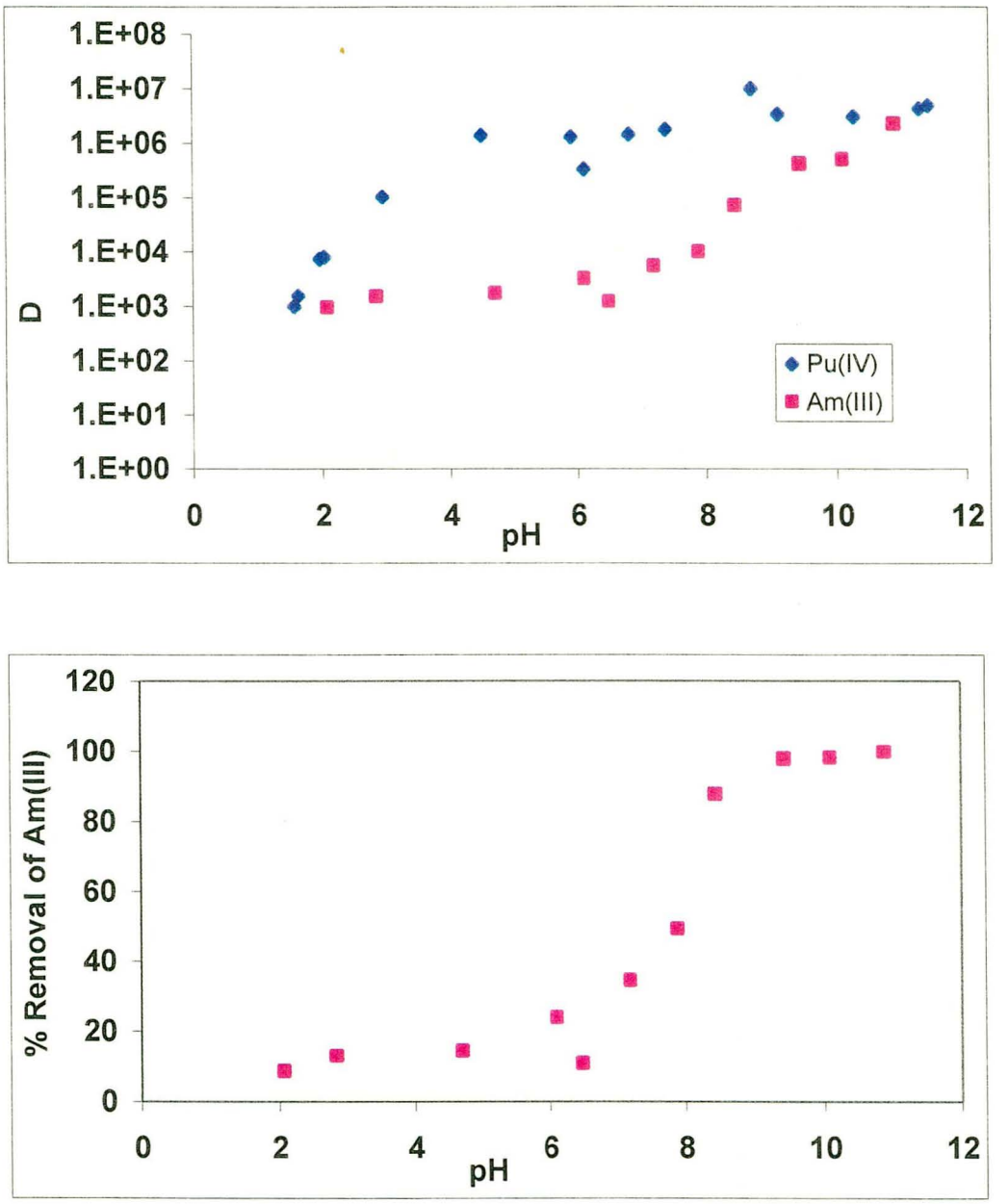

Figure 5-10. A comparision of Am(III) (pink squares) and Pu(IV) (blue diamonds) uptake by PDT is shown in the plot of D vs. pH on the top. The same Am(III) data are graphed as % uptake vs. pH on the bottom.

The concentration of PDT was also varied to see if there was an effect on Pu(IV) uptake (Figure 5-11). The typical experiment involves 0.01% PDT, and it was found that varying the concentration an order of magnitude in either direction to 0.1% and 0.001% had no effect on D. It would be expected that less PDT in solution (hence lower ligand concentration and larger phase ratio) would lead to less uptake of Pu(IV), as is the case here. The phase ratio (100,000 for the 0.001% solution, and 1,000 for the 0.1% solution) allows the experiments to be normalized for differences in ligand concentration, and yields the same distribution coefficient, regardless of PDT concentration.

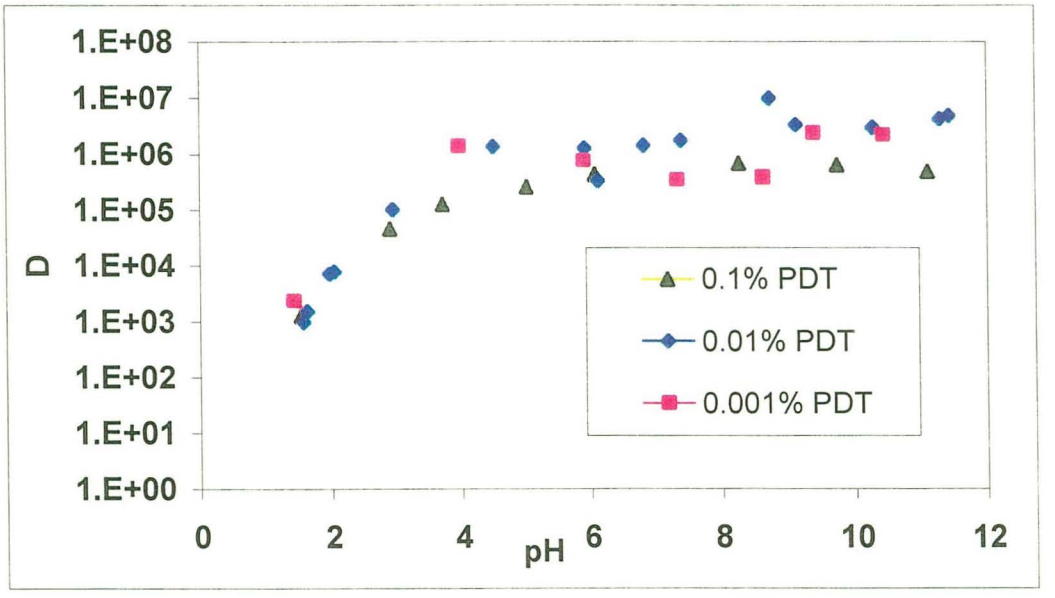

Figure 5-11. The graph of D vs. pH shows no difference in D for Pu(IV) uptake as the concentration of PDT varies from 0.1% to 0.001%.

The PF process is being tested for removing Pu(IV) from two waste streams at LANL. One is the Radioactive Waste Treatment Facility (RWTF, or TA-50) on site at

LANL that treats waste generated in the labs. The PF process is currently being examined to determine if this procedure can be used at the RWTF. The second waste stream originates from TA-55, which is the plutonium research and reprocessing lab. About half of the aqueous Pu waste treated at the RWTF originates at TA-55, therefore this is clearly a target for Pu removal to alleviate the amount that is treated at the RWTF.

The major Pu processing operation is the production of highly pure PuO_2. During this procedure the Pu(IV) is first reduced to Pu(III) with hydroxylamine nitrate (HAN) then precipitated as the oxalate complex. Thus the waste stream contains large quantities of HAN and oxalate. Due to the high stability of the Pu(IV)-catecholate complex, the metal quickly oxidizes to Pu(IV) upon binding of a catecholate to Pu(III).[22] In the presence of the reducing agent HAN we wanted to ensure that this would still happen. Pu(III) was prepared by reduction of Pu(IV) with HAN and the solution was stored with excess HAN. These Pu uptake experiments were conducted in the same way and the assumption is that if the Pu remained Pu(III) then the graph of D vs. pH would resemble the Am(III) graph. However, the graph resembles the Pu(IV) curve, indicating that the Pu(III) oxidized to Pu (IV) (Figure 5-12).

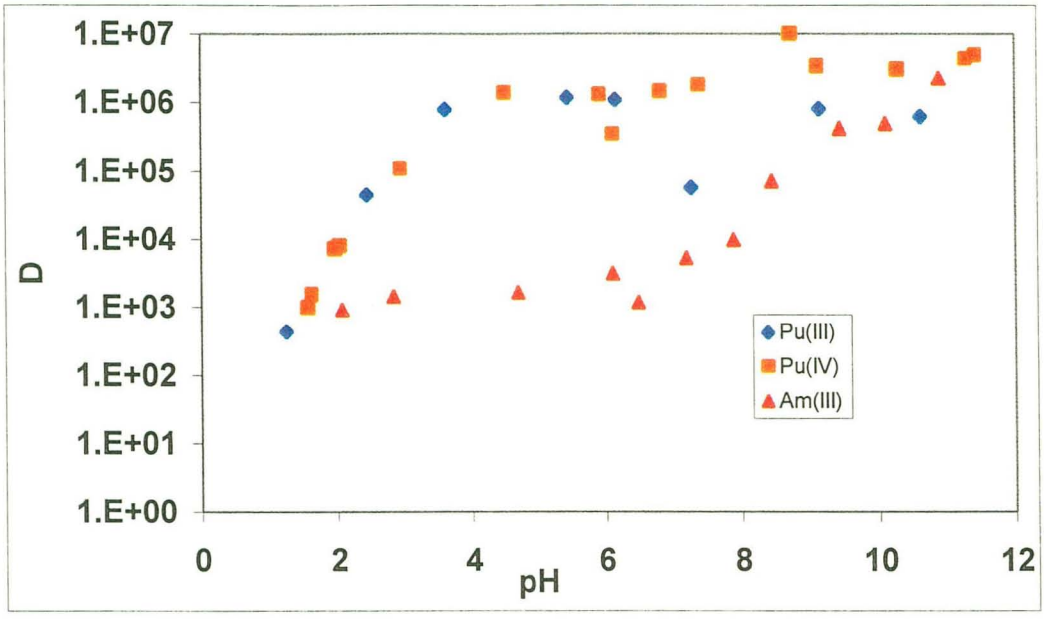

Figure 5-12. The graph of D vs. pH for the uptake of Pu(III) (blue diamonds) in the presence of HAN compared with Am(III) (red triangles) and Pu(IV) (orange squares).

Pu is known to form a soluble polymer in basic solutions and to adsorb to glass surfaces. This was always a concern during the experiments, thus the cpm for the feed solutions were examined at every point to ensure they were not decreasing over time. In addition, an experiment was conducted to see if PDT could solubilize the adsorbed Pu. This was done by adding Pu(IV) to two basic solutions of 0.1M $NaNO_3$ and counting the feed and permeate solutions at regular intervals. Although the permeate solutions should not have any cpm because polymerized Pu(IV) will not permeate the membrane, the solutions were ultrafiltered for comparison to other experiments. As expected the cpm of the feed solution decreased with time as the Pu(IV) adsorbed to the glass surfaces, shown in Figure 5-13. After four hours PDT was added to one of the solutions and the cpm of

the feed solution slowly recovered to normal cpm after 2 days indicating that the TAMs can solubilize Pu(IV) that has adsorbed to a glass surface.

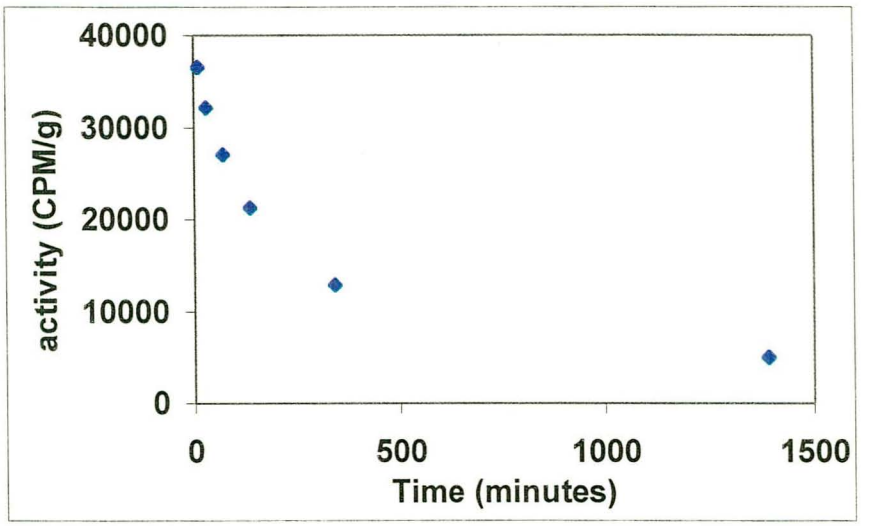

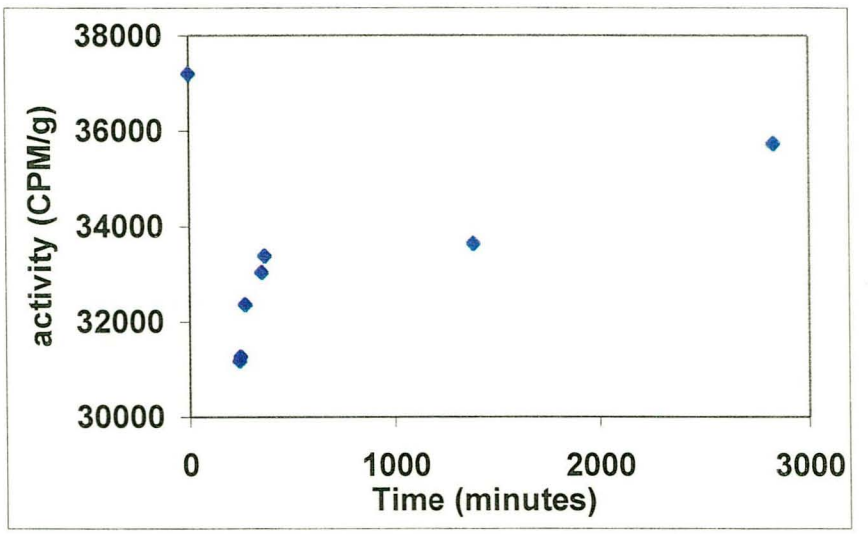

Figure 5-13. The graph on top shows the decrease of cpm over time of a basic Pu(IV) solution. The graph on the bottom illustrates the recovery of the cpm when PDT is added after four hours.

Conclusions and Future work

Two water-soluble chelating polymers, PST and PDT, have been designed as Pu(IV) chelators for the polymer filtration method of removing metals from waste streams. PDT functioned better than PST, as it was soluble in water throughout the pH range. PDT exhibited strong uptake of Pu(IV), particularly in basic solutions, and preference for this tetravalent actinide over Am(III).

A qualitative pH titration was also conducted in 1M $NaNO_3$ and PDT remained mostly soluble at this higher ionic strength. Some cloudyness was observed between pH 2.5 and 4, however it will still be interesting to see if this affects the Pu(IV) uptake. PDT may also be suitable for binding other metals such as UO_2^{2+} or Tc(IV). Since waste streams can contain a variety of organic and inorganic material, competition experiments with metals such as Fe(III) and Al(III) or ligands such as EDTA will elucidate the effectiveness of PDT in a complex waste stream.

The comparison of these results with the WSCP currently in use at LANL, PEIP, indicates that PDT is a good alternative to PEIP, and may be desirable to use since it is totally oxidizable.

Experimental

General. All reagents and solvents other than PEI were purchased from Aldrich Chemical Company or Fisher Scientific and used as purchased. All solvents were dried over activated alumina and stored over 4Å molecular sieves. All reactions were carried out under Ar. Thionyl chloride was purified by distillation from triphenyl phosphite. Water was distilled and further purified by a Millipore cartridge system (resisitivity 18 x

10^6 Ω). Thin layer chromatography (TLC) was performed using alumina-backed silica plates and visualized with a 254 nm UV lamp. All organic extracts were dried over $MgSO_4$ and solvents were removed with a rotary evaporator. ^1H and ^{13}C NMR spectra were obtained on a Bruker DRX500 (500 MHz) or Bruker AMX400 spectrometer (400 MHz) as noted. All NMR samples were taken in $CDCl_3$ or D_6-DMSO as noted. All Microanalyses were performed by the Microanalytical Services Laboratory in the College of Chemistry, University of California, Berkeley. Compound **5-2** was prepared as previously reported.[16,17] The polymer filtration unit consisted of a QuixStand Benchtop system fitted with a feed reservoir and a 30,000 MWCO filtration membrane (Xampler (UFP-30-C4A) AG Technology Corporation) and a peristaltic pump (EasyLoad Masterflex, Cole Parmer Instrument Co.). Pu-239 and Am-241 stock solutions in 8M HNO_3 were obtained from Los Alamos analytical supplies as previously reported.[4] Pu(III) preparation was performed as previously described.[8] Ultrafiltration cartridges were Amicon-Centricon-10. Samples were counted on a Packard Liquid scintillation analyzer (model Tri-Carb 2200CA) or Beckman scintillation counter (model LS6000) in 20 mL of Ultima Gold scintillation cocktail. PEI was purchased from BASF and purified to a minimum molecular weight of 30,000 by Dr. Tom Robison with the Xampler filtration membrane.

Polymer preparation:

5-4: **5-2** (1g, 2.6 mmol) was suspended in 20 mL of toluene and one drop of DMF. Oxalyl chloride (0.7 mL, 8.1 mmol) was added under N_2. Over three hours the milky white suspension dissolved and the solvent was removed by rotary evaporation to yield a

white oily solid **5-3**. In a separate flask, 2-mercaptothiazolide (0.67 g, 5.6 mmol) was dissolved in 10 mL of THF and 1 mL of TEA. This was added slowly to the acid chloride cooled with a dry ice/ethylene glycol bath and a yellow solution resulted. This was allowed to warm to room temperature and stirred for 12 hours then cooled to 0 °C and filtered. The white solid (TEA HCl) was washed with THF. The yellow THF solution was diluted with 20 mL of CH_2Cl_2 and extracted with 2 x 75 mL of 1M KOH / brine, dried with $MgSO_4$, and rotary evaporated to a yellow oil (1.42 g, 93%).

5-5: **5-4** (1.4g, 2.5 mmol) was dissolved in 350 mL CH_2Cl_2 and N,N-dimethylethylenediamine (0.14 mL, 1.25 mmol) dissolved in 100 mL CH_2Cl_2 was added dropwise over 20 hours. This was evaporated to 75 mL and extracted with 2 x 50 mL 1M KOH / brine, dried over $MgSO_4$, filtered, and rotary evaporated to a yellow oil. The excess **5-4** was eluted from a silica gel column with CH_2Cl_2 / 1% MeOH and the product **5-5** was eluted with 5% MeOH. The fractions containing **5-5** were rotary evaporated to a yellow oil (0.35g, 51%).

5-6: Polyethyleneimine (minimum weight 30,000; 0.109g, approximately 1 equivalent of primary N) dissolved in 20 mL of CH_2Cl_2 was added slowly to **5-5** dissolved in 20 mL CH_2Cl_2. After stirring for 12 hours 2mL of MeOH was added to the cloudy pale yellow solution to complete the dissolution. After stirring for 3 days, the reaction was only faintly yellow, so it was evaporated, dissolved in 250 mL distilled H_2O, and all small molecule impurities were removed by ultrafiltration.

5-7: **5-6** (1g) was dissolved in 25 mL of glacial acetic acid and 25 mL of 48% HBr under N_2, stirred for 5 days and evaporated to an off-white solid. Upon addition of distilled H_2O, the solution turned a pale pink, indicating the presence of Fe(III). EDTA was added and the pH was adjusted to 3 with HCl to remove the Fe(III) from the WSCP and ultrafiltration separated the FeEDTA and other small molecules from the polymer. A clear light brown film resulted upon rotary evaporation.

5-8: Taurine (0.18g, 1.4 mmol) was dissolved in 5 mL of MeOH and 3 mL of distilled H_2O and NaH (0.053g, 1.3 mmol) was added. This mixture was then added to a solution of **5-4** (2.1g, 3.7 mmol) dissolved in 150 mL of THF and 100 mL of distilled H_2O and stirred overnight. The volume was reduced to 30 mL and the majority of the excess **5-4** precipitated and was filtered. The supernatant was evaporated to a thick yellow oil and addition of distilled H_2O dissolved the product. The NMR and mass spectrum indicated the product was present however the NMR also showed free 2-mercaptothiazoline that could not be separated and the mass spectrum indicated no **5-4** was present. The weight of **5-8** was estimated between 0.64 and 0.85g.

5-9: All of **5-8** was dissolved in 20 mL of distilled H_2O and added over one hour to PEI (0.35g) dissolved in 80 mL of distilled H_2O with small additions of 1M KOH to ensure dissolution. This was diluted to 200 mL and purified with ultrafiltration and rotary evaporated to a white solid.

5-10: All of **5-9** was suspended in 15 mL glacial acetic acid / 10 mL 48 % HBr and stirred for 3 weeks. This was evaporated to a white solid and upon addition of distilled H_2O, the solution turned a pale pink, indicating the presence of Fe(III). EDTA was added and the pH was adjusted to 3 to remove the Fe(III) from the WSCP and ultrafiltration separated the FeEDTA and other small molecules from the polymer. A clear light brown film resulted upon rotary evaporation (0.52 g).

Pu(IV) uptake studies:

The raw data (weight of each sample, counts per minute, pH) are in Appendix 2.

Preparation of stock solution: A 1% stock solution of PST was prepared by dissolving 100 mg of the polymer in 10.03 g of distilled H_2O and the pH was adjusted to 7 with the addition of 0.05 mL 10M NaOH to aid dissolution. This solution was filtered through 5 micron and 0.5 micron filters. A 1% stock solution of PDT was prepared by dissolving 0.102 mg of PDT in 10.106 g of distilled H_2O. This solution was filtered through 5.0, 0.45, and 0.22 micron filters and used as the stock for all of the experiments.

Actinide uptake experiments: A 0.01% solution of either PST or PDT was prepared by diluting 0.100 mL of the stock solution with 10 mL of 0.1M $NaNO_3$. For PST, the pH was adjusted to 12.4 by addition of 80 microliters of 10M NaOH. To this was added 0.05 mL of Pu(IV) solution or 0.20 mL of an Am(III) solution (final activity 35,000 counts per minute per gram). The solution was allowed 15 minutes to equilibrate with stirring, the pH was recorded and two samples were removed. The first sample is the "feed" and the exact weight was recorded by tareing a scintillation vial containing 20 mL of Ultima Gold Scintillation Cocktail and recording the weight after the addition of approximately

0.1 mL of the feed sample. The second sample would become the "permeate" and is obtained after centrifuging approximately 1.0 mL for 25 minutes in a 10,000 MWCO Centricon tube. The exact weight of the sample that permeated the membrane was recorded in the same manner. To monitor the uptake of Pu(IV) as a function of pH, either 1M or 10M NaOH or 1M or conc. HNO_3 was added, and this procedure was repeated. Up to 8 data points at different pH values could be obtained in this manner.

Pu(III) uptake: The procedure was conducted in the same manner as above except the solution was prepared with 5 mL of 0.1M $NaNO_3$ and 5.0 mL of Pu(III) solution (in 0.5M HAN and 0.5M HNO_3, final activity 35,000 counts per minute per gram).

Varying concentration of PDT: The procedure was conducted in the same manner as above except: for the 0.001% solution 0.010mL of the PDT stock solution added to 10 mL of 0.1M $NaNO_3$, and for the 0.1% solution, 1.00mL of the PDT stock solution was added to 9.0 mL of 0.1M $NaNO_3$.

Dissolution of Pu(IV) in a basic solution: Two solutions were prepared by adjusting the pH of 10 mL of 0.1M $NaNO_3$ to 12.3 with NaOH, then adding 0.05 mL of Pu(IV). The "feed" was sampled as described above at regular intervals. At four hours, PDT (0.1mL, final concentration 0.01%) was added to one solution and the "feed" was sampled as described above at regular intervals.

References

(1) Bond, A. H.; Dietz, M. L.; Chiarizia, R. *Ind Eng Chem Res* **2000**, *39*, 3442-3464.

(2) Alexandratos, S. D.; Natesan, S. *Ind Eng Chem Res* **2000**, *39*, 3998-4010.

(3) Romanovskiy, V. N.; Smirnov, I. V.; Babain, V. A.; Todd, T. A.; Herbst, R. S.; Law, J. D.; Brewer, K. N. *Solvent Extr Ion Exch* **2001**, *19*, 1-21.

(4) Horwitz, E. P.; Kalina, D. G.; Diamond, H.; Vandegrift, G. F. *Solvent Extr. Ion Exch.* **1985**, *3*, 75-109.

(5) Mathur, J. N.; Murali, M. S.; Nash, K. L. *Solvent Extr Ion Exch* **2001**, *19*, 357-390.

(6) Alexandratos, S. D.; Crick, D. W. *Ind Eng Chem Res* **1996**, *35*, 635-644.

(7) Horwitz, E. P.; Chiarizia, R.; Diamond, H.; Gatrone, R. C.; Alexandratos, S. D.; Trochimczuk, A. Q.; Crick, D. W. *Solvent Extr Ion Exch* **1993**, *11*, 943-966.

(8) Kimura, T. *J Radioanal Nucl Chem Art* **1990**, *141*, 307-316.

(9) Kimura, T.; Akatsu, J. *J Radioanal Nucl Chem Art* **1991**, *149*, 25-34.

(10) Thompson, J. A.; Jarvinen, G. D. *Filtration and Separation* **1999**, *36*, 28-32.

(11) Smith, B. F.; Robison, T. W. US Patent #5,643,456, 1998.

(12) Smith, B. F.; Gibson, R. R.; Jarvinen, G. D.; Jones, M. M.; Lu, M. T.; Robison, T. W.; Schroeder, N. C.; Stalnaker, N. *J Radioanal Nucl Chem* **1998**, *234*, 219-223.

(13) Smith, B. F.; Gibson, R. R.; Jarvinen, G. D.; Robison, T. W.; Schroeder, N. C.; Stalnaker, N. D. *J Radioanal Nucl Chem* **1998**, *234*, 225-229.

(14) Geckeler, K. E.; Volcheck, K. *Environ. Sci. Tech.* **1996**, *30*, 725-734.

(15) Michaels, A. S. In *Advances in Separation and Purification*; Perry, E. S., Ed.; John Wiley: New York, 1968.

(16) Horn, D. In *Polymeric Amines and Ammonium Salts*; Goethals, E. J., Ed.; Pergamon Press: New York, 1980.

(17) Schulte, L. D.; Purdy, G. M.; Jarvinen, G. D.; Ramsey, K. B.; Silver, G. L.; Espinoza, J.; Rinehart, G. H. Internal LANL Report.

(18) Raymond, K. N.; Garrett, T. M.; Miller, P. W. US Patent 5,049,280, 1991.

(19) Garrett, T. M.; Miller, P. W.; Raymond, K. N. *Inorg. Chem.* **1989**, *28*, 128-133.

(20) Weitl, F. L.; Raymond, K. N.; Smith, W. L.; Howard, T. R. *J. Am. Chem. Soc.* **1978**, *100*, 1170-1172.

(21) Sofen, S. R.; Cooper, S. R.; Raymond, K. N. *Inorg. Chem.* **1979**, *18*, 1611-1616.

(22) Kappel, M. J.; Nitsche, H.; Raymond, K. N. *Inorg. Chem.* **1985**, *24*, 605-611.

(23) Haddad, S. F.; Raymond, K. N. *Inorg. Chim. Acta* **1986**, *122*, 111-118.

(24) Freeman, G. E.; Raymond, K. N. *Inorg. Chem.* **1985**, *24*, 1410-1417.

(25) Weitl, F. L.; Raymond, K. N.; Durbin, P. W. *J. Med. Chem.* **1981**, *24*, 203-206.

Appendix 1

X-Ray Structure Details of $K_4[Zr(C_{12}H_{12}O_4N_2)_4]$ · diethylether · 3 ethanol · x (solvent)

EXPERIMENTAL DETAILS

A. Crystal Data

Empirical Formula	$C_{48}H_{56}O_{16}N_8ZrK_4$
Formula Weight	1248.63
Crystal Color, Habit	clear, tablet
Crystal Dimensions	0.27 X 0.40 X 0.15 mm
Crystal System	monoclinic
Lattice Type	C-centered
No. of Reflections Used for Unit Cell Determination (2θ range)	2931 (3.5 - 45.0°)
Lattice Parameters	a = 27.576(2)Å
	b = 29.345(1) Å
	c = 15.2659(8) Å
	β = 118.688(2)°
	V = 10837.0(9) Å^3
Space Group	C2/c (#15)
Z value	8
Dcalc	1.530 g/cm3
F000	5152.00
μ(MoKα)	5.86 cm-1

B. Intensity Measurements

Diffractometer	SMART
Radiation	MoKα (λ = 0.71069 Å)
	graphite monochromated
Crystal to Detector Distance	60.0 mm
Temperature	-114.0°C
Scan Type	ω (0.3° per frame)
Scan Rate	20 seconds per frame.
2θ max	46.6o
No. of Reflections Measured	Total: 17556 Unique: 7358 (Rint = 0.136)
Corrections	Lorentz-polarization Absorption (Tmax = 0.94 Tmin = 0.20)

C. Structure Solution and Refinement

Structure Solution	Direct Methods (SIR92)
Refinement	Full-matrix least-squares
Function Minimized	$\sigma w (\|Fo\| - \|Fc\|)^2$
Least Squares Weights	$1/\sigma^2(F_o) = 4F_o^2/\sigma^2(F_o^2)$
p-factor	0.030
Anomalous Dispersion	All non-hydrogen atoms
No. Observations (I>3.00sigma(I))	1848
No. Variables	300
Reflection/Parameter Ratio	6.16
Residuals: R; Rw	0.111 ;

Goodness of Fit Indicator	1.016
Max Shift/Error in Final Cycle	0.001
Maximum peak in Final Diff. Map	0.60 e-/Å^3
Minimum peak in Final Diff. Map	-1.01 e-/Å^3

Table A-1. Atomic coordinates and Biso/Beq for $K_4[Zr(ETAM)_4]$.

atom	x	y	z	Beq
Zr(1)	0	0.1354(1)	0	4.0(1)
K(1)	0.0727(3)	0.1143(2)	0.0331(5)	5.7(2)
K(2)	-0.3071(3)	0.1369(2)	-0.3784(6)	7.5(2)
O(1)	0.0830(7)	0.1127(6)	-0.137(1)	5.0(4)
O(2)	0.0403(7)	0.1896(6)	-0.151(1)	4.7(4)
O(3)	0.2573(8)	0.0944(7)	-0.025(1)	6.8(5)
O(4)	0.1415(10)	0.3047(8)	-0.012(2)	9.0(6)
O(5)	-0.0579(6)	0.1586(6)	-0.192(1)	4.3(4)
O(6)	-0.0120(6)	0.0821(5)	-0.167(1)	4.2(4)
O(7)	-0.0824(8)	-0.0350(7)	-0.117(1)	6.9(5)
O(8)	-0.2193(8)	0.1744(7)	-0.228(1)	7.1(5)
O(9)	0.172(1)	0.149(1)	0.195(2)	13.4(9)
O(10)	-0.0015(10)	0.1816(8)	0.005(2)	9.2(6)
O(11)	-0.358(9)	0.173(6)	-0.22(1)	28(4)
O(14)	-0.255(1)	0.204(1)	-0.104(2)	13.2(8)
O(16)	-0.361(3)	0.056(3)	-0.407(6)	19(2)
O(17)	0.340(3)	0.060(3)	0.127(5)	13(1)
O(18)	0.352(3)	0.059(2)	0.078(5)	13(1)
O(19)	-0.351(7)	0.169(5)	-0.26(1)	22(4)
N(1)	0.1748(9)	0.0609(8)	-0.086(2)	4.9(5)
N(2)	0.051(1)	0.2761(9)	-0.107(2)	6.6(6)
N(3)	-0.1442(10)	0.2059(8)	-0.216(2)	6.0(6)
N(4)	-0.0116(9)	-0.0045(7)	-0.131(1)	4.7(5)
C(1)	0.177(1)	0.1417(9)	-0.054(2)	4.3(6)
C(2)	0.121(1)	0.1440(10)	-0.101(2)	5.4(7)
C(3)	0.097(1)	0.1895(10)	-0.098(2)	5.1(7)
C(4)	0.132(1)	0.2252(9)	-0.058(2)	4.1(6)
C(5)	0.189(1)	0.2226(9)	-0.012(2)	3.9(6)
C(6)	0.215(1)	0.183(1)	-0.013(2)	6.3(8)
C(7)	0.207(1)	0.0953(10)	-0.053(2)	4.7(7)
C(8)	0.195(1)	0.0181(10)	-0.103(2)	6.4(8)
C(9)	0.225(2)	-0.009(1)	0.002(3)	9(1)
C(10)	0.103(2)	0.275(1)	-0.061(2)	6.6(8)

C(11)	0.025(2)	0.322(1)	-0.107(3)	8(1)
C(12)	0.019(3)	0.322(3)	-0.010(6)	7(1)
C(13)	-0.136(1)	0.1273(9)	-0.186(2)	4.4(6)
C(14)	-0.089(1)	0.1273(9)	-0.184(2)	4.3(6)
C(15)	-0.060(1)	0.0825(9)	-0.165(2)	4.1(6)
C(16)	-0.086(1)	0.0409(9)	-0.153(2)	3.9(6)
C(17)	-0.136(1)	0.0469(9)	-0.153(2)	4.9(7)
C(18)	-0.161(1)	0.0872(9)	-0.168(2)	5.0(7)
C(19)	-0.054(1)	-0.0014(10)	-0.129(2)	4.4(6)
C(20)	0.022(1)	-0.049(1)	-0.109(2)	6.8(8)
C(22)	0.074(1)	-0.041(1)	-0.105(2)	6.5(7)
C(23)	-0.172(1)	0.171(1)	-0.208(2)	6.6(8)
C(24)	-0.177(1)	0.253(1)	-0.250(3)	9.0(10)
C(25)	-0.156(3)	0.291(2)	-0.157(5)	7(1)
C(26)	-0.127(3)	0.290(2)	-0.212(5)	6(1)
C(27)	0.185(2)	0.195(2)	0.219(3)	11(1)
C(28)	0.137(2)	0.221(1)	0.193(3)	11(1)
C(29)	0.226(3)	0.128(2)	0.223(5)	7(1)
C(30)	0.215(2)	0.078(2)	0.201(3)	3(1)
C(32)	-0.037(3)	0.193(2)	0.050(6)	17(2)
C(33)	-0.054(9)	0.163(7)	0.02(2)	31(6)
C(34)	-0.030(4)	0.180(3)	0.136(6)	11(2)
C(35)	-0.352(5)	0.179(3)	-0.142(7)	11(2)
C(36)	-0.397(5)	0.179(4)	-0.19(1)	17(3)
C(37)	-0.190(4)	0.198(3)	0.022(7)	9(2)
C(45)	-0.365(5)	0.057(4)	-0.263(9)	20(3)
C(46)	-0.095(9)	0.189(7)	0.13(2)	34(5)
C(47)	0.365(4)	0.101(3)	0.179(7)	8(2)
C(48)	-0.315(4)	0.042(4)	-0.286(8)	15(2)
C(49)	0.383(5)	0.085(4)	0.150(10)	12(2)
C(50)	0.436(8)	0.047(7)	0.51(1)	33(4)
C(51)	0.500(7)	-0.002(6)	0.56(1)	34(5)
C(52)	0.409(6)	0.086(6)	0.23(1)	24(4)
C(53)	-0.168(4)	0.155(3)	0.056(6)	9(2)
C(54)	-0.23(1)	0.187(7)	-0.03(2)	29(4)
C(55)	-0.003(6)	0.325(5)	-0.06(1)	20(4)
C(56)	-0.376(4)	0.185(3)	-0.066(8)	15(2)
C(57)	-0.207(5)	0.150(3)	0.021(9)	10(2)
C(58)	0.351(5)	0.063(4)	0.483(8)	19(2)

Table A-2. Anisotropic Displacement Parameters for $K_4[Zr(ETAM)_4]$.

atom	U11	U22	U33	U12	U13	U23
Zr(1)	0.075(3)	0.017(2)	0.081(3)	0	0.044(3)	0
K(1)	0.115(6)	0.048(4)	0.091(6)	-0.018(4)	0.059(5)	0.004(4)
K(2)	0.111(6)	0.067(5)	0.116(6)	0.009(5)	0.057(5)	0.015(5)

Table A-3. Selected bond lengths for $K_4[Zr(ETAM)_4]$.

atom	atom	distance	atom	atom	distance
Zr1	O2	2.135(7)	Zr1	O2	2.135(7)
Zr1	O6	2.150(7)	Zr1	O6	2.150(7)
Zr1	O1	2.239(8)	Zr1	O1	2.240(8)
Zr1	O5	2.267(7)	Zr1	O5	2.267(7)
Zr1	K1	3.836(3)	Zr1	K1	3.836(3)
K1	O7	2.561(10)	K1	O10	2.670(12)
K1	O1	2.774(8)	K1	O9	2.82(2)
K1	O6	2.967(8)	K1	C2	3.039(12)
K1	C3	3.290(13)	K1	O2	3.334(9)
K2	O4	2.521(10)	K2	C60	2.57(5)
K2	O8	2.667(11)	K2	O3	2.696(9)
K2	O16	2.86(6)	K2	O11	2.86(4)
K2	C48	3.45(6)	K2	C23	3.51(2)
O1	C2	1.307(14)	O2	C3	1.346(14)
O3	C7	1.228(14)	O3	K2	2.696(9)
O4	C10	1.25(2)	O4	K2	2.521(10)
O5	C14	1.330(14)	O6	C15	1.353(12)
O7	C19	1.24(2)	O7	K1	2.561(10)
O8	C23	1.216(15)	O9	C29	1.48(3)
O9	C27	1.63(2)	O10	C32	1.40(3)
O11	C60	1.64(6)	O11	C35	1.70(6)
O14	C37	1.42(4)	O16	C58	1.31(8)
O16	C48	1.54(7)	O17	C59	0.98(5)
O17	C49	1.36(5)	O17	C47	1.57(6)
N1	C7	1.34(2)	N1	C8	1.47(2)
N2	C10	1.29(2)	N2	C11	1.47(2)
N3	C23	1.31(2)	N3	C24	1.51(2)
N4	C19	1.316(15)	N4	C20	1.43(2)
C1	C2	1.36(2)	C1	C6	1.43(2)
C1	C7	1.51(2)	C2	C3	1.46(2)
C3	C4	1.43(2)	C4	C5	1.38(2)
C4	C10	1.52(2)	C5	C6	1.40(2)
C8	C9	1.51(2)	C11	C55	1.21(5)
C11	C12	1.90(5)	C12	C55	0.72(6)
C13	C14	1.36(2)	C13	C18	1.45(2)
C13	C23	1.49(2)	C14	C15	1.45(2)
C15	C16	1.37(2)	C16	C17	1.36(2)
C16	C19	1.51(2)	C17	C18	1.36(2)
C20	C22	1.50(2)	C24	C26	1.43(3)

C24	C25	1.56(4)	C25	C26	1.53(4)
C27	C28	1.42(3)	C29	C30	1.31(4)
C32	C33	0.98(6)	C32	C46	1.46(12)
C32	C34	1.52(5)	C33	C46	1.29(13)
C33	C34	1.38(7)	C34	C46	1.32(12)
C35	C56	1.48(8)	C35	C36	1.53(9)
C36	C56	1.11(10)	C37	C53	0.93(7)
C37	C57	1.48(5)	C37	C54	1.46(6)
C45	C48	1.31(9)	C45	C60	1.72(10)
C47	C49	1.01(6)	C47	C52	1.65(7)
C49	C52	1.48(7)	C49	C59	1.54(6)
C53	C57	1.66(8)	C54	C57	1.04(5)
C58	O16	1.31(8)	C58	C59	1.74(8)
C59	C58	1.74(8)			

Distances are in angstroms. Estimated standard deviations in the least significant figure are given in parentheses.

Table A-4. Selected bond angles for $K_4[Zr(ETAM)_4]$.

atom	atom	atom	angle	atom	atom	atom	angle
O2	Zr1	O2	82.4(5)	O6	Zr1	O5	142.0(3)
O2	Zr1	O6	107.7(3)	O6	Zr1	O5	69.7(3)
O2	Zr1	O6	143.2(3)	O1	Zr1	O5	73.7(3)
O2	Zr1	O6	143.2(3)	O1	Zr1	O5	117.6(3)
O2	Zr1	O6	107.7(3)	O5	Zr1	O5	145.1(4)
O6	Zr1	O6	85.5(4)	O2	Zr1	K1	60.1(2)
O2	Zr1	O1	71.5(3)	O2	Zr1	K1	138.1(2)
O2	Zr1	O1	141.1(3)	O6	Zr1	K1	50.3(2)
O6	Zr1	O1	73.9(3)	O6	Zr1	K1	113.5(2)
O6	Zr1	O1	80.1(3)	O1	Zr1	K1	45.5(2)
O2	Zr1	O1	141.1(3)	O1	Zr1	K1	126.9(2)
O2	Zr1	O1	71.5(3)	O5	Zr1	K1	72.3(2)
O6	Zr1	O1	80.1(3)	O5	Zr1	K1	113.6(2)
O6	Zr1	O1	73.9(3)	O2	Zr1	K1	138.1(2)
O1	Zr1	O1	144.3(4)	O2	Zr1	K1	60.1(2)
O2	Zr1	O5	73.8(3)	O6	Zr1	K1	113.5(2)
O2	Zr1	O5	80.1(3)	O6	Zr1	K1	50.3(2)
O6	Zr1	O5	69.7(3)	O1	Zr1	K1	126.9(2)
O6	Zr1	O5	141.9(3)	O1	Zr1	K1	45.5(2)
O1	Zr1	O5	117.6(3)	O5	Zr1	K1	113.6(2)
O1	Zr1	O5	73.7(3)	O5	Zr1	K1	72.3(2)
O2	Zr1	O5	80.1(3)	K1	Zr1	K1	161.22(11)
O2	Zr1	O5	73.8(3)	O7	K1	O10	127.5(3)

O7	K1	O1	114.8(3)
O10	K1	O1	107.6(3)
O7	K1	O9	91.8(4)
O10	K1	O9	103.4(4)
O1	K1	O9	108.2(4)
O7	K1	O6	94.5(3)
O10	K1	O6	85.5(3)
O1	K1	O6	54.6(2)
O9	K1	O6	162.7(3)
O7	K1	C2	127.9(3)
O10	K1	C2	103.6(3)
O1	K1	C2	25.5(3)
O9	K1	C2	85.2(4)
O6	K1	C2	78.2(3)
O7	K1	C3	154.1(3)
O10	K1	C3	78.1(3)
O1	K1	C3	43.5(3)
O9	K1	C3	85.1(4)
O6	K1	C3	82.2(3)
C2	K1	C3	26.2(3)
O7	K1	O2	159.4(3)
O10	K1	O2	61.3(3)
O1	K1	O2	48.5(2)
O9	K1	O2	104.6(4)
O6	K1	O2	66.3(2)
C2	K1	O2	43.6(3)
C3	K1	O2	23.4(2)
O7	K1	Zr1	125.9(2)
O10	K1	Zr1	76.9(2)
O1	K1	Zr1	35.2(2)
O9	K1	Zr1	133.1(3)
O6	K1	Zr1	33.88(15)
C2	K1	Zr1	50.7(2)
C3	K1	Zr1	48.5(2)
O2	K1	Zr1	33.74(13)
O4	K2	C60	119.1(13)
O4	K2	O8	112.9(4)
C60	K2	O8	96.5(12)
O4	K2	O3	95.3(3)
C60	K2	O3	133.1(15)
O8	K2	O3	98.1(3)
O4	K2	O16	113.0(15)
C60	K2	O16	49.0(19)
O8	K2	O16	132.3(16)
O3	K2	O16	90.0(13)
O4	K2	O11	98.2(9)
C60	K2	O11	34.6(14)
O8	K2	O11	80.0(8)
O3	K2	O11	166.0(9)
O16	K2	O11	81.3(16)
O4	K2	C48	139.0(10)
C60	K2	C48	47.8(17)
O8	K2	C48	107.6(11)
O3	K2	C48	85.3(11)
O16	K2	C48	26.2(14)
O11	K2	C48	82.1(14)
O4	K2	C23	113.6(4)
C60	K2	C23	108.6(12)
O8	K2	C23	16.4(3)
O3	K2	C23	81.7(3)
O16	K2	C23	133.3(15)
O11	K2	C23	96.2(8)
C48	K2	C23	107.1(11)
C2	O1	Zr1	114.8(7)
C2	O1	K1	88.7(6)
Zr1	O1	K1	99.3(3)
C3	O2	Zr1	115.3(7)
C3	O2	K1	76.5(7)
Zr1	O2	K1	86.2(2)
C7	O3	K2	127.8(8)
C10	O4	K2	156.9(10)
C14	O5	Zr1	113.6(7)
C15	O6	Zr1	117.0(7)
C15	O6	K1	107.5(6)
Zr1	O6	K1	95.8(3)
C19	O7	K1	147.4(10)
C23	O8	K2	125.4(9)
C29	O9	C27	113.1(19)
C29	O9	K1	120.1(16)
C27	O9	K1	118.6(12)
C32	O10	K1	140.8(15)
C60	O11	C35	117.8(38)
C60	O11	K2	63.0(22)
C35	O11	K2	152.9(30)
C58	O16	C48	127.1(76)
C58	O16	K2	91.3(56)
C48	O16	K2	98.7(38)
C59	O17	C49	80.7(43)
C59	O17	C47	120.2(52)
C49	O17	C47	39.5(26)
C7	N1	C8	121.1(11)
C10	N2	C11	122.4(13)

C23	N3	C24	121.1(12)
C19	N4	C20	124.5(12)
C2	C1	C6	121.9(13)
C2	C1	C7	122.1(12)
C6	C1	C7	116.0(11)
O1	C2	C1	128.7(12)
O1	C2	C3	112.5(10)
C1	C2	C3	118.7(13)
O1	C2	K1	65.8(6)
C1	C2	K1	115.6(9)
C3	C2	K1	86.6(7)
O2	C3	C4	124.5(12)
O2	C3	C2	116.5(12)
C4	C3	C2	119.0(12)
O2	C3	K1	80.1(7)
C4	C3	K1	121.1(8)
C2	C3	K1	67.2(7)
C5	C4	C3	120.3(13)
C5	C4	C10	118.7(13)
C3	C4	C10	120.9(11)
C4	C5	C6	120.3(13)
C5	C6	C1	119.7(12)
O3	C7	N1	123.4(13)
O3	C7	C1	120.9(13)
N1	C7	C1	115.6(12)
N1	C8	C9	112.5(11)
O4	C10	N2	124.3(14)
O4	C10	C4	118.5(12)
N2	C10	C4	117.3(14)
C55	C11	N2	111.5(26)
C55	C11	C12	6.3(31)
N2	C11	C12	107.2(18)
C55	C12	C11	10.6(53)
C14	C13	C18	118.4(13)
C14	C13	C23	125.7(13)
C18	C13	C23	115.9(12)
O5	C14	C13	126.2(12)
O5	C14	C15	114.0(10)
C13	C14	C15	119.9(13)
O6	C15	C16	126.8(11)
O6	C15	C14	113.4(11)
C16	C15	C14	119.7(11)
C17	C16	C15	120.0(13)
C17	C16	C19	117.9(13)
C15	C16	C19	122.1(11)
C18	C17	C16	122.3(14)
C17	C18	C13	119.6(12)
O7	C19	N4	121.5(14)
O7	C19	C16	121.3(13)
N4	C19	C16	117.1(13)
N4	C20	C22	111.8(12)
O8	C23	N3	122.0(14)
O8	C23	C13	124.2(14)
N3	C23	C13	113.8(13)
O8	C23	K2	38.2(7)
N3	C23	K2	126.4(10)
C13	C23	K2	104.9(9)
C26	C24	N3	107.6(17)
C26	C24	C25	61.2(19)
N3	C24	C25	111.6(19)
C26	C25	C24	55.2(19)
C24	C26	C25	63.6(20)
C28	C27	O9	111.4(20)
C30	C29	O9	107.5(26)
C33	C32	O10	120.3(55)
C33	C32	C46	59.8(60)
O10	C32	C46	169.6(52)
C33	C32	C34	62.5(43)
O10	C32	C34	117.6(25)
C46	C32	C34	52.4(46)
C32	C33	C46	78.8(75)
C32	C33	C34	78.2(51)
C46	C33	C34	59.1(61)
C33	C34	C46	56.9(60)
C33	C34	C32	39.3(28)
C46	C34	C32	61.4(58)
C56	C35	C36	43.1(43)
C56	C35	O11	153.1(58)
C36	C35	O11	110.2(56)
C56	C36	C35	66.1(65)
C53	C37	O14	106.1(62)
C53	C37	C57	83.8(57)
O14	C37	C57	121.4(32)
C53	C37	C54	121.0(66)
O14	C37	C54	91.7(34)
C57	C37	C54	41.4(24)
C48	C45	C60	115.0(78)
C33	C46	C32	41.4(46)
C33	C46	C34	63.9(70)
C32	C46	C34	66.2(59)
C49	C47	O17	59.2(44)
C49	C47	C52	62.3(45)

O17	C47	C52	89.8(43)
C45	C48	O16	82.8(61)
C45	C48	K2	85.2(58)
O16	C48	K2	55.2(32)
C47	C49	O17	81.3(50)
C47	C49	C52	80.5(51)
O17	C49	C52	106.1(44)
C47	C49	C59	120.1(60)
O17	C49	C59	38.8(24)
C52	C49	C59	112.0(45)
C49	C52	C47	37.2(27)
C37	C53	C57	62.4(53)
C57	C54	C37	70.2(42)
C12	C55	C11	163.1(84)
C36	C56	C35	70.8(69)
C54	C57	C37	68.4(40)
C54	C57	C53	99.5(51)
C37	C57	C53	33.8(25)
O16	C58	C59	146.0(74)
O17	C59	C49	60.5(38)
O17	C59	C58	177.6(63)
C49	C59	C58	118.4(48)
O11	C60	C45	160.9(54)
O11	C60	K2	82.4(28)
C45	C60	K2	111.6(44)

Angles are in degrees. Estimated standard deviations in the least significant figure are given in parentheses.

X-Ray Structure Details of $[(C_6H_5CH_2)_3NCH_3]_4 \cdot [Th(C_{12}H_{12}O_4N_2)_4]$

EXPERIMENTAL DETAILS

A. Crystal Data

Empirical Formula	ThC88H120N12O16
Formula Weight	1834.02
Crystal Color, Habit	tan, block
Crystal Dimensions	0.23 X 0.17 X 0.12 mm
Crystal System	triclinic
Lattice Type	Primitive
No. of Reflections Used for Unit	
Cell Determination (2θ range)	8192 (0.0 - 0.0 °)
Lattice Parameters	a = 13.7570(3)Å
	b = 13.9293(3) Å
	c = 26.9124(6) Å
	α = 99.941(1)°
	β = 94.972(1)°
	γ = 103.160(1)°
	V = 4903.4(2) Å^3
Space Group	P$\bar{1}$ (#2)
Z value	2
Dcalc	1.242 g/cm3

F000	1900.00
μ(MoKα)	15.93 cm-1

B. Intensity Measurements

Diffractometer	SMART
Radiation	MoKα (λ = 0.71069 Å)
	graphite monochromated
Crystal to Detector Distance	60.0 mm
Temperature	-124.0 ° C
Scan Type	ω (0.3 ° per frame)
Scan Rate	10.0 seconds per frame.
2θmax	51.2 °
No. of Reflections Measured	Total: 25460 Unique: 15569 (Rint = 0.044)
Corrections	Lorentz-polarization Absorption (Tmax = 0.83 Tmin = 0.41)

C. Structure Solution and Refinement

Structure Solution	Direct Methods (SIR92)
Refinement	Full-matrix least-squares
Function Minimized	Σ w (|Fo| - |Fc|)2
Least Squares Weights	1/σ2(Fo) = 4Fo2/σ2(Fo2)
p-factor	0.030
Anomalous Dispersion	All non-hydrogen atoms

No. Observations (I>3.00σ(I))	11123
No. Variables	874
Reflection/Parameter Ratio	12.73
Residuals: R; Rw; Rall	0.052 ; 0.060; 0.077
Goodness of Fit Indicator	1.58
Max Shift/Error in Final Cycle	0.00
Maximum peak in Final Diff. Map	4.31 e-/Å^3
Minimum peak in Final Diff. Map	-2.67 e-/Å^3

Table A-5. Atomic coordinates and Biso/Beq for $4Bn_3NCH_3[Th(ETAM)_4]$.

atom	x	y	z	Beq
Th(1)	0.11022(2)	-0.08238(2)	0.23597(1)	1.500(6)
O(1)	-0.0184(4)	-0.0346(4)	0.1860(2)	2.0(1)
O(2)	0.0246(4)	-0.2065(4)	0.1619(2)	2.2(1)
O(3)	-0.1983(5)	0.0689(5)	0.0810(2)	3.3(2)
O(4)	-0.0744(5)	-0.3913(6)	0.0170(2)	4.6(2)
O(5)	0.2016(4)	0.0277(4)	0.1825(2)	1.9(1)
O(6)	0.2745(4)	-0.1022(4)	0.2216(2)	1.9(1)
O(7)	0.3903(5)	0.2651(5)	0.1304(2)	3.2(2)
O(8)	0.5848(5)	-0.0637(5)	0.2601(2)	3.4(2)
O(9)	0.2238(4)	0.0041(4)	0.3121(2)	2.0(1)
O(10)	0.0526(4)	0.0468(4)	0.2896(2)	2.0(1)
O(11)	0.3659(5)	0.0661(6)	0.4627(2)	4.4(2)
O(12)	-0.0979(5)	0.1729(5)	0.4050(2)	2.9(2)
O(13)	0.0064(4)	-0.1610(4)	0.2944(2)	1.9(1)
O(14)	0.1332(4)	-0.2419(4)	0.2474(2)	2.0(1)
O(15)	-0.1381(4)	-0.2957(4)	0.4067(2)	2.9(1)
O(16)	0.1704(5)	-0.5285(4)	0.2598(2)	3.3(2)
O(17)	0.484(1)	0.3986(10)	0.4194(5)	11.3(4)
O(18)	0.4672(6)	0.3927(6)	0.9269(3)	6.0(2)
N(1)	-0.1122(5)	0.0998(5)	0.1607(3)	2.4(2)
N(2)	-0.0036(6)	-0.3823(6)	0.0968(3)	3.4(2)
N(3)	0.2310(5)	0.1759(5)	0.1297(3)	2.4(2)
N(4)	0.4268(5)	-0.1479(5)	0.2672(3)	2.1(2)
N(5)	0.3883(6)	0.0372(6)	0.3790(3)	3.0(2)
N(6)	-0.0997(5)	0.1173(5)	0.3199(2)	2.5(2)

N(7)	-0.1009(5)	-0.1554(5)	0.3728(2)	2.4(2)
N(8)	0.2074(5)	-0.3972(5)	0.2201(3)	2.5(2)
N(9)	0.3075(5)	0.3069(5)	0.2969(2)	2.3(1)
N(10)	0.8344(5)	0.2171(5)	0.5286(3)	2.4(1)
N(11)	0.2904(5)	0.2542(6)	0.7950(3)	2.8(1)
N(12)	0.7911(5)	0.1359(5)	0.9621(2)	2.1(1)
N(13)	0.5192(8)	0.3709(8)	0.4978(4)	5.7(2)
N(14)	0.6197(7)	0.4757(7)	0.9727(3)	4.6(2)
C(1)	-0.0573(6)	-0.0872(6)	0.1395(3)	1.8(2)
C(2)	-0.1194(6)	-0.0547(6)	0.1041(3)	2.2(2)
C(3)	-0.1566(7)	-0.1221(8)	0.0565(3)	2.7(2)
C(4)	-0.1361(7)	-0.2141(7)	0.0447(3)	2.7(2)
C(5)	-0.0736(7)	-0.2462(7)	0.0792(3)	2.5(2)
C(6)	-0.0356(6)	-0.1828(6)	0.1264(3)	1.8(2)
C(7)	-0.1466(6)	0.0426(7)	0.1141(3)	2.5(2)
C(8)	-0.1257(7)	0.2009(7)	0.1755(3)	3.0(2)
C(9)	-0.0339(8)	0.2689(8)	0.2088(4)	3.7(3)
C(10)	-0.0514(7)	-0.3465(7)	0.0620(3)	2.9(2)
C(11)	0.0206(8)	-0.4789(8)	0.0872(4)	4.1(3)
C(12)	-0.043(1)	-0.5536(10)	0.1104(5)	7.0(5)
C(13)	0.3025(6)	0.0436(6)	0.1873(3)	2.1(2)
C(14)	0.3423(6)	-0.0256(6)	0.2113(3)	1.6(2)
C(15)	0.4466(6)	-0.0117(6)	0.2219(3)	2.0(2)
C(16)	0.5109(6)	0.0693(7)	0.2063(3)	2.4(2)
C(17)	0.4722(7)	0.1318(7)	0.1808(3)	2.7(2)
C(18)	0.3668(6)	0.1215(6)	0.1704(3)	1.8(2)
C(19)	0.3303(6)	0.1920(6)	0.1415(3)	2.0(2)
C(20)	0.1861(7)	0.2421(7)	0.1032(4)	3.3(2)
C(21)	0.0804(7)	0.1929(8)	0.0804(3)	3.3(2)
C(22)	0.4924(6)	-0.0758(7)	0.2509(3)	2.3(2)
C(23)	0.4563(7)	-0.2107(7)	0.3012(3)	2.7(2)
C(24)	0.3786(7)	-0.2341(7)	0.3368(3)	3.0(2)
C(25)	0.1855(6)	0.0489(6)	0.3509(3)	1.8(2)
C(26)	0.0909(6)	0.0707(6)	0.3389(3)	1.7(2)
C(27)	0.0446(6)	0.1172(6)	0.3778(3)	1.9(2)
C(28)	0.0936(7)	0.1417(6)	0.4282(3)	2.6(2)
C(29)	0.1846(7)	0.1203(6)	0.4398(3)	2.4(2)
C(30)	0.2331(6)	0.0736(6)	0.4020(3)	2.1(2)
C(31)	0.3336(7)	0.0579(7)	0.4165(4)	2.7(2)
C(32)	0.4956(7)	0.0396(9)	0.3869(4)	3.8(3)
C(33)	0.5603(9)	0.134(1)	0.3775(5)	6.0(4)
C(34)	-0.0559(6)	0.1386(6)	0.3688(3)	2.2(2)
C(35)	-0.2023(7)	0.1260(8)	0.3064(4)	3.7(2)
C(36)	-0.2108(8)	0.2340(8)	0.3111(3)	3.8(3)
C(37)	0.0107(6)	-0.2531(6)	0.3024(3)	1.6(2)
C(38)	0.0779(6)	-0.2987(6)	0.2753(3)	1.7(2)

C(39)	0.0860(6)	-0.3959(6)	0.2795(3)	1.9(2)
C(40)	0.0266(6)	-0.4464(6)	0.3109(3)	2.5(2)
C(41)	-0.0349(6)	-0.4009(6)	0.3388(3)	2.3(2)
C(42)	-0.0425(6)	-0.3015(6)	0.3369(3)	1.8(2)
C(43)	-0.0992(6)	-0.2512(7)	0.3739(3)	2.0(2)
C(44)	-0.1435(7)	-0.0971(7)	0.4107(3)	2.7(2)
C(45)	-0.2542(8)	-0.1080(8)	0.3981(4)	4.7(3)
C(46)	0.1579(6)	-0.4452(6)	0.2530(3)	2.3(2)
C(47)	0.2833(7)	-0.4344(7)	0.1920(3)	3.5(2)
C(48)	0.3180(8)	-0.3663(8)	0.1553(3)	3.5(3)
C(49)	0.2132(7)	0.2478(7)	0.2637(3)	2.9(2)
C(50)	0.3668(8)	0.2366(8)	0.3121(4)	3.6(2)
C(51)	0.2811(7)	0.3659(7)	0.3417(3)	3.0(2)
C(52)	0.3677(7)	0.3728(7)	0.2648(3)	2.7(2)
C(53)	0.4665(7)	0.4397(7)	0.2931(3)	2.6(2)
C(54)	0.4692(8)	0.5350(8)	0.3186(4)	4.0(2)
C(55)	0.5596(9)	0.5972(9)	0.3458(4)	4.6(2)
C(56)	0.6455(9)	0.5618(9)	0.3455(4)	4.6(2)
C(57)	0.6435(9)	0.4689(9)	0.3195(4)	5.0(3)
C(58)	0.5549(8)	0.4098(8)	0.2931(4)	4.1(2)
C(59)	0.7487(7)	0.1887(7)	0.4874(3)	3.3(2)
C(60)	0.8800(7)	0.1284(7)	0.5291(4)	3.5(2)
C(61)	0.7991(7)	0.2458(7)	0.5790(3)	3.0(2)
C(62)	0.9187(6)	0.3062(6)	0.5193(3)	2.3(2)
C(63)	0.8854(6)	0.3970(6)	0.5122(3)	2.3(2)
C(64)	0.8541(7)	0.4103(7)	0.4642(3)	2.7(2)
C(65)	0.8305(7)	0.5004(8)	0.4579(4)	3.4(2)
C(66)	0.8373(7)	0.5765(7)	0.4982(4)	3.4(2)
C(67)	0.8694(7)	0.5658(7)	0.5465(3)	3.2(2)
C(68)	0.8927(7)	0.4766(7)	0.5533(3)	2.8(2)
C(69)	0.4030(9)	0.2921(9)	0.8075(4)	5.0(3)
C(70)	0.2642(9)	0.1506(9)	0.8085(4)	5.0(3)
C(71)	0.2596(9)	0.2458(9)	0.7405(4)	4.7(2)
C(72)	0.2365(8)	0.3208(8)	0.8275(4)	3.9(2)
C(73)	0.2564(7)	0.4273(7)	0.8212(3)	3.1(2)
C(74)	0.1952(8)	0.4584(8)	0.7877(4)	3.9(2)
C(75)	0.2135(9)	0.5566(9)	0.7825(4)	5.1(3)
C(76)	0.2950(9)	0.6258(9)	0.8081(4)	4.9(2)
C(77)	0.3600(9)	0.6004(9)	0.8420(4)	5.2(3)
C(78)	0.3422(8)	0.4992(8)	0.8488(4)	4.4(2)
C(79)	0.8207(6)	0.2226(6)	1.0044(3)	2.3(2)
C(80)	0.8724(7)	0.0808(7)	0.9605(3)	3.3(2)
C(81)	0.7748(7)	0.1721(7)	0.9134(3)	3.1(2)
C(82)	0.6940(6)	0.0589(6)	0.9691(3)	2.3(2)
C(83)	0.6053(6)	0.0986(6)	0.9760(3)	2.4(2)
C(84)	0.5330(8)	0.0943(8)	0.9347(4)	3.8(2)

C(85)	0.4448(9)	0.1267(9)	0.9444(4)	4.9(2)
C(86)	0.4323(10)	0.1668(10)	0.9917(5)	6.0(3)
C(87)	0.4996(8)	0.1733(8)	1.0326(4)	4.1(2)
C(88)	0.5867(7)	0.1389(7)	1.0246(3)	3.0(2)
C(89)	0.546(1)	0.406(1)	0.4570(6)	7.6(4)
C(90)	0.417(1)	0.327(1)	0.5036(6)	9.6(5)
C(91)	0.594(1)	0.383(1)	0.5446(5)	6.5(3)
C(92)	0.5394(8)	0.4014(8)	0.9607(4)	4.2(2)
C(93)	0.631(1)	0.560(1)	0.9487(5)	7.7(4)
C(94)	0.697(1)	0.476(1)	1.0137(5)	7.6(4)

Table A-6. Anisotropic Displacement Parameters for $4Bn_3NCH_3[Th(ETAM)_4]$.

atom	U11	U22	U33	U12	U13	U23
Th(1)	0.0178(2)	0.0188(2)	0.0164(2)	0.0043(1)	0.0028(1)	0.0062(1)
O(1)	0.031(3)	0.024(3)	0.016(3)	0.006(3)	0.003(3)	0.003(3)
O(2)	0.033(4)	0.021(3)	0.023(3)	0.004(3)	0.006(3)	0.002(3)
O(3)	0.037(4)	0.053(4)	0.035(4)	0.012(3)	-0.015(3)	0.018(3)
O(4)	0.060(5)	0.071(5)	0.034(4)	0.015(4)	-0.002(4)	-0.015(4)
O(5)	0.021(3)	0.032(4)	0.026(3)	0.008(3)	0.005(3)	0.015(3)
O(6)	0.024(3)	0.023(3)	0.026(3)	0.006(3)	0.006(3)	0.011(3)
O(7)	0.038(4)	0.042(4)	0.051(4)	0.003(3)	0.009(3)	0.029(3)
O(8)	0.024(4)	0.054(5)	0.051(4)	0.010(3)	0.001(3)	0.020(3)
O(9)	0.018(3)	0.036(4)	0.022(3)	0.010(3)	0.003(2)	0.007(3)
O(10)	0.025(3)	0.029(3)	0.020(3)	0.008(3)	0.002(2)	0.007(3)
O(11)	0.053(5)	0.081(6)	0.032(4)	0.025(4)	-0.016(3)	0.006(4)
O(12)	0.043(4)	0.043(4)	0.029(3)	0.022(3)	0.013(3)	0.000(3)
O(13)	0.027(3)	0.022(3)	0.024(3)	0.009(3)	0.006(3)	0.009(3)
O(14)	0.028(3)	0.023(3)	0.024(3)	0.003(3)	0.011(3)	0.007(3)
O(15)	0.036(4)	0.039(4)	0.034(3)	0.005(3)	0.014(3)	0.021(3)
O(16)	0.043(4)	0.029(4)	0.054(4)	0.014(3)	0.014(3)	0.014(3)
N(1)	0.040(5)	0.035(5)	0.025(4)	0.017(4)	0.001(4)	0.011(4)
N(2)	0.060(6)	0.027(5)	0.031(4)	0.007(4)	0.010(4)	-0.009(4)
N(3)	0.028(5)	0.031(5)	0.041(5)	0.006(4)	0.004(4)	0.024(4)
N(4)	0.025(4)	0.032(4)	0.037(4)	0.013(3)	0.005(3)	0.019(4)
N(5)	0.040(5)	0.057(6)	0.021(4)	0.023(4)	-0.002(4)	0.000(4)
N(6)	0.025(4)	0.042(5)	0.027(4)	0.014(4)	0.004(3)	0.003(3)
N(7)	0.039(5)	0.029(4)	0.023(4)	0.009(4)	0.015(3)	0.011(3)
N(8)	0.042(5)	0.024(4)	0.040(4)	0.018(4)	0.015(4)	0.014(4)
C(1)	0.026(5)	0.027(5)	0.020(5)	0.004(4)	0.011(4)	0.010(4)
C(2)	0.024(5)	0.033(5)	0.018(4)	0.006(4)	-0.001(4)	0.008(4)
C(3)	0.027(5)	0.058(7)	0.019(5)	0.001(5)	-0.005(4)	0.016(5)
C(4)	0.038(6)	0.035(6)	0.020(5)	0.002(5)	0.002(4)	-0.002(4)
C(5)	0.028(5)	0.036(6)	0.023(5)	-0.006(4)	0.001(4)	0.009(4)
C(6)	0.017(4)	0.028(5)	0.022(5)	0.001(4)	0.009(4)	0.013(4)

C(7)	0.026(5)	0.043(6)	0.029(5)	0.002(5)	0.002(4)	0.018(5)
C(8)	0.038(6)	0.037(6)	0.037(5)	0.016(5)	0.000(4)	0.011(5)
C(9)	0.046(7)	0.048(7)	0.047(6)	0.014(5)	0.010(5)	0.006(5)
C(10)	0.034(6)	0.041(6)	0.029(6)	0.004(5)	0.008(5)	0.003(5)
C(11)	0.057(7)	0.036(6)	0.054(7)	0.012(5)	0.003(6)	-0.014(5)
C(12)	0.17(2)	0.047(8)	0.12(1)	0.057(9)	0.08(1)	0.035(8)
C(13)	0.020(5)	0.027(5)	0.024(5)	0.007(4)	0.004(4)	0.001(4)
C(14)	0.026(5)	0.016(4)	0.018(4)	0.005(4)	0.007(4)	0.002(3)
C(15)	0.020(5)	0.026(5)	0.030(5)	0.008(4)	0.006(4)	0.007(4)
C(16)	0.016(5)	0.036(6)	0.038(5)	0.007(4)	0.003(4)	0.012(4)
C(17)	0.028(5)	0.033(6)	0.038(5)	0.000(4)	0.007(4)	0.015(4)
C(18)	0.025(5)	0.028(5)	0.018(4)	0.005(4)	0.007(4)	0.005(4)
C(19)	0.029(5)	0.024(5)	0.021(4)	0.004(4)	0.001(4)	0.005(4)
C(20)	0.033(6)	0.045(6)	0.051(6)	0.008(5)	-0.001(5)	0.031(5)
C(21)	0.038(6)	0.057(7)	0.040(6)	0.023(5)	0.004(5)	0.020(5)
C(22)	0.025(5)	0.036(6)	0.025(5)	0.014(4)	0.003(4)	0.005(4)
C(23)	0.039(6)	0.044(6)	0.032(5)	0.021(5)	0.008(4)	0.017(4)
C(24)	0.044(6)	0.049(7)	0.034(6)	0.016(5)	0.008(5)	0.019(5)
C(25)	0.023(5)	0.014(4)	0.022(4)	0.001(4)	-0.002(4)	0.005(4)
C(26)	0.024(5)	0.018(5)	0.021(4)	0.000(4)	0.000(4)	0.007(4)
C(27)	0.023(5)	0.017(4)	0.030(5)	0.003(4)	0.008(4)	0.012(4)
C(28)	0.040(6)	0.031(5)	0.024(5)	0.010(4)	0.005(4)	0.002(4)
C(29)	0.044(6)	0.027(5)	0.019(5)	0.004(4)	0.001(4)	0.006(4)
C(30)	0.029(5)	0.023(5)	0.028(5)	0.004(4)	-0.001(4)	0.009(4)
C(31)	0.036(6)	0.030(6)	0.039(6)	0.010(5)	-0.014(5)	0.007(5)
C(32)	0.026(6)	0.072(8)	0.044(6)	0.024(6)	-0.011(5)	0.001(6)
C(33)	0.036(7)	0.09(1)	0.12(1)	0.012(7)	0.000(8)	0.014(9)
C(34)	0.032(5)	0.016(5)	0.035(5)	0.006(4)	0.007(4)	0.004(4)
C(35)	0.028(6)	0.057(7)	0.048(6)	0.013(5)	0.004(5)	0.006(5)
C(36)	0.056(7)	0.059(7)	0.039(6)	0.037(6)	0.009(5)	0.011(5)
C(37)	0.023(5)	0.020(5)	0.019(4)	0.003(4)	-0.001(4)	0.008(4)
C(38)	0.020(5)	0.024(5)	0.019(4)	0.003(4)	-0.003(4)	-0.001(4)
C(39)	0.025(5)	0.023(5)	0.023(4)	0.004(4)	0.002(4)	0.005(4)
C(40)	0.031(5)	0.024(5)	0.031(5)	-0.003(4)	-0.003(4)	0.012(4)
C(41)	0.028(5)	0.029(5)	0.030(5)	-0.001(4)	0.005(4)	0.021(4)
C(42)	0.022(5)	0.025(5)	0.016(4)	0.000(4)	-0.004(4)	0.010(4)
C(43)	0.025(5)	0.038(6)	0.011(4)	-0.001(4)	-0.005(4)	0.004(4)
C(44)	0.048(6)	0.028(5)	0.035(5)	0.010(5)	0.018(5)	0.011(4)
C(45)	0.045(7)	0.056(8)	0.067(7)	0.022(6)	0.006(6)	-0.006(6)
C(46)	0.032(5)	0.015(5)	0.036(5)	0.001(4)	-0.001(4)	0.006(4)
C(47)	0.046(6)	0.038(6)	0.044(6)	0.015(5)	0.012(5)	0.009(5)
C(48)	0.058(7)	0.052(7)	0.041(6)	0.024(6)	0.024(5)	0.017(5)

Table A-7. Selected bond lengths for $4Bn_3NCH_3[Th(ETAM)_4]$.

atom	atom	distance
Th(1)	O(1)	2.410(5)
Th(1)	O(2)	2.413(5)
Th(1)	O(5)	2.490(5)
Th(1)	O(6)	2.395(5)
Th(1)	O(9)	2.414(5)
Th(1)	O(10)	2.428(5)
Th(1)	O(13)	2.445(5)
Th(1)	O(14)	2.381(5)
O(1)	C(1)	1.335(9)
O(2)	C(6)	1.343(9)
O(3)	C(7)	1.25(1)
O(4)	C(10)	1.24(1)
O(5)	C(13)	1.346(9)
O(6)	C(14)	1.333(9)
O(7)	C(19)	1.25(1)
O(8)	C(22)	1.24(1)
O(9)	C(25)	1.333(9)
O(10)	C(26)	1.340(9)
O(11)	C(31)	1.26(1)
O(12)	C(34)	1.253(9)
O(13)	C(37)	1.350(9)
O(14)	C(38)	1.342(9)
O(15)	C(43)	1.253(9)
O(16)	C(46)	1.252(9)
O(17)	C(89)	1.24(2)
O(18)	C(92)	1.26(1)
N(11)	C(71)	1.47(1)
N(11)	C(72)	1.52(1)
N(12)	C(79)	1.46(1)
N(12)	C(80)	1.49(1)
N(12)	C(81)	1.50(1)
N(12)	C(82)	1.56(1)
N(13)	C(89)	1.32(2)
N(13)	C(90)	1.43(2)
N(13)	C(91)	1.51(1)
N(14)	C(92)	1.30(1)
N(14)	C(93)	1.42(2)
N(14)	C(94)	1.46(2)
C(1)	C(2)	1.42(1)
C(1)	C(6)	1.42(1)
C(2)	C(3)	1.43(1)
C(2)	C(7)	1.47(1)
C(3)	C(4)	1.37(1)
C(4)	C(5)	1.41(1)

atom	atom	distance
N(1)	C(7)	1.35(1)
N(1)	C(8)	1.45(1)
N(2)	C(10)	1.33(1)
N(2)	C(11)	1.44(1)
N(3)	C(19)	1.33(1)
N(3)	C(20)	1.47(1)
N(4)	C(22)	1.35(1)
N(4)	C(23)	1.46(1)
N(5)	C(31)	1.34(1)
N(5)	C(32)	1.47(1)
N(6)	C(34)	1.35(1)
N(6)	C(35)	1.46(1)
N(7)	C(43)	1.35(1)
N(7)	C(44)	1.44(1)
N(8)	C(46)	1.34(1)
N(8)	C(47)	1.47(1)
N(9)	C(49)	1.49(1)
N(9)	C(50)	1.50(1)
N(9)	C(51)	1.46(1)
N(9)	C(52)	1.52(1)
N(10)	C(59)	1.48(1)
N(10)	C(60)	1.51(1)
N(10)	C(61)	1.50(1)
N(10)	C(62)	1.56(1)
N(11)	C(69)	1.51(1)
N(11)	C(70)	1.52(1)
C(15)	C(22)	1.49(1)
C(16)	C(17)	1.37(1)
C(17)	C(18)	1.42(1)
C(18)	C(19)	1.50(1)
C(20)	C(21)	1.49(1)
C(23)	C(24)	1.51(1)
C(25)	C(26)	1.43(1)
C(25)	C(30)	1.42(1)
C(26)	C(27)	1.41(1)
C(27)	C(28)	1.41(1)
C(27)	C(34)	1.49(1)
C(28)	C(29)	1.37(1)
C(29)	C(30)	1.41(1)
C(30)	C(31)	1.48(1)
C(32)	C(33)	1.48(2)
C(35)	C(36)	1.52(1)
C(37)	C(38)	1.42(1)
C(37)	C(42)	1.40(1)

C(5)	C(6)	1.40(1)		C(38)	C(39)	1.41(1)	
C(5)	C(10)	1.50(1)		C(39)	C(40)	1.39(1)	
C(8)	C(9)	1.50(1)		C(39)	C(46)	1.49(1)	
C(11)	C(12)	1.47(2)		C(40)	C(41)	1.37(1)	
C(13)	C(14)	1.43(1)		C(41)	C(42)	1.42(1)	
C(13)	C(18)	1.40(1)		C(42)	C(43)	1.49(1)	
C(14)	C(15)	1.40(1)		C(44)	C(45)	1.50(1)	
C(15)	C(16)	1.42(1)		C(47)	C(48)	1.52(1)	
C(52)	C(53)	1.52(1)		C(86)	C(87)	1.35(1)	
C(53)	C(54)	1.38(1)		C(87)	C(88)	1.41(1)	
C(53)	C(58)	1.37(1)		C(56)	C(57)	1.35(1)	
C(54)	C(55)	1.40(1)		C(57)	C(58)	1.36(1)	
C(55)	C(56)	1.38(1)		C(62)	C(63)	1.48(1)	
C(63)	C(64)	1.38(1)		C(63)	C(68)	1.40(1)	
C(64)	C(65)	1.40(1)		C(65)	C(66)	1.36(1)	
C(66)	C(67)	1.38(1)		C(67)	C(68)	1.39(1)	
C(72)	C(73)	1.49(1)		C(73)	C(74)	1.37(1)	
C(73)	C(78)	1.42(1)		C(74)	C(75)	1.37(1)	
C(75)	C(76)	1.34(2)		C(76)	C(77)	1.37(2)	
C(77)	C(78)	1.42(1)		C(82)	C(83)	1.46(1)	
C(83)	C(84)	1.41(1)		C(83)	C(88)	1.40(1)	
C(84)	C(85)	1.42(1)		C(85)	C(86)	1.34(1)	

Distances are in angstroms. Estimated standard deviations in the least significant figure are given in parentheses.

Table A-8. Selected bond angles for $4Bn_3NCH_3[Th(ETAM)_4]$.

atom	atom	atom	angle	atom	atom	atom	angle
O(1)	Th(1)	O(2)	64.8(2)	O(10)	Th(1)	O(14)	132.3(2)
O(1)	Th(1)	O(5)	74.5(2)	O(13)	Th(1)	O(14)	64.8(2)
O(1)	Th(1)	O(6)	132.9(2)	Th(1)	O(1)	C(1)	120.8(5)
O(1)	Th(1)	O(9)	132.4(2)	Th(1)	O(2)	C(6)	120.8(5)
O(1)	Th(1)	O(10)	71.2(2)	Th(1)	O(5)	C(13)	117.2(4)
O(1)	Th(1)	O(13)	98.8(2)	Th(1)	O(6)	C(14)	119.5(4)
O(1)	Th(1)	O(14)	132.3(2)	Th(1)	O(9)	C(25)	117.9(4)
O(2)	Th(1)	O(5)	91.8(2)	Th(1)	O(10)	C(26)	116.9(5)
O(2)	Th(1)	O(6)	94.5(2)	Th(1)	O(13)	C(37)	120.3(4)
O(2)	Th(1)	O(9)	162.8(2)	Th(1)	O(14)	C(38)	123.2(5)
O(2)	Th(1)	O(10)	130.7(2)	C(7)	N(1)	C(8)	122.8(7)
O(2)	Th(1)	O(13)	93.9(2)	C(10)	N(2)	C(11)	123.8(8)
O(2)	Th(1)	O(14)	71.8(2)	C(19)	N(3)	C(20)	122.1(7)
O(5)	Th(1)	O(6)	63.9(2)	C(22)	N(4)	C(23)	124.2(7)
O(5)	Th(1)	O(9)	92.9(2)	C(31)	N(5)	C(32)	124.4(7)
O(5)	Th(1)	O(10)	97.1(2)	C(34)	N(6)	C(35)	121.7(7)
O(5)	Th(1)	O(13)	168.3(2)	C(43)	N(7)	C(44)	121.6(6)

O(5)	Th(1)	O(14)	126.8(2)
O(6)	Th(1)	O(9)	72.8(2)
O(6)	Th(1)	O(10)	132.7(2)
O(6)	Th(1)	O(13)	125.7(2)
O(6)	Th(1)	O(14)	67.4(2)
O(9)	Th(1)	O(10)	65.0(2)
O(9)	Th(1)	O(13)	84.6(2)
O(9)	Th(1)	O(14)	92.2(2)
O(10)	Th(1)	O(13)	71.5(2)
C(59)	N(10)	C(62)	111.2(6)
C(60)	N(10)	C(61)	109.7(6)
C(60)	N(10)	C(62)	107.4(6)
C(61)	N(10)	C(62)	109.7(6)
C(69)	N(11)	C(70)	106.1(8)
C(69)	N(11)	C(71)	110.4(8)
C(69)	N(11)	C(72)	111.2(7)
C(70)	N(11)	C(71)	109.6(8)
C(70)	N(11)	C(72)	107.9(7)
C(71)	N(11)	C(72)	111.4(8)
C(79)	N(12)	C(80)	108.8(7)
C(79)	N(12)	C(81)	109.0(6)
C(79)	N(12)	C(82)	112.2(6)
C(80)	N(12)	C(81)	110.7(6)
C(80)	N(12)	C(82)	106.1(6)
C(81)	N(12)	C(82)	109.9(6)
C(89)	N(13)	C(90)	123(1)
C(89)	N(13)	C(91)	122(1)
C(90)	N(13)	C(91)	114(1)
C(92)	N(14)	C(93)	121(1)
C(92)	N(14)	C(94)	120(1)
C(93)	N(14)	C(94)	119(1)
O(1)	C(1)	C(2)	124.3(7)
O(1)	C(1)	C(6)	115.8(7)
C(2)	C(1)	C(6)	119.8(7)
C(1)	C(2)	C(3)	116.6(8)
C(16)	C(15)	C(22)	118.7(7)
C(15)	C(16)	C(17)	120.8(8)
C(16)	C(17)	C(18)	122.2(7)
C(13)	C(18)	C(17)	117.4(7)
C(13)	C(18)	C(19)	123.6(7)
C(17)	C(18)	C(19)	118.9(7)
O(7)	C(19)	N(3)	121.4(7)
O(7)	C(19)	C(18)	121.4(8)
N(3)	C(19)	C(18)	117.1(7)
N(3)	C(20)	C(21)	111.6(7)
O(8)	C(22)	N(4)	121.6(7)

C(46)	N(8)	C(47)	123.4(7)
C(49)	N(9)	C(50)	109.4(7)
C(49)	N(9)	C(51)	108.8(7)
C(49)	N(9)	C(52)	106.5(6)
C(50)	N(9)	C(51)	110.5(7)
C(50)	N(9)	C(52)	109.0(6)
C(51)	N(9)	C(52)	112.4(7)
C(59)	N(10)	C(60)	108.7(7)
C(59)	N(10)	C(61)	110.2(7)
C(1))	C(2)	C(7)	124.0(7)
C(3)	C(2)	C(7)	119.4(7)
C(2)	C(3)	C(4)	122.9(8)
C(3)	C(4)	C(5)	120.7(8)
C(4)	C(5)	C(6)	118.3(8)
C(4)	C(5)	C(10)	116.9(8)
C(6)	C(5)	C(10)	124.7(8)
O(2)	C(6)	C(1)	115.6(7)
O(2)	C(6)	C(5)	122.9(8)
C(1)	C(6)	C(5)	121.5(7)
O(3)	C(7)	N(1)	123.0(9)
O(3)	C(7)	C(2)	121.3(8)
N(1)	C(7)	C(2)	115.7(7)
N(1)	C(8)	C(9)	110.9(7)
O(4)	C(10)	N(2)	122.5(9)
O(4)	C(10)	C(5)	121.0(8)
N(2)	C(10)	C(5)	116.5(8)
N(2)	C(11)	C(12)	112.6(9)
O(5)	C(13)	C(14)	115.3(7)
O(5)	C(13)	C(18)	124.1(7)
C(14)	C(13)	C(18)	120.6(7)
O(6)	C(14)	C(13)	115.8(7)
O(6)	C(14)	C(15)	124.0(7)
C(13)	C(14)	C(15)	120.2(7)
C(14)	C(15)	C(16)	118.6(7)
C(14)	C(15)	C(22)	122.6(7)
C(25)	C(30)	C(31)	122.8(8)
C(29)	C(30)	C(31)	118.9(8)
O(11)	C(31)	N(5)	122.3(9)
O(11)	C(31)	C(30)	120.2(9)
N(5)	C(31)	C(30)	117.4(8)
N(5)	C(32)	C(33)	112.4(9)
O(12)	C(34)	N(6)	122.2(8)
O(12)	C(34)	C(27)	121.4(8)
N(6)	C(34)	C(27)	116.4(7)
N(6)	C(35)	C(36)	113.6(8)
O(13)	C(37)	C(38)	116.0(7)

O(8)	C(22)	C(15)	122.6(8)
N(4)	C(22)	C(15)	115.7(7)
N(4)	C(23)	C(24)	111.0(7)
O(9)	C(25)	C(26)	116.3(7)
O(9)	C(25)	C(30)	123.5(7)
C(26)	C(25)	C(30)	120.2(7)
O(10)	C(26)	C(25)	116.0(7)
O(10)	C(26)	C(27)	124.0(7)
C(25)	C(26)	C(27)	120.0(7)
C(26)	C(27)	C(28)	118.9(7)
C(26)	C(27)	C(34)	123.4(7)
C(28)	C(27)	C(34)	117.7(7)
C(27)	C(28)	C(29)	121.1(8)
C(28)	C(29)	C(30)	121.7(8)
C(25)	C(30)	C(29)	118.2(8)
N(7)	C(43)	C(42)	117.8(7)
N(7)	C(44)	C(45)	113.9(8)
O(16)	C(46)	N(8)	120.9(8)
O(16)	C(46)	C(39)	122.4(7)
N(8)	C(46)	C(39)	116.7(7)
N(8)	C(47)	C(48)	109.3(7)
N(9)	C(52)	C(53)	113.7(7)
C(52)	C(53)	C(54)	119.4(9)
C(52)	C(53)	C(58)	122.3(9)
C(54)	C(53)	C(58)	118.3(9)
C(53)	C(54)	C(55)	120(1)
C(54)	C(55)	C(56)	119(1)
C(55)	C(56)	C(57)	121(1)
C(56)	C(57)	C(58)	119(1)
C(53)	C(58)	C(57)	122(1)
N(10)	C(62)	C(63)	115.3(7)
C(62)	C(63)	C(64)	121.1(8)
C(62)	C(63)	C(68)	121.1(8)
C(64)	C(63)	C(68)	117.6(8)
C(63)	C(64)	C(65)	120.1(9)
C(66)	C(67)	C(68)	119.4(9)
C(63)	C(68)	C(67)	121.7(8)
O(13)	C(37)	C(42)	124.0(7)
C(38)	C(37)	C(42)	120.0(7)
O(14)	C(38)	C(37)	115.4(7)
O(14)	C(38)	C(39)	123.7(7)
C(37)	C(38)	C(39)	120.8(7)
C(38)	C(39)	C(40)	118.5(7)
C(38)	C(39)	C(46)	122.5(7)
C(40)	C(39)	C(46)	119.0(7)
C(39)	C(40)	C(41)	120.9(8)
C(40)	C(41)	C(42)	122.2(7)
C(37)	C(42)	C(41)	117.3(7)
C(37)	C(42)	C(43)	123.4(7)
C(41)	C(42)	C(43)	119.2(7)
O(15)	C(43)	N(7)	121.8(8)
O(15)	C(43)	C(42)	120.3(8)
C(72)	C(73)	C(78)	120.2(9)
C(74)	C(73)	C(78)	117.9(9)
C(73)	C(74)	C(75)	121(1)
C(74)	C(75)	C(76)	122(1)
C(75)	C(76)	C(77)	120(1)
C(76)	C(77)	C(78)	119(1)
C(73)	C(78)	C(77)	119(1)
N(12)	C(82)	C(83)	116.1(7)
C(82)	C(83)	C(84)	121.9(8)
C(82)	C(83)	C(88)	121.0(8)
C(84)	C(83)	C(88)	117.0(8)
C(83)	C(84)	C(85)	119.1(9)
C(84)	C(85)	C(86)	121(1)
C(85)	C(86)	C(87)	122(1)
C(86)	C(87)	C(88)	118(1)
C(83)	C(88)	C(87)	122.2(9)
O(17)	C(89)	N(13)	122(2)
O(18)	C(92)	N(14)	126(1)
C(64)	C(65)	C(66)	121.5(9)
C(65)	C(66)	C(67)	119.7(9)
N(11)	C(72)	C(73)	115.8(8)
C(72)	C(73)	C(74)	121.9(9)

Angles are in degrees. Estimated standard deviations in the least significant figure are given in parentheses.

X-Ray Structure Details of $[Th(C_{12}H_{12}O_4N_2)_3(CH_3OH)]_2 \cdot 4\ N(CH_3)_4 \cdot 3\ CH_3OH \cdot x$(solvent) (first Th_2ETAM_6 dimer)

EXPERIMENTAL DETAILS

A. Crystal Data

Empirical Formula	$Th_2C_{90}H_{140}O_{26}N_{16}$
Formula Weight	2326.26
Crystal Color, Habit	brown, tablet
Crystal Dimensions	0.24 X 0.10 X 0.10 mm
Crystal System	monoclinic
Lattice Type	Primitive
No. of Reflections Used for Unit Cell Determination (2θ range)	4827 (3.5 - 45.0°)
Lattice Parameters	a = 13.2437(3)Å
	b = 26.7048(2) Å
	c = 16.6384(3) Å
	β = 106.830(1)°
	V = 5632.5(2) Å^3
Space Group	P21/c (#14)
Z value	2
Dcalc	1.372 g/cm^3
F000	2360.00
μ(MoKα)	27.23 cm^{-1}

B. Intensity Measurements

Diffractometer	SMART
Radiation	MoKα (λ = 0.71069 Å) graphite monochromated
Crystal to Detector Distance	60.0 mm
Temperature	-117.0°C
Scan Type	ω (0.3° per frame)
Scan Rate	20 seconds per frame.
2θ max	51.9°
No. of Reflections Measured	Total: 25878 Unique: 9888 (Rint = 0.090)
Corrections	Lorentz-polarization Absorption (Tmax = 0.75 Tmin = 0.59)

C. Structure Solution and Refinement

Structure Solution	Direct Methods (SIR92)
Refinement	Full-matrix least-squares
Function Minimized	$\sigma\ w\ (\lvert Fo\rvert - \lvert Fc\rvert)^2$
Least Squares Weights	$1/\sigma^2(F_o) = 4F_o^2/\sigma^2(F_o^2)$
p-factor	0.030
Anomalous Dispersion	All non-hydrogen atoms
No. Observations (I>3.00σ(I))	4064
No. Variables	347
Reflection/Parameter Ratio	11.71
Residuals: R; Rw	0.067 ; 0.077

Goodness of Fit Indicator	1.73
Max Shift/Error in Final Cycle	0.02
Maximum peak in Final Diff. Map	1.91 e-/Å^3
Minimum peak in Final Diff. Map	-1.25 e-/Å^3

Table A-9. Atomic coordinates and Biso/Beq for Th_2ETAM_6 dimer #1

atom	x	y	z	Beq
Th()	1.03495(6)	-0.01766(3)	0.12632(5)	2.03(2)
O(1)	1.0630(9)	0.0168(5)	0.2598(7)	2.8(3)
O(2)	1.127(1)	-0.0712(5)	0.2406(9)	2.1(4)
O(3)	1.072(1)	-0.0955(4)	0.0664(9)	3.4(4)
O(4)	0.907(1)	-0.0813(5)	0.1173(9)	3.3(4)
O(5)	0.8927(9)	0.0015(4)	-0.0069(7)	1.7(3)
O(6)	0.8815(9)	0.0217(5)	0.1418(7)	2.1(3)
O(7)	1.040(1)	0.0795(5)	0.0999(8)	2.4(4)
O(8)	1.176(1)	0.0978(6)	0.482(1)	6.2(4)
O(9)	1.404(5)	-0.115(2)	0.428(4)	7(1)
O(10)	1.338(2)	-0.1513(10)	0.428(2)	5.2(8)
O(11)	1.174(2)	-0.242(1)	0.040(2)	11.8(8)
O(12)	0.715(1)	-0.2012(7)	0.145(1)	7.1(5)
O(13)	0.600(1)	0.0534(7)	0.197(1)	7.0(5)
O(14)	0.780(1)	-0.0046(5)	-0.1742(9)	4.0(3)
O(15)	1.293(2)	-0.173(1)	0.580(2)	4.9(7)
N(1)	1.083(1)	0.0982(7)	0.347(1)	4.1(4)
N(2)	1.266(2)	-0.142(1)	0.289(2)	9.3(7)
N(3)	1.212(2)	-0.1588(9)	0.036(1)	7.1(6)
N(4)	0.732(2)	-0.1172(7)	0.137(1)	4.7(4)
N(5)	0.612(2)	-0.0170(10)	-0.200(1)	7.2(5)
N(6)	0.776(2)	0.0402(7)	0.249(1)	4.6(4)
N(7)	0.981(2)	-0.1506(9)	0.386(2)	7.1(6)
N(8)	0.609(4)	-0.320(2)	0.054(3)	12
C(1)	1.138(2)	0.0001(6)	0.326(1)	2.2(4)
C(2)	1.175(2)	-0.0507(9)	0.315(2)	4.3(5)
C(3)	1.253(2)	-0.071(1)	0.379(2)	6.0(6)
C(4)	1.293(2)	-0.045(1)	0.450(2)	6.5(7)
C(5)	1.259(2)	0.0035(9)	0.462(2)	5.0(6)
C(6)	1.177(2)	0.0249(8)	0.398(1)	3.1(4)
C(7)	1.145(2)	0.0767(9)	0.409(2)	3.9(5)
C(8)	1.041(2)	0.148(1)	0.344(2)	7.0(7)
C(9)	0.992(3)	0.168(1)	0.260(3)	11(1)
C(11)	1.303(4)	-0.121(2)	0.363(3)	11(1)

C(12)	1.295(3)	-0.201(1)	0.278(2)	10(1)
C(13)	1.378(5)	-0.181(2)	0.250(4)	20(1)
C(14)	1.024(2)	-0.1365(8)	0.083(1)	3.0(4)
C(15)	0.931(2)	-0.1275(9)	0.107(1)	3.9(5)
C(16)	0.871(2)	-0.1694(9)	0.120(1)	4.4(5)
C(17)	0.908(2)	-0.219(1)	0.115(2)	6.1(6)
C(18)	1.000(2)	-0.226(1)	0.098(2)	5.8(6)
C(19)	1.058(2)	-0.185(1)	0.078(2)	6.4(7)
C(20)	1.153(3)	-0.193(2)	0.048(2)	9.9(10)
C(21)	1.304(3)	-0.165(1)	0.005(2)	8.4(8)
C(22)	1.274(3)	-0.170(1)	-0.082(2)	9.0(9)
C(23)	0.771(2)	-0.163(1)	0.134(2)	5.7(6)
C(24)	0.622(3)	-0.105(1)	0.141(2)	8.7(9)
C(25)	0.630(3)	-0.096(1)	0.227(2)	10.0(10)
C(26)	0.796(2)	0.0097(8)	-0.001(1)	3.1(4)
C(27)	0.793(2)	0.0237(8)	0.082(1)	2.8(4)
C(28)	0.697(2)	0.0354(8)	0.097(1)	4.1(5)
C(29)	0.610(2)	0.0365(10)	0.030(2)	6.4(7)
C(30)	0.607(2)	0.025(1)	-0.052(2)	6.6(7)
C(31)	0.705(2)	0.0115(9)	-0.069(1)	4.2(5)
C(32)	0.703(2)	-0.0029(9)	-0.148(2)	5.3(6)
C(33)	0.592(3)	-0.031(1)	-0.290(2)	8.8(9)
C(34)	0.515(3)	0.003(1)	-0.347(2)	9.6(9)
C(35)	0.696(2)	0.0437(10)	0.187(2)	5.3(6)
C(36)	0.776(2)	0.045(1)	0.332(2)	6.3(7)
C(37)	0.873(2)	0.021(1)	0.388(2)	5.9(6)
C(38)	1.132(2)	0.1065(10)	0.108(2)	4.8(8)
C(39)	0.911(3)	-0.115(1)	0.335(2)	9.2(9)
C(40)	0.914(4)	-0.191(2)	0.410(3)	14(1)
C(41)	1.045(3)	-0.178(1)	0.336(2)	10.1(10)
C(42)	1.047(3)	-0.129(1)	0.454(3)	10(1)
C(43)	0.681(5)	-0.320(2)	0.151(4)	12
C(44)	0.515(4)	-0.278(2)	0.045(4)	12
C(45)	0.512(5)	-0.306(3)	0.118(5)	12
C(46)	0.617(5)	-0.362(2)	-0.051(4)	12
C(47)	0.555(7)	-0.372(3)	0.035(5)	12.3(7)
C(48)	0.673(4)	-0.296(2)	-0.002(3)	12
C(53)	1.248(7)	-0.169(3)	0.641(5)	11(1)
C(54)	0.422(3)	-0.353(1)	0.211(2)	12
C(55)	0.529(5)	-0.366(2)	0.337(4)	12
C(56)	0.598(3)	-0.351(1)	0.415(3)	12

Table A-10. Anisotropic Displacement Parameters for Th_2ETAM_6 dimer #1

atom	U11	U22	U33	U12	U13	U23
Th()	0.0245(4)	0.0284(4)	0.0346(4)	0.0061(6)	0.0163(3)	0.0008(6)
O(1)	0.026(7)	0.036(7)	0.042(8)	0.015(8)	0.006(6)	0.013(9)
O(2)	0.06(1)	0.06(1)	0.04(1)	0.030(8)	0.022(9)	0.004(8)
O(3)	0.06(1)	0.017(8)	0.07(1)	0.011(7)	0.047(9)	0.013(7)
O(4)	0.050(10)	0.024(8)	0.06(1)	0.007(7)	0.030(9)	-0.003(8)
O(5)	0.028(8)	0.026(8)	0.031(8)	0.005(5)	0.021(6)	0.002(5)
O(6)	0.020(7)	0.033(7)	0.031(7)	0.002(7)	0.009(6)	-0.008(8)
O(7)	0.030(8)	0.031(8)	0.06(1)	-0.021(7)	0.027(8)	-0.010(7)
C(38)	0.09(2)	0.08(2)	0.05(2)	-0.03(2)	0.03(2)	-0.01(1)

Table A-11. Selected bond lengths for Th_2ETAM_6 dimer #1.

atom	atom	distance
Th	O(1)	2.33(1)
Th	O(2)	2.41(1)
Th	O(3)	2.42(1)
Th	O(4)	2.38(1)
Th	O(5)	2.51(1)
Th	O(5)	2.48(1)
Th	O(6)	2.37(1)
Th	O(7)	2.64(1)
Th	O(14)	2.42(1)
O(1)	C(1)	1.32(2)
O(2)	C(2)	1.33(3)
O(3)	C(14)	1.33(3)
O(4)	C(15)	1.30(3)
O(5)	C(26)	1.33(2)
O(6)	C(27)	1.30(2)
O(7)	C(38)	1.39(3)
O(8)	C(7)	1.29(3)
O(9)	O(10)	1.30(7)
O(9)	C(11)	1.47(7)
O(10)	C(11)	1.33(5)
O(11)	C(20)	1.34(5)
O(12)	C(23)	1.31(4)
O(13)	C(35)	1.36(4)
O(14)	C(32)	1.22(3)
O(15)	C(53)	1.3(1)
N(1)	C(7)	1.26(3)
C(6)	C(7)	1.48(3)
N(1)	C(8)	1.44(4)
N(2)	C(11)	1.31(5)
N(2)	C(12)	1.65(5)
N(3)	C(20)	1.25(5)
N(3)	C(21)	1.47(5)
N(4)	C(23)	1.33(3)
N(4)	C(24)	1.51(4)
N(5)	C(32)	1.32(3)
N(5)	C(33)	1.50(4)
N(6)	C(35)	1.24(3)
N(6)	C(36)	1.39(4)
N(7)	C(39)	1.43(4)
N(7)	C(40)	1.53(6)
N(7)	C(41)	1.53(5)
N(7)	C(42)	1.34(4)
N(8)	C(43)	1.61(8)
N(8)	C(44)	1.65(8)
N(8)	C(47)	1.6(1)
N(8)	C(48)	1.58(8)
C(1)	C(2)	1.47(3)
C(1)	C(6)	1.34(3)
C(2)	C(3)	1.37(3)
C(3)	C(4)	1.34(4)
C(3)	C(11)	1.54(6)
C(4)	C(5)	1.41(4)
C(5)	C(6)	1.40(3)
C(8)	C(9)	1.46(5)

C(12)	C(13)	1.42(9)		C(14)	C(15)	1.42(4)	
C(14)	C(19)	1.39(4)		C(15)	C(16)	1.43(3)	
C(16)	C(17)	1.43(4)		C(16)	C(23)	1.42(4)	
C(17)	C(18)	1.34(4)		C(18)	C(19)	1.42(4)	
C(19)	C(20)	1.50(6)		C(21)	C(22)	1.40(5)	
C(24)	C(25)	1.43(6)		C(26)	C(27)	1.45(3)	
C(26)	C(31)	1.38(3)		C(27)	C(28)	1.40(3)	
C(28)	C(29)	1.36(3)		C(28)	C(35)	1.52(4)	
C(29)	C(30)	1.38(4)		C(30)	C(31)	1.46(4)	
C(31)	C(32)	1.36(4)		C(33)	C(34)	1.47(4)	
C(36)	C(37)	1.50(3)		C(44)	C(45)	1.4(1)	
C(55)	C(56)	1.40(7)					

Distances are in angstroms. Estimated standard deviations in the least significant figure are given in parentheses.

Table A-12. Selected bond angles for Th_2ETAM_6 dimer #1.

atom	atom	atom	angle	atom	atom	atom	angle
O(1)	Th	O(2)	65.0(5)	O(5)	Th	O(5)	67.8(5)
O(1)	Th	O(3)	137.4(5)	O(5)	Th	O(6)	63.7(4)
O(1)	Th	O(4)	104.8(5)	O(5)	Th	O(7)	72.7(3)
O(1)	Th	O(5)	129.2(4)	O(5)	Th	O(14)	132.0(4)
O(1)	Th	O(5)	134.6(4)	O(5)	Th	O(6)	123.5(4)
O(1)	Th	O(6)	68.1(4)	O(5)	Th	O(7)	70.1(4)
O(1)	Th	O(7)	76.5(5)	O(5)	Th	O(14)	68.4(4)
O(1)	Th	O(14)	73.9(5)	O(6)	Th	O(7)	69.3(4)
O(2)	Th	O(3)	72.4(5)	O(6)	Th	O(14)	132.4(4)
O(2)	Th	O(4)	79.3(5)	O(7)	Th	O(14)	74.9(4)
O(2)	Th	O(5)	153.7(4)	Th	O(1)	C(1)	122(1)
O(2)	Th	O(5)	120.8(5)	Th	O(2)	C(2)	119(1)
O(2)	Th	O(6)	115.5(5)	Th	O(3)	C(14)	117(1)
O(2)	Th	O(7)	133.1(4)	Th	O(4)	C(15)	119(1)
O(2)	Th	O(14)	69.7(5)	Th	O(5)	Th	112.2(5)
O(3)	Th	O(4)	65.6(5)	Th	O(5)	C(26)	118(1)
O(3)	Th	O(5)	90.1(4)	Th	O(5)	C(26)	129(1)
O(3)	Th	O(5)	69.4(4)	Th	O(6)	C(27)	123(1)
O(3)	Th	O(6)	135.3(4)	Th	O(7)	C(38)	124(1)
O(3)	Th	O(7)	139.4(5)	O(10)	O(9)	C(11)	57(3)
O(3)	Th	O(14)	92.2(5)	O(9)	O(10)	C(11)	68(3)
O(4)	Th	O(5)	75.5(4)	Th	O(14)	C(32)	138(1)
O(4)	Th	O(5)	120.6(4)	C(7)	N(1)	C(8)	127(2)
O(4)	Th	O(6)	72.8(5)	C(11)	N(2)	C(12)	118(3)
O(4)	Th	O(7)	138.3(4)	C(20)	N(3)	C(21)	125(3)
O(4)	Th	O(14)	146.4(4)	C(23)	N(4)	C(24)	126(2)

C(32)	N(5)	C(33)	127(3)
C(35)	N(6)	C(36)	125(3)
C(39)	N(7)	C(40)	107(3)
C(39)	N(7)	C(41)	112(3)
C(39)	N(7)	C(42)	112(3)
C(40)	N(7)	C(41)	105(3)
C(40)	N(7)	C(42)	112(3)
C(41)	N(7)	C(42)	109(3)
C(43)	N(8)	C(44)	108(4)
C(43)	N(8)	C(47)	108(5)
C(43)	N(8)	C(48)	109(4)
C(44)	N(8)	C(47)	108(5)
C(44)	N(8)	C(48)	101(4)
C(47)	N(8)	C(48)	122(5)
O(1)	C(1)	C(2)	114(2)
O(1)	C(1)	C(6)	125(2)
C(2)	C(1)	C(6)	120(2)
O(2)	C(2)	C(1)	114(2)
O(2)	C(2)	C(3)	127(2)
C(1)	C(2)	C(3)	119(2)
C(2)	C(3)	C(4)	120(3)
C(2)	C(3)	C(11)	118(3)
C(4)	C(3)	C(11)	121(3)
C(3)	C(4)	C(5)	123(2)
C(4)	C(5)	C(6)	118(2)
C(1)	C(6)	C(5)	120(2)
C(18)	C(19)	C(20)	122(3)
O(11)	C(20)	N(3)	123(4)
O(11)	C(20)	C(19)	113(3)
N(3)	C(20)	C(19)	124(4)
N(3)	C(21)	C(22)	111(3)
O(12)	C(23)	N(4)	117(3)
O(12)	C(23)	C(16)	122(2)
N(4)	C(24)	C(25)	107(3)
O(5)	C(26)	C(31)	125(2)
O(6)	C(27)	C(26)	117(2)
C(26)	C(27)	C(28)	120(2)
C(27)	C(28)	C(35)	119(2)
C(28)	C(29)	C(30)	126(3)
C(26)	C(31)	C(30)	117(2)
C(30)	C(31)	C(32)	119(2)
O(14)	C(32)	C(31)	125(2)

C(1)	C(6)	C(7)	122(2)
C(5)	C(6)	C(7)	118(2)
O(8)	C(7)	N(1)	122(2)
O(8)	C(7)	C(6)	120(2)
N(1)	C(7)	C(6)	118(2)
N(1)	C(8)	C(9)	115(3)
O(9)	C(11)	O(10)	55(3)
O(9)	C(11)	N(2)	139(5)
O(9)	C(11)	C(3)	98(4)
O(10)	C(11)	N(2)	117(4)
O(10)	C(11)	C(3)	117(4)
N(2)	C(11)	C(3)	118(3)
N(2)	C(12)	C(13)	85(4)
O(3)	C(14)	C(15)	115(2)
O(3)	C(14)	C(19)	125(2)
C(15)	C(14)	C(19)	120(2)
O(4)	C(15)	C(14)	118(2)
O(4)	C(15)	C(16)	124(2)
C(14)	C(15)	C(16)	119(2)
C(15)	C(16)	C(17)	120(2)
C(15)	C(16)	C(23)	121(2)
C(17)	C(16)	C(23)	119(2)
C(16)	C(17)	C(18)	119(3)
C(177)	C(18)	C(19)	122(3)
C(14)	C(19)	C(18)	120(3)
C(14)	C(19)	C(20)	118(3)
N(5)	C(33)	C(34)	113(3)
O(13)	C(35)	N(6)	121(3)
O(13)	C(35)	C(28)	115(2)
N(6)	C(35)	C(28)	123(3)
N(6)	C(36)	C(37)	110(2)
N(8)	C(44)	C(45)	77(4)
N(4)	C(23)	C(16)	121(2)
O(5)	C(26)	C(27)	114(1)
C(27)	C(26)	C(31)	121(2)
O(6)	C(27)	C(28)	122(2)
C(27)	C(28)	C(29)	117(2)
C(29)	C(28)	C(35)	124(3)
C(29)	C(30)	C(31)	118(2)
C(26)	C(31)	C(32)	123(2)
O(14)	C(32)	N(5)	117(2)
N(5)	C(32)	C(31)	119(3)

Angles are in degrees. Estimated standard deviations in the least significant figure are given in parentheses.

X-Ray Structure Details for $[Th(C_{12}H_{12}O_4N_2)_3(CH_3OH)]_2 \cdot 4\ N(CH_3)_4 \cdot 6\ CH_3OH \cdot 3\ H_2O$ (second Th_2ETAM_6 dimer)

EXPERIMENTAL DETAILS

A. Crystal Data

Empirical Formula	$Th_2C_{90}H_{140}O_{26}N_{16}$
Formula Weight	1529.63
Crystal Color, Habit	tan, tablet
Crystal Dimensions	0.16 X 0.10 X 0.09 mm
Crystal System	monoclinic
Lattice Type	Primitive
No. of Reflections Used for Unit Cell Determination (2θ range)	4521 (3.5 - 45.0°)
Lattice Parameters	a = 18.2603(9)Å
	b = 18.5002(9) Å
	c = 19.675(1) Å
	β = 117.298(1)°
	V = 5906.3(5) Å^3
Space Group	P21/c (#14)
Z value	4
Dcalc	1.720 g/cm^3
F000	3160.00
μ(MoKα)	26.25 cm^{-1}

B. Intensity Measurements

Diffractometer	SMART
Radiation	MoKα (λ = 0.71069 Å) graphite monochromated
Crystal to Detector Distance	60.0 mm
Temperature	-117.0°C
Scan Type	ω (0.3o per frame)
Scan Rate	30 seconds per frame.
2θ max	46.5°
No. of Reflections Measured	Total: 24261 Unique: 8795 (Rint = 0.074)
Corrections	Lorentz-polarization Absorption (Tmax = 0.75 Tmin = 0.65)

C. Structure Solution and Refinement

Structure Solution	Direct Methods (SIR92)
Refinement Function Minimized	Full-matrix least-squares σ w $(\|Fo\| - \|Fc\|)^2$
Least Squares Weights	$1/\sigma^2(F_o) = 4F_o^2/\sigma^2(F_o^2)$
p-factor	0.003
Anomalous Dispersion	All non-hydrogen atoms
No. Observations (I>3.00 σ(I)) No. Variables	4195 585

Reflection/Parameter Ratio	7.17
Residuals: R; Rw	0.032 ; 0.030
Goodness of Fit Indicator	1.04
Max Shift/Error in Final Cycle	0.00
Maximum peak in Final Diff. Map	0.79 e-/Å^3
Minimum peak in Final Diff. Map	-0.68 e-/Å^3

Table A-13. Atomic coordinates and Biso/Beq for Th_2ETAM_6 dimer #2

atom	x	y	z	Beq
Th()	0.61963(2)	0.03437(2)	0.52341(2)	1.394(7)
O(1)	0.7275(4)	0.0424(4)	0.4870(3)	2.0(2)
O(2)	0.7235(4)	0.1257(3)	0.5910(4)	2.0(2)
O(3)	0.8749(4)	0.0909(4)	0.3806(4)	3.0(2)
O(4)	0.8510(4)	0.3246(4)	0.6478(4)	3.0(2)
O(5)	0.6785(4)	-0.0841(3)	0.5490(4)	2.0(2)
O(6)	0.5779(4)	-0.0439(4)	0.4123(3)	2.3(2)
O(7)	0.8187(5)	-0.2747(4)	0.5914(4)	2.4(2)
O(8)	0.5736(4)	-0.1475(3)	0.2188(4)	2.7(2)
O(9)	0.6757(4)	0.0138(3)	0.6565(3)	1.9(2)
O(10)	0.5311(4)	-0.0436(4)	0.5653(3)	1.4(2)
O(11)	0.8132(4)	-0.0524(4)	0.8832(4)	2.8(2)
O(12)	0.4103(4)	-0.1387(3)	0.5604(4)	2.4(2)
O(13)	0.5468(4)	0.1210(3)	0.5790(4)	3.1(2)
O(14)	0.0525(5)	0.1388(4)	0.0596(5)	5.7(2)
O(15)	0.0687(5)	0.1423(4)	0.7960(4)	4.7(2)
O(16)	0.4313(6)	0.1050(5)	0.9191(6)	8.1(3)
O(17)	1.0022(4)	0.1277(4)	0.1740(4)	4.2(2)
O(18)	1.4202(8)	-0.0253(8)	0.9855(7)	4.0(3)
N(1)	0.7748(5)	0.0190(4)	0.3791(5)	2.7(2)
N(2)	0.7728(6)	0.2460(4)	0.6726(5)	2.5(3)
N(3)	0.5282(5)	-0.0551(4)	0.2632(4)	2.8(2)
N(4)	0.7666(6)	-0.1887(4)	0.6401(5)	2.5(3)
N(5)	0.8076(5)	0.0215(5)	0.7899(4)	3.5(2)
N(6)	0.4632(5)	-0.2366(4)	0.6313(5)	2.3(2)
N(7)	0.9501(5)	-0.0513(4)	0.6417(4)	2.3(2)
N(8)	1.2121(6)	0.0072(4)	0.9505(5)	3.7(2)
C(1)	0.7698(6)	0.1020(5)	0.4997(5)	1.3(2)
C(2)	0.7685(6)	0.1491(5)	0.5580(6)	1.6(3)

C(3)	0.8137(6)	0.2147(5)	0.5759(6)	2.6(3)
C(4)	0.8592(6)	0.2327(5)	0.5360(6)	2.5(3)
C(5)	0.8609(6)	0.1889(5)	0.4825(6)	2.4(3)
C(6)	0.8170(6)	0.1228(5)	0.4621(5)	1.9(3)
C(7)	0.8240(7)	0.0758(5)	0.4039(6)	2.3(3)
C(8)	0.7803(7)	-0.0319(7)	0.3258(6)	3.7(3)
C(9)	0.8495(8)	-0.0846(7)	0.3660(8)	4.9(4)
C(10)	0.8145(7)	0.2665(6)	0.6347(6)	2.3(3)
C(11)	0.7682(8)	0.2906(6)	0.7333(7)	3.4(4)
C(12)	0.6926(10)	0.3392(7)	0.7028(8)	5.2(5)
C(13)	0.6781(6)	-0.1240(5)	0.4932(6)	1.3(3)
C(14)	0.6263(6)	-0.1004(5)	0.4166(6)	1.7(3)
C(15)	0.6243(6)	-0.1370(5)	0.3535(6)	2.0(3)
C(16)	0.6744(6)	-0.1988(5)	0.3683(6)	1.6(3)
C(17)	0.7222(6)	-0.2241(5)	0.4404(6)	1.9(3)
C(18)	0.7251(6)	-0.1881(5)	0.5049(6)	2.8(3)
C(19)	0.7748(7)	-0.2202(6)	0.5824(7)	2.5(3)
C(20)	0.8056(8)	-0.2157(6)	0.7186(8)	4.2(4)
C(21)	0.7547(9)	-0.2733(8)	0.7254(8)	5.7(5)
C(22)	0.5726(6)	-0.1132(6)	0.2736(6)	2.0(3)
C(23)	0.4792(6)	-0.0200(6)	0.1895(6)	2.9(3)
C(24)	0.5223(7)	0.0424(7)	0.1763(6)	4.6(3)
C(25)	0.6501(5)	-0.0371(6)	0.6857(5)	1.7(2)
C(26)	0.5716(6)	-0.0709(5)	0.6365(6)	1.6(3)
C(27)	0.5451(6)	-0.1295(5)	0.6645(5)	1.4(3)
C(28)	0.5910(7)	-0.1513(5)	0.7403(6)	2.2(3)
C(29)	0.6635(8)	-0.1185(6)	0.7871(6)	2.0(3)
C(30)	0.6955(6)	-0.0599(5)	0.7606(6)	1.7(3)
C(31)	0.7765(6)	-0.0292(6)	0.8159(6)	2.4(3)
C(32)	0.8889(7)	0.0559(6)	0.8374(6)	3.7(3)
C(33)	0.8831(10)	0.1225(9)	0.871(1)	7.7(6)
C(34)	0.4693(7)	-0.1666(5)	0.6161(6)	2.4(3)
C(35)	0.3889(7)	-0.2790(6)	0.5921(6)	3.5(3)
C(36)	0.3455(9)	-0.2906(7)	0.6402(9)	5.6(5)
C(37)	0.519(1)	0.190(1)	0.555(1)	2.4(4)
C(38)	0.574(2)	0.170(1)	0.638(2)	4.9(6)
C(39)	0.8786(6)	-0.0319(7)	0.6542(6)	3.5(2)
C(40)	0.9390(7)	-0.0187(6)	0.5692(7)	4.7(3)
C(41)	0.9563(7)	-0.1316(6)	0.6369(6)	3.9(3)
C(42)	1.0268(6)	-0.0229(6)	0.7052(5)	3.1(2)
C(43)	1.1260(7)	0.0130(6)	0.9348(6)	4.1(3)
C(44)	1.2597(8)	0.0718(6)	0.9915(7)	4.7(3)
C(45)	1.2502(9)	-0.0575(7)	0.9975(8)	7.0(4)
C(46)	1.2168(7)	0.0006(6)	0.8768(7)	4.9(3)
C(47)	0.0733(8)	0.2096(7)	0.0413(8)	6.2(4)
C(48)	-0.0044(8)	0.1810(7)	0.7438(8)	5.2(3)

C(49)	0.4346(8)	0.1692(8)	0.9615(8)	6.4(4)

Table A-14. Anisotropic Displacement Parameters for Th_2ETAM_6 dimer #2

atom	U11	U22	U33	U12	U13	U23
Th()	0.0209(2)	0.0160(2)	0.0193(2)	-0.0022(3)	0.0105(1)	-0.0015(3)
O(1)	0.027(4)	0.017(4)	0.032(4)	-0.008(4)	0.015(3)	-0.004(4)
O(2)	0.031(5)	0.022(4)	0.025(4)	-0.003(3)	0.016(4)	-0.003(3)
O(3)	0.044(5)	0.033(5)	0.049(5)	-0.007(4)	0.036(5)	-0.005(4)
O(4)	0.046(5)	0.029(5)	0.054(5)	-0.013(4)	0.028(4)	-0.010(4)
O(5)	0.026(5)	0.020(4)	0.025(4)	-0.003(3)	0.012(4)	-0.005(3)
O(6)	0.032(4)	0.019(4)	0.030(4)	0.002(4)	0.015(3)	0.001(4)
O(7)	0.050(6)	0.030(5)	0.037(5)	0.019(4)	0.019(5)	0.004(4)
O(8)	0.040(5)	0.034(5)	0.028(5)	-0.002(4)	0.014(4)	-0.012(4)
O(9)	0.028(4)	0.022(5)	0.020(4)	-0.011(3)	0.014(3)	-0.001(3)
O(10)	0.030(4)	0.015(4)	0.020(4)	0.004(4)	0.015(3)	0.000(4)
O(11)	0.039(5)	0.052(6)	0.022(4)	-0.009(4)	0.001(4)	0.005(4)
O(12)	0.021(5)	0.026(4)	0.033(5)	-0.002(3)	0.009(4)	0.008(4)
O(13)	0.031(5)	0.022(5)	0.043(5)	-0.004(3)	0.023(4)	-0.016(4)
N(1)	0.030(6)	0.036(7)	0.043(6)	-0.013(5)	0.026(5)	-0.025(5)
N(2)	0.044(7)	0.026(5)	0.046(7)	-0.019(5)	0.027(6)	-0.019(5)
N(3)	0.038(6)	0.030(6)	0.011(5)	0.008(4)	0.004(5)	-0.008(4)
N(4)	0.053(7)	0.030(6)	0.023(6)	0.016(5)	0.017(6)	0.008(5)
N(5)	0.037(6)	0.046(7)	0.021(5)	-0.004(5)	0.000(4)	0.006(5)
N(6)	0.034(6)	0.021(5)	0.034(6)	-0.005(4)	0.008(5)	0.009(4)
C(1)	0.015(7)	0.016(6)	0.021(6)	0.003(5)	0.005(5)	-0.004(5)
C(2)	0.014(7)	0.028(7)	0.022(7)	0.007(5)	0.008(6)	0.007(5)
C(3)	0.025(7)	0.021(7)	0.029(7)	-0.002(5)	0.003(6)	-0.008(6)
C(4)	0.035(8)	0.026(7)	0.041(8)	-0.014(5)	0.025(7)	0.006(6)
C(5)	0.028(8)	0.032(7)	0.034(7)	-0.008(5)	0.021(6)	-0.002(6)
C(6)	0.034(7)	0.017(6)	0.023(7)	0.000(5)	0.019(6)	0.002(5)
C(7)	0.032(8)	0.027(7)	0.028(7)	0.003(6)	0.019(7)	0.004(6)
C(8)	0.067(9)	0.045(7)	0.069(9)	-0.027(9)	0.056(8)	-0.020(9)
C(9)	0.10(1)	0.047(9)	0.09(1)	-0.016(8)	0.07(1)	-0.019(8)
C(10)	0.031(8)	0.031(7)	0.040(8)	-0.010(6)	0.021(7)	0.001(6)
C(11)	0.07(1)	0.041(8)	0.053(9)	-0.016(7)	0.037(8)	-0.020(7)
C(12)	0.13(1)	0.055(9)	0.08(1)	0.002(9)	0.08(1)	-0.030(8)
C(13)	0.025(7)	0.015(6)	0.031(7)	-0.001(5)	0.026(6)	0.001(5)
C(14)	0.022(7)	0.021(6)	0.029(7)	-0.013(5)	0.014(6)	0.002(6)
C(15)	0.031(7)	0.016(6)	0.026(7)	-0.008(5)	0.014(6)	-0.005(5)
C(16)	0.030(7)	0.021(6)	0.021(7)	-0.007(5)	0.012(6)	-0.011(5)
C(17)	0.030(7)	0.019(6)	0.034(7)	0.005(5)	0.017(6)	0.000(5)
C(18)	0.031(8)	0.021(7)	0.034(8)	-0.011(6)	0.015(6)	0.000(6)
C(19)	0.043(9)	0.030(8)	0.037(9)	-0.006(6)	0.029(7)	0.000(7)
C(20)	0.07(1)	0.039(8)	0.07(1)	0.008(7)	0.041(9)	0.017(7)

C(21)	0.10(1)	0.09(1)	0.051(10)	0.00(1)	0.038(10)	0.003(9)
C(22)	0.021(7)	0.019(7)	0.025(7)	-0.007(5)	0.003(6)	-0.001(6)
C(23)	0.040(7)	0.044(9)	0.029(7)	0.013(6)	0.013(6)	-0.001(6)
C(24)	0.086(10)	0.047(8)	0.049(8)	0.006(9)	0.034(7)	0.016(8)
C(25)	0.032(6)	0.016(5)	0.020(6)	-0.001(6)	0.014(5)	-0.005(6)
C(26)	0.022(7)	0.017(6)	0.023(7)	0.004(5)	0.011(6)	0.003(5)
C(27)	0.024(7)	0.018(6)	0.017(6)	0.004(5)	0.012(6)	0.010(5)
C(28)	0.029(7)	0.020(6)	0.029(7)	-0.005(5)	0.007(6)	0.007(5)
C(29)	0.054(9)	0.034(8)	0.022(7)	0.013(7)	0.025(7)	0.014(6)
C(30)	0.022(7)	0.034(8)	0.019(7)	-0.001(5)	0.009(6)	-0.003(5)
C(31)	0.032(7)	0.028(6)	0.028(7)	-0.001(7)	0.012(6)	0.001(7)
C(32)	0.042(8)	0.054(10)	0.039(8)	-0.017(6)	0.006(6)	-0.002(6)
C(33)	0.08(1)	0.08(1)	0.18(2)	-0.02(1)	0.03(1)	-0.05(1)
C(34)	0.030(8)	0.022(7)	0.032(7)	-0.002(6)	0.018(6)	0.000(6)
C(35)	0.047(9)	0.030(7)	0.042(8)	-0.019(6)	0.001(7)	0.007(6)
C(36)	0.07(1)	0.08(1)	0.10(1)	-0.019(9)	0.06(1)	-0.021(9)

Table A-15. Selected bond lengths for Th_2ETAM_6 dimer #2.

atom	atom	distance	atom	atom	distance
Th	O(1)	2.389(6)	N(1)	C(7)	1.32(1)
Th	O(2)	2.431(6)	N(1)	C(8)	1.45(1)
Th	O(5)	2.391(6)	N(2)	C(10)	1.34(1)
Th	O(6)	2.435(6)	N(2)	C(11)	1.49(1)
Th	O(9)	2.364(6)	N(3)	C(22)	1.31(1)
Th	O(10)	2.569(6)	N(3)	C(23)	1.46(1)
Th	O(10)	2.499(6)	N(4)	C(19)	1.34(1)
Th	O(12)	2.432(6)	N(4)	C(20)	1.46(1)
Th	O(13)	2.620(6)	N(5)	C(31)	1.32(1)
O(1)	C(1)	1.30(1)	N(5)	C(32)	1.49(1)
O(2)	C(2)	1.33(1)	N(6)	C(34)	1.35(1)
O(3)	C(7)	1.24(1)	N(6)	C(35)	1.45(1)
O(4)	C(10)	1.23(1)	N(7)	C(39)	1.48(1)
O(5)	C(13)	1.32(1)	N(7)	C(40)	1.48(1)
O(6)	C(14)	1.35(1)	N(7)	C(41)	1.50(1)
O(7)	C(19)	1.25(1)	N(7)	C(42)	1.48(1)
O(8)	C(22)	1.26(1)	N(8)	C(43)	1.46(1)
O(9)	C(25)	1.30(1)	N(8)	C(44)	1.48(1)
O(10)	C(26)	1.35(1)	N(8)	C(45)	1.48(1)
O(11)	C(31)	1.25(1)	N(8)	C(46)	1.50(1)
O(12)	C(34)	1.24(1)	C(1)	C(2)	1.45(1)
O(13)	C(37)	1.38(2)	C(1)	C(6)	1.42(1)
O(13)	C(38)	1.37(3)	C(2)	C(3)	1.42(1)
O(14)	C(47)	1.46(1)	C(3)	C(4)	1.42(1)
O(15)	C(48)	1.45(1)	C(3)	C(10)	1.50(1)
O(16)	C(49)	1.44(1)	C(4)	C(5)	1.34(1)

C(5)	C(6)	1.42(1)		C(6)	C(7)	1.49(1)	
C(8)	C(9)	1.50(2)		C(11)	C(12)	1.52(2)	
C(13)	C(14)	1.43(1)		C(13)	C(18)	1.42(1)	
C(14)	C(15)	1.40(1)		C(15)	C(16)	1.41(1)	
C(15)	C(22)	1.48(1)		C(17)	C(18)	1.41(1)	
C(16)	C(17)	1.36(1)		C(20)	C(21)	1.46(2)	
C(18)	C(19)	1.49(1)		C(25)	C(30)	1.38(1)	
C(23)	C(24)	1.49(1)		C(25)	C(26)	1.45(1)	
C(26)	C(27)	1.40(1)		C(27)	C(28)	1.39(1)	
C(27)	C(34)	1.44(1)		C(28)	C(29)	1.36(1)	
C(29)	C(30)	1.44(1)		C(30)	C(31)	1.49(1)	
C(32)	C(33)	1.43(2)		C(35)	C(36)	1.50(2)	
C(37)	C(38)	1.51(3)					

Distances are in angstroms. Estimated standard deviations in the least significant figure are given in parentheses.

Table A-16. Selected bond angles for Th_2ETAM_6 dimer #2.

atom	atom	atom	angle	atom	atom	atom	angle
O(1)	Th	O(2)	65.0(2)	O(9)	Th	O(10)	64.6(2)
O(1)	Th	O(5)	76.6(2)	O(9)	Th	O(10)	124.3(2)
O(1)	Th	O(6)	74.3(2)	O(9)	Th	O(12)	136.6(2)
O(1)	Th	O(9)	110.1(2)	O(9)	Th	O(13)	71.4(2)
O(1)	Th	O(10)	149.1(2)	O(10)	Th	O(10)	67.0(2)
O(1)	Th	O(10)	125.5(2)	O(10)	Th	O(12)	133.2(2)
O(1)	Th	O(12)	73.0(2)	O(10)	Th	O(13)	72.2(2)
O(1)	Th	O(13)	137.1(2)	O(10)	Th	O(12)	68.8(2)
O(2)	Th	O(5)	111.1(2)	O(10)	Th	O(13)	69.0(2)
O(2)	Th	O(6)	138.5(2)	O(12)	Th	O(13)	78.4(2)
O(2)	Th	O(9)	70.9(2)	Th	O(1)	C(1)	119.6(6)
O(2)	Th	O(10)	131.5(2)	Th	O(2)	C(2)	117.4(6)
O(2)	Th	O(10)	131.9(2)	Th	O(5)	C(13)	120.4(5)
O(2)	Th	O(12)	72.3(2)	Th	O(6)	C(14)	118.6(6)
O(2)	Th	O(13)	76.4(2)	Th	O(9)	C(25)	123.1(5)
O(5)	Th	O(6)	64.5(2)	Th	O(10)	Th	113.0(2)
O(5)	Th	O(9)	72.2(2)	Th	O(10)	C(26)	114.7(5)
O(5)	Th	O(10)	72.9(2)	Th	O(10)	C(26)	131.0(6)
O(5)	Th	O(10)	117.0(2)	Th	O(12)	C(34)	139.6(6)
O(5)	Th	O(12)	144.1(2)	Th	O(13)	C(37)	127(1)
O(5)	Th	O(13)	137.6(2)	Th	O(13)	C(38)	135(1)
O(6)	Th	O(9)	134.2(2)	C(37)	O(13)	C(38)	67(1)
O(6)	Th	O(10)	88.3(2)	C(7)	N(1)	C(8)	121.5(9)
O(6)	Th	O(10)	67.8(2)	C(10)	N(2)	C(11)	123.1(9)

O(6)	Th	O(12)	89.0(2)
O(6)	Th	O(13)	136.8(2)
C(31)	N(5)	C(32)	123.1(8)
C(34)	N(6)	C(35)	123.9(9)
C(39)	N(7)	C(40)	108.7(8)
C(39)	N(7)	C(41)	110.5(8)
C(39)	N(7)	C(42)	109.8(7)
C(40)	N(7)	C(41)	109.0(8)
C(40)	N(7)	C(42)	109.1(8)
C(41)	N(7)	C(42)	109.6(8)
C(43)	N(8)	C(44)	111.2(9)
C(43)	N(8)	C(45)	110.1(9)
C(43)	N(8)	C(46)	109.6(9)
C(44)	N(8)	C(45)	108.8(9)
C(44)	N(8)	C(46)	108.3(9)
C(45)	N(8)	C(46)	108.8(9)
O(1)	C(1)	C(2)	115.9(9)
O(1)	C(1)	C(6)	125.3(9)
C(2)	C(1)	C(6)	118.8(9)
O(2)	C(2)	C(1)	115.4(9)
O(2)	C(2)	C(3)	125(1)
C(1)	C(2)	C(3)	119(1)
C(2)	C(3)	C(4)	119(1)
C(2)	C(3)	C(10)	122(1)
C(4)	C(3)	C(10)	119(1)
C(3)	C(4)	C(5)	121.5(9)
C(4)	C(5)	C(6)	122.1(9)
C(1)	C(6)	C(5)	119.1(9)
N(4)	C(19)	C(18)	116(1)
N(4)	C(20)	C(21)	109(1)
O(8)	C(22)	N(3)	122(1)
O(8)	C(22)	C(15)	120(1)
N(3)	C(22)	C(15)	117(1)
O(9)	C(25)	C(26)	117.6(8)
C(26)	C(25)	C(30)	120(1)
O(10)	C(26)	C(27)	125.1(9)
C(26)	C(27)	C(28)	119.9(9)
C(28)	C(27)	C(34)	119.5(9)
C(28)	C(29)	C(30)	121(1)
C(25)	C(30)	C(31)	125(1)
O(11)	C(31)	N(5)	123(1)
N(5)	C(31)	C(30)	116.7(9)
O(12)	C(34)	N(6)	118.0(9)

C(22)	N(3)	C(23)	125.1(9)
C(19)	N(4)	C(20)	124(1)
C(1))	C(6)	C(7)	121.8(9)
C(5)	C(6)	C(7)	119.0(9)
O(3)	C(7)	N(1)	123(1)
O(3)	C(7)	C(6)	120(1)
N(1)	C(7)	C(6)	117.6(9)
N(1)	C(8)	C(9)	111(1)
O(4)	C(10)	N(2)	121(1)
O(4)	C(10)	C(3)	122(1)
N(2)	C(10)	C(3)	116(1)
N(2)	C(11)	C(12)	113(1)
O(5)	C(13)	C(14)	117.0(9)
O(5)	C(13)	C(18)	124.0(9)
C(14)	C(13)	C(18)	119.0(9)
O(6)	C(14)	C(13)	113.6(9)
O(6)	C(14)	C(15)	124.8(9)
C(13)	C(14)	C(15)	121(1)
C(14)	C(15)	C(16)	117.4(9)
C(14)	C(15)	C(22)	122.8(9)
C(16)	C(15)	C(22)	119.8(9)
C(15)	C(16)	C(17)	122.6(9)
C(16)	C(17)	C(18)	121.0(9)
C(13)	C(18)	C(17)	118.5(9)
C(13)	C(18)	C(19)	122(1)
C(17)	C(18)	C(19)	119(1)
O(7)	C(19)	N(4)	123(1)
O(7)	C(19)	C(18)	121(1)
N(6)	C(34)	C(27)	117.6(9)
N(6)	C(35)	C(36)	112(1)
O(13)	C(37)	C(38)	56(1)
O(13)	C(38)	C(37)	57(1)
N(3)	C(23)	C(24)	112.7(9)
O(9)	C(25)	C(30)	122.0(9)
O(10)	C(26)	C(25)	115.8(8)
C(25)	C(26)	C(27)	119.0(9)
C(26)	C(27)	C(34)	120.6(9)
C(27)	C(28)	C(29)	121.1(9)
C(25)	C(30)	C(29)	118(1)
C(29)	C(30)	C(31)	117(1)
O(11)	C(31)	C(30)	121(1)
N(5)	C(32)	C(33)	113(1)
O(12)	C(34)	C(27)	124.4(9)

Angles are in degrees. Estimated standard deviations in the least significant figure are given in parentheses.

X-Ray Structure Details for 2,3-Dihydroxyterephthaloyl Chloride

EXPERIMENTAL DETAILS

A. Crystal Data

Empirical Formula	Cl2C8O4H4
Formula Weight	235.02
Crystal Color, Habit	yellow, tablet
Crystal Dimensions	0.50 x 0.14 x 0.05 mm
Crystal System	orthorhombic
Lattice Type	Primitive
No. of Reflections Used for Unit	
Cell Determination (2θ range)	933 (3.5 - 45.0o)
Lattice Parameters	a = 13.781(3) Å
	b = 4.835(1) Å
	c = 13.241(3) Å
	V = 882.3(8) Å3
Space Group	Pccn (#56)
Z value	4
Dcalc	1.769 g/cm3
F000	472.00
μ(MoKα)	7.15 cm-1

B. Intensity Measurements

Diffractometer	SMART
Radiation	MoKα (λ = 0.71069 Å)
	graphite monochromated
Crystal to Detector Distance	0.0 mm
Temperature	-109.0oC
Scan Type	ω (0.3o per frame)
Scan Rate	0.0 seconds per frame
2θmax	49.4o
No. of Reflections Measured	Total: 3949 Unique: 899 (Rint = 0.050)
Corrections	Lorentz-polarization
	Absorption (Tmax = 1.00, Tmin = 1.00)

C. Structure Solution and Refinement

Structure Solution	Direct Methods (SIR92)
Refinement	Full-matrix least-squares
Function Minimized	Σ w (|Fo| - |Fc|)2
Least Squares Weights	1/σ2(Fo) = 4Fo2/σ2(Fo2)
p-factor	0.030
Anomalous Dispersion	All non-hydrogen atoms

No. Observations (I>3.00σ(I))	402
No. Variables	64
Reflection/Parameter Ratio	6.28
Residuals: R; Rw; Rall	0.050; 0.061; 0.000
Goodness of Fit Indicator	1.81
Max Shift/Error in Final Cycle	0.56
Maximum peak in Final Diff. Map	0.36 e-/Å3
Minimum peak in Final Diff. Map	-0.28 e-/Å3

Table A-17. Atomic coordinates and Biso/Beq for 2,3-Dihydroxyterephthaloyl Chloride

atom	x	y	z	Beq
Cl(1)	0.94954(8)	0.7613(3)	0.08453(10)	4.09(3)
O(1)	0.9252(2)	0.7817(7)	0.2762(3)	3.62(9)
O(2)	0.8130(2)	0.4444(8)	0.3807(2)	3.09(8)
C(1)	0.7858(3)	0.3536(10)	0.2888(3)	2.12(9)
C(3)	0.8215(3)	0.450(1)	0.1974(3)	2.41(9)
C(4)	0.8972(3)	0.6709(10)	0.2007(4)	3.01(9)
C(5)	0.7851(3)	0.347(1)	0.1061(3)	2.9(1)

Table A-18. Anisotropic Displacement Parameters for 2,3-Dihydroxyterephthaloyl Chloride

atom	U11	U22	U33	U12	U13	U23
Cl(1)	0.0527(7)	0.0481(9)	0.0612(8)	-0.0108(8)	0.0047(7)	0.0187(9)
O(1)	0.051(2)	0.029(2)	0.065(2)	-0.004(2)	-0.004(2)	-0.009(2)
O(2)	0.047(2)	0.046(3)	0.037(2)	-0.015(2)	-0.003(2)	-0.010(2)
C(1)	0.034(2)	0.027(3)	0.030(1)	0.007(2)	-0.004(2)	-0.005(2)
C(3)	0.030(2)	0.030(3)	0.035(2)	-0.002(2)	0.001(2)	0.002(2)
C(4)	0.035(3)	0.022(3)	0.058(2)	0.002(2)	-0.002(2)	0.004(2)
C(5)	0.050(3)	0.042(4)	0.029(2)	-0.007(2)	-0.002(2)	0.006(2)

Table A-19. Selected bond lengths for 2,3-Dihydroxyterephthaloyl Chloride

atom	atom	distance	atom	atom	distance
Cl1	C4	1.755(7)	O1	C4	1.198(7)
O2	C1	1.347(7)	C1	C1	1.41(1)
C1	C3	1.388(8)	C3	C4	1.493(8)
C3	C5	1.401(8)	C5	C5	1.35(1)

Table A-20. Selected bond angles for 2,3-Dihydroxyterephthaloyl Chloride

atom	atom	atom	angle	atom	atom	atom	angle
O2	C1	C1	115.3(3)	O2	C1	C3	125.5(5)
C1	C1	C3	119.2(3)	C1	C3	C4	117.5(6)
C1	C3	C5	120.4(5)	C4	C3	C5	122.1(6)
Cl1	C4	O1	119.1(5)	Cl1	C4	C3	116.1(5)
O1	C4	C3	124.8(6)	C3	C5	C5	120.4(3)

References

(1) SIR92: Altomare, A., Burla, M.C., Camalli, M., Cascarano, M., Giacovazzo, C., Guagliardi, A., Polidori, G. (1993). J. Appl. Cryst., 26, 343.

(2) DIRDIF92: Beurskens, P.T., Admiraal, G., Beurskens, G., Bosman, W.P., Garcia-Granda, S., Gould, R.O., Smits, J.M.M. and Smykalla, C. (1992). The DIRDIF program system, Technical Report of the Crystallography Laboratory, University of Nijmegen, The Netherlands.

(3) Least-Squares:

Function minimized: $\Sigma w(|F_o|-|F_c|)^2$

where $w = \frac{1}{\sigma^2(F_0^2)} = \frac{4F_0^2}{\sigma^2(F_0^2)}$

and $\sigma^2(F_o^2) = [S^2(C+R^2B) + (pF_o^2)^2]/Lp^2$

S = Scan rate
C = Total integrated peak count
R = Ratio of scan time to background counting time
B = Total background count
Lp = Lorentz-polarization factor
p = p-factor

(4) Standard deviation of an observation of unit weight:

$[\Sigma w(|F_o|-|F_c|)^2/(N_o-N_v)]^{1/2}$

where No = number of observations
Nv = number of variables

(5) Cromer, D. T. & Waber, J. T.; "International Tables for X-ray Crystallography", Vol. IV, The Kynoch Press, Birmingham, England, Table 2.2 A (1974).

(6) Ibers, J. A. & Hamilton, W. C.; Acta Crystallogr., 17, 781 (1964).

(7) Creagh, D. C. & McAuley, W.J .; "International Tables for Crystallography", Vol C, (A.J.C. Wilson, ed.), Kluwer Academic Publishers, Boston, Table 4.2.6.8, pages 219-222 (1992).

(8) Creagh, D. C. & Hubbell, J.H..; "International Tables for Crystallography", Vol C, (A.J.C. Wilson, ed.), Kluwer Academic Publishers, Boston, Table 4.2.4.3, pages 200-206 (1992).

(9) teXsan: Crystal Structure Analysis Package, Molecular Structure Corporation (1985 & 1992).

(10) SMART: Area-Detector Software Package, Siemens Industrial Automation, Inc.: Madison, WI, (1995)

(11) SAINT: SAX Area-Dectector Integration Program, V4.024; Siemens Industrial Automation, Inc.: Madison, WI, (1995)

(12) XPREP:(v 5.03) Part of the SHELXTL Crystal Structure Determination Package, Siemens Industrial Automation, Inc.: Madison, WI, (1995)

(13) SADABS: Siemens Area Detector ABSorption correction program, George Sheldrick, (1996).
Advance copy, private communication.

Appendix 2

Raw Data for Chapter 5 – Pu(IV) and Am(III) uptake by PDT and PST

Weight in grams, cpm = counts per minute, cpm normalized has background cpm subtracted.

PDT (0.01%) + Pu(IV)								
				cpm/gram	cpm/gram			
sample name	weight(g)	cpm gross	cpm normalized	feed	permeate	D	% Extraction	pH
101A	0.097	3227.37	3208.605	33078.4		9.81E+02	8.93	1.56
101b	0.6494	19580.67	19561.905		30123.04			
101c	0.0984	3251.77	3233.005	32855.74		1.54E+03	13.33	1.62
101d	0.6439	18353.47	18334.705		28474.46			
101e	0.1003	3079.8	3061.035	30518.79		9.74E+06	99.90	8.71
101f	0.6231	38.27	19.505		31.30316			
101g	0.1001	3157.33	3138.565	31354.3		4.81E+06	99.79	11.42
101h	0.6392	60.33	41.565		65.0266			
101i	0.0994	3057.6	3037.8	30561.37		4.24E+06	99.76	11.28
101j	0.5414	58.7	38.9		71.85076			
102a	0.0937	3071.3	3051.5	32566.7		1.74E+06	99.43	7.38
102b	0.5917	130	110.2		186.243			
102c	0.0887	2767.3	2747.5	30975.2		1.42E+06	99.30	6.81
102d	0.602	150.5	130.7		217.1096			
102e	0.0999	3153.8	3134	31371.37		3.31E+05	97.07	6.11
102f	0.5988	570.4	550.6		919.5057			
102g	0.0963	2909.4	2889.6	30006.23		7.13E+03	41.61	1.96
102h	0.5952	10448.5	10428.7		17521.34			
103A	0.0995	3051.8	3032.4	30476.38		7.85E+03	43.99	2.03
103b	0.6087	10409.2	10389.8		17068.84			
103c	0.0852	2603.6	2584.2	30330.99		1.03E+05	91.14	2.94
103d	0.495	1347	1330.3		2687.475			
103e	0.0757	2293.8	2277.1	30080.58		1.35E+06	99.26	4.49
103f	0.67	165	148.3		221.3433			
103g	0.0969	2953	2936.3	30302.37		2.99E+06	99.67	10.27
103h	0.6398	81.3	64.6		100.9691			
103i	0.0969	2859.8	2843.1	29340.56		3.33E+06	99.70	9.11
103j	0.4719	58.2	41.5		87.94236			
103k	0.0964	2823.3	2808.7	29135.89		1.28E+06	99.22	5.91
103l	0.5694	143.3	128.7		226.0274			

PDT (0.01%) + Am(III)								
				cpm/gram	cpm/gram			
sample name	weight(g)	cpm gross	cpm normalized	feed	permeate	D	% Extraction	pH
104a	0.0997	2367.1	2357.95	23650.45		-6.31E+02	-6.74	1.13
104b	0.6307	15930.5	15921.35		25243.94			
104c	0.1015	2671.8	2662.65	26233		9.09E+02	8.33	2.07
104d	0.5466	13153.2	13144.05		24046.93			
104e	0.0968	2304.9	2295.75	23716.43		-4.01E+02	-4.18	3
104f	0.6572	16246.9	16237.75		24707.47			
104g	0.0979	2510.9	2501.75	25554.14		-4.76E+02	-5.00	3.86
104h	0.6167	16556.2	16547.05		26831.6			
104i	0.0939	2489.5	2480.35	26414.8		3.11E+03	23.70	6.1
104j	0.6054	12210.5	12201.35		20154.2			
104k	0.0863	2126.9	2117.75	24539.4		1.18E+03	10.55	6.48
104l	0.5779	12694.6	12685.45		21950.94			
105a	0.0908	2590.7	2576.9	28379.96		6.93E+04	87.39	8.44
105b	0.5971	2151.2	2137.4		3579.635			
105c	0.0979	2527.5	2513.7	25676.2		4.08E+05	97.61	9.43
105d	0.6048	385.4	371.6		614.418			
105e	0.0931	2284.1	2270.3	24385.61		4.80E+05	97.96	10.1
105f	0.678	351.2	337.4		497.6401			
112a	0.099	3545.8	3536.65	35723.74		1.45E+03	12.66	2.83
b	0.5195	16217.9	16208.75		31200.67			
c	0.0847	2467	2457.85	29018.3		9.60E+03	48.99	7.88
d	0.5949	8815.7	8806.55		14803.41			
e	0.0601	1960	1950.85	32460.07		-5.11E+02	-5.39	5.12
f	0.4772	16333.4	16324.25		34208.4			
g	0.0958	3621.4	3612.25	37706.16		1.65E+03	14.20	4.69
h	0.5484	17751.9	17742.75		32353.67			
I	0.0776	2548	2538.85	32717.14		2.19E+06	99.55	10.88
j	0.5344	88.7	79.55		148.8585			
k	0.092	3251	3241.85	35237.5		5.23E+03	34.36	7.19
l	0.5645	13066.8	13057.65		23131.36			

PDT (0.01%) + Pu(III)								
				cpm/gram	cpm/gram			
sample name	weight(g)	cpm gross	cpm normalized	feed	permeate	D	% Extraction	pH
113 a	0.0941	3153.8	3153.8	33515.41		4.65E+02	4.44	1.24
b	0.4972	15923.6	15923.6		32026.55			
c	0.0839	2672.4	2672.4	31852.21		4.40E+04	81.47	2.44
d	0.4629	2732.4	2732.4		5902.787			

e	0.0734	2320.7	2320.7	31617.17		7.32E+05	98.65	3.61
f	0.5143	219.2	219.2		426.2104			
g	0.0889	2762.7	2762.7	31076.49		1.07E+06	99.07	5.43
h	0.4895	140.9	140.9		287.8447			
I	0.0826	2582.8	2582.8	31268.77		9.98E+05	99.01	6.15
j	0.463	143.6	143.6		310.1512			
114 a	0.0939	2866.8	2866.8	30530.35		7.38E+05	98.66	9.13
b	0.4537	185.3	185.3		408.4197			
c	0.0935	3006.4	3006.4	32154.01		5.83E+05	98.31	10.61
d	0.539	292.2	292.2		542.115			
e	0.0953	2984.7	2984.7	31318.99		4.72E+05	97.93	8.03
f	0.5184	336.5	336.5		649.1127			

PDT (0.1%) + Pu(IV)								
				cpm/gram	cpm/gram			
sample name	weight(g)	cpm gross	cpm normalized	feed	permeate	D	% Extraction	pH
115a	0.0837	2809.9	2799.9	33451.61		1.28E+03	56.08	1.53
b	0.476	7003.6	6993.6		14692.44			
c	0.0947	3174.6	3164.6	33417.11		4.68E+04	97.91	2.9
d	0.6014	430.2	420.2		698.703			
e	0.096	3281.4	3271.4	34077.08		1.29E+05	99.23	3.71
f	0.4798	136.2	126.2		263.0263			
g	0.0904	3120.5	3110.5	34408.19		2.58E+05	99.61	5.01
h	0.5266	79.9	69.9		132.7383			
I	0.0903	3073.1	3063.1	33921.37		4.31E+05	99.77	6.07
j	0.553	53.4	43.4		78.48101			
m	0.0902	3085.9	3075.9	34100.89		6.64E+05	99.85	8.26
n	0.5503	38.2	28.2		51.24478			
o	0.095	3279.7	3269.7	34417.89		6.26E+05	99.84	9.73
p	0.5499	40.2	30.2		54.91908			
q	0.0836	3057.3	3047.3	36450.96		4.84E+05	99.79	11.1
r	0.585	54	44		75.21368			

PDT (0.001% + Pu(IV)								
				cpm/gram	cpm/gram			
sample name	weight(g)	cpm gross	cpm normalized	feed	permeate	D	% Extraction	pH
116a	0.085	3082.7	3072.7	36149.41		2.31E+03	2.25	1.42
b	0.6036	21338.1	21328.1		35334.82			
c	0.0979	2545.7	2535.7	25900.92		2.36E+06	95.93	9.37
d	0.6035	645.9	635.9		1053.687			
e	0.0984	2612.2	2602.2	26445.12		2.18E+06	95.61	10.42
f	0.5801	683.6	673.6		1161.179			
g	0.1008	3037.1	3027.1	30030.75		1.40E+06	93.35	3.96

h	0.5159	1040.6	1030.6		1997.674			
i	0.0916	2495.7	2485.7	27136.46		7.58E+05	88.35	5.89
j	0.6232	1981	1971		3162.709			
k	0.0986	2147.3	2137.3	21676.47		3.74E+05	78.92	8.61
l	0.4966	2279.7	2269.7		4570.479			
m	0.0993	1960.1	1950.1	19638.47		3.38E+05	77.17	7.31
n	0.5415	2437.9	2427.9		4483.657			

Pu polymer formation, no PDT, pH 12.3

sample name	weight(g)	cpm gross	cpm normalized	cpm/gram feed	time (min) after add. of Pu(IV)
106a	0.096	3514.6	3504.1	36501.04	10
106c	0.0964	3113.3	3102.8	32186.72	30
106e	0.0975	2655.6	2645.1	27129.23	70
106g	0.0972	2078.2	2067.7	21272.63	135
106i	0.0887	1155.8	1145.3	12912.06	340
k	0.0917	466.2	456.2	4974.918	1390
m	0.0728	1509	1498.5	20583.79	1430
o	0.0759	2843.8	2833.3	37329.38	

Pu polymer dissolution, pH 12.3

sample name	weight(g)	cpm gross	cpm normalized	cpm/g feed	time (min) after addition of: Pu(IV)	PDT
1	0.1003	3741.4	3730.9	37197.41	0	0
2	0.0903	2825	2814.5	31168.33	240	0
2a	0.0841	2639.7	2629.2	31262.78	245	5
2c	0.0726	2359.8	2349.3	32359.5	270	30
2e	0.0903	2994	2983.5	33039.87	350	110
2g	0.0961	3217.8	3207.3	33374.61	365	125
2i	0.0861	2906.5	2896	33635.31	1390	1150
2k	0.0983	3522.4	3512.4	35731.43	2830	2590

PST + Pu(IV)

sample name	weight(g)	cpm gross	cpm normalized	cpm/gram feed	cpm/gram permeate	D	% Extraction	pH
78A	0.101	3378.7	3359.8	33266		2.20E+03	18.06	1.29
78B	0.7567	20646	20627		27259			
78C	0.1039	3021.3	3002.4	28897		2.88E+05	96.65	9.86
78D	0.7073	704.1	685.25		968.83			
78E	0.1	3089.5	3070.6	30706		7.35E+05	98.66	10.87
78F	0.7538	329.7	310.85		412.38			
79A	0.1033	3246.1	3227.3	31242		6.71E+05	98.53	10.77
79B	0.6248	305.3	286.45		458.47			
79C	0.1039	2578.5	2559.6	24636		7.55E+05	98.69	7.87
79D	0.6026	213	194.15		322.19			

79E	0.1054	2709.8	2690.9	25531		5.30E+05	98.15	6.16
79F	0.5782	292.1	273.25		472.59			
79G	0.1054	2432.9	2414	22904		4.82E+05	97.97	5.02
79H	0.4122	210.9	192.05		465.91			
79I	0.102	1867.5	1848.7	18124		2.63E+05	96.33	3.74
79J	0.5482	383.4	364.55		664.99			
80A	0.101	3167.8	3148.9	31178		5.99E+05	98.36	3.69
80B	0.7567	406.3	387.45		512.03			
80C	0.1039	2646.5	2627.6	25290		1.06E+07	99.91	9.59
80D	0.7073	35.7	16.85		23.823			
80E	0.1	2788.9	2770	27700		2.21E+07	99.95	11.66
80F	0.7538	28.3	9.45		12.536			
81A	0.1033	2558.7	2539.8	24587		3.89E+06	99.74	6.74
81B	0.6248	58.2	39.35		62.98			
81C	0.1039	2453.5	2434.6	23433		3.40E+06	99.71	5.66
81D	0.6026	60.2	41.35		68.619			
81E	0.1054	2108.2	2089.3	19823		1.46E+06	99.32	4.12
81F	0.5782	97	78.15		135.16			
81G	0.1054	1778.7	1759.8	16697		2.00E+05	95.24	3.43
81H	0.4122	346.5	327.65		794.88			
82A	0.0523	1808.4	1791.8	34260		8.71E+06	99.89	12.07
82B	0.6386	41.7	25.1		39.305			
82C	0.1018	3672.6	3656	35914		1.11E+07	99.91	11.97
82D	0.6126	36.4	19.8		32.321			
82E	0.1013	3651.4	3634.8	35882		7.34E+06	99.86	11.89
82F	0.6063	46.2	29.6		48.821			
83G	0.1032	3706.1	3689.5	35751		1.07E+07	99.91	12.1
82H	0.5113	33.6	17		33.249			
83A	0.1015	3610.4	3593.8	35407		8.49E+06	99.88	9.88
83B	0.598	41.5	24.9		41.639			
83C	0.1015	3654.8	3638.2	35844		1.22E+07	99.92	9.82
83D	0.5758	33.5	16.9		29.35			
83E	0.0995	3534.3	3517.7	35354		8.87E+06	99.89	9.1
83F	0.6429	42.2	25.6		39.82			
83G	0.0826	2943.9	2927.3	35439		1.03E+07	99.90	8.76
83H	0.6569	39.1	22.5		34.252			
86A	0.0989	3365.5	3347.4	33846		1.36E+07	99.93	9.02
86B	0.6558	34.4	16.3		24.855			
86C	0.1046	3491	3472.9	33202		1.65E+07	99.94	8.02
86D	0.611	30.4	12.3		20.131			
86E	0.104	3416.6	3398.5	32678		8.72E+06	99.89	7.03
86F	0.6788	43.5	25.4		37.419			
86G	0.1043	1416.9	1398.8	13411		1.73E+06	99.43	6.45
86H	0.6453	67.7	49.6		76.863			
88A	0.1041	1912.6	1894.5	18199		1.62E+06	99.39	4.46
88B	0.5838	83.2	65.1		111.51			
88C	0.1043	1137.6	1119.5	10733		6.00E+05	98.36	3.63

88D	0.6207	127.3	109.2		175.93			
88E	0.1042	1042.5	1024.4	9831.1		1.08E+05	91.50	3.03
88F	0.5383	468.1	450		835.97			
88G	0.1018	929.5	911.4	8952.8		4.40E+04	81.48	2.28
88H	0.7034	1184.5	1166.4		1658.2			

PST + Am(III)								
				cpm/gram	cpm/gram			
sample name	weight(g)	cpm gross	cpm normalized	feed	permeate	D	% Extraction	pH
85A	0.1007	1466.8	1448.7	14386		7.01E+06	99.86	11.59
85B	0.6395	31.2	13.1		20.485			
85C	0.1035	1559.7	1541.6	14895		2.74E+05	96.48	11.99
85D	0.5513	307.5	289.4		524.94			
85E	0.1032	1560.9	1542.8	14950		8.59E+04	89.57	9.81
85F	0.6606	1048.1	1030		1559.2			
85G	0.105	1604.7	1586.6	15110		5.14E+04	83.70	9.14
85H	0.6443	1604.9	1586.8		2462.8			
85I	0.1051	1549.1	1531	14567		3.06E+04	75.35	7.82
85J	0.591	2140.1	2122		3590.5			
87A	0.1015	1360.5	1342.4	13226		6.08E+02	5.73	5.3
87B	0.6373	7963.7	7945.6		12468			
87C	0.1059	1391.7	1373.6	12971		1.07E+03	9.66	3.66
87D	0.5735	6738.6	6720.5		11718			
87E	0.1046	1630.6	1612.5	15416		2.80E+02	2.72	2.21
87F	0.4104	6172.5	6154.4		14996			

Ernest Orlando Lawrence Berkeley National Laboratory
One Cyclotron Road | Berkeley, California 94720

Prepared for the U.S. Department of Energy under Contract No. DE-AC03-76SF00098